SYNTHESIS OF GUANIDINO ANALOGUES AS POTENTIAL NITRIC OXIDE SYNTHASE INHIBITORS

BONG YONG KOY

NATIONAL UNIVERSITY OF SINGAPORE

2004

SYNTHESIS OF GUANIDINO ANALOGUES
AS POTENTIAL NITRIC OXIDE SYNTHASE INHIBITORS

BONG YONG KOY **2004**

SYNTHESIS OF GUANIDINO ANALOGUES AS POTENTIAL NITRIC OXIDE SYNTHASE INHIBITORS

BONG YONG KOY
(B.Sc.(Pharm.)(Hons.), NUS)

A THESIS SUBMITTED

FOR THE DEGREE OF DOCTOR OF PHILOSOPHY

DEPARTMENT OF PHARMACY

NATIONAL UNIVERSITY OF SINGAPORE

2004

To the beautiful world, those who love me, and those I love.

Acknowledgements

I wish to express my highest gratitude and appreciations towards Dr. Chui Wai Keung for his invaluable guidance, teaching, advice, support and understandings throughout the course of the study. Under his supervision, I have learnt a lot and emerged as a better scientist as well as a better person.

I wish to extend my special thanks to Assoc. Prof. Paul Heng W. S., head of Department of Pharmacy, for providing support and facilities for carrying out the study; and the National University of Singapore for providing the research scholarship.

I also wish to thank Assoc. Prof. Peter Wong T. H. from Department of Pharmacology for his guidance and advice, as well as providing the facilities to perform the biological studies.

My appreciations to the laboratory officers in Department of Pharmacy and Department of Pharmacology, especially Miss Christin Ang L. K., Miss Ng S. E., Mdm. Oh T. B., and Mdm. Ting W. L., for their assistance and technical supports. The support from administrative staff and office support staff are also appreciated.

I am also gratitude for the friendship and support from my fellow friends in Department of Pharmacy and Department of Pharmacology, notably, but not limited to, Dr. Jeyanti C. T., Dr. Poon T.Y., Mr. Chen W. S., Mr. Ma X., Miss Lau A. J. and Miss Lee H. Y. I also wish to thank co-workers Miss Tan Y.K., Mr Ng K. P. and Mr. Tan J. M. in Pharmacy Department.

Last but not least, I would like to thank my family for their understanding and emotional support.

Table of Contents

Summary

Nitric oxide (NO) is produced by three isoforms of nitric oxide synthase (nNOS, iNOS and eNOS). Depending on the concentration, NO functions as either a signalling agent or a cytotoxic agent. Overproduction of nNOS-derived NO is implicated in various neurodegenerative diseases. Hence, selective inhibition nNOS is desirable.

Numerous NOS inhibitors have been developed, but relatively few are nNOS selective and none is clinically available yet. Most of the NOS inhibitors contain a guanidino-mimicking group, which is essential for inhibitor binding. In addition, several active site interacting groups modify the binding affinity and isoform selectivity of the inhibitors.

Among the ligand-interacting sites, the region adjacent to the guanidino binding site (RegG) was less studied. Limited data suggested the involvement of hydrophobic interaction in RegG; and hydrophobic interaction is the major driving force in the induced-fitting of a ligand to its binding site. Hence, it was hypothesised that by exploiting the RegG, selective nNOS inhibition and improved nNOS binding affinity could be achieved through differently substituted guanidino compounds, and thus may give rise to useful therapeutic values.

63 compounds from six series of guanidino analogues were synthesised and evaluated as selective nNOS inhibitor and molecular probe of RegG. While the syntheses of N^1-alkylguanidines, N^1-alkyl-N^2-nitroguanidines and 1-alkyl-4-nitroimino-1,3,5-triazinanes (TZN) were rather straight forward, the syntheses of N^1,N^2-dialkylguanidines, 2-(2-nitroguanidino)alkanoic acids (NGAA) and 6-anilino-4-amino-1,2-dihydro-2,2-dimethyl-1,3,5-triazines (TZA) were challenging and time

consuming, and the reaction optimisation required a good understanding of the reaction mechanisms.

As compared to N^1-alkylguanidines, N^1,N^2-(disubstituted)guanidines were more potent and nNOS selective inhibition was achievable, provided the haem iron (Fe_{haem}) interacting groups were able to bind to the size-restricted proximal guanidino binding site. Both Fe_{haem}-interacting N^2-nitro and N^2-propyl substituents showed similar activity profile. For the N^1-alkyl-N^2-nitroguanidines, N^1-benzyl substituent resulted in enhanced binding affinity and a tendency towards nNOS inhibition. Ring substituents on the N^1-benzyl group modified the binding affinity but provided no improvement in nNOS selectivity. However, with large and hydrophobic aromatic group, as in compound **XXXXII** (N^1-(diphenyl)methyl-N^2-nitroguanidine), nNOS selective inhibition was achieved together with improved binding affinity (IC_{50} 58±5 μM). On the other hand, compounds with charged groups (NGAA, TZN and TZA) were inactive.

Hence, hydrophobic and π-π stacking interactions were involved in the RegG, while charged species were not tolerated. The surface topology of the RegG seemed to be highly conserved provided the RegG-interacting group was not steric challenging. With bulky, hydrophobic and aromatic RegG-interacting group, the RegG of nNOS, but not iNOS or eNOS, could undergo induced-conformational change to accommodate the compound. Thus, nNOS inhibition was achievable *via* a size-exclusion mechanism in the RegG.

The lead compound, compound **XXXXII**, was tested using PTZ and rotarod tests. Compound **XXXXII** exhibited partial *in vivo* nNOS inhibition with minimum neuromotor side effects. Although compound **XXXXII** could not prevent the initialisation of convulsion, it minimised convulsion-induced neurological injuries. In

conclusion, the current study suggested that selective nNOS inhibition could be achieved *via* a size-exclusion mechanism in the RegG, and the *in vitro* nNOS inhibition was translatable into *in vivo* neuroprotective activity.

Keywords: Nitric oxide synthase; Selective inhibition; Size-exclusion mechanism; Neuroprotection; N^1-(Diphenyl)methyl-N^2-nitroguanidine.

Abbreviations

$\%yield_{adj}$	% yield (adjusted to purity)
[ ]	concentration term
$[Ca^{2+}]_{i,f}$	intracellular free Ca^{2+} concentration
1,14-BITU	N^1,N^{14}-bis((S-methyl)isothioureido)tetradecane (1,14-BITU
1,3-PBITU	S,S'-(1,3-phenylenebis(1,2-ethanediyl))bisisothiourea
1,4-PBITU	S,S'-(1,4-phenylenebis(1,2-ethanediyl))bisisothiourea
1400W	N-(*m*-(aminomethyl)benzyl)acetamide
BH_4	(6R)-5,6,7,8-tetrahydro-L-biopterin
CaM	calmodulin
CBS	α-acid binding site
cNOS	constitutive NOS
cpm	count per minute
DCM	dichloromethane
dGBS	distal guanino binding site
DIEA	N,N-diisopropyl-N-ethylamine
DMF	N,N-dimethylformamide
DMSO	N,N-dimethylsulphoxide
DRIFT	diffuse reflectance infrared Fourier transformed spectroscopy
DTT	DL-Dithiothreitol
DZP	diazepam
eNOS	endothelial nitric oxide synthase
EPITU	S-ethyl-N-phenyl-isothiourea
ESI	electron spray ionisation

FAD	flavin adenine dinucleotide
FMN	flavin mononucleotide
FTIR	Fourier transformed infrared spectroscopy
$GABA_A$	γ-aminobutyric acid receptor subtype A
GBS	guanino binding site
GMEC	global minimum energy conformer
HEPES	4-(2-hydroxyethyl)-1-piperazineethanesulfonic acid
HOONO	peroxynitrous acid
IC_{50}	inhibitory concentration at 50 % inhibition
iNOS	inducible nitric oxide synthase
iPrNHG	N^1-isopropyl-N^3-hydroxyguanidine
K_i	coefficient of inhibition
L-AMMA	L-N^G,N^G-dimethyl-arginine
L-Arg	L-Arginine
L-Cit	L-citrulline
L-NA	L-N^G-nitro-arginine
L-NAME	L-N^G-nitro-arginine methyl ester
L-NHA	N^ω-hydroxy-L-arginine
L-NIO	L-N^5-(1-iminoethyl)-ornithine
L-NMMA	L-N^G-monomethyl-arginine
L-NPA	L-N^G-propylarginine
L-OH-Arg	N^φ-hydroxyl-L-Arginine
MALDI	matrix-assisted laser desorption ionisation
NADPH	β-Nicotinamide adenine dinucleotide 2'-phosphate reduced tetrasodium salt

NBS	α-amino binding site
nBuNHG	N^1-butyl-N^3-hydroxyguanidine
NGAA	2-(2-nitroguanidino)alkanoic acids
NIL	L-N-iminoethyllysine
NIO	L-N-iminoethylornitine
nNOS	neuronal nitric oxide synthase
NO	nitric oxide
NOS	nitric oxide synthase
PDZ	postsynaptic density zipper
pGBS	proximal guanino binding site
p-NO_2PhOCOCl	p-nitrophenyl chloroformate
PS	polystyrene
PTC	phase transfer catalyst
PTZ	pentylenetetrazol
RegG	region adjacent to GBS
rpm	rotation per minute
RS_{NO}	reactive nitric oxide species
SacBS	substrate access channel binding site
SAR	structural-activity relationship
SMITUSO4	S-methylisothiouronium sulphate
SMNNITU	S-methyl-N-nitroisothiourea
SOD	superoxide dismutase
SPOS	solid phase organic synthesis
$t_{½}$	half-life

TEA	N,N,N-triethylamine
TFA	trifluoroacetic acid
THF	tetrahydrofuran
TosylCl	*p*-methylphenylsulphonyl chloride
TZA	6-anilino-4-amino-1,2-dihydro-2,2-dimethyl-1,3,5-triazines
TZN	1-alkyl-4-nitroimino-1,3,5-triazinane
TZP	1-(substituted)phenyl-4,6-diamino-1,2-dihydro-2,2-dimethyl-1,3,5-triazine

List of Figures

List of Schemes

List of Tables

Chapter 1 Nitric Oxide and Nitric Oxide Synthase

In 1998, the Nobel Prize in Biology / Medicine was awarded to three scientists, Robert Furchgott, Louis Ignarro and Ferid Murad[1]. In the same year, Pfizer Inc. introduced a blockbuster drug, sildenafil (Viagra®), which attracted much public attention[2]. Both events were related to each other *via* nitric oxide (NO), which was named as "Molecule of The Year" in 1992 for being a startlingly simple molecule uniting neuroscience, physiology, and immunology[3].

Nitric Oxide (NO): Properties and Biological Effects

NO is a diatomic gaseous molecule which is hydrophobic and uncharged. NO has low water solubility of 1.9×10^{-3} M (25 °C, P_{NO} 1 atm), comparable to other non-hydrolysable gases such as nitrogen and carbon monoxide[4,5]. NO is a radical with eleven valence shell electrons, but the occupation of the unpaired electron in the π antibonding orbital resulted in the higher stability of NO as compared to other radicals[6]. Although NO is almost inert to water, the half-life ($t_{½}$) of NO is relatively short in the physiological system (5 to 15 seconds[7]) due to the redox breakdown of NO, the reactions of NO with O_2 and O_2^{-}, and the scavenging systems of NO.

By itself, NO is not a nitrosating agent. The NO-related chemical reactions are attributable to the redox products (NO^+ and NO^-) and the autoxidative product (RS_{NO}) of NO[8]. NO is readily oxidised and reduced into NO^+ and NO^- (conjugate base of HNO) respectively, but the roles of NO^+ and NO^- are limited physiologically[9]. The major physiological nitrosating agent is the reactive nitric oxide species (RS_{NO}) (**Scheme 1**[9]), which serves as NO^+ donor[9].

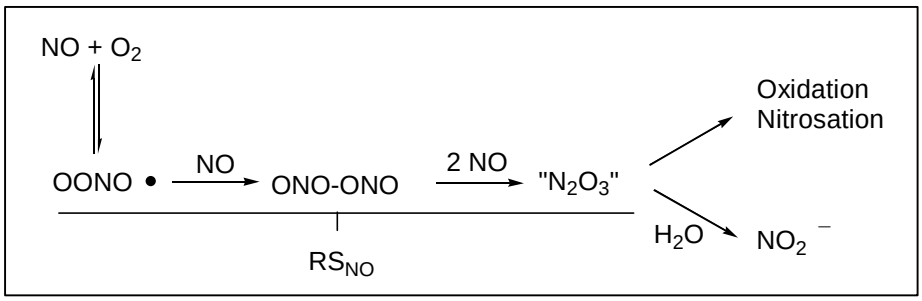

Scheme 1. The autoxidation of NO.

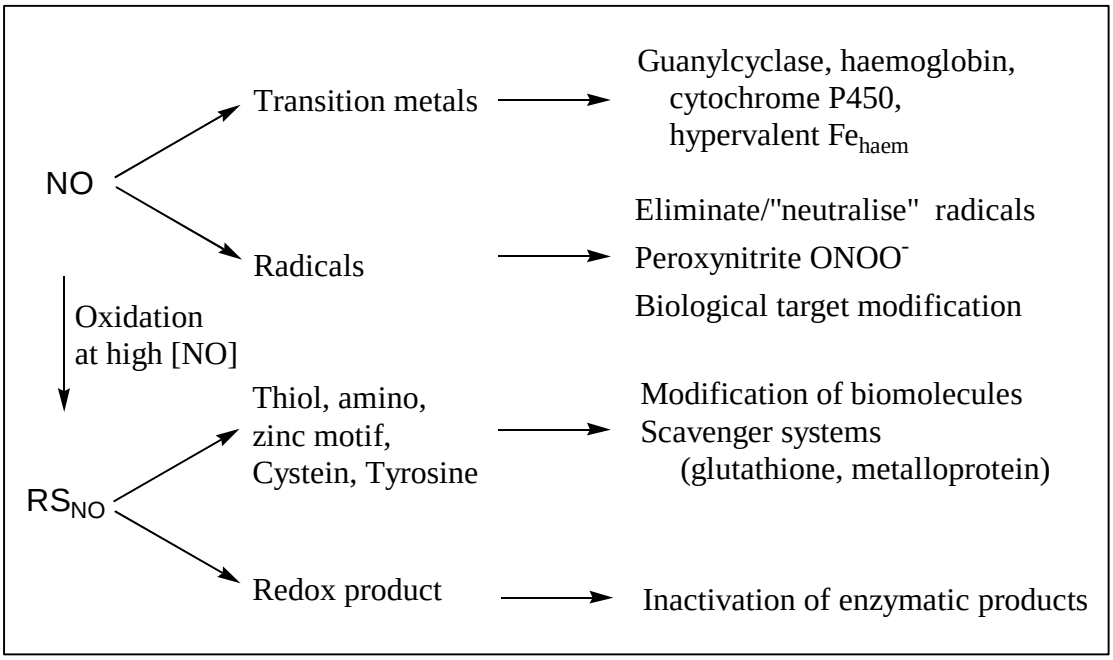

Scheme 2. Direct and indirect biological effects of NO.

The RS_{NO} formation is dependent on [NO] and [O_2]. Since [O_2] is high in physiological systems, NO becomes the limiting reagent. The kinetics of RS_{NO} formation has a second order dependency on [NO][10,11]. At low [NO], the $t_{½}$ of NO is long. Thus NO remains intact for a longer duration and responsible for the biological effects at low [NO]. In contrary, at high [NO], the $t_{½}$ of NO is short. NO is rapidly oxidised into RS_{NO}, which is responsible for the biological effects observed at high [NO]. As a result, the second order [NO] dependency separates the direct and indirect biological effects of NO. The direct biological effects of NO are attributed to NO itself while the indirect biological effects of NO are attributed to the oxidative products of NO (mainly the RS_{NO}) (**Scheme 2**).

The direct biological effects of NO are resulted from the reactions of NO with metals and other radicals. NO has an affinity to react with some transition metals such as Fe^{2+} and Fe^{3+} to give metal-NO^{+} adducts[9,12]. Hence, NO interacts with various metalloproteins such as guanyl cyclase[13], cytochrome P450 enzymes[14], haemoglobin[15], and myoglobin[15]. The interaction between NO and guanyl cyclase is the basis for physiological effects of NO. The guanyl cyclase is stimulated by NO and produces the second messenger cGMP, which initiates a cascade of downstream signalling events. Besides that, through the interruption of the Fe-O_2 complex formation and the subsequent oxidative reactions, NO reversibly inhibits the cytochrome P450 enzymes. NO also reacts with oxyhaemoglobin and oxymyoglobin to give methaemoglobin and metmyoglobin respectively, with the generation of nitrate. Hence, the haemoglobin and the intact red blood cells are NO scavengers that prevent NO related oxidative damages. Furthermore, the affinity of NO towards high valent Fe(IV/V)[16], an intermediary product of peroxide-induced toxicity, also helps to minimise peroxide related injuries.

NO reacts with various radicals, such as nitrogen dioxide[9], hydroxyl radical[17], peroxide radical, superoxide (O_2^-) radical, alkyl radical, alkoxy radical, and alkylperoxide radicals[18], thus consuming and inactivating the radicals. Physiologically the most important reaction is the formation of peroxynitrite ($OONO^-$) from NO and O_2^-. The formation of $OONO^-$, which is 5 times faster than superoxide dismutase (SOD)[9], can be both detoxifying[19] and potentially deleterious[20]. Under basic pH, the $OONO^-$ is relatively inert and slowly dismutates into nitrite and oxygen[21], thus serves to inactivate O_2^-. Under acidic pH, $OONO^-$ is protonated as peroxynitrous acid (HOONO), which either self-isomerises into nitrate or oxidises

various biological substrates. Since HOONO is a weaker oxidant as compared to O_2^-, less overall oxidative damage is resulted as compared to O_2^- [9,22].

Other than being an oxidant, HOONO also exhibits destructive roles through reaction with sulfhydryl (–SH) to give disulfide[23], and in the presence of metal ions, nitriation of tyrosine[24]. As a result, the structures, and thus the activities, of the proteins are modified. Nevertheless, the formation (which is in competition with high level of SOD) and oxidising effect of $OONO^-$ (which is scavenged by SOD and GSH) are tightly regulated, and thus the toxicity due to $OONO^-$ is rather limited.

The indirect effect of NO is mainly attributed to RS_{NO}[9]. In aqueous system, the primary RS_{NO} is NO_X, which is postulated to have the empirical formula of N_2O_3[25]. In physiological system, NO_X is rapidly hydrolysed to nitrite[9]. The aqueous hydrolysis of NO_X is in competition with the nitrosation and oxidation reactions, in which NO_X nitrosates, and thus modifies the functions of, amine- and thiol-containing biomolecules, as well as oxidizes redox-active complexes[9,10,26]. RS_{NO} covalently modifies the thiol moieties or zinc motifs of various enzymes, such as ribonucleotide reductase[27], protein kinase C[28], glyceraldehydes-3-phophate dehydrogenase[29], DNA alkyltransferase[30], and Fpq protein[31], and thus inhibiting the enzymes. In addition, NO_X reacts with thiol groups in glutathione, which is an important NO scavenger, to give S-nitrosothiol adducts[26]. The thiol-rich metallothionein also provides scavenging protection against NO_X toxicity[32]. On the other hand, instead of acting directly on enzyme, the NO_X is shown to oxidise the redox-active enzymatic products. For example, although the xanthine oxidase activity is not affected by NO_X, the enzymatic effect is limited as the O_2^- that is produced is rapidly intercepted by NO_X[9,19,33,34].

The interplay between direct and indirect effects of NO is [NO] dependence[9]. Since the [NO] changes as the NO diffuses away from the NO producing source, the

observed NO effects are varied[35]. Generally at low [NO] on a cellular scale, the diffusion diameter is 150 – 300 μm and a rather wide area of cells (typical cell radius is 4 – 15 μm) is regulated to varying degree[35]. In cases of high local [NO] production, the destructive damage is rather localised at the high [NO] producing source, and normal regulatory effects of NO are observed at the peripheral low [NO] regions as the NO diffuses away[35].

As a result, the overall *in vivo* effect of NO is regulated by the reactivity, selectivity and diffusibility of NO[35]. NO is produced *in vivo* under both constitutive and inducible mode[9,36]. In constitutive mode, NO is produced in concentration of picomolar range, at which regulatory direct biological NO effects are involved. On the other hand, micromolar range of [NO] is produced under inducible mode, and the high [NO] is associated with mainly destructive indirect NO biological effects.

***In vivo* NO Production: Nitric Oxide Synthase (NOS)**

NO is produced in human body by a family of enzymes known as nitric oxide synthase (NOS; EC1.14.13.39). NOS oxidises L-arginine (L-Arg) into NO and L-citrulline (L-Cit). There are three isoforms of NOS, the neuronal NOS (nNOS), inducible NOS (iNOS) and endothelial NOS (eNOS), each with different structures, expression modes, regulations, localisations and functions.

When NOS is represented as a single peptidic chain, it has a reductase domain on its C-terminus and an oxygenase domain on its N-terminus (**Figure 1**). The reductase domain bears more than 50% sequence similarity with NADPH-cytochrome P450 reductases from different species[36]. The electrons produced through NADPH oxidation are transferred through flavin adenine dinucleotide (FAD) to flavin mononucleotide (FMN), and subsequently into the oxygenase domain. The oxygenase domain consists of binding sites for L-Arg, (6R)-5,6,7,8-tetrahydro-L-

biopterin (BH_4), and iron protoporphyrin IX (haem)[37,38,39]. The haem is the catalytic site for oxidising the substrate L-Arg, and it shows a reduced CO (carbon monoxide) difference spectrum characteristic of cytochrome P450 enzymes[40,41,42]. In the absence of L-Arg and BH_4, the Fe_{haem} exists predominantly in six-coordinated low spin inactive form (λ_{max} at 420 nm), but it is activated to the five-coordinated high spin form (λ_{max} at 450 nm) in the presence of L-Arg and BH_4. The role of BH_4 has been controversial[36]. It has been suggested to act as allosteric modulator[43], high-spin state promoter[41], protein stabilizer[44] and activity enhancer[45]. Interconnecting the reductase and oxygenase domains is the calmodulin (CaM) binding domain[36]. The enzyme is inactive without CaM, the binding of which is essential for intra-reductase and reductase-oxygenase electron transfers, and thus the initiation of the enzyme catalytic machinery[46,47,48].

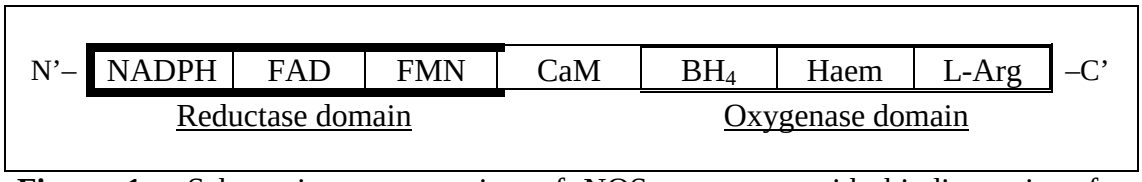

Figure 1. Schematic representation of NOS structures with bindings sites for substrates and cofactors.

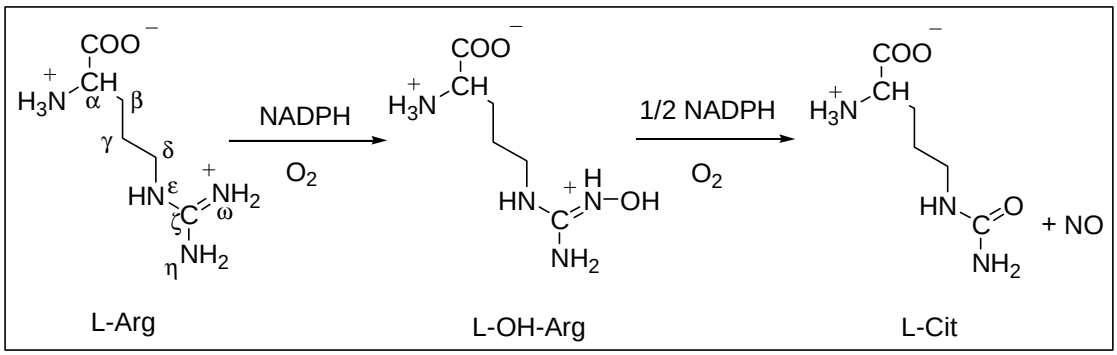

Scheme 3. Two-monooxygenations enzymatic synthesis of NO.

Despite having a self-sufficient redox system on single monomer, NOS is active only in the homodimeric form. The dimerisation enables proper orientation of

the functional domains, thus allowing efficient inter-domain electron transfer[49,50]. As a catalytically active NOS dimer, an electron is transferred from the reductase domain of one monomer into the oxygenase domain of the other monomer. It was found that both haem and BH_4 are essential for the formation and stabilization of the dimeric conformation[44,51,52].

The catalytically active NOS produces NO *via* oxidation of L-Arg, with stoichiometric production of L-Cit[36] (**Scheme 3**). The NO is synthesised through two constitutive steps. The first step is the monooxygenation of L-Arg, which results in the hydroxylation of the N^{ω} of the guanidino moiety[53]. In order to oxidise 1 mole of L-Arg, 1 mole of NADPH (provides 2 moles of electrons) and 1 mole of O_2 are required. This is a classical cytochrome P450 mixed-function hydroxylation. Initially, an electron derived from NADPH reduces the Fe_{haem}, which is subsequently bound to O_2. After that, a second NADPH-derived electron reduces the bound O_2 to give Fe_{haem}-$O_{2(reduced)}$. Subsequently a proton is abstracted from the L-Arg guanidino moiety to give prooxo-Fe_{haem} complex, which loses a water molecule to generate hypervalent oxo-Fe radical. This hypervalent oxo-Fe radical is responsible for the radical-based hydroxylation of the guanidino moiety of L-Arg, giving rise to the product N^{ω}-hydroxyl-L-Arg (L-NHA)[54].

With the L-NHA tightly bound at the NOS active site, the second monooxygenation reaction occurs. The reaction requires 0.5 mole of NADPH (provides 1 moles of electrons) and 1 mole of O_2 for every 1 mole of L-NHA, and generates equimolar of L-Cit and NO as final products[54]. This single NADPH-derived electron monooxygenation step is unique and different from other reported monooxygenases. The reaction is initiated by the reduction of Fe_{haem} by an NADPH-derived electron. Another reducing electron is derived from the L-NHA[55], and results

in Fe_{haem}- $O_{2(reduced)}$ complex. By abstracting a proton from L-NHA, peroxo-Fe complex is generated. Subsequently the peroxo-Fe complex attacks the N-OH-Arg radical to give L-Cit and NO.

Isoforms of Nitric Oxide Synthase

Three distinct NOS isoforms are identified in mammals[42] (**Table 1**). These isoforms are named according to the cell types or conditions in which they were first discovered, namely the neuronal NOS (nNOS, Type I), inducible or inflammatory NOS (iNOS, Type II) and endothelial NOS (eNOS, Type III). All the isoforms contain the basic structural domains as described above. The smallest among the three isoforms is iNOS (125 kDa monomeric molecular mass). On the other hand, the largest among all the isoforms is nNOS (155 kDa monomeric molecular mass). The extra mass in nNOS is attributed to an additional 250 amino acids sequence at the N-terminal which contains a postsynaptic density zipper (PDZ) motif that is responsible for the subcellular targeting of nNOS[56]. The eNOS (monomeric molecular weight of 133 kDa) is acylated at the N-terminal. Post-translational acylation such as myristoylation and palmitoylation are required for stabilising the association of eNOS to cell membrane and targeting eNOS to caveolae[57].

	nNOS	iNOS	eNOS
Monomer size	155 kDa	125 kDa	133 kDa
Major location	Neural system	Immune system	Endothelium
Expression	Constitutive	Inducible	Constitutive
Ca^{2+} dependency	Dependent	Independent	Dependent

Table 1. A brief comparison of the three isoforms of NOS.

The NOS isoforms vary in their localisation[36,58]. Each NOS isoform is distributed in wider ranges of tissues and cells than being suggested by the name alone. While found mainly on the neurons of both central and peripheral nervous systems, nNOS is also highly expressed in skeletal muscles, and also found in cardiac muscle and kidneys. The iNOS is mainly distributed in the macrophages and other cells of immune system, and is also isolated in hepatocytes, chondrocytes, myocytes, asterocytes, endothelium and unstriped muscles. The eNOS is mainly found in endothelium, as well as the heart and the brain.

Each NOS isoform is highly conversed when compared across different mammalian species. The amino acid sequences of nNOS and eNOS show more than 90 % homology across the mammalian species, while the iNOS shows more than 80 % homology. For example, the rat nNOS shares 94% and 98% sequence homology with human nNOS and murine nNOS respectively[59]. Hence, the high inter-species homology of NOS isoforms enable the extrapolation the experimental results from one species to the other. However, the inter-isoform sequence homology is less within the same species. In human, the three NOS isoforms share less than 59% homology in the amino acid sequences[60].

The three NOS isoforms are expressed from distinct DNA sequences, and the modes of protein expression are varied among the isoforms[61]. Both nNOS and eNOS are constitutively expressed in human body, and collectively they are known as constitutive NOS (cNOS). The nNOS expression may be varied to give differently spliced enzymes[60], while the activity of eNOS may be modified post-translationally[60]. On the other hand, iNOS is usually unexpressed in healthy cells, but is rapidly expressed upon a variety of inflammatory and immunological stimuli, such as lipopolysaccharides (endotoxins), cytokines and glucocorticoids[62]. Interestingly,

some variants of iNOS are constitutively expressed in intestines[63], while the expression of nNOS and eNOS are induced by elevated oestrogen level and shear stress in vascular endothelium respectively[64,65].

The enzymatic activity of the three NOS isoforms is regulated by different mechanisms[36]. The constitutive NOS (nNOS and eNOS) is regulated by intracellular free Ca^{2+} concentration ($[Ca^{2+}]_{i,f}$). In contrast, the activity of iNOS is independent on $[Ca^{2+}]_{i,f}$ and is instead determined by protein expression. An autoinhibitory domain, that is present in the FMN binding domain of constitutive NOS but absent in iNOS, prevents the binding of CaM to constitutive NOS at physiological $[Ca^{2+}]_{i,f}$ (~80 nM)[66]. At elevated $[Ca^{2+}]_{i,f}$, the autoinhibitory domain is displaced by CaM and thus the constitutive NOS is activated. The constitutive NOS remains catalytically active until the $[Ca^{2+}]_{i,f}$ returns to resting level, at which the CaM dissociates from constitutive NOS. During this brief period of elevated $[Ca^{2+}]_{i,f}$, NO is produced in picomolar concentration[36]. On the other hand, CaM is tightly bound to iNOS[67]. Hence, once iNOS is expressed and dimerised, it is able to generate NO in micromolar range for a prolonged period of time[36]. Other than Ca^{2+}/CaM regulation, the activity of NOS is affected by protein-protein interactions and post-translational modifications[60]. The nNOS is inhibited by PIN (protein inhibitor of nNOS)[68], while the eNOS activity is increased with phosphorylation of Ser1179 [69] and is reduced by association with membrane protein caveolin-1[70].

Physiological Roles of NO and Pathology of NO Overproduction

NO performs diverse and important physiological roles in the human body. The diverse physiological roles of NO have been elucidated mainly through the use of NOS inhibitors (nonselective and selective) and NOS knockout animals[58]. An appreciation of the physiological roles of NO is important for the understanding of the

possible consequences in modulating NOS activity. It is generally accepted that long-term inhibition of eNOS (except under special circumstances such as septic shock) is unfavourable[58]. On the other hand, the inhibition of both nNOS and iNOS can be potentially beneficial and harmful[58].

In the nervous system, nNOS plays an important physiological role in producing NO as a neurotransmitter. In the peripheral nervous system, NO induces the relaxation of vascular and non-vascular smooth muscle[71], leading to the relaxation of intestinal sphincters, corpus cavernosum, urinary bladders, urethra, and bronchi[58]. In the central nervous system, nNOS is widely expressed but the role of the produced NO is not precisely identified[58]. Due to the abundance of nNOS in the cerebellum, nNOS knockout and inhibition lead to abnormality in balancing and coordination, especially in dark environment when visual cues are reduced[72]. The nNOS knockout mice also show an increase in inappropriate mounting and aggressive behaviours, thus suggesting the role of NO in behavioural inhibition[72]. Studies using NOS inhibitors suggest the involvement of nNOS-derived NO in long-term memory potentiation, but this is not apparent in NOS knockout animals[71]. The nNOS-derived NO is also implicated in pain-perception, neuronal plasticity and fertility[56,73].

Highly expressed in skeletal muscle[74], the nNOS is associated with dystrophin in fast-twitch fibres and the produced NO prevents muscular dystrophy[75]. The nNOS-derived NO also regulates myotube development, innervation and contractility of skeletal muscles, as well as the muscular arteriolar tone and exercise-induced glucose uptake in the muscles[56]. The nNOS is also expressed in renal tissue, and the produced NO plays a role in regulating rennin-angiotensin system[76]. Besides that, nNOS-derived NO is also shown to exert positive inotropic response in the heart[77] and prevent ovalbumin-induced airway hyperreponsiveness[78].

On the other hand, the iNOS-derived NO plays important cytotoxic and cytostatic roles for host defence against invading pathogens (such as protozoa, bacteria, fungi and viruses) and tumour cells[79,80]. The iNOS-derived NO also regulates the cytokine production and T-helper (Type I) cell expansion[81]. On the other hand, some evidence from iNOS knockout studies indicated the involvement of iNOS in normal physiological processes, such as oesteoclastic bone resorption[82], ischaemic preconditioning of heart[83], wound healing (angiogenesis and collagen synthesis)[84], and resolution of certain inflammations[62].

Through smooth muscle relaxation, the eNOS-derived NO plays a very critical role in maintaining the basal vasculature tone, and thus the basal blood pressure[85]. This forms the basis of the life-saving effect of nitroglycerin[1]. Besides that, the NO produced is also involved in the regulation of platelet aggregation, white blood cells adhesion, vascular-endothelial growth factor expression and angiogenesis[58]. The eNOS-derived NO is found to exert negative inotropic response in the heart[77], and involved in long-term potentiation of memory[86].

Inhibition of eNOS has been shown to be beneficial in cases such as hyperoxia-induced retinopathy and septic shock[87]. However, most data suggested that prolonged eNOS inhibition is harmful in view of its important cardioprotective roles[36,58]. On the other hand, over-expression of iNOS has been observed in chronic inflammations. Improper induction of iNOS as a result of chronic inflammation leads to the high production of NO, which, on top of eradicating pathogens, damages the host cells as observed in various autoimmune diseases, such as diabetes and rheumatoid arthritis[36]. Induction of iNOS has been observed in septic shock[88], asthma[89], pain[90,91], and others inflammatory diseases[58].

In pathological condition with elevated $[Ca^{2+}]_{i,f}$, nNOS is constantly activated, leading to NO overproduction and neurotoxicity. Various neurodegenerative conditions such as Parkinsonism, Alzheimer's disease, Huntington's disease, and brain ischaemias are implicated with nNOS-derived NO overproduction[36,56,92-96]. The neurotoxicity of NO has been attributed to DNA damage[59,97]. Following DNA damage, repair mechanism involving PARS (Poly (ADP ribose) synthetase), which consumes a lot of ATPs, is activated. Continual activation of PARS, an abundant enzyme in the cell, leads to energy depletion and cell death. Furthermore, O_2^- is produced through NADPH oxidation in the reductase domain of nNOS in conditions of high consumption and low supply of L-Arg and/or BH_4[58,60]. Either by itself or through $OONO^-$, O_2^- leads to cellular damages and aggravates the acute ischaemic injuries.

As a result, NOS represents a viable biological target in terms of drug design, in view of the ubiquitous presence and important roles of NO in virtually every part of human body, as well as the devastating effects of NO overproduction. The selective inhibition of either nNOS or iNOS is highly desirable. For the current study, it is of interest to search for selective nNOS inhibitors.

Inhibition of Nitric Oxide Synthase

Literature reviews often reveal contradictory views on the beneficial or harmful roles of NO[58]. The dual effects of NO are resulted from the conflicting roles of different NOS isoforms, the rate of NO synthesis and the cellular redox state. Furthermore, the diverse roles of NO in virtually every part of the body implied that attempts to control NO production on one site might turn out to be harmful to other sites. Thus, any attempt to regulate NO should be carefully planned.

Several pharmacological interventions in the production and downstream effects of NO have been suggested[98], which include interferences on enzyme expression; interferences on enzyme dimerisation and protein-protein interactions; interferences on availability and accessibility of L-Arg; interferences on availability and accessibility of co-factors (Ca^{2+}, CaM, BH_4); interferences on haem, NADPH, FAD and FMN; and inactivation of NO produced.

Among the available approaches, the most commonly applied and extensively studied approach is the use of NOS inhibitors[98], which prevent the binding of the L-Arg to the NOS active site. A lot of studies have been carried out on NOS inhibition. However, the complex roles of NO complicate the use of NOS inhibitors. The isoform selectivity is an important consideration for minimising the disruptions on physiological functioning of NO, especially the regulatory role of eNOS-derived NO on basal pressure. However, it is often difficult to achieve isoform selectivity with appropriate degree of inhibition, not mentioning selected targeting of tissues and cells[58,98]. Furthermore, it is important to have inhibitors showing minimum side effects on non-NOS targets[58].

A review on NOS inhibitors and their selectivity will be presented (**Chapter 2**). Prior to that, it is necessary to understand the active site and its environment. The X-ray Crystallography and molecular probing studies provided useful information regarding the active site of NOS.

X-Ray Crystallographic Structure of NOS

The first x-ray crystallography of NOS was published by Crane *et. al.* in 1997[99]. However, this was a report on the inactive monomeric iNOS. The dimeric X-ray crystallographic structure of murine iNOS was reported in the following year, setting the foundation for understanding the protein structure and the active site[100]. In

the same year, bovine eNOS haem domain structure was also reported, and a novel zinc tetrathiolate motif was identified[101]. Subsequently in 1999, Fischmann *et. al.* reported the X-ray crystallography of the more clinically relevant human iNOS and eNOS[102]. It was shown that the active sites of human iNOS and eNOS are highly conserved. Similar conclusion was obtained by Li *et. al.* by comparing the structure of human iNOS to bovine eNOS[103,104].

At the initiation of the current research in year 2000, the X-ray crystallographies of iNOS and eNOS were available. However, no report on nNOS X-ray crystallographic structure was available until the mid of 2002[105]. The year 2000 seemed to be a turning point for NOS X-ray crystallography research. Prior to the year 2000, more effort were put in understanding the native structure of NOS and the L-Arg binding in the active site. However, after the year 2000, the focus was shifted to the understanding of the inhibitor binding, elucidation of metabolic pathways and exploration of structural variation for isoform selectivity.

The monomeric NOS oxygenase resembles a "left-handed baseball catcher's mitt", with a shallow (~10 Å depth) haem pocket[100]. Upon dimerisation (**Figure 2**), the mobile and exposed hydrophobic region refolds and becomes part of the substrate-access channel and substrate-binding site, and at the same time sequesters two molecules of BH_4 at the centre of the dimer interface[100]. Incomplete complementarities at the dimer interface result in two water-filled cavities, one of which was located near to the cavity opening and adjacent to BH_4[102].

Protein dimerisation produces a deep (~ 30 Å) substrate access channel towards the active site[100]. The substrate access channel has the shape of a funnel, with the larger opening being the channel opening (~ 10×15 Å^2 in cross section), which is large enough for the diffusion of both L-Arg and L-Cit[102]. The narrow end

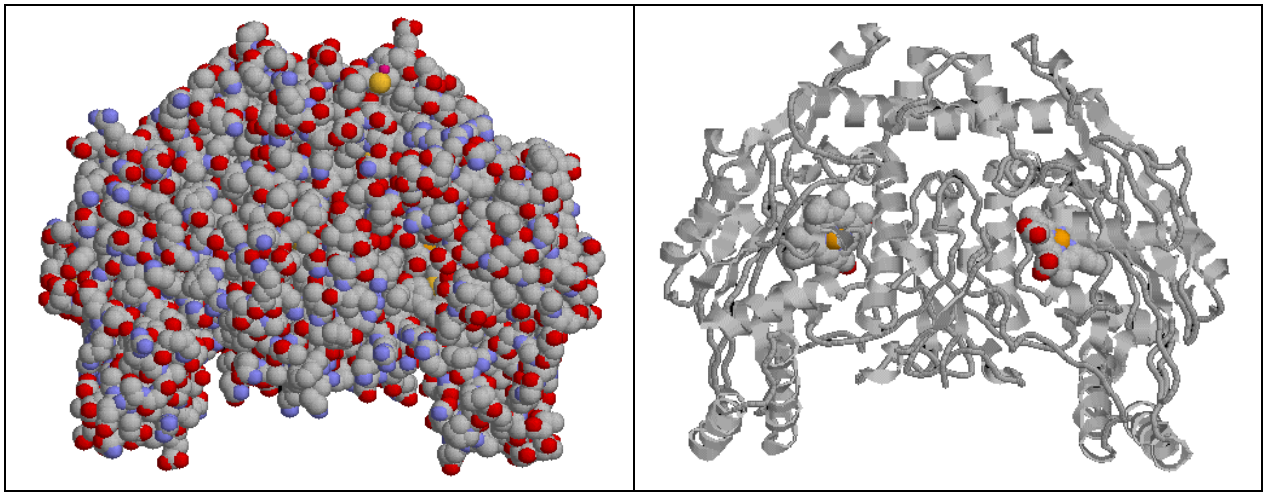

Figure 2. *Left*: Active dimer of NOS (Brookhaven code: 2NSE) consists of two monomers interfacing at the centre. The active site opening is located on near to the dimer interface, and the catalytic haem moiety is visible (the right monomer). *Right*: Cartoon view of the NOS dimer with the haem (in CPK view) located at the centre of each monomer.

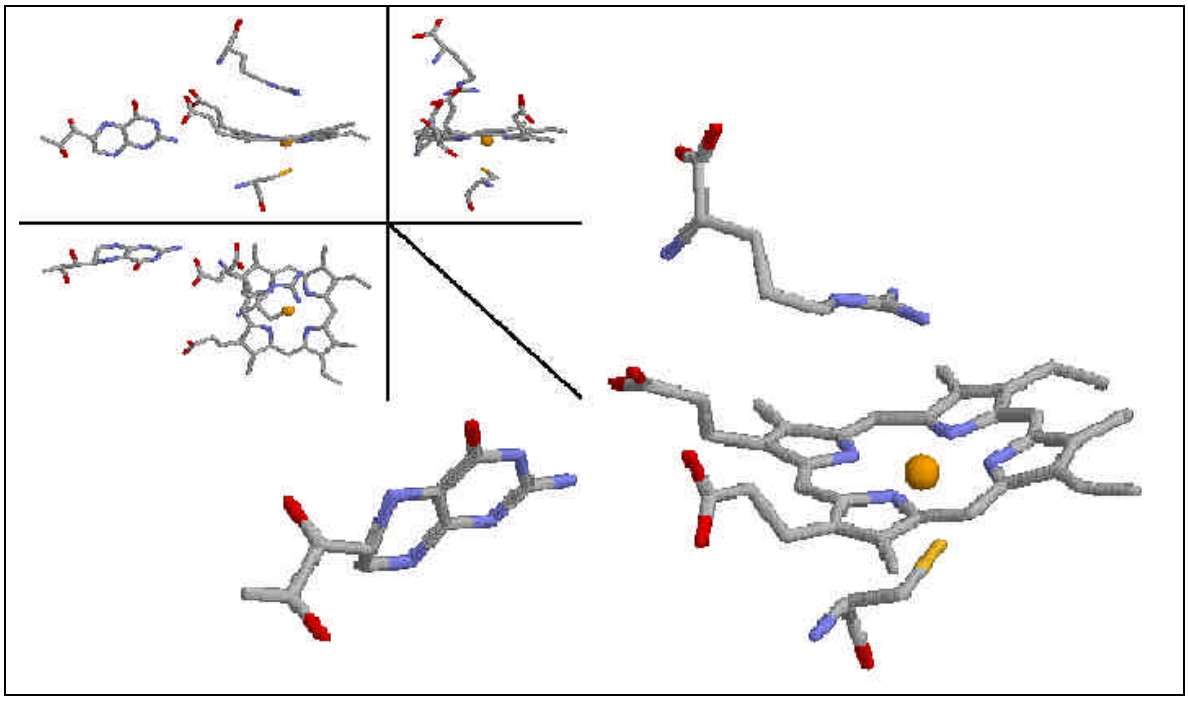

Figure 3. Various views of haem, L-Arg and BH_4 in NOS (Brookhaven code: 2NSE). The Fe_{haem} is coordinated by the pyrrole nitrogens of haem, a cysteine residue, and the guanidino N^{ω} of the L-Arg. The haem is slightly concave. The BH_4 is roughly perpendicular to the haem, which comprises of four pyrrole rings (ring A, B, C and D), with the ring A located nearest to the BH_4. Both ring A and ring D have propionate side chains.

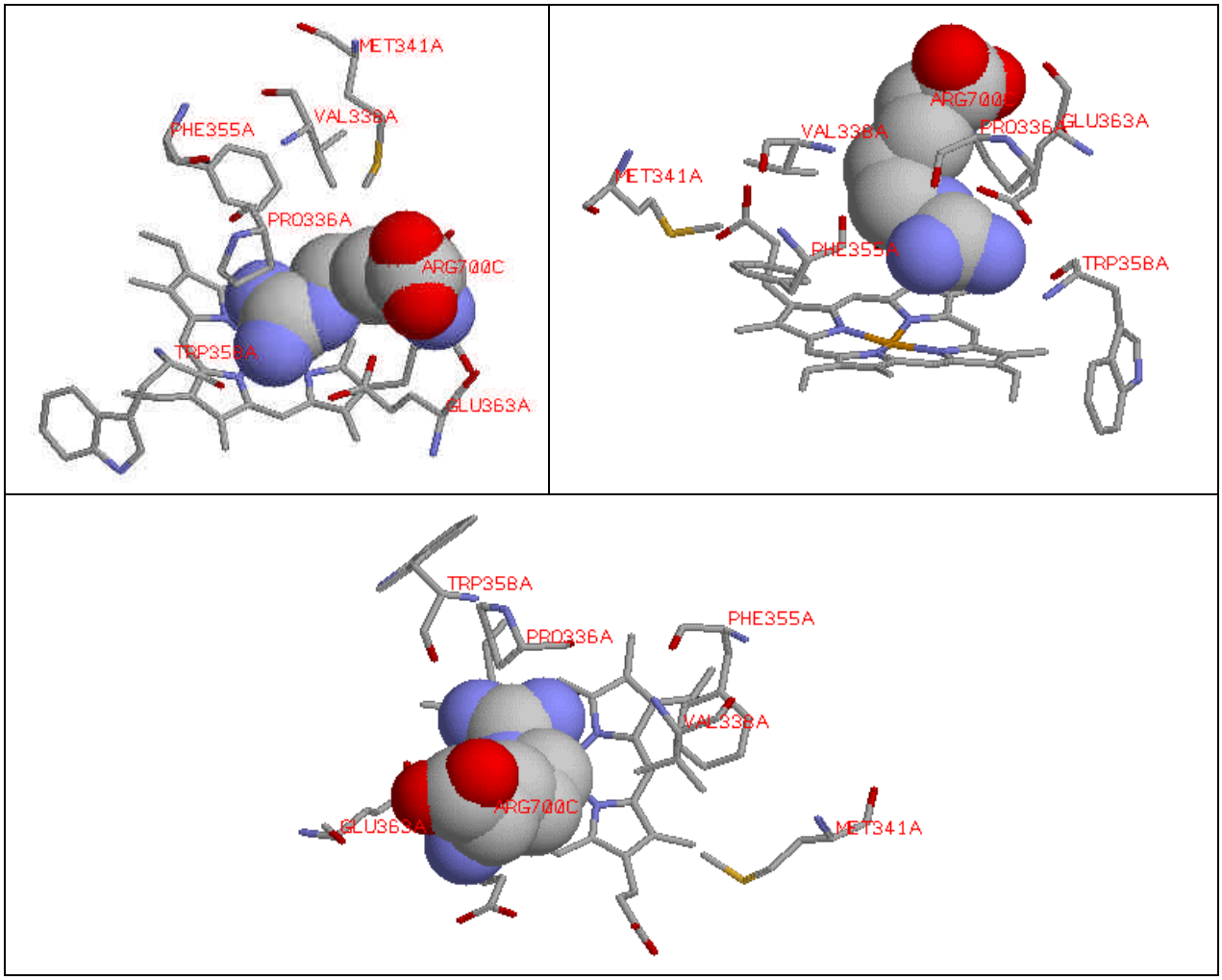

Figure 4. Binding environment around the guanidino group of L-Arg in NOS active site (Brookhaven code: 2NSE). *Upper left*: The N^{φ} of guanidino group of L-Arg is hydrogen bonded to both Trp and Glu. The Glu is involved in bidendate interaction with both N_{φ} and N_{ε} of guanidino group. *Upper right*: The residues Pro, Phe and Val form a hydrophobic cavity above pyrrole ring C of haem. The N_{η} of guanidino group of L-Arg is pointed towards the Fe_{haem}. *Lower*: The alkyl chain of L-Arg is in slight non-bonded contact with Val residue.

of this channel is a small opening on the opposite surface of the enzyme, which only allows one molecule of water to pass through[102]. The catalytic site (haem) is located at the centre of the funnel shaped substrate access channel[102].

The oxygenase domain has an elongated shape with three structural sub-domains[102]. The first sub-domain is a crescent shaped substrate-binding sub-domain, and the haem group is located between the closing tips of the crescent. The second sub-domain is the ellipsoidal shaped BH_4-binding sub-domain, which caps the cavity

of the crescent shaped substrate-binding sub-domain. The third sub-domain consists of hydrophobic two-helix bundles that bear structural role, as compared to the enzymatic role of the other two sub-domains.

The haem (**Figure 3**), located opposite to the dimer interface, is buried in the protein interior through *van der Waals* (VDW) forces, with the one of the haem surface making most of the contact with protein (residue Trp, Met, Trp, Phe/Tyr)[102]. The pyrrole ring A and ring D of the haem possess propionate groups which are oriented towards the dimer interface, facing the substrate access channel, and forming several hydrogen bonds with water molecules inside the large catalytic cavity [r1504]. At the centre of the haem, the iron is penta-coordinated by the pyrrole nitrogens and cysteine thiol, thus providing a single axial coordination available for O_2 binding[102]. On the whole, the haem has a curved shape with the haem iron being significantly out of plane, and the protein-interacting surface being the protruding side[102].

The BH_4-binding sub-domain is located adjacent to the dimerisation interface, and is found at the side of the access channel and away from the bulk solvent[102]. The BH_4 is sequestered into protein interior though various hydrophobic, aromatic π-π stacking, and hydrogen bonding interactions[100]. This BH_4-binding sub-domain is positioned proximal and perpendicular to the haem, and the BH_4 is hydrogen bonded with the propionate of pyrrole ring A of haem[100].

The L-Arg binds to the active site in an extended conformation with the side chain terminal fitting tightly into the narrow corner of the active site cavity[102] (**Figure 4**). The guanidino group is found to be coplanar to the haem, forming π-π stacking interaction with pyrrole ring A of haem, and the $N_\varepsilon H$ and $N_\eta H_2$ of the guanidino moiety are involved in a bidendate interaction with the Trp and Glu residues[100,102]. A closer examination on the charged guanidino group shows that terminal amino ($N_\eta H_2$)

and imino ($N_\omega H_2^+$) groups, despite being chemically equivalent under physiological pH, are located in distinctly different environments[106]. The distal, non-hydroxylated NH_2 is positioned in a narrow cavity, and the two hydrogens are respectively hydrogen bonded to the backbone carbonyl oxygen of Trp and one of the side chain carbonyl oxygen of Glu[102]. On the other hand, the proximal NH_2 is oriented towards the Fe_{haem}, and ready to be hydroxylated. The binding cavity for the proximal guanidino NH_2 is larger than that of the distal guanidino NH_2[102-104]. In addition, a hydrophobic cavity is identified above pyrrole ring C of haem[104]. The hydrophobic cavity forms a rather rigid roof over the active site. Inside the hydrophobic cavity, the side chains of Pro, Val and Phe are orientated inward to the active site[104].

The alkyl moiety ($-C_\beta H_2-C_\gamma H_2-C_\delta H_2-$) between the guanidino group and the C_α is found to be involved in slight non-bonded contact with the hydrophobic Val residue[102]. The α-NH_2 group of L-Arg is found to be hydrogen bonded to the propionate of the pyrrole ring A of haem. On the other hand, the α-COOH group of L-Arg is found to be hydrogen bonded to various residues, namely Arg, Gln, Tyr and Asp/Asn (an Asp is found in iNOS but an Asn is found in both eNOS and nNOS)[100,102]. The Asn residue in eNOS or nNOS is not a hydrogen bond acceptor and does not interact with the adjacent protein Arg residue as the alternative Asp residue in iNOS does. This is the only protein structural difference that comes in contact with L-Arg[103]. Acting together, the α-amino and α-acid binding pockets are specific for the L-α-amino acids. On the other hand, the propionate of the pyrrole ring A of haem is hydrogen bonded to N_2H and N_3 of BH_4 as well as water-bridged to O_4 of BH_4[100]. The protein Arg residue adjacent to the Asn/Asp residue is also hydrogen bonded with BH_4. As a result, an extensive network of hydrogen bonding between dimerisation elements, the haem propionates and the BH_4 is formed upon L-Arg binding, and this

explains the cooperativity observed among the events such as BH_4 binding, L-Arg binding, and enzyme dimerisation[103].

At the initiation of this work at year 2000, the X-ray crystallographic data suggested that the active site of the iNOS and eNOS are highly conserved[102,103]. While the X-ray crystallographic data of nNOS was not available, there were reports citing unpublished data claiming the nNOS active site to be highly similar to that of iNOS and eNOS. Subsequent publication of nNOS X-ray crystallography by end of 2002 finally justified the claim[105]. The report by Li *et. al*. in 2002 is the first report on nNOS X-ray crystallography. The binding of L-NHA in nNOS is identical to the binding in human eNOS and murine iNOS, thus supporting the common claims on the conservation of active sites among the three NOS isoforms. As a result, the design of isoform specific inhibitors is suggested to be a great challenge. However, the availability of existing isoform selective NOS inhibitors suggests that isoform selectivity can be achieved despite conserved active site.

Several strategies to achieve selectivity have been proposed. The variation in protein residue (Asn/Asp) of α-COOH binding pocket can be exploited for selective inhibition[103]. On the other hand, some of the amino acid side chains that do not make direct contact with the substrate but line the periphery of the active site are also different, thus can be used to achieve isoform selectivity[102,103]. Another suggested approach is to design inhibitor that extends out of the L-Arg binding site into the substrate access channel where more variation in protein residues exists[102].

Molecular Probing on NOS Active Site

The main limitation of X-ray crystallography is the loss of information on protein dynamics when the protein is crystallized[107]. The theory of induced-fitting enjoys popular acceptance over the traditional theory of rigid lock-and-key for

explaining the interaction between a drug and its biological target[108]. The induced-fit of a drug molecule to a target is widely observed[107,108]. However, X-ray crystallography is ineffective for studying the induced-fit of a ligand to a protein. In addition, the structure observed in a crystal lattice might be different from the native state of a protein. As a result, the X-ray crystallographic data is to be interpreted with caution.

Protein NMR study is useful in providing complementary information on the native protein structures in solution, and the protein dynamics[109]. However, no NMR study on NOS is reported to date because the molecular weight of the dimeric NOS is too large for NMR protein study. As a result, in order to understand the native structure of the NOS the active site, and dynamic interactions in involved, molecular probing study emerges as a useful tool.

Using resonance Raman spectroscopy of Fe_{haem} coordinated with carbon monoxide, it has been shown that the structures of guanidino binding sites are different among the NOS isoforms[110]. The guanidino binding site is more open in the direction of the haem iron, than that of iNOS and eNOS. This inference is consistent with the observed nNOS selective inhibition demonstrated by L-N^{ω}-propylarginine (L-NPA)[111]. Besides that, as suggested by the study on rate of phenyl-iron complex formation, the size of the ceiling forming the haem active site is also different[112]. The ceiling is found to be larger in nNOS, followed by iNOS and smallest in eNOS.

The molecular probing study on the guanidino binding site conducted by Babu *et. al.*[106] further suggested that the distal non-hydroxylated NH_2 binding pocket is small and less hydrophobic. It cannot even accommodate methyl substitution on the distal guanidino NH_2 group. In addition, replacement of distal guanidino NH_2 with methyl resulted in weaker binding. As a result, it is proposed that the distal guanidino

binding pocket has highest affinity for $–NH_2$ and $=NH_2^+$, moderate affinity for =S, substantially less affinity for =O, and very little affinity for $–CH_3$. On the other hand, the proximal N (near haem) is relatively larger in size, and shows highest affinity for =S (and –S-alkyl), moderate affinity for alkyl, -NH-R, $-NH_2/=NH_2^+$ (approximate order), and very little affinity for =O.

The Glu residue, the only charged residue that points into the guanidino binding site[100], is involved in four hydrogen bonding interactions, namely two hydrogen bondings with the L-Arg guanidino group, one hydrogen bonding with the α-NH_2, and another hydrogen bonding with the backbone amide NH of Met residue. However, thermodynamic calculation shows that the hydrogen bonding of the distal non-hydroxylated NH_2 with Glu residue is rather weak (< 2 kcal/mol), much weaker than the expected normal value of a hydrogen bond (3-6 kcal/mol)[106]. This relative weakness reflects either unfavourable hydrogen bond length, or very favourable interaction of Glu residue with water molecules which are lost upon inhibitor binding. Hence, the importance of bidendate interaction with Glu residue is less than expected. The hydrogen bonding network with Glu alone is insufficient for ensuring the binding of inhibitors. Indeed, unsubstituted thiourea is found to be inactive as NOS inhibitor despite capable of forming the hydrogen bonding network with Glu residue.

Binding sites around the active site of NOS

The active site of NOS is the enzymatic site that binds to and oxidises the guanidino moiety of L-Arg. Based on the understanding of the interaction of L-Arg with the active site through the molecular probing and the X-ray crystallographic studies, several binding sites are identified in the NOS active sites (**Figure 5**).

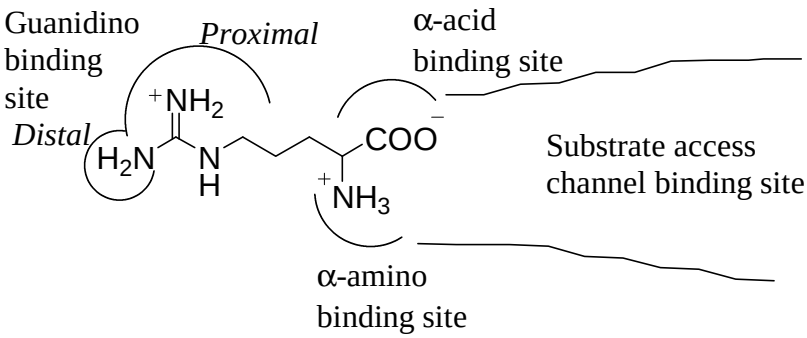

Figure 5. The active site of NOS bound with L-Arg, showing potential binding sites for inhibitor interaction.

The guanidino binding site (GBS) is the catalytic site generating NO from L-Arg. The GBS can be subdivided into proximal GBS and distal GBS. In the proximal GBS, the Fe_{haem} binds to one of the terminal guanidino NH_2 of L-Arg, and oxidises the NH_2 to give NO. The binding cavity of proximal GBS is able to accommodate moderately sized groups, such as propyl and allyl, in a hydrophobic pocket identified above the haem. The size and ligand-compatibility of proximal GBS vary among the NOS isoforms, thus enabling some degree of isoform selectivity to be achieved[110]. On the other hand, the distal GBS accommodates the other non-oxidised terminal NH_2 of L-Arg. This cavity is small and cannot tolerate even methyl substitution on NH_2 group. Extensive hydrogen bonding network is found around the distal GBS, and a positively charge Glu residue was located in adjacent to the distal GBS. Hence distal GBS is suited for the binding of hydrogen-bond donating and polar groups.

The α-amino binding site (NBS) and α-acid binding site (CBS) are extensively exploited in the design of inhibitors. Extensive hydrogen bonding networks and electrostatic interactions are found around these binding sites. With both binding sites acting together, stereospecific preference towards L-amino acids is observed. Interaction with either one or both of the binding sites greatly enhances the binding affinity of an inhibitor, usually resulting in IC_{50} values in the low μM or nM range, provided the inhibitor fulfils other binding requirements. However, in terms of

isoform selectivity, both binding sites do not allow much differentiation of the isoforms. The only difference of protein residues that contact directly with the L-Arg is identified in CBS, in which Asp is found in iNOS and Asn is found in both nNOS and eNOS.

Further away from the Fe_{haem} is the substrate access channel binding site (SacBS). Several differences in protein residues are identified, thus providing promise for isoform selectivity[113]. However, more work is needed to further characterise the SacBS.

Not all the reported inhibitors binds to all the available binding sites mentioned above. Generally, the groups binding to GBS is essential, and this interaction determines the binding affinity of the inhibitors, as well as the selectivity of the inhibitors. Groups binding to NBS and CBS usually provide enhancement in inhibitor binding. The SacBS, though being relatively unexplored area, offers potential for isoform selective binding.

From literature reviews, it is found that the region adjacent to the GBS (RegG) is often neglected (**Figure 6**). The RegG is not regarded as a key binding site, and it is rarely discussed in literature. The only information about RegG is that the hydrophobic portions of inhibitors, such as the alkyl and phenyl groups, are often found in this region. The general tendency to ignore RegG might be attributed to a biased perception that only hydrophobic interaction, a weaker interaction than ionic and hydrogen bonding interactions, is involved in this region.

However, the importance of RegG should not be dismissed due to its strategic location. The RegG is located in immediate vicinity of GBS. It is an important bridging region between the GBS and NBS/CBS, not mentioning the SacBS. Hence,

in order for a compound to bind to the active site, inevitably it has to interact with RegG. The lack of compatibility with RegG will result in reduced binding affinity.

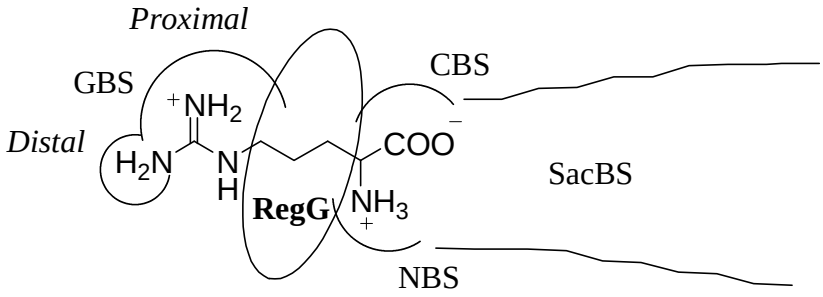

Figure 6. The often neglected, yet strategically located, RegG.

Furthermore, dissimilarities are found in the protein core near to the periphery of the active site, and thus the NOS isoforms may have different abilities to undergo conformational changes caused by induced fitting of inhibitors. Since the hydrophobic interaction is non-specific and weak, the reorganisation of hydrophobic moieties bound by hydrophobic interactions is likely be involved in the ligand-induced conformational change. As a result, the RegG, likely to be hydrophobic based on limited data, could possibly play a role in terms of ligand-induced conformational changes and result in improved inhibitor binding to, as well as selective inhibition of, the NOS.

Chapter 2 NOS Inhibitors Interacting with Guanidino Binding Site

A large number of NOS inhibitors have been developed to date. To review these NOS inhibitors, the compounds are classified according to the groups that bind to the GBS. For each GBS-interacting group, discussions are elaborated on structural modifications of the RegG-interacting groups, NBS-interacting groups, CBS-interacting groups and SacBS-interacting groups.

The isoform selectivity has not been clearly defined and applied across various studies. In this review, the selectivity of an inhibitor between two isoforms is measured by comparing the *in vitro* IC_{50} (or K_i) values of the inhibitor against both isoforms. A compound with IC_{50} (or K_i) value that is at least 20 folds lower towards an isoform over that of the other isoform is a selective inhibitor of the former isoform. Since there are three NOS isoforms, for a compound to be considered as a NOS isoform selective inhibitor, its IC_{50} (or K_i) value against a particular NOS isoform has to be at least 20-fold lower than those of the remaining two (but not either one) NOS isoforms.

A few limitations of the current reviews on NOS inhibitors should be noted. The review is focused on inhibitors with GBS-interacting groups that mimic the guanidino moiety of L-Arg, and show similar binding interactions in GBS as the guanidino moiety of L-Arg. As a result, some of the heterocyclic inhibitors, which bind to the active site through different binding interactions as compared to guanidino moiety of L-Arg, are not included in the review. Besides that, in some reports, the compounds are not tested against all three isoforms, and thus no selectivity information can be derived for these compounds. In addition, the inhibitors in the review are sourced from journal publications while patented compounds are not

included. Nevertheless, it is believed that the information obtained is sufficient to give a rather complete picture of the NOS inhibitors and their isoform selectivity.

Inhibitors with Guanidino Moiety

Alkylguanidino compounds have been reported to be NOS inhibitors. Methylguanidine (**01**) is a weak and nonselective inhibitor of NOS[114]. Disubstituted guanidines, without NBS-interacting group and CBS-interacting group, are weak inhibitors. For example, N^1-propyl-N^3-butylguanidine (**02**) has been reported as a non-selective, weak binding inhibitor[115]. Cyclic 2-iminodiazanane (**03**) is shown to be weaker than the corresponding amidine counterpart, the 2-iminopiperidine (**25**)[116].

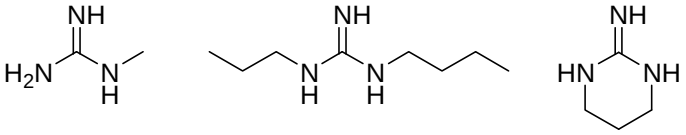

01 **02** **03**

The binding affinity of guanidino compounds is enhanced by the presence of NBS-interacting group and/or CBS-interacting group. The prototypical inhibitor, L-N^G-monomethyl-arginine (L-NMMA) (**04**), is one of the earliest discovered NOS inhibitor[117]. L-NMMA is a non-selective, competitive inhibitor of NOS[36]. With additional methylation on the terminal guanidino group, L-N^G,N^G-dimethyl-arginine (L-AMMA) (**05**) is a non-selective NOS inhibitor which is present naturally in the body[118]. With slightly longer alkyl substituent, L-N^G-allylarginine (**06**) is a nonselective inhibitor, while L-N^G-propylarginine (L-NPA) (**07**) and L-N^G-cyclopropylarginine (**08**) has been found to be a potent nNOS selective inhibitor[111,119]. This suggests that the proximal GBS of nNOS is larger than those of the other isoforms. Structural constraint has been introduced on guanidino moiety of L-Arg using N^δ,N^ω-ethylene bridge, resulting in cyclic guanidine. However, no biological activity has been reported with this series of compounds[120]. The phenylguanidino

based amino-acids (**09**) are nonselective inhibitors (eNOS inhibitory data is not reported)[121]. The activities of these compounds are less than that of phenylthioureido counterparts (**55**), while the activity profiles are different from those of N-phenylamidino counterparts (**43**), which have been demonstrated as nNOS selective[122]. In order to constrain the flexibility of the alkyl chain in L-Arg, alkenyl, carbonyl and ring structures have been introduced. However, the compounds are found to be nonselective[123,124]. **10** and **11** are both substrates and inhibitors of NOS, while **12** and **13** are pure inhibitors.

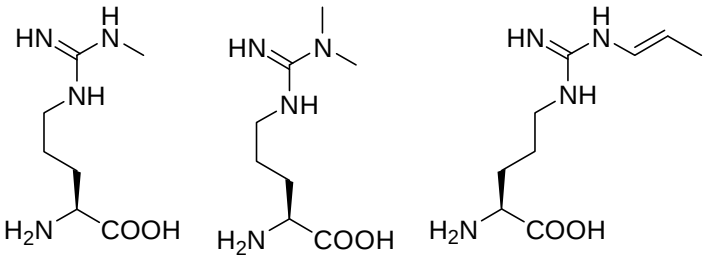

04 **05** **06**

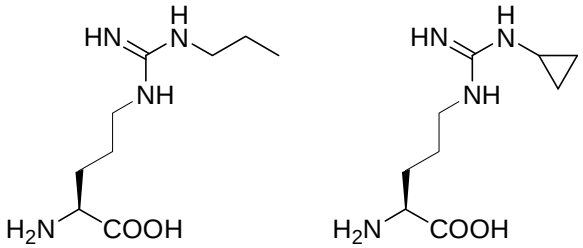

07 **08**

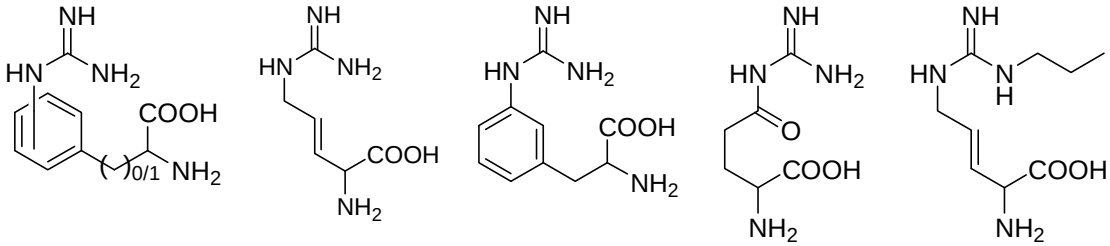

09 **10** **11** **12** **13**

The removal of NBS-interacting group with the retention of CBS-interacting group has been demonstrated in α-guanidinoglutaric acid (**11**). This endogenous convulsant is an nNOS inhibitor (iNOS and eNOS inhibitory data is not reported)[125]. For some inhibitors, the CBS-interacting group is removed while modifying the NBS-

interacting group. Simple aminoguanidines (**12**) and agmatine (**13**) are weak nonselective inhibitors of NOS[114]. Imidazole has been also used as NBS-interacting group, leading to weak inhibitors[126] (**14**). With three methylene spacing between the imidazole and the guanidines, iNOS selective inhibition is achieved. However, this information should be interpreted with caution, as it is possible to have imidazole instead of guanidine acting as the haem interfering entity.

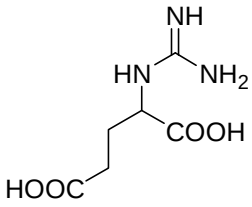

11

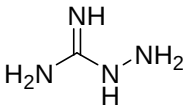

12

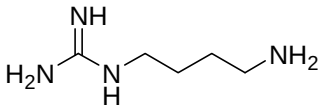

13

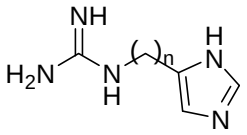

14

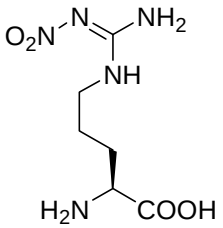

15

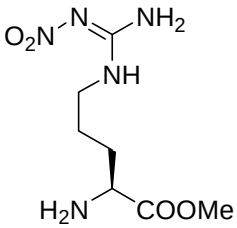

16

Nitro substitution confers NOS inhibitory activity to guanidino compounds and demonstrates distinct inhibitory profile. With the presence of NBS-interacting group and/or CBS-interacting group, potent inhibitions are achievable. L-N^G-nitro-arginine (L-NA) (**15**) is a potent prototypical NOS inhibitor[127]. It is isoform non-selective, despite showing a tendency of inhibiting constitutive NOS selectively over iNOS. The inhibition is competitive in nature, but prolonged incubation results in tight-binding complex with nNOS. Due to the poor oral bioavailability, L-NA has been formulated as L-N^G-nitro-arginine methyl ester (L-NAME)[128] (**16**). By itself, L-NAME is a non-selective NOS inhibitor, and it is less potent than L-NA due to either a lack of CBS-interacting group or the incompatibility of the methyl group with the CBS.

Dipeptides and peptidomimetics, with L-NA as one of the residues, have been evaluated as NOS inhibitors, and selective inhibition of various isoforms is achievable[129]. Selective nNOS inhibition has been reported for dipeptides and peptidomimetics containing L-NA[130-133]. It is believed that the enhanced nNOS selectivity is attributed to structural differences in the SacBS. Other than nNOS selectivity, dipeptides have also been suggested as iNOS selective with limited data (eNOS inhibitory data is not reported)[134].

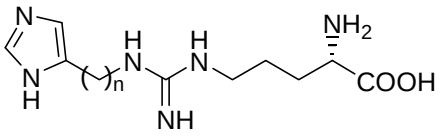

17

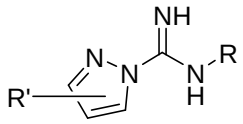

18

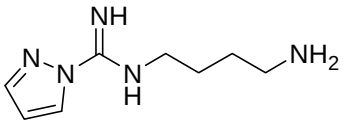

19

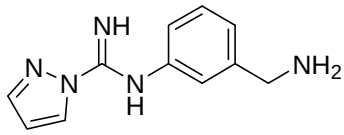

20

Another modification of the guanidino moeity involves the use of heterocyclic substitution. N^G-(Imidazolylalkyl)arginines (**17**) are shown to display weak nonselective NOS inhibition[126]. With one of the guanidino nitrogen incorporated into a heterocycle, 1H-pyrazole-1-carboxamidines (**18**) have been shown to be nonselective NOS inhibitors[115]. The presence of terminal amino function (**19**) results in increased potency but not selectivity. With phenyl substitution (**20**), no selective inhibition is achieved, which is different from the case of nNOS selective N-phenylamidines[122] (**43**).

Amidine and Related Inhibitors

Amidine based inhibitors represent a large group of NOS inhibitors. The amidino group is bioisosteric with the guanidino group, with the non-nitrogen group interfering with the haem. The simplest form of amidine, formamidine (**21**), is a nonselective inhibitor[135]. Substitutions on the central carbon of amidino group (**22**)

with various alkyl, heterocyclic, heteroatom-containing alkyl chains produce non-selective inhibitors[114]. Cyclopropylamidine (**23**) and 2-thienylamidine (**24**) are found to be potent inhibitors in this series.

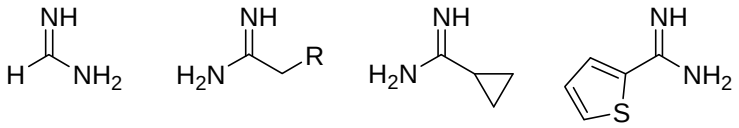

21 **22** **23** **24**

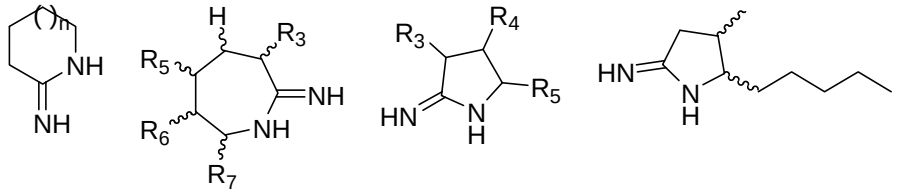

25 **26** **27** **28**

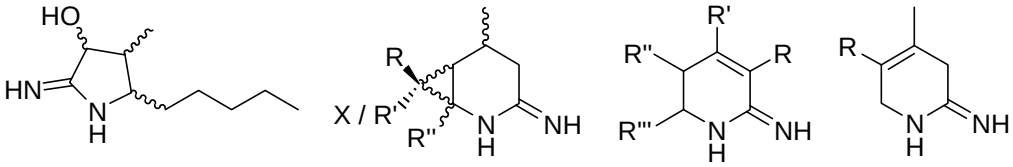

29 **30** **31** **32**

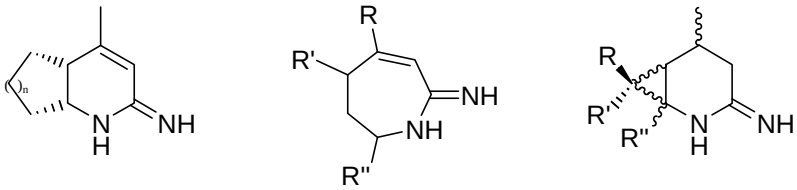

33 **34** **35**

Cyclic amidines are able to inhibit NOS. 2-iminoazaheterocycles (**25**) are non-selective inhibitors despite displaying iNOS selectivity over eNOS[116,136]. Similar inhibition profile is observed for 2-iminohomopeperidine[137] (**26**), 2-iminopyrrolidines (**27**), 4-methyl-5-pentyl-2-iminopyrrolidines (**28**) and the 3-hydroxyl analogues (**29**)[138,139]. Interestingly for the 3-hydroxyl substituted analogues, one of the stereoisomers is an iNOS selective inhibitor. Bicyclic amidines are highly potent with IC_{50} in nanomolar range, but the inhibitors are non-selective (nNOS inhibitory data is not reported)[140] (**30**). Dihydropyridin-2-imines and analogues (**31**) (**32**) (**33**) (**34**) have been shown to be isoform nonselective (nNOS inhibitory data is not

reported)[141,142]. With the appropriate substituents, azepines are better than piperidines in terms of iNOS selectivity over eNOS (nNOS inhibitory data is not reported). 2-Azabicyclo[4.1.0]heptan3-imine (**35**) has been evaluated and shown to be nonselective[143].

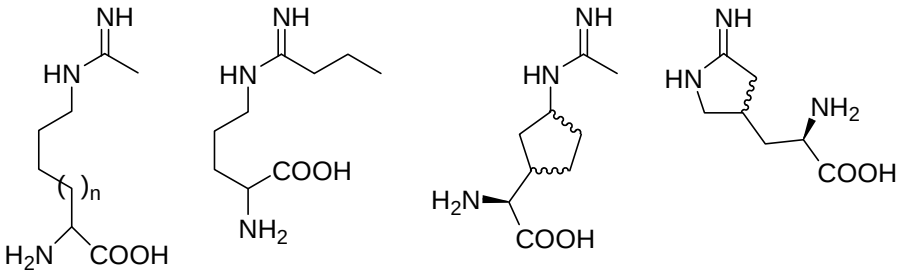

36 **37** **38** **39**

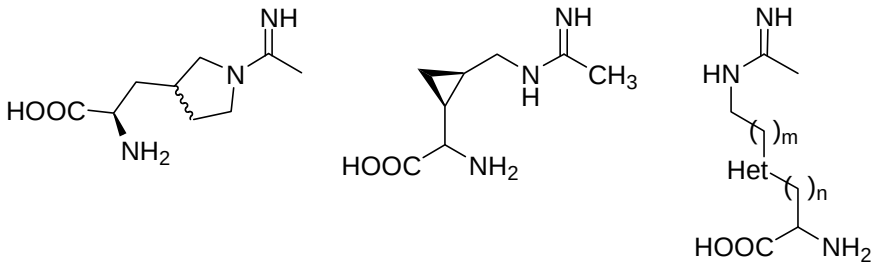

40 **41** **42**

Similar to guanidino compounds, amidino compounds with NBS-interacting group and/or CBS-interacting group generally demonstate good binding affinity. L-N-iminoethyllysine (L-NIL) (**36**, n=1) is iNOS selective over eNOS (nNOS inhibitory data is not reported). With shorter alkyl bridge, the L-N-iminoethylornitine (L-NIO) (**36**, n=0) is more potent than NIL, but with longer alkyl bridge, L-N-iminoethylhomolysine (**36**, n=2) is less potent[114]. A prodrug of L-NIL has been developed[144]. L-NIL with tetrazole-amide group is reported to be inactive, thus implying either the carboxylic group is important, or the protonated tetrazole is incompatible with CBS. Based on L-NIL, N^5-(1-imino-3-butenyl)-L-ornithine (**37**) is an nNOS selective inhibitor[145]. In addition, several conformationally restricted amidinyl amino acids (**38**) (**39**) (**40**) have been synthesised and shown to inhibit iNOS (nNOS and eNOS inhibitory data is not reported)[146]. On the other hand, selective

iNOS inhibition is observed for 3,4-cyclopropylarginine analogue (**41**)[147]. With the introduction of heteroatom into the alkyl bridge between the amidine and the amino-acid groups, the resultant compounds (**42**) are iNOS selective, and the inhibitory activities are dependent on the position of the heteroatom[148]. When conformational restriction being applied to these compounds, they are shown to be inactive as NOS inhibitor[149].

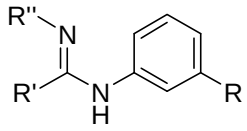

43

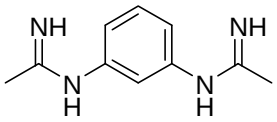

44

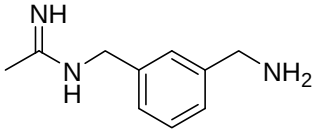

45

Attempts to remove the NBS-interacting group and/or CBS-interacting group have been performed. The α-amino and α-acid groups of L-NIL are not required for iNOS inhibition, but the hydrogen bonding of α-amino is important for catalysis[150]. L-NIL analogues with vicinal diol, which is an isostere of the carboxylic acid, are non-selective[151]. On the other hand, CBS-interacting group is often left out in the design of NOS inhibitor, while NBS-interacting group is retained. An extensive study has been performed to elucidate the tolerence of the guanidino binding site using phenyl substituted amidines (**43**)[122]. The imino nitrogen is to be kept unsubstituted. This is consistent with the guanidino binding site model, which dictates that the distal GBS is small and intolerant with simple methyl substitution[106]. On the other hand, for nNOS but not iNOS or eNOS, the proximal GBS is able to accommodate a range of alkyl, alkyl with heteroatom terminal, and hetorocylic ring, and hence nNOS selective inhibition is achieved. For the substitution on the phenyl ring, several nitrogen containing *meta*-substituents have been shown to result in nNOS selectivity, but bulky and electronic groups, except aminomethyl, result in weak or inactive compounds. The phenylenebisamidine (**44**) is reported to be nNOS selective. On the other hand,

with benzyl substitution, a prototypical highly iNOS selective inhibitor, N-(m-(aminomethyl)benzyl)acetamide (1400W) (**45**), is obtained, and 1400W has been used extensively in *in vivo* research since its discovery in 1997[152].

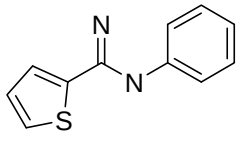

46

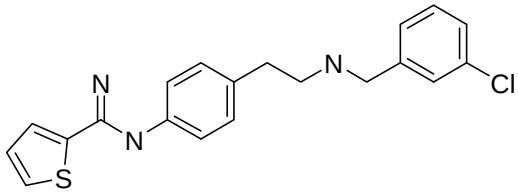

47

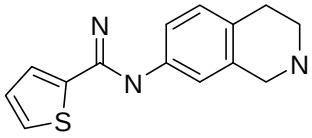

48

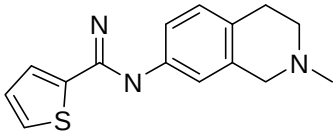

49

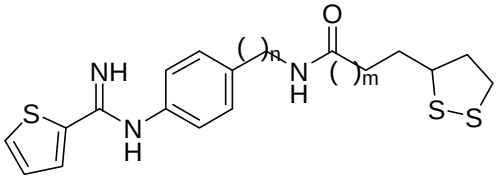

50

Another series of amidine evaluated is the thiazole-containing amidine with phenyl substitution. Without NBS-interacting group on the phenyl ring, the compound are weakly selective (**46**). However, with amino-containing moiety, nNOS selective inhibition is achieved[153] (**47**) (**48**) (**49**). Acylation of the terminal nitrogen with lipoic acid (**50**) results in an nNOS inhibitor (iNOS and eNOS inhibitory data is not reported), which offers protection against cell model of glutamate toxicity[154].

Thiourea and Isothiourea Based Inhibitors

L-Citrulline, with a urea function showing low affinity to GBS, prompts the use of thiourea as an inhibitor. Thiourea and isothiourea are commonly found in NOS inhibitors, but the latter is more commonly employed. Unsubstituted thiourea is inactive as NOS inhibitor. Phenylthiourea (**51**) and benzylthiourea (**52**) are non-selective NOS inhibitors (eNOS inhibitory data is not reported), and hydroxylethyl substitution on thiouronium nitrogen (**53**) results in nonselective inhibitor[155].

L-Thiocitrulline is a isoform nonselective NOS inhibitor[156]. Modifications on the alkyl bridge between the thiourea and the amino acid groups have been performed.

Lengthening the alkyl bridge of L-Cit with an methylene group produced nonselective inhibitor (eNOS inhibitory data is not reported) (**54**)[157]. Phenylthiourea analogues with amino acid group (**55**) are nonselective (NOS inhibitory data is not reported)[121]. The presence of oxygen in the alkyl bridge (**56**) produces iNOS inhibitor (nNOS and eNOS inhibitory data is not reported)[158], and the thiourea-containing compounds are weaker than isothiourea-containing compounds for this series of inhibitors.

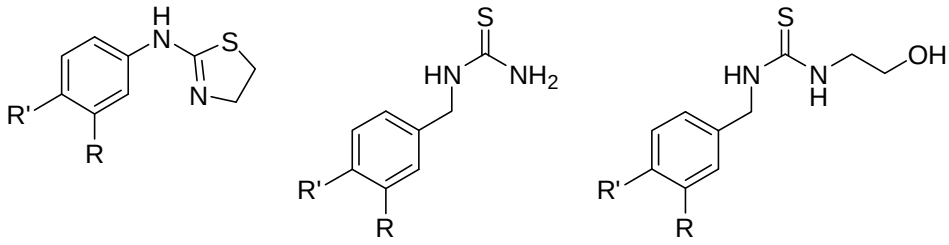

51 **52** **53**

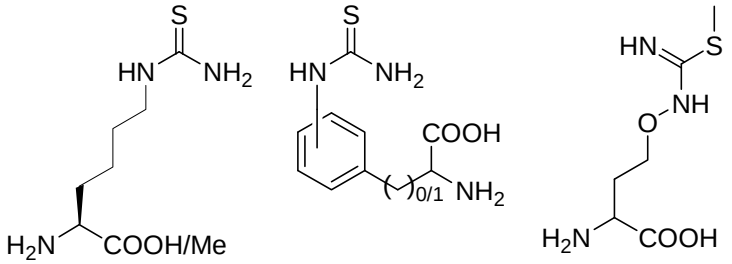

54 **55** **56**

An extensive study using alkylisothiourea[159] (**57**) has been conducted for iNOS inhibition (nNOS and eNOS inhibitory data is not reported). The S-alkyl group is to be kept small for iNOS inhibition. Larger alkyl groups decreases the inhibitory activities and n-butyl results in inactive compound. Benzyl group and heteroatom-containing chains, such as methoxy and cyanomethyl, are tolerated at the active site, and S-aminomethyl results in potent inhibition. The imino nitrogen is preferably unsubstituted, while the amino nitrogen can be substituted with various groups, ranging from small amino group to large benzyl group. Heterocyclic analogues are also evaluated. The 2-aminothiazole (**58**) and 2-aminothiazoline (**59**) are found to be active. Another extensive study providing information on isoform selectivity has

been conducted, and laid the foundation for the popular use of isothiourea derivatives as NOS inhibitors[160]. Isothiourea, thiazole (**58**), thiazoline (**59**) and bisisothiourea (**60**) are evaluated and shown to be nonselective NOS inhibitors. With alkylbenzene as the bridging element, potent inhibition has been observed in **60**. Further study on S-alkylthiourea reveals that S-ethylisothiourea is iNOS selective. The cyclic amidines, as in 2-amino-5,6-dihydro-6-methyl-4H-1,3-thiazine (**61**), are shown to be nonselective but more potent than ethylisothiourea[161]. N-phenylisothioureas (**62**) have been evaluated[162], and the thioureido sulphur should only be substituted with short alkyl chain like methyl and ethyl. Bulkier S-substituents like propyl, isopropyl, butyl and benzyl are not tolerated in NOS. With suitable ring substituents (mostly hydrophobic, and some bulky aromatic), nNOS selective inhibition is achieved for this series of compounds.

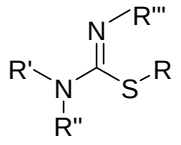

57

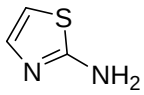

58

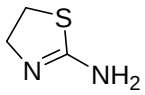

59

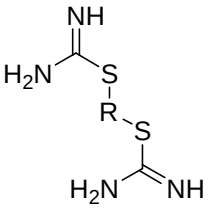

60

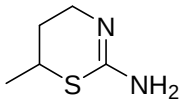

61

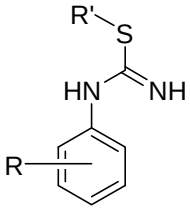

62

Based on L-Cit, S-methyl and S-ethyl-L-thiocitrulline (**63**) are evaluated and the latter is shown to be nNOS selective inhibitors[163]. Additional alkyl substitutions on the imino nitrogen lead to inactive compounds, with the exception of methyl substitution (**64**), which exhibits weak inhibition[164]. This is rather unexpected because the distal GBS is known to the small and intolerable to even methyl substitution[106]. Thus this suggests that the affinity-enhancing effect of NBS-

interacting group and CBS-interacting group can overcome the steric incompatibility of GBS-interacting group in the distal GBS.

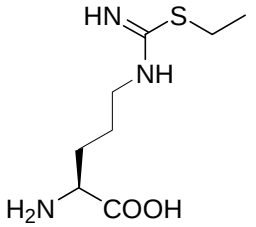

63

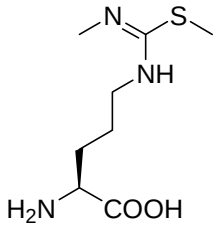

64

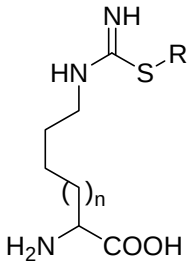

65

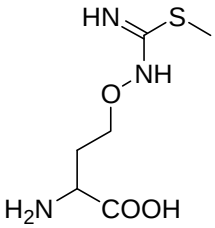

66

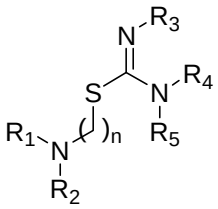

67

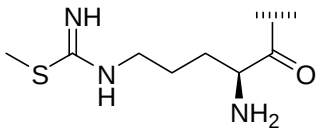

68

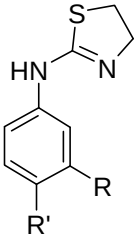

69

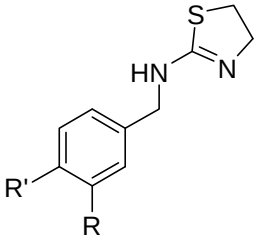

70

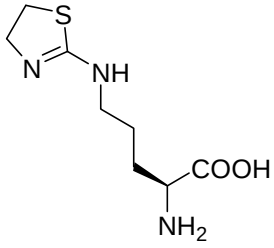

71

Modification on the chain length of the alkyl chain of isothiocitrulline leads to nonselective inhibitor (eNOS inhibitory data is not reported) (**65**)[165]. L-Canavanine (**66**), with oxygen in the alkyl bridge, is shown to inhibit iNOS (nNOS and eNOS inhibitory data is not reported)[166]. Analogues without CBS-interacting group are also evaluated. The analogues of dimaprit (**67**) show inhibition against nNOS (iNOS and eNOS inhibitory data is available)[167]. The analogues of dimaprit are different from the rest of the isothiourea-based inhibitors because the sulphur is located on the bridging chain, and can be substituted by the terminal nitrogen to give guanidines, which are suspected to be the active forms. Compounds with SacBS-interacting groups are synthesised to explore isoform selective inhibition. Dipeptides with S-

methylisothiourea terminal are iNOS selective over nNOS (eNOS inhibitory data is not reported) (**68**)[134]. Another series of dipeptides is also evaluated and shown to be non-selective[168].

The incorporation of the sulphur and the imino nitrogen as part of a thiazole ring represents another series of thiourea related inhibitors. As stated previously, the thiazole and thiazoline are nonselective inhibitors[160]. With phenyl (**69**) and benzyl substitution (**70**), the compounds are shown to be non-selective (eNOS inhibitory data is not reported)[155]. Thiazole-containing amino acids are shown to be nonselective (**71**) (eNOS inhibitory data is not reported)[169]. Other than thiazole, a series of heterocyclic rings, such as isothiourea, thiazine, pyrimidine and oxazole, as well as non-cyclic isothiourea have been evaluated, but the inhibitory potencies are lower than that of thiazole-containing compounds. In addition, the CBS-interacting group is shown to be not essential but desirable. Lengthening the alkyl bridge by a methylene function, with or without the presence of CBS-interacting group, results in inactive compound[157].

Heterocyclic Based Inhibitors

Although several heterocycles are reported to be NOS inhibitors, however, not all of them meet the inclusion criteria for this review, thus are not extensively presented here. These heterocycles show different binding mechanisms around the Fe_{haem} as compared to guanidino mimetics. For example, some NOS inhibitors containing the imidazole or indazole groups are known to bind to the haem through different interaction forces as compared to the guanidino group of L-Arg[170,171].

2-Aminopyridine (**72**), a close analogue of iminopiperidine, is generally nonselective[172]. With the appropriate 4,6-disubstitution in the phenyl ring, the potency towards iNOS has increased. This is reflected in the shift of the IC_{50} values

to the nanomolar range, however no enhancement in selectivity is observed. Further study on 6-(4-(substituted)phenyl)-2-aminopyridines (**73**) shows that selective inhibition of NOS can be achieved[173]. With aminoalkyl-containing bulky 6-substituents on the aminopyridine, nNOS selective inhibitors have been obtained[174].

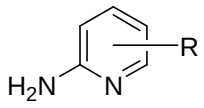

72

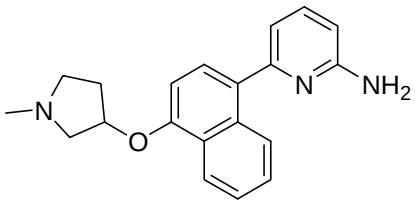

73

From the review, it is found that relatively few selective inhibitors are available for inhibitors with GBS-interacting groups. None of the guanidino mimetics, such as guanidines, amidines, thioureas and isothioureas, is superior to the others in terms of affinity or selectivity. Among the GBS-interacting groups, the ability of the guanidino group to interact with GBS is without doubt. Furthermore, the guanidino group is the natural anchoring moiety of the substrate L-Arg. In addition, in term of structural modification, a variety of substitution can be introduced to the guanidino moiety. As a result, it is of interest to evaluate the potential of guanidino compounds as inhibitors and molecular probes of NOS active site though a series of SAR and molecular probing studies.

Besides that, it is observed that a lot of inhibitors interacting with either one or both of NBS and CBS show increased potency but not necessarily increased selectivity. Hence, the NBS-interacting group and/or CBS-interacting group alone are insufficient in providing good isoform selectivity. Nevertheless, the good potency achievable with either NBS-interacting group or CBS-interacting group is dependent on a condition, which specifies that the compound should possess the appropriate GBS-interacting group and (the generally ignored) RegG-interacting group. Hence, it

is of interest to study the contribution of RegG-interacting group in improving the binding and isoform selectivity of an inhibitor, using a guanidino group as the GBS-interacting group.

X-Ray Crystallography of Inhibitors Bound to The NOS Active Site

It is of interest to understand the binding of the inhibitors to the NOS active site by X-ray crystallography studies. As compared to the X-ray crystallographic studies published before the year 2000 (**Chapter 1**), those reported after the year 2000 have been more focused on elucidating the binding conformation of the inhibitors, the interactive forces involved, and the structural variations that determine isoform selectivity.

The N^1-butyl-N^3-hydroxyguanidine (**74**)[105] binds to nNOS in similar fashion as N^{ω}-hydroxy-L-arginine (L-NHA) (**75**), which in turn binds similarly as L-Arg. Compound **75** establishes extensive hydrogen bonding network around GBS, as well as stereospecific interactions with NBS and CBS. The hydroxyl group on the guanidino moiety points away from Fe_{haem} toward the backbone amide of Gly forming weak hydrogen bonding or nonbonding contact. As for **74**, the hydroxyl group is also orientated away from the Fe_{haem}. However, as compared to the alkyl chain of L-NHA, the n-butyl group is curled toward Gln and Val residues, away from the NBS and CBS, and forms hydrophobic ineractions with Val residues. Besides that, the side chain of Gln residue is shifted in order to avoid close contact with the butyl group.

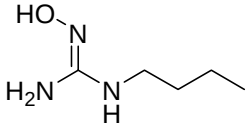

74

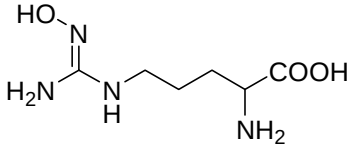

75

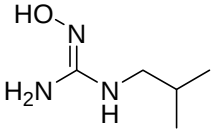

76

In contrast, the binding conformation of N^1-isopropyl-N^3-hydroxyguanidine (**76**)[105] is different from **74** and **75**. The isopropyl group is located in the hydrophobic

cavity above the haem, in which the hydroxyl groups of **74** and **75** occupy, with the two ultimate methyl groups make favourable VDW interactions with both Val and Phe residues. Furthermore, the hydroxyl group is located in the distal GBS, which is known to be sterically restricted. The hydroxyl group is hydrogen bonded to the backbone carbonyl of Trp residue, while both N^2H and N^3H of guanidino group are involved in bifurcate hydrogen bondings with Glu residue. To accommodate hydroxyl in the distal GBS, the guanidino plane of **76** is shifted slightly away from the Trp residue as compared to that of **74** and **75**.

For simple S-alkylisothiourea (**57**), the sulphur is located above the haem pyrrole ring B nitrogen. The ethyl group of S-ethylisothiourea protrudes into the hydrophobic cavity above heam, interacting with the Phe residue[102,104]. As for isopropyl group of S-isopropylisothiourea, one of the terminal methyl groups is in close VDW contact with the haem as limited by the space in the hydrophobic pocket above the haem. For 2-amino-1,3-thiazolidine (**59**), the thiazolidine ring remains puckered but is approximately parallel to the haem plane. The thioureaido fragment occupies the same position as simple S-alkylthiourea, with the ethyl bridge protruding into the hydrophobic pocket above the haem.

For S-ethyl-N-phenyl-isothiourea (EPITU) (**62**)[175], the terminal thioureido amino group (NH_2) binds to the distal GBS. In proximal GBS, the S-ethyl group of EPITU is in close contact with the carbonyl of Pro in the hydrophobic pocket above haem, which is different from that of S-ethylisothiourea described above. The N-phenyl ring is orientated at an angle of 153° relative to the thioureido plane, making hydrophobic interaction with Val residue, which is a critical interaction for the binding of EPITU.

As for the S,S'-(1,4-phenylenebis(1,2-ethanediyl))bisisothiourea (**77**) and S,S'-(1,3-phenylenebis(1,2-ethanediyl))bisisothiourea (**78**)[175], the first thioureido group fits into the GBS forming similar hydrogen bonding network as the L-Arg. Compounds **77** and **78** bind to NOS in twisted conformation, with the energetic incentive derived from hydrogen bonding between the second thioureido group and propionate of pyrrole ring D of haem. Compound **77** interacts better with the propionate than **78**. Besides that, the phenyl ring of **77** is perpendicular to the plane of first thioureido group and establishes hydrophobic interaction with Val residue, while the phenyl ring of **78** is tilted with less perfect hydrophobic contact. This explains the higher potency of **77** than **78**. As for N^1,N^{14}-bis((S-methyl)isothioureido)tetradecane (**79**)[175], the X-ray crystallographic image is disordered except the first thioureido group and subsequent four carbons. Nevertheless, this implies that a bulky ligand with an alkyl chain as long as $C_{14}H_{28}$ can bind to the active site, as long as the compound possesses a suitable GBS-interacting group such as guanidino, amidino or ureido group, and the remaining portion of the lengthy molecules is accommodated in the substrate access channel.

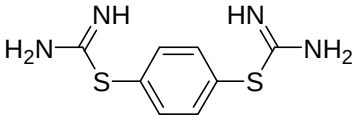

77

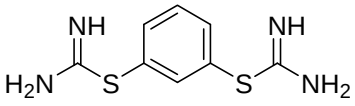

78

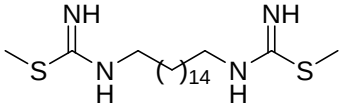

79

Study of the binding of N-(*m*-(aminomethyl)benzyl)acetamide (1400W) (**45**) in nNOS and iNOS has been performed[176]. The amidino group mimics the guanidino group of L-Arg and is hydrogen bonded to Glu residue in GBS. The phenyl ring of **45** is positioned on top of the pyrrole ring A of haem, and the *m*-aminomethyl group interacts with both haem propionates, which are in turn hydrogen bonded to Tyr residue and BH_4 respectively. The binding of **45** in eNOS has also been reported[177], in which the amidino group is hydrogen bonded with Glu and Trp in the GBS, and the

amidinyl methyl group of **45** is directed towards the Fe_{haem}. In contrast to both nNOS and iNOS, the phenyl ring is positioned above the haem propionates in eNOS, and the position of *m*-aminomethyl group is not clearly defined, though it shows a tendency to bind to the propionate of pyrrole ring D of haem. The amino group could not bind to NBS as judged from the position of the phenyl ring.

Compound **45** is known to be iNOS selective inhibitor. The iNOS selectivity arises from the conformational flexibility of the iNOS active site, which can accommodate **45** with greater conformational complementarity than the other two isoforms. In order for all the three nitrogens of **45** to interact strongly with the Glu residue as well as the haem propionates in iNOS, the **45** moves closer towards the propionates and Glu, and causes the shifting of helix H11 strand. However, this shift of the helix strand is not possible in nNOS because of the hydrogen bonding (between Try and Lys residues in H11) that immobilises the helix strand. In iNOS, a hydrophobic Phe residue replaces Try residue, thus the hydrogen bonding is absent and the shifting of the helix strand is allowed.

The prototypical NOS inhibitor, L-NA (**15**)[170], binds to active site in a similar fashion as L-Arg, with the nitro group positioned in the proximal GBS. The nitro group provides additional interactions (hydrogen bonding and non-bonding) with the protein as compared to L-Arg. The backbone amides Gly and Trp residue is hydrogen bonded with the nitro group, and various non-bonded contacts are formed between nitro and protein (Pro, Phe, Ser, Gly, Trp residues).

Another NOS inhibitor, L-N^5-(1-iminoethyl)-ornithine (L-NIO) (**36**, n=1)[177], binds in a similar fashion as L-Arg with a network of hydrogen bonds in the GBS. The amidino methyl group is directed towards the Fe_{haem}. A bridging water molecule originally found between the carbonyl oxygen of Pro residue and the guanidino $N_\eta H_2$

of L-Arg is absent in the case of L-NIO, probably due to the increased hydrophobicity upon L-NIO binding.

The binding of L-NPA (**07**)[176], known as nNOS selective, is similar to that of L-Arg. The propyl group is directed towards the Fe_{haem} and resides in the hydrophobic cavity above the haem. Slight differences between the bindings of L-NPA to nNOS and iNOS are observed, forming the structural basis of nNOS selective binding. The active site of iNOS is smaller than nNOS and eNOS by 13 $Å^2$ and 8.4 $Å^2$ respectively. A spacer is created in the protein core of iNOS through hydrogen bonding between the side chain amide of Asn residue with the backbone carbonyl of Ala residue, thus decreasing the space available in the active site of iNOS. This explains the inability of the hydrophobic cavity above the haem iNOS to accommodate compounds with large or inflexible Fe_{haem}-facing group. By having a Ser residue in place of Asn residue, the spacer is absent in the protein core of nNOS and eNOS, thus the active sites are larger. Since the active site cavity eNOS is only slightly smaller than that of nNOS (4.6 A^2), both active sites show relatively similar steric tolerance. This size differences among the active sites of the three isoforms are likely to be clinically relevant, because the same protein sequential difference is also found in all the three human NOS isoforms. Furthermore, the 3D structures of human iNOS and nNOS are also found to align nicely over those of murine iNOS and rat nNOS.

In addition to the size variation in the active site, other differences are observed between the binding of L-NPA in iNOS and nNOS[176]. A hydrogen bond is present between the α-amino of L-NPA with Trp residue in nNOS but is absent in iNOS. Besides that, the α-acid of L-NPA forms hydrogen bond to Gln residue of nNOS while the interaction is not possible in iNOS. These differences are attributed

to the Asn residue located in SacBS in nNOS (Asn residue replaced by Thr residue in iNOS). The Thr (iNOS) residue is too short for interaction with adjacent Arg residue, thus interacts with Gln residue instead. In contrast, the Asn (nNOS) is hydrogen bonded with adjacent Arg residue, thus unable to interact with Gln residue. Hence, the Gln residue in iNOS is not available for hydrogen bonding with α-acid of L-NPA, but the Gln residue in nNOS is free to interact with α-acid of L-NPA. Nevertheless, these interactions might not be clinically significant, because an Asn residue (instead of Thr residue) is found in human iNOS. Thus nNOS selectivity might not be achieved in human by exploiting the residue difference in this site.

It is of interest to carry out X-ray crystallographic study on nNOS selective dipeptidic inhibitors. The selectivity of isoform selective dipeptidic inhibitors has been attributed to the structural differences in ZacBS. However, a recent study using L-N$^{\omega}$-nitroarginine-2,4-L-diaminobutyramide (**80**), (4S)-N-(4-amino-5-(aminoethyl)aminopentyl)N'-nitroguanidine (**81**) and L-N$^{\omega}$-nitroarginine-(4R)-aminoL-proline amide (**82**) suggests that the selectivity is attributed to the differences in the CBS[178].

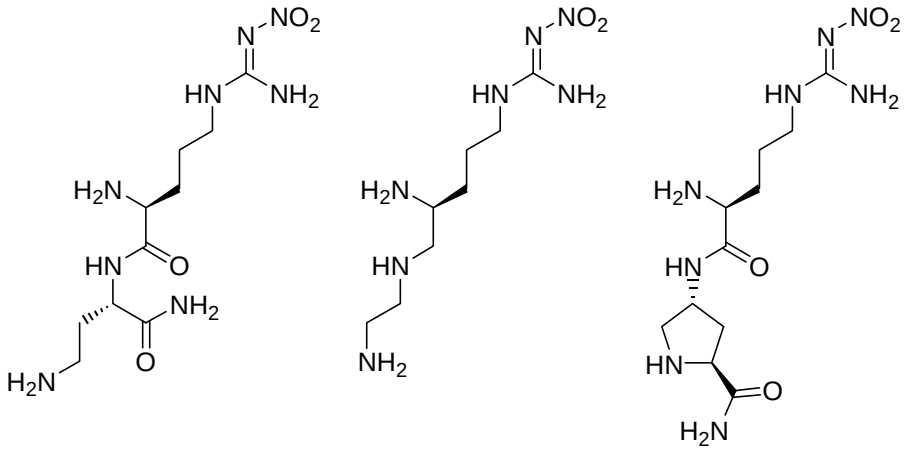

80 **81** **82**

The nitroguanidino group binds to the GBS in a similar fashion as L-Arg, with an extensive hydrogen bonding network[178]. The N-nitro group forms additional

hydrogen bondings with the protein backbone, thus strengthening the binding. However, the fitting of nitroguanidino group in nNOS is better than that of eNOS. In eNOS, either the hydrogen bonding between the terminal guanidino nitrogen and Glu residue, or the hydrogen bonding between the nitro and protein backbone, or both, is stretched slightly beyond favourable distance. In nNOS, the nitro group is consistently found to be ~ 0.1 Åcloser to the protein backbone than in eNOS.

Due to the lack of CBS-interacting group, these dipeptidic inhibitors cannot fit into the L-amino acid specific NBS and CBS in both nNOS and eNOS, but extends into the ZacBS instead[178]. The NBS-interacting group (α-amino group of L-NA portion) of the dipeptidic inhibitor is hydrogen bonded directly to the Glu residue of GBS, but it is hydrogen bonded *via* a water bridge to the Glu residue in eNOS. Interestingly, in nNOS, the NBS-interacting group can also interact with CBS, which is originally interacting with α-COOH in case of L-Arg binding. Hence, in nNOS, the inhibitors adopt curled conformation for maximum electrostatic interaction between NBS-interacting group and both Asp and Glu residues. However, an Asn (in eNOS) residue is found in place of the Asp (in nNOS) residue. The Asn (in eNOS) residue is uncharged, and the mono hydrogen of Asn residue is already bonded to an adjacent Arg residue. As a result, the eNOS is unable to establish the similar electrostatic interaction with the dipeptidic inhibitors as in nNOS, and thus the inhibitors are fully extended in eNOS. Furthermore, it is found that the same contacts are available in both isoforms and yet the inhibitors make different contacts in nNOS and eNOS. Hence, the difference in binding conformation is due to the varying adaptabilities of the dipeptidic inhibitors in the active sites of the two isoforms. Importantly, this structural difference in CBS is likely to be clinically significant as the difference is also found in human isoforms.

Although nitroindazole is not considered a guanidino mimicking GBS-interacting group, the X-ray crystallographic information of nitroindazoles[170,171] provides additional information about the NOS active site, and is briefly reviewed here. As compared to L-Arg, the nitroindazoles bind through a different set of interactive forces, such as π-π stacking interactions, hydrophobic interactions and hydrogen bonding interactions. The potency of nitroindazole is mainly attributed to π-π stacking interaction, which is an important noncovalent intermolecular forces that can contribute at least as much energy as hydrogen bonding[179]. On the other hand, the importance of hydrophobic interactions around the active site is highlighted by the improved potency of 3-bromo-7-nitroindazole as compared to 7-nitroindazole, which is a result of significant hydrophobic interactions around the bromo group. Besides that, the nitroindazoles also exhibit interactions with BH_4. Interestingly, the Glu residue in the GBS adopts a new rotameric form upon the binding of 7-nitroindazoles. Besides that, the haem propionates are found to adopt different conformation as composed to the X-ray crystallography of L-Arg. This highlights that the active site is not rigid and can adopt some structural variations upon inhibitor binding.

Early X-ray crystallographic studies tend to suggest that the active sites of NOS are highly conserved and rigid. However, recent reports suggest that ligand-induced changes in the active site conformation are possible[171,176]. The selectivity of both 1400W and NPA is attributed to the isoform-specific structural differences outside the active site, which in turn confer conformational flexibilities in the protein active site. The study on nitroindazoles further suggests that the Glu residue of GBS and haem propionates can undergo conformational changes in response to ligand binding. As a result, the active site of NOS is not a rigid entity, but is indeed flexible and accommodative to the ligand.

Chapter 3 Hypothesis, Objectives and Experimental Design

NO is found ubiquitously in the human body, acting as a neurotransmitter, a paracrine agent, an autocrine agent, as well as a cytotoxic agent. Overproduction of NO is implicated in a variety of pathological conditions, which can be controlled by modulating the NO production. Hence, the NO-producing enzyme, NOS, is a valid and important target for drug design. Of the three NOS isoforms, nNOS is the focus of the current study. Overproduction of nNOS-derived NO in high concentration produces destructive RS_{NO}, which is detrimental to the neurons. The hyperactivity of nNOS is often associated with neurodegenerative diseases, thus inhibition of nNOS is a suitable approach in curbing neurodegeneration. However, there is a lack of therapeutically useful nNOS inhibitors available in clinical settings, and hence it is of interest to search for novel nNOS inhibitors.

The inhibition of nNOS should be selective, with minimal interference with the normal functioning of iNOS and eNOS. However, the conservation of the active site topology of the three NOS isoforms presents a challenge in achieving selective isoform inhibition. Nevertheless, several selective inhibitors of iNOS and nNOS have been reported, suggesting that the selective inhibition of nNOS is not impossible. The selectivity of the inhibitors is believed to be related to the differences in the capacity of the topologically conserved active sites to accommodate the inhibitors through induced fit. Among the binding sites identified in the NOS active site, the region adjacent to GBS (RegG), despite being strategically located, has not been extensively exploited in drug design. Based on limited data, hydrophobic interactions, which are often associated with conformational changes of active site, are likely to be the major interactive forces in the RegG. Thus the RegG offers promise for improving inhibitor's binding affinity and isoform selectivity.

Since X-ray crystallography is unable to capture the dynamics of NOS active site and NMR study of NOS is infeasible, the molecular probing study is a useful strategy for characterising the RegG. Being part of the substrate L-Arg, the guanidino group is known to bind to the GBS with high affinity. Besides that, the guanidino moiety can be modified through various N-substitutions. Hence, guanidino compounds are suitable for molecular probing study of the RegG. In addition, while several classes of guanidino compounds have been developed as NOS inhibitors, relatively few are isoform selective. Thus it is of interest to investigate the potential in capitalising the RegG for improving the affinity and selectivity of guanidino based NOS inhibitors.

Therefore, based on the information retrieved from the literature reports, the following hypothesis was proposed for this study: "That by exploiting the region adjacent to the guanidino binding site, selective nNOS inhibition and improved nNOS binding affinity can be achieved through differently substituted guanidino compounds, thus may give rise to useful therapeutic value."

In order to prove the above hypothesis, the current study was designed to meet the following objectives:

1. To synthesise with rationale several series of guanidino compounds that can bind to both the GBS and the RegG.
2. To evaluate the binding affinity and isoform selectivity of the guanidino compounds using the [^{3}H]-L-citrulline assay.
3. To evaluate the *in vivo* activity of the lead compound(s) identified from the current study.

Achieving these objectives would in turn provide a better understanding of the RegG.

In order to meet the above objectives, a general experimental design was outlined. The guanidino compounds should be suitably substituted in order to be accessible to the GBS, and at the same time able to interfere with the catalytic functioning of the GBS for NO production. Besides that, the guanidino compounds should possess suitable groups for interaction with the RegG. These RegG interacting groups should be structurally diverse in order to perform SAR and molecular probing studies. Although hydrophobic forces seemed to be involved in the RegG, as suggested by limited data, it would be necessary to evaluate the presence of other interactive forces (such as ionic, hydrogen bonding and π-π stacking interactions) in the RegG.

A guanidino group can be N-substituted with various groups. With respect to binding to NOS, it would be of interest to evaluate the inhibitory activity by synthesising N^1,N^2-(disubstituted)guanidines. At the active site of NOS, one of the unsubstituted guanidino nitrogen atoms of a N^1-(monosubstituted)guanidine is likely be orientated towards the Fe_{haem}, while the N^1-substituted nitrogen is orientated towards the access channel. Thus, N^1-(monosubstituted)guanidines are likely to be substrates of NOS. In order to disrupt the catalytic mechanism of the enzyme, the nitrogen facing the Fe_{haem} should be substituted and the substituents should be kept relatively small in size in order to fit into the binding cavity in the proximal GBS. On the other hand, the distal GBS cannot accommodate substituted nitrogen, thus N^1,N^2,N^3-(trisubstituted)guanidines are unlikely to be accessible to the active site. As a result, N^1,N^2-(disubstituted)guanidines are more suitable candidates to be developed as NOS inhibitors. In addition, other than simple guanidino group, it is also of interest to evaluate the inhibitory potential of heterocycles, in which the guanidino group is incorporated structurally in a heterocyclic ring.

Hence, several series of compounds are proposed. As a preliminary study, a series of N^1-alkylguanidines would be useful in providing preliminary information for subsequent studies, despite being likely to be metabolised by NOS. Subsequently, two series of disubstituted guanidines are proposed, the N^1,N^2-dialkylguanidines and N^1-alkyl-N^2-nitroguanidines, with reference to the prototypical inhibitor L-NA. In addition, in order to evaluate the possibility of the presence of anionic interaction in the RegG, a series of 2-(2-nitroguanidino)alkanoic acids is to be synthesised. On the other hand, for evaluating the involvement of cationic interaction in RegG, two series of heterocycles, 1-alkyl-4-nitroimino-1,3,5-triazinanes and 6-anilino-4-amino-1,2-dihydro-2,2-dimethyl-1,3,5-triazines, are to be synthesised.

In addition, the [^{3}H]-L-citrulline assay is to be optimised for evaluating the NOS inhibitory activities of the compounds synthesised. The compounds are to be tested against all three isoforms of NOS. The lead compound (ideally be potent and nNOS selective) identified from the study is to be subjected to *in vivo* test to elucidate the clinical potential of the lead compound, as well as to establish the clinical benefits of nNOS inhibition.

Subsequently, from the results obtained, SAR of guanidino analogues as NOS inhibitors, and information regarding the environment of RegG can be extracted. The potential of RegG for enhancing the binding of the inhibitors shall be evaluated, and the potential contribution of RegG to nNOS selective inhibition shall be assessed. As a result, structural requirements for future design of selective nNOS inhibitors can be identified.

Chapter 4 Preliminary Studies on N^1-Alkylguanidines

A series of N^1-alkylguanidines was synthesised in the preliminary study to evaluate the nNOS inhibiting potential of guanidino compounds. While compound **01** has been shown to be a weak and nonselective NOS inhibitor[114], limited information is available about the use of N^1-alkylguanidine as NOS inhibitor. Hence, it was of interest to study the SAR of N^1-alkylguanidine. Furthermore, the preliminary study was also aimed at obtaining information about various aspects of the current study, range from the synthetic efficiency, handling of guanidino compound, execution of L-citrulline assays, to preliminary understanding of RegG.

An Introduction to Guanidines

The guanidino group exhibits distinctive physicochemical properties. Guanidine is highly basic (pKa (guanidine sulphate) = 13.6)[180]. The guanidino moiety can actively take part in hydrogen bonding interactions, as either a H-bond donor or acceptor. Once protonated, a guanidinium ion can participate in ionic interactions and behaves similarly as Na^+ and K^+. The basicity of guanidino group can be moderated by various N-substituents[181], which also modulates the hydrogen bonding patterns and metal coordination properties of guanidines. In addition, the extensive π-electron conjugation in the guanidino moiety enables it to participate in π-π conjugation interactions with aromatic systems[182].

Since the discovery of guanidine in 1861 by Strecker, hundreds of naturally occurring guanidino compounds have been identified[183]. Guanidine-containing compounds have been shown to exhibit various physiological, pharmacological and toxicological effects[184]. Physiologically, guanidino compounds are known to function as both phosphate-carriers and nitrogen-sinks (from which organisms derive various nitrogen-containing compounds)[184]. On the other hand, naturally occurring guanidino

compounds are found to exhibit several toxicological effects[184], which include the disruption of protein complex, blockade of membrane sodium or chloride channels, modulation of NO production[185], hypotension and hypoglycaemia. Interestingly, these physiological and toxicological effects are capitalised for pharmacological applications[184,186]. The guanidino group is found in several pharmacological classes of drug molecules, such as antidiabetic, antimalarial, diuretics, sympatholytics, antimicrobial, antifungal, antiviral, NMDA receptor antagonists and DNA binding agents[181,184].

Synthesis of Guanidines

Guanidines can be synthesised by several approaches as depicted in the following scheme (**Scheme 4**)[187]. In general, the guanidines can be synthesised through substitution reactions or addition reactions. The substitution reactions involve the substitution of amines on activated imino-containing functions, with the leaving group being less basic than the incoming amine. On the other hand, the addition reactions involved the addition of amines on linear carbodiimide- or cyanamide- containing groups with an electron deficient carbon centre.

The classical pathway of guanidine synthesis is the Rathke synthesis, a reaction developed in 1884[187]. The guanidine is synthesised *via* the substitution of S-methylisothiouronium salts by amines. Many variants of Rathke synthesis has been developed, mainly using thiourea or urea as the starting materials. Starting with a thiourea, the amidino function is activated by either converting the thiocarbonyl sulphur into thioether function, or replacing the sulphur with a more electronegative chloride. Subsequently, the activated amidino function is substituted by amines. Similarly, a urea can be activated as O-methylisouronium, chloroformamidinium (Vilsmeier salt)[188] or O-phosphorylisouronium[189] groups for subsequent nucleophilic

substitution. Besides that, there is another variant of Rathke synthesis where the leaving groups are heterocyclic, such as 3,5-dimethyl-1H-pyrazole-1-carboxamidine nitrate[190] and 1H-pyrazole-1-carboxamidine hydrocholoride[126]. Generally these heterocyclic-activated amidines are superior to S-methylisothiouronium sulphate for the synthesis of monoalkylguanidines, but less suitable for reaction with secondary amines[187].

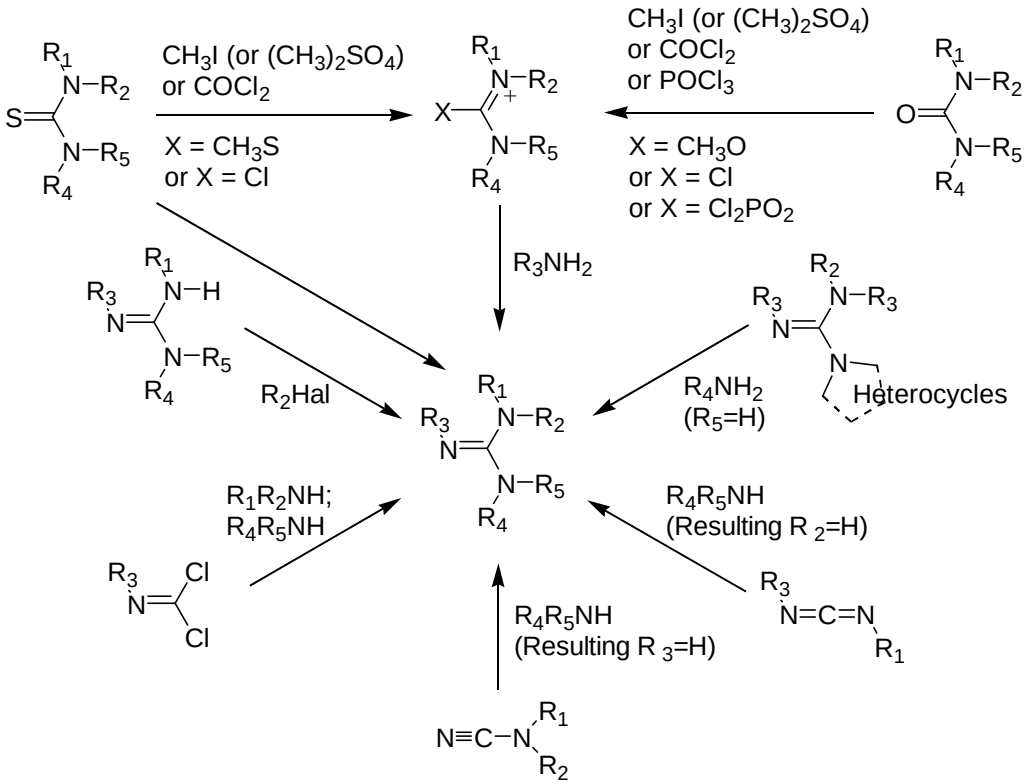

Scheme 4. Synthesis of Guanidine.

A non-Rathke synthesis of highly substituted guanidines involves the synthesis of guanidine from carbonimidic dichloride, the chloro groups of which are substituted with amines (with Vilsmeier salt as intermediate)[191]. On the other hand, direct alkylation of existing guanidines offers another route to synthesise guanidines with higher degree of substitutions. In addition, a thiourea can be converted directly into urea with the use of a suitable catalyst[192].

The addition of amine to carbodiimide[193] and cyanamide[194] represents a different approach to the synthesise of guanidine. It is of interest to highlight that in contrast to the Rathke synthesis, the highest degree of substitution possible with the addition reaction is tetra-substitution. Nevertheless, pentasubstitution has been demonstrated with the reaction of cyanamide and hexachloroantimonates at –78 °C[195]. Interestingly, carbodiimide has been used as a coupling agent for the synthesis of guanidine by reacting thiourea and alkylamine[196].

As shown above, several methods are available for the synthesis of differently substituted guanidines, ranging from unsubstituted guanidines to pentasubstituted guanidines. Each of the methods is associated with its strengths and weaknesses. The traditional Rathke synthesis is probably the most commonly adopted approach for the synthesis of guanidines. The reaction is more facile for ammonia and primary amines, but is less favourable with more hindered secondary amine[187]. Highly steric amines, such as t-butylamine, fail to react through traditional Rathke synthesis. Besides, if the incoming amine is lower in nucleophilicity, such as aniline, the alkylthiol may not be a good leaving group. As such, stronger leaving groups, such as S-chloro- and O-phosphoryl-isouronim salt, are more desirable. The Vilsmeier salt is suitable for the synthesis of sterically hindered and highly substituted guanidines[187]. Besides that, the methylthiol that is liberated during the traditional Rathke synthesis has an unpleasant odour, thus the use of alternative leaving groups if preferred. The aminoiminomethane sulphonic acid, a product of direct oxidation of thiourea with peracids, reacts at room temperature to give non-volatile sulphuric acid which is soluble in the reaction medium[197]. As for urea, it is generally used in a similar way as thiourea, with the alcohol (in place of alkylthiol) as the leaving group. However,

alcohol is a less favourable leaving group than alkylthiol, and thus the thiourea approach remains as a favourite choice.

The direct substitution on guanidines is usually performed with the use of alkyl halide[187]. However, the reaction usually results in a multicomponent mixture [r4006]. As a result, it is a less applied synthetic approach. Aromatic substitution on guanidine can also be performed through electrophilic substitution (Friedel-Crafts reaction) of guanidino group on a benzene ring[198]. As for the carbonimidic dihalides, it is reported that the reactivities of the starting dihalides and the intermediate Vilsmeier salts are different, thus enabling reaction with two different amines[191]. Although this represents an interesting approach for guanidine synthesis, precise control of substitution is not easily achieved, thus most of the reported reactions are on the synthesis of symmetrical guanidine with the same alkyl substitution on both guanidinium nitrogens[191].

Synthesis of N^1-Alkylguanidines

The traditional Rathke synthesis is used for the synthesis of N^1-alkylguanidine in the current study because the reaction is reported to give good yield with the use of simple primary and secondary amines, and the reagents are readily available commercially. A series of N^1-alkylguanidine sulphates was synthesised through the nucleophilic substitution of a variety of alkylamines on S-methylisothiourea sulphate (SMITUSO4) (**Scheme 5**). In order to achieve structural diversity of N^1-alkyl group, various subclasses of alkylamines, which include the aliphatic alkylamines, branched aliphatic alkylamines, cycloalkylamines, heterocyclic alkylamines and benzylamines, were used for the synthesis.

The synthesis of N^1-alkylguanidine sulphate from SMITUSO4 and alkylamine was rather straightforward. Generally the yield of the reaction was satisfactory (56%

- 98%). The N^1-alkylguanidines were found to have good water solubility. However, with bulkier alkyl substituents, the water solubility of N^1-alkylguanidine decreased, and some of the benzyl substituted compounds became rather water insoluble.

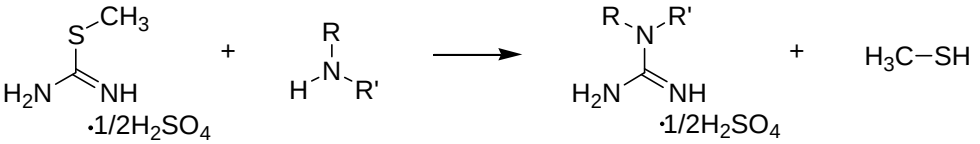

Scheme 5. Synthesis of guanidine sulphate *via* nucleophilic substitution of SMITUSO4 by amines.

It was observed that in order to achieve satisfactory reaction rate and yield, one of the reagents should be used as a salt while the other was preferable to be a free base. Both reagents in the same form would deter the progress of the reaction. It was found that no reaction occurred when both reagents were charged, and it was reported[182] that the rate and yield of reaction were low when both reagents were uncharged.

Biological Evaluation of N^1-Alkylguanidines

The compounds were screened for inhibitory activity against the three isoforms of NOS and those compounds with more than 10% inhibition at 125 μM were identified and evaluated for their IC_{50} values (**Table 2**). As shown in the table, the compounds were shown to be non-selective and relatively few compounds showed more than 10% inhibition at 125 μM. As compared to the rest of the series, compound **I** was the only compound showing inhibitory activities against all the three isoforms, with slight selectivity towards iNOS. Compound **III** (2-piperidinylamidine) showed a different inhibitory profile by being inactive against iNOS but showed weak inhibition against the constitutive NOS. On the other hand, compound **IX,** the most potent nNOS inhibitor among the N^1-alkylguanidines, demonstrated yet another inhibitory profile with some selectivity against nNOS.

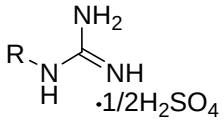

		nNOS		iNOS		eNOS	
	R	%Inh	$IC_{50} \pm SEM$	%Inh	$IC_{50} \pm SEM$	%Inh	$IC_{50} \pm SEM$
I	propyl	21.8	411.1 ± 23.8	51.7	99.3 ± 19.3	18.2	611.3 ± 103
II	isobutyl	< 10		< 10		< 10	
III	$–C_5H_{10}–$	21.6	468.5 ± 45.3	< 10		15.1	709.6 ± 151
IV	benzyl	< 10		< 10		< 10	
V	*p*-Cl-benzyl	< 10		< 10		< 10	
VI	*p*-CH_3-benzyl	< 10		< 10		< 10	
VII	*p*-NO_2-benzyl	< 10		< 10		< 10	
VIII	*p*-NH_2-benzyl	< 10		< 10		< 10	
IX	*m*,*p*-diCl-benzyl	31	261.8 ± 45.3	13.2	1849 ± 524	< 10	

Table 2. The % Inhibition at 125 μM and IC_{50} (μM) of N^1-alkylguanidines.

As indicated by X-ray crystallographic studies, the hydrophobic cavity above the haem was rather limited in size, as it could only accommodate alkyl groups as large as propyl or isopropyl group [r2056], but a butyl group (as in S-butylisothiourea) was found to be orientated out of the GBS into the $RegG^{105}$. As a result, among the N^1-alkylguanidines tested, only compound **I** was likely to bind to the hydrophobic pocket. Compound **I** was indeed found to show a tendency towards iNOS selective inhibition. The observed tendency towards iNOS inhibition was not surprising because S-ethylisothiourea was known to be iNOS selective. In contrast, the L-NPA, with a N-propylguanidino terminal, was found to be nNOS selective. As a result, it is postulated that simple alkylguanidine by itself could inhibit iNOS

selectively, but with the presence of other enzyme interacting groups, as in L-NPA, nNOS selectivity could be achieved. On the other hand, the inactivity of compound **II**, the isobutyl group of which was likely to be located in the RegG, suggested that the hydrophobic interaction, if any, in the RegG was weaker than the hydrophobic interaction the hydrophobic pocket above haem in proximal GBS (as shown by **I**), and that the weak hydrophobic interaction in the RegG, by itself, was insufficient for imparting good binding affinity to the N^1-alkylguanidine. As for compound **III**, it was found to inhibit constitutive NOS with similar IC_{50} values as compound **I**. However, it was not sure whether the cyclopentyl chain was fitted into the hydrophobic pocket above the haem, or orientated towards the substrate access channel.

For the rest of the series (**IV – IX**), the N-benzyl substituents were too bulky for binding to the hydrophobic cavity above the haem in proximal GBS, thus these substituents probably interacted with the RegG. However, the N^1-benzylguanidines were inactive, except compound **IX**, thus suggesting that the interaction of benzyl group in the RegG was rather weak. Nevertheless, the inhibitory activity displayed by compound **IX** was rather promising. The compound **IX** was the most potent nNOS inhibitor in the N^1-alkylguanidine series, and it showed a tendency of nNOS selectivity over iNOS and eNOS. Hence, the benzyl group, with suitable ring substitution, could contribute towards improved binding affinity and nNOS selectivity. This was a rather encouraging preliminary result that supported the hypothesis on the possible contribution of RegG towards inhibitor binding and nNOS selectivity.

Preliminary Protein Visualisation and Analysis

In order to understand the possible interactions of the alkylguanidino compounds in the nNOS active site, molecular protein viewer was used to elucidate the active site topology qualitatively. By early 2001, the X-ray crystallography of nNOS was not reported. As a result, eNOS-Arg complex crystal structure (Brookhaven code: 2NSE) was evaluated using the software Rasmol instead, assuming that nNOS active site was similar to that of eNOS as cited as unpublished data in literatures[175].

On close examination of the X-ray crystal structure of eNOS-Arg complex, four hydrophobic residues, namely Pro336, Val338, Met341 and Phe355, were identified around GBS with side chains protruding into the catalytic cavity. Detailed investigation showed that Pro residue was located above the guanidinium plane of the substrate L-Arg, outlining the non-reactive distal GBS. As a result, Pro residue would not be an ideal binding site because it was not readily accessible. On the other hand, a cluster of hydrophobic amino acids (Phe, Val and Met) was located very closely to the substrate L-Arg.

The Pro, Phe and Val were known as structural elements of the small hydrophobic cavity above the haem in the proximal GBS. On the other hand, through computational protein visualisation, it was found that Val and Met formed a hydrophobic zone above the haem group, and faced the substrate access channel. This hydrophobic zone was connected to the exposed hydrophobic surface of haem (the pyrrole ring A and D, and the associated propylene arm), forming a rather large area of hydrophobic region (**Figure 7**). This hydrophobic region might account for the hypothesised RegG. It was of interest to evaluate the presence of a similar

hydrophobic zone in nNOS (as part of the RegG), and availability of the hydrophobic zone for potential inhibitor binding.

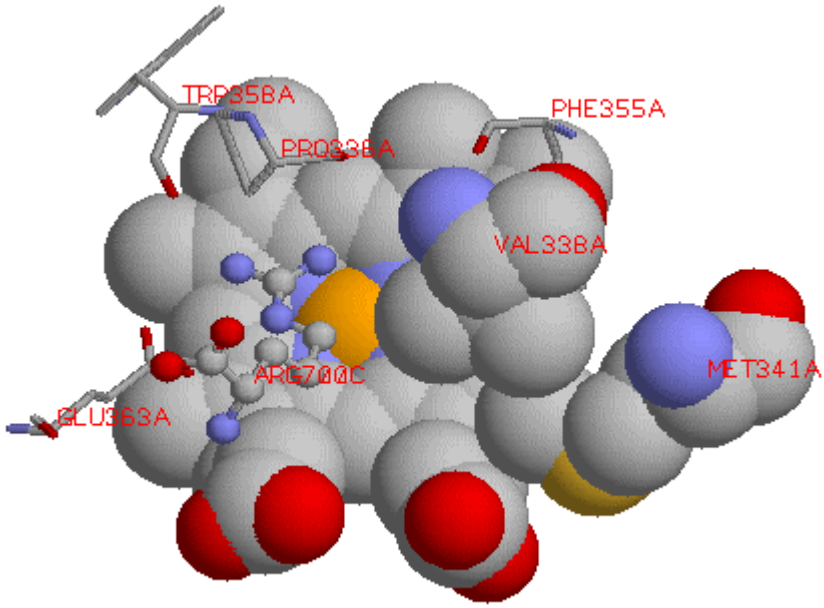

Figure 7. Hydrophobic region formed by Val, Met and haem.

Further analysis showed that the substrate L-Arg showed minimal interaction with the hydrophobic region. The distances from guanidino C_ζ of the L-Arg to the side chain of Phe, Val and Met were 7.47 Å, 5.659 Å and 8.388 Å respectively. While Phe and Met seemed to be involved in hydrophobic interaction with the haem, and Val appeared to be involved in some hydrophobic interaction with the aliphatic backbone of L-Arg (C_γ of Val is 3.824 Å from the C_δ of substrate L-Arg). This suggested that the hydrophobic region would play a minor role in the binding of L-Arg, and presumably, the binding of L-Arg based inhibitors to the NOS active site. The potential of this hydrophobic region of RegG for improved binding and selectivity remained to be explored.

Chapter 5 Solid Phase Organic Synthesis of N^1,N^2-dialkylguanidines. Part I.

The synthesis of N^1,N^2-dialkylguanidines is not as straightforward as N^1-alkylguanidines. A versatile synthetic scheme of N^1,N^2-dialkylguandines, in which the N^1-alkyl and N^2-alkyl are derived from chemically diverse and commercially available alkylamines, is sought after. As discussed in **Chapter 4**, the precise control of different substitutions on carbonimidic dihalides is not easily achieved, and the reaction produces multicomponent mixture. As for the substitution using alkylhalides on guanidines, multicomponent mixture is produced and protective groups are to be employed. On the other hand, the Rathke synthesis and its variants requires the synthesis of N-alkyl substituted guanylating precursors prior to the synthesis of N^1,N^2-dialkylguanidine. Similarly, the use of cyanamides and carbodiimides is also limited by the need of synthesising N-alkyl substituted cyanamide and carbodiimide in advance. As a result, regardless of the synthetic approach, the synthesis of N^1,N^2-dialkylguanidine involves multisteps of reactions, for which the solid phase organic synthesis (SPOS) is a preferred approach.

Solid Phase Organic Synthesis (SPOS)

Since the Merrifield's report[199] on solid-supported peptide synthesis in 1963, SPOS has captured the attention of the community of chemists; and the technology has been employed for the synthesis of DNA, RNA, small organic molecules, new materials and catalysts. The field of chemistry is revolutionised by this ingenious synthetic approach and Merrifield was awarded the Noble Prize in Chemistry for his great contributions[200].

In SPOS, a reagent is attached to a suitable solid support, while the other reagent(s) are introduced as solution (in which the solid phase is immersed) and the reaction takes place on the solid support. The yield and rate of the reaction can be

increased by the addition of excess reagents. The removal of excess reagents and solvents, as well as the isolation of final compounds can be easily accomplished through simple filtration and washing. In addition, the use of solid support results in a "pseudo-dilution" effect[201], in which the polymeric framework separates the functional groups from each other, and thus reducing the inter-site reactions even with the use of excess reagent. These unique characteristics position SPOS as a suitable approach for multisteps reactions.

However, SPOS is not without drawbacks. The loading of the solid phase is low, and thus the yield of compounds is low in absolute term. Being a recent advancement in chemistry, limited literatures are available, and the range of reaction permitted on solid phase is also limited. Furthermore, not all solution phase reactions are transferable (or yet to be transferred) as solid phase reactions. Hence, a lot of time is often spent on the development and optimisation of a solid phase reaction, a process that is quoted as the most time-consuming process in SPOS[202]. As compared to solution phase synthesis, several additional factors, such as the solid support, spacer and linker, are influencing the outcome of the SPOS. The lack of suitable analytical techniques for the analysis of SPOS further complicates the optimisation work[203,204]. However, once the optimised condition is identified, the subsequent large-scale synthesis of compound libraries can be performed in a relatively short duration.

The solid support is an insoluble functionalised, polymeric material to which library members or reagents may be attached, allowing them to be readily separated (by filtration, centrifugation, etc.) from excess reagents, soluble reaction by-products or solvents[201]. The purification process is simplified as washing-filtration cycles, which is convenient and timesaving. The solid supports for synthesising small organic molecules include crosslinked organic polymers, linear organic polymers, dendrimers

and inorganic supports[205]. In practice, the most commonly used solid support is the commercially available small spherical resin (cross-linked polymer) beads. Several criteria have to be considered in the selection of solid support[206]. The solid phase should be insoluble (or can be precipitated after the reaction), in order to capitalise on the filtration process, but swellable (or soluble) in the reaction medium, to maximise the rate and extent of the reaction. A linker and probably a spacer should be present to link the substrate to the solid phase, and the solid support, spacer and linker should be inert to the reagents and the reaction conditions used. A spacer is usually an inert functionality flanked between the polymeric support and the linker[206]. The spacer serves to distant the reaction site from solid support, and to modify the swellability of polymer. As a result, a spacer allows the functional groups to rotate more freely and increases the accessibility of dissolved reagents to the site of reaction. A linker is a bifunctional chemical moiety attaching a compound to a solid support, which can be cleaved to release compounds from the support[201]. A careful choice of linker allows cleavage to be performed under suitable conditions. The linkers should be quantitatively loaded onto the solid phase and the attachment of linkers to solid supports or spacers should be chemically stable throughout the synthesis. The attachment of the linker to the solid support is generally realised *via* stable covalent bonding (such as ether, amide or alkyl bonds)[207]. A large number of linkers have been developed for various reaction conditions and cleavage condition[206].

To meet the specific needs of various reactions, a variety of cleavage approaches for releasing the products from the linkers have been developed, such as electrophilic cleavage, nucleophilic cleavage, light cleavage, metal-assisted cleavage, reductive cleavage, cyclisation-based cleavage, and safe-catch cleavage[207,208]. Even for the same linker, different cleavage conditions are developed to suit the need of the

attached compounds[207]. After cleavage, some of the released products may carry residual portion (remnant) of the linker and this may limit the utility of the linker. In addition, due to the reversibility of some cleavage reaction, scavengers are to be added to drive the reaction forward and to minimise the side reactions[207]. The success of cleavage is dependent on the spacer, degree of polymer crosslinking, resin loading, resin bead size, and resin swellability in cleavage solution[207].

With the advancement in SPOS technologies and the mass production of libraries of compounds, the conventional analytical techniques are not well equipped to meet the specific needs of SPOS in terms of speed and compatibility[203-204]. The analysis of SPOS products can be classified into on-bead analysis and off-bead analysis[203]. The on-bead analysis of immobilised intermediates and products provides real-time information about the reaction, but several characteristics of SPOS chemistry limits the choice of analytical techniques for on-bead analysis[203]. The solid support interferes with analysis by generating extra signals and noises. Besides that, the analysis is complicated by the heterogeneous reaction condition and the high equivalence of reagents used. As a result, the on-bead analysis is often complemented with off-bead analysis, in which the compound is detached from the solid support for analysis. A wide range of analytical techniques can be applied for the off-bead analysis. However, off-bead analysis is often time-consuming and destructive[203-204], and uncertainty arises on whether the on-bead compound is the same as the cleaved compound analysed after to the cleavage reaction.

Both FTIR and NMR are useful techniques for on-bead analysis, while techniques such as MS, UV and NMR are applicable for off-bead analysis. FTIR is the technique of choice for rapid real-time monitoring of the progress of reaction[203-204] by detecting the transformation of functional groups. However, FTIR does not provide

sufficient information for structural elucidation and the analysis is interfered by background noises from the solid support. The most recommended FTIR technique is the microscopic one-bead FTIR, and diffuse reflectance infrared Fourier transformed spectroscopy (DRIFT) is a commonly used alternative. Solid state NMR is another on-bead analytical technique[203-204]. NMR is useful in elucidating the structures of the compounds and indicating the degree of reaction completion. However, NMR requires high power NMR spectrometer and long analytical duration, which is a limiting factor for the high-throughput analysis of chemical libraries. The frequently suggested on-bead NMR technique is the magic-angle NMR, which eliminates most of the signal-broadening effects originated from solid support. Alternatively, gel phase NMR, in which the resins are swollen in a solvent to form a pseudo-homogenous gel like system, can also be performed using conventional NMR techniques. MS is a useful but destructive off-bead analysis[203-204]. MALDI and TFA-vapour cleavage strategies have been applied to accelerate the rate of analysis. The use of MS coupled HPLC (LCMS) is a very useful technique for analysing the components of the mixture of compounds, and estimating the progress and yield of reaction. UV and fluorescence spectrophotometry are also used as off-bead quantitative techniques in SPOS[203-204]. Besides that, functional group specific reactions can be performed to quantity the functional group on the solid support. The elemental combustion analysis has also been performed on the resin to determine the yield of the compounds[204].

SPOS of Guanidines

A range of SPOS of guanidino group had been developed, and the general principle of synthesis was the same as the synthetic routes described previously (**Chapter 4**). The traditional Rathke's synthesis had been adapted as solid phase reaction. In one of the reports, the guanidine precursor, isothiourea, was produced by

the methylation of thiourea, which was in turn obtained through reacting a resin bound amino group with fluorenylmethoxycarbonyl isothiocyanate[209]. However, upon cleavage, part of the linker was incorporated as one of the N-substituent, thus limiting the versatility of the reaction. Variants of Rathke's synthesis were also reported as SPOS, in which a thiourea was introduced onto the Wang resin *via* a carbonylimidazole linker[210]. The attractiveness of this reaction was the traceless cleavage, but long procedures were involved. Furthermore, the versatility of the reaction was limited because one of the N-alkyl substituents was to be introduced as N-alkylthioureas, the availability and variety of which were limited commercially. Another reported variant of Rathke's synthesis produced N-acyl-N'-carbamylguanidine, and heavy metal (mercury) was used[211]. The use of pyrazole carboxamidine linkage to a solid support was also reported[212]. The guanidine was formed through the reaction with an amine and guanidine produced was N-acylated.

An ingenious isothiourea-based reaction using the thio group as the anchor to the solid support was reported[213], but the reaction produced N-(mono)alkylguanidine (instead of N^1,N^2-diaklylguanidine). In another study, the solid-linked acylisothiocyanate reacted with an amine to give thiourea, which was subsequently activated by carbodiimide and reacted with another amine to give acylated guanidine[214]. Carbodiimide activated thiourea was also reported in another study where the thioureas was synthesised from (preferably aromatic) isothiocyanate[215]. A study on solid phase synthesis of oligomeric guanidines suggested that the method of choice to synthesise guanidine was to react resin bound amine with carbodiimide-activated thiourea[216]. However, considering the need for diversification of the N-substitution, the carbodiimide-activated thiourea approach was limited in versatility because of the limited variety of commercially available thioureas. On the other hand, electrophilic

guanylating agent had also been reported to guanylate a resin bound amine[217], and a variation using PEG support was also reported[218]. A pyrazole-based guanylating agent was also used for guanidine synthesis[219]. Generally, these reactions were limited by commercial availability and versatility of the guanylating agents. In some cases, the guanidine itself was used as the anchoring moiety to the solid phase *via* sulphonyl chloride based linker[220]. Attachment of guanidino group to the solid support *via* sulphonylamide and isothiourea were also reported[221].

Some synthetic schemes involved the use of reactive or harmful reagents. A highly versatile reaction through the carbonimidic dichloride approach was reported but this method required the use of reactive phosgene[181]. On the other hand, heavy metal was employed in a SPOS scheme where a thiourea was converted to guanidine by use of amine and mercury[222]. The thiourea was formed on the diazonium linker though the use of thioisocyanate, the variety of which was rather limited commercially.

Several carbodiimide-based syntheses had been reported[223-225]. The carbodiimide was obtained through aza-Wittig reactions using isothiocyanate or isocyanate. However, limited commercial supply iso(thio)cyanates, from which one of the guanidino N-alkyl substituents was derived, limited the versatility of the reactions. In some of the synthesis, part of the linker was incorporated to the final guanidine product, which might be undesirable. A novel synthesis was reported by synthesising guanidine through the coupling of azide and phosphine with aromatic isothiocyanate, but one of the N-substituents of the resultant guanidine contained an amide group[226].

As shown above, not all the reported SPOS of guanidines were suitable for the synthesis of N^1,N^2-dialkylguanidines. Some of the reported reactions yielded only monosubstituted guanidines[227]. In some cases, the reaction was suitable for the synthesis of N^1-alkyl-N^2-arylguanidines rather than N^1,N^2-dialkylguanidines[215]. On the

other hand, some of the cleaved guanidines were substituted with part of the linker fragments, which usually contain acyl terminal moeities[212,226,228]. For those SPOS suitable for the synthesis of N^1,N^2-dialkylguanidines, the synthetic schemes were generally limited in terms of the choice of reagents, diversity of the building blocks, presence of linker remnant on the product, duration of reaction and cost of reaction. Among the reported reactions, three of the reactions seemed to be more versatile and universal[181,213,225], however each of these is not without drawbacks (as discussed above). As a result, there was a lack of versatile and relatively safe SPOS of N^1,N^2-dialkylguanidine. Hence it was of interest to devise a new synthetic route for synthesising guanidine from carbodiimide. The SPOS of guanidine through the addition of alkylamine to carbodiimide had been reported[226], but the syntheses of the intermediate carbodiimide were not versatile.

Synthesis of Carbodiimides

Carbodiimide belongs to the heterocumulene family, which possesses an integral carbon-nitrogen double bond. Like other heterocumulenes, the cumulative double bond in carbodiimide results in high reactivity towards nucleophilic and cycloaddition reactions. A carbodiimide can be synthesised from various routes (**Scheme 6**). The phosgeneimines (route **A**) are useful starting reagents for the synthesis of heterocumulenes due to their enhanced reactivity[229]. Prolonged heating of phosgeneimines with alkylamine hydrochlorides produces carbodiimides with the evolution of hydrogen chloride[205,230]. Elimination reaction involving isothioureas, thioureas or ureas (route **B**, **C**, **D**) represents a general practical approach for synthesising heterocumulenes. In particular both ureas and thioureas are useful starting materials for synthesising carbodiimides[229]. Carbodiimides can be obtained through thermal[229] or heavy metal ($AgNO_3$, HgO, $HgCl_2$)[229,231] catalysed desulphurisation of S-

alkyl or S-acyl-isothioureas, or the based-catalysed[232] decomposition of the S-(N-methylpyridinium)isothioureas (route **B**). Heavy metal catalysed desulphurisation of 1,3-dialkyl- and 1,3-diaryl-thioureas, assisted by dehydrating agents (or azeotropic distillation) for the removal of water, provided a good general preparative method for carbodiimides[229,233] (route **C**). Carbodiimides can also be obtained *via* the dehydration of 1,3-dialkyl and 1,3-diaryl-ureas using a variety of chlorinating agents, such as phosphorus pentachloride[234], phosphorus oxychloride[229], toluene-p-sulphonyl chloride[235] and phosgene[231,234] (route **D**). Carbodiimide can also be synthesised from the rearrangement of heterocycles (route **E**). Triphenylphosphine-catalysed breakdown of 5-imino-1,2,4-thiadiazolines generates imidoylcarbodimides[236]. Besides that, the thermal-induced rearrangement of 1,5-disubstituted tetrazoles produces carbodiimide[231]. The carbodiimide synthesis using isocyanates and isocyanides (route **F**) is applicable to the synthesis of symmetrical and unsymmetrical carbodiimides containing alkyl, aryl, and alkenyl substituents[229,233,237-239].

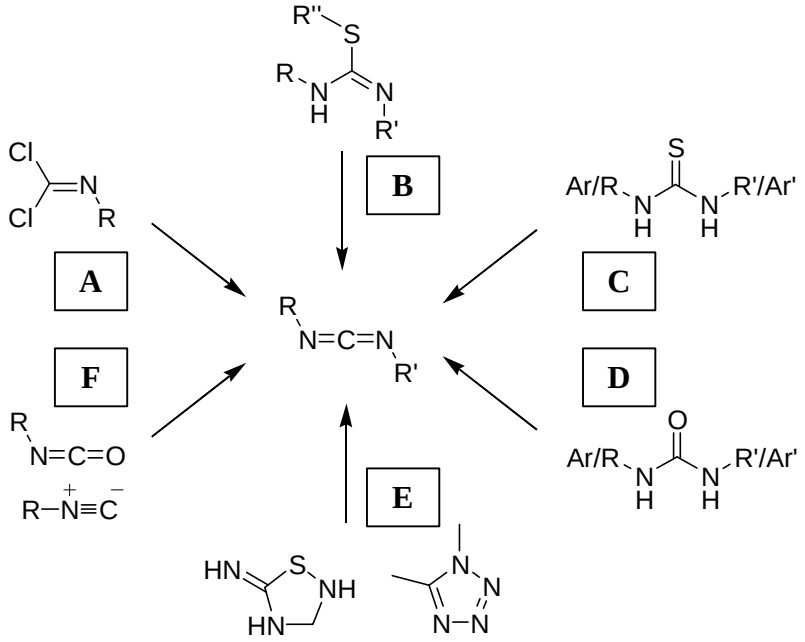

Scheme 6. Synthetic routes to carbodiimide.

For the current study, the need to introduce alkylamines as N-alkyl substituents disqualified heterocycles (route **E**) to be used as carbodiimide precursors. For the remaining synthetic routes, the use of reactive phosphogiminium (route **A**) was out of favour due to safety concerns, and the use of isocyanates (route **F**) was not ideal for synthesis because isocyanates themselves are synthesised through similar synthetic routes as carbodiimides. As a result, the employment of urea, thiourea or isothiourea (route **B**-**D**) as carbodiimide precursor was preferred. In this study, it was decided to synthesise carbodiimide *via* the dehydration of urea.

A review on the SPOS of carbodiimide showed that the most commonly synthetic approach was through the use of isocyanate (route **F**)[223-225]. However, the reaction lacked general applicability and versatility due to the employment of limited availability of iso(thio)cyanate instead of alkylamines as building blocks. In another report, carbodiimide was synthesised from urea through the use of p-toluenesulphonyl chloride as dehydrating agent. However, the synthesis of urea in this report involved the use of isocyanate, which is limited in commercial availability and molecular diversity, as building blocks. Nevertheless, a very versatile SPOS of urea had been reported in good yield[240,241]. The SPOS of urea employed alkylamines as the building blocks to give N^1-alkyl-N^2-(RinkResin)urea. With the on-bead urea, subsequent dehydration reaction would produce the N^1-alkyl-N^2-(RinkResin)carbodiimide, which could react with alkylamine to give N^1,N^2-dialkyl-N^3-(RinkResin)guanidine, and thus generate the N^1,N^2-dialkylguanidine upon cleavage. As a result, the reaction scheme was able to fulfil the objective of this study for achieving versatility in synthesis and to maximise the structural diversity of the guanidines, in which both N^1-alkyl and N^2-alkyl would preferably be derived individually from different alkylamine building blocks, while the N^3 was kept unsubstituted.

A Proposed SPOS of N^1,N^2-dialkylguanidine

A six-step SPOS reaction scheme was devised for the synthesis of N^1,N^2-dialkylguanidines, starting from the Rink resin (**Scheme 7**).

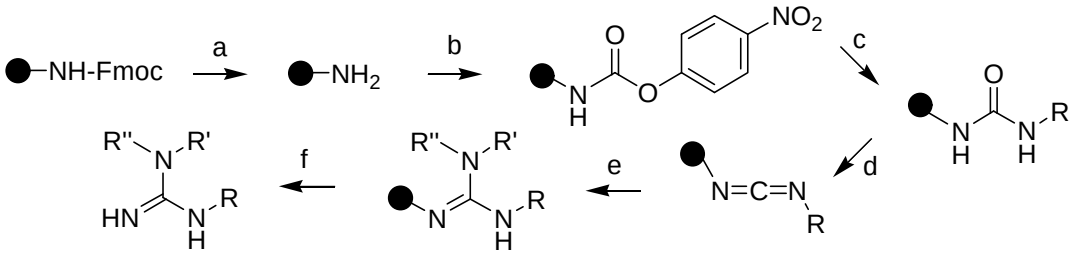

Scheme 7. SPOS reaction scheme proposed.

Deprotection of the Rink resin was carried out first in step (a). This was followed by carbamylation of amino function (step (b)). Step (c) involved the formation of urea, and the dehydration of urea was carried out in step (d). This was followed by the formation of guanidine in step (e). The last step (f) was the cleavage of guanidine from the resin. The synthesis of urea on Rink linker (steps (a) to (c)), and the cleavage of urea directly from the Rink linker were reported as SPOS[240,241]. Besides that, step (d) was reported as solid phase reaction[242] while steps (e) and (f) were reported as SPOS of guanidines[226,241]. Hence, the reaction conditions for steps (a), (b), (c), (d), (e) and (f) could be modified from literature reports. Nevertheless, the reported reaction schemes for each reaction employed different solid supports and linkers, and hence the reaction conditions might need to be optimised when applied in the current study.

In order to ensure that the reaction sites in the interior of the resins were accessible to the reagents, the resins were immersed and allowed to swell in DCM for at least 8 hours prior to synthesis[243]. Being lighter than DCM, the resins were found floating on the surface of DCM, and a significant increase in the volume of the resin was observed. The swollen resins were slightly yellowish white in colour.

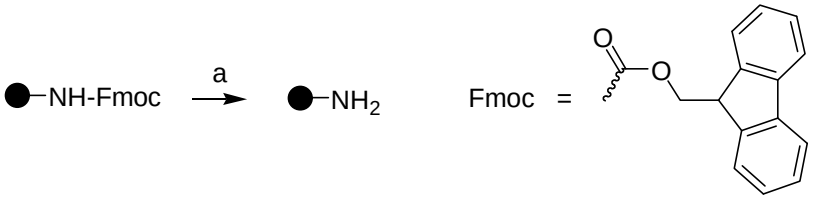

The amino group of the Rink resin was protected by Fmoc through carbamate linkage. Fmoc was stable to acidic condition and quite resistant to catalytic hydrogenolysis, but was cleavable by a base[244,245]. In this study, Fmoc was deprotected using piperidine[246]. The deprotection procedure was formulated as a 30-minute reaction at room temperature with the use of 20 %v/v piperidine in DMF [r8704]. The deprotected resin was whitish in colour.

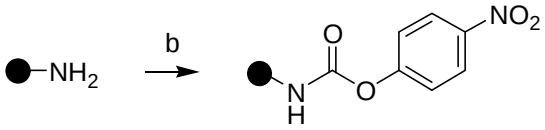

The free amino group was carbamylated by p-nitrophenyl chloroformate (p-NO_2PhOCOCl), which was a carbonyl group donor with two different leaving groups of varying reactivity. The formulated reaction condition was a 30-minute reaction at room temperature with the use of a mixture of 0.5 M p-NO_2PhOCOCl and 0.5 M DIEA in THF/DCM (1:1)[221,240]. After the reaction, the resins turned yellow in colour, which is characteristic of nitro-containing compounds.

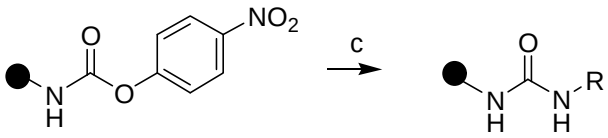

Subsequently, alkylamine was added to the on-bead carbamates to give urea. The leaving group, p-nitrophenol, gave a characteristically intense yellow coloured solution, while the resin was milky white in colour. Excess alkylamine was used to ensure complete reaction and good yield, and the production of the urea was

ascertained by using LC-MS. The reaction was carried out for 30 minutes at room temperature with the use of a mixture of 0.5 M alkylamine and 0.5 M TEA in DMF[221,240].

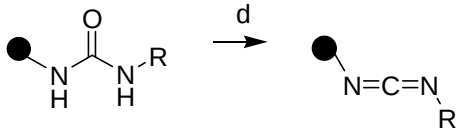

The dehydration of urea into carbodiimide was reported as a solid phase reaction, which involved refluxing the urea with 1.5 equivalents of TosylCl and 5 equivalents of TEA in DCM for 50 hours[242]. However, when the reaction condition was adopted in this study, the yield of carbodiimide was low. Furthermore, the reaction duration of 50 hours which was less then optimal. As a result, the reaction condition was to be optimised (**Chapter 6**).

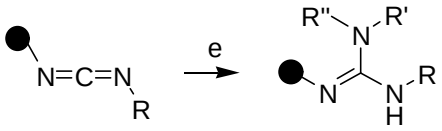

The guanidine was formed *via* a nucleophilic addition of alkylamine to the carbodiimide[226]. Both primary and secondary amines were used in the reaction. The reaction condition was designed as a 24-hour reaction at 50 °C with the addition of 0.5 M (mono/di)alkylamine in THF/DCM (1:1).

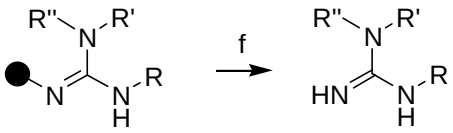

Cleavage of guanidine and urea from the Rink resin had been reported, and the conditions were adapted for this synthesis[221,240]. Prior to cleavage, the resins were washed thoroughly with several cycles of various solvents (DCM, THF, acetone, methanol and water). The cleavage was effected using 5% TFA in DCM[247]. In early

studies, a pink colouration was observed in the solution upon cleavage. The pink colouration due to the partial cleavage of the Rink linker could be minimised with the use of 1% methanol as scavenger[247]. The resin became black in colour upon cleavage, probably due to the formation of carbocation on the resin. This visual change was also a good indication of the progress of the cleavage process.

In order to increase the yield and enhance the resultant purity of the compounds, the post-cleavage purification was optimised (**Chapter 6**). The solution containing the product was concentrated using rotary evaporation, and solvent-solvent extraction was subsequently performed. The product was isolated as a yellow liquid and stored in a desiccator.

Chapter 6 Solid Phase Organic Synthesis of N^1,N^2-dialkylguanidines. Part II.

In the previous chapter, a synthetic scheme for N^1,N^2-dialkylguanidine was designed, in which the carbodiimide intermediate was to be generated through dehydration of urea. However, then the reaction condition for dehydration of urea to carbodiimide was applied in the current study, the yield was low despite 48 hours of reaction. As a result, it was necessary to optimise the formation of carbodiimide. Besides that, the post-cleavage purification was also optimised for better yield and purity of the final product. However, the optimisation of the synthetic conditions turned out to be challenging and time-consuming.

Dehydration of Urea in Solution Phase Reaction

In solution phase synthesis, various dehydrating agents have been used for the synthesis of carbodiimide from urea. An early method developed for urea dehydration involved the use of p-toluenesulphonyl chloride (TosylCl) in pyridine, which served as both the base and the solvent[235]. The use of large amount of pyridine was replaced by the use of triethylamine (TEA) as the base and methylene chloride (DCM) as the solvent in the reaction[248]. An optimised protocol of this reaction was reported as the slow addition of reagent mixture (TosylCl/TEA in DCM) to the urea at less than 10 °C, followed by 3 hours of reflux[235].

Besides that, dehydration using triphenylbromophosphonium bromide (Ph_3PBr_2) was also reported[249]. Urea dehydration was achieved by refluxing the urea with a mixture of Ph_3PBr_2 and TEA in benzene. Subsequent study eliminated the use of benzene as solvent. The urea was added to a suspension of Ph_3PBr_2 in cold DCM with TEA as base. The reaction was monitored using FTIR and good yields were reported[249]. Another reported reaction utilised triphenylphosphine in tetrachloromethane as the dehydrating system[250].

Phosphorous pentoxide (P_2O_5) was also used to dehydrate urea[251]. The urea was refluxed with 5 equivalents of P_2O_5 in pyridine for 135 minutes and reasonable yield was obtained. However, this was a stand-alone case report of synthesis with no further follow up studies. On the other hand, phosgene ($COCl_2$) had been used to chlorinate the urea to give imidochloride, which generated carbodiimide through base-induced dehydrohalogenation[248]. Phosphorous pentachloride (PCl_5) was reported to react with urea and, after a series of intermediary reactions, generated carbodiimide and phosphorous oxychloride $POCl_3$[207]. It was postulated that the PCl_5 reacted with urea to give chloroformamidinium chloride and thiophosphoryl chloride, with the later to be removed before the formation of carbodiimides.

Among the urea-dehydrating agents, the most commonly applied reagent was TosylCl, with reported yield in the range of 50 – 80%. As for the Ph_3PBr_2, the good yield was reported in 70-75%, while the efficiency of the Ph_3P/CCl_4 was comparable to the Ph_3PBr_2. The reaction using P_2O_5 was an unoptimised case report. As a result, two of the dehydrating agents, TosylCl and Ph_3PBr_2, were selected for further SPOS development for this study.

Dehydration of Urea in Solid Phase Reaction

The only report on the dehydration of urea into carbodiimide was through the use of TosylCl as dehydrating agent[242]. However, the reaction required long hours (50 hours) of reflux, and the reported condition resulted in low yield when applied in the current study. Hence there was a need to optimise the reaction condition, and the reaction condition for solution phase reaction was used as a reference.

The optimisation study relied heavily on the availability of appropriate analytical techniques. Since the carbodiimide has a characteristic spectroscopic profile as compared to urea, FTIR was a suitable tool to monitor the change in functional

group. During the early phase of the optimisation, the dehydration of urea was monitored using FTIR, and the sample was prepared as KBr disc. However, it was reported that the polystyrene resin could not be compressed easily into a disc[204]. Thus diffuse reflectance infrared fourier transform (DRIFT) was used instead. Using a large number of scans (n=512), DRIFT gave good IR spectra, with an acceptable sample preparation and analytical duration of around 15 minutes per sample. The data was acquired in transmission mode (%T), but was converted to absolute absorbance scale (Abs) for determining the peak area. Through DRIFT, the success of the dehydration of urea was indicated by the appearance of the carbodiimide $\nu_{C=N}$ band in the region of 2120-2130 cm^{-1}. The 2120-30 cm^{-1} region was rather clean and practically free from interference by the resin matrix, but the urea $\nu_{C=O}$ band (~ 1650 cm^{-1}) could not be easily detected due to background interference of the resin polymer. As a result, DRIFT analysis was unable to monitor the degree of urea-to-carbodiimide inter-conversion. Nevertheless, DRIFT analysis provided information on the generation of carbodiimide group, and the extent of carbodiimide formation could be interpreted as the ratio of the peak area of the carbodiimide $\nu_{C=N}$ peak to the peak area of a reference peak. The selected reference peak (which was a signal originated from the solid support) was the twin-peak at 1845 – 1995 cm^{-1}, the peak area of which remained consistent in size and shape regardless of the group immobilised on the resin. Comparison of the peak ratios over time provided a good indication of the progress of the dehydration.

Since DRIFT did not indicate the consumption of urea, LCMS was used instead as a tool to monitor the progress of the dehydration. However, as an off-bead analysis, LCMS requires the cleavage of the product from the resin using TFA. Since the carbodiimide could react with TFA to give urea and acid anhydride, it was necessary to

convert the carbodiimide into guanidine prior to cleavage. This was achieved by the addition of (2-methyl)propylamine to the carbodiimide to give guanidine. Subsequently the guanidine was cleaved from the resin and subjected to LCMS analysis. The use of methanol-water mixture as mobile phase resulted in a tailing of the highly basic guanidines over a long duration on the Eclipse XDB-C8 column (4.6 mm x 15 cm). As a result, the mobile phase was changed to 0.01%TFA methanol-water misture, which eliminated the tailing problem. However, the resolution of the two peaks was poor. The N^1-substituted urea was eluted slightly earlier than the N^1,N^2-disubstituted guanidine. As a result, high proportion of water was used initially during the gradient elution to suppress the elution of the more hydrophobic guanidine, followed by an increasing proportion of methanol at the later phase of elution.

The validity of using LCMS as a tool to monitor the extent of reaction was supported by gel phase ^{13}C NMR. The off-bead analysis through LCMS cast doubts on whether the urea detected was the unreacted urea or the reaction product of TFA and carbodiimide during cleavage. As a result, on-bead ^{13}C NMR was performed. It was found that the peak ratio of guanidino carbon to ureido carbon in the NMR study was consistent with the peak ratio of guanidine to urea in LCMS study. This indicated that the urea detected in the LCMS was not a reaction product of acidic cleavage.

Using the above analytical techniques, the dehydration efficiency of two dehydrating agents, TosylCl and Ph_3PBr_2, was evaluated. The initial conditions used on solid phase were modified from the solution phase reaction conditions, with an increased equivalence of the reagents (5 equivalents). The urea-bound resin was reacted with Ph_3PBr_2 in DCM at 0 °C, and progress of the reaction was monitored using DRIFT. After two hours of reaction at ice bath temperature (as suggested by the solution phase reaction), the yield was found to be low, according to the intensity of the

carbodiimide $\nu_{C=N}$ band appearing at 2123 cm^{-1}. The ineffective dehydration might be attributed to the heterogenous reaction condition where both the resin and Ph_3PBr_2 were suspended in DCM. Hence, THF/DCM (1:1) was used instead in order to immerse the resins and increase the yield. However, a strong IR band was observed at 2200 cm^{-1} instead, indicating that the carbodiimide was not formed. The lack of carbodiimide formation was further supported by the lack of reaction between the functional group responsible for 2200 cm^{-1} and (2-methyl)propylamine.

On the other hand, the dehydration reaction using TosylCl was initiated by the addition of TosylCl at less than 10 °C to the urea-bound resin, followed by refluxing (the solution phase synthetic condition). DRIFT showed that after two hours of reflux the peak area of carbodiimide $\nu_{C=N}$ peak showed no further increment. The carbodiimide formed was indicated by the appearance of $\nu_{C=N}$ at 2120-30 cm^{-1}, while no IR band at 2200 cm^{-1} was observed.

According to this comparative study on the efficiency of the dehydrating agents, TosylCl was considered superior to Ph_3PBr_2 as suggested by its dehydration efficiency, and the lack of side products. In addition, in terms of cost, Ph_3PBr_2 was almost 20 times more expensive than TosylCl. As a result, TosylCl was selected as the dehydrating agent for the subsequent optimisation study.

Optimisation of Dehydration of Urea by TosylCl

With the use of LCMS, it was surprising to find that the reaction did not proceed to completion (i.e. urea still present), even with 5 equivalents of TosylCl, long reaction time, and replacement with fresh reagent. Solvents with different refluxing temperatures were used, with the aim to modify the rate and the yield of the reaction. The use of tetrahydrofuran (THF) and toluene resulted in similar yield of carbodiimide as compared to the original dichloromethane (DCM). High boiling point solvent, N,N-

dimethylformamide (DMF), was also used but DMF was found to react with the carbodiimide formed. In addition, attempts to use diisopropylamine (DIEA), instead of triethylamine (TEA), as a base gave no significant improvement in carbodiimide yield.

Hence, the reaction was not optimised, and it was necessary to understand the mechanism of the dehydration in order to troubleshoot the problem encountered. There was no report on the mechanism of urea dehydration by TosylCl. However, a related dehydration mechanism involving amide and TosylCl was suggested[252]. With reference to the mechanism of amide dehydration, a mechanism of urea dehydration was proposed (**Scheme 8**). The carbonyl oxygen of urea was sulphonylated to give O-(p-toluenesulphonyl)-N-alkyl-N'-(RinkResin)-isourea. The hydrochloric acid liberated was trapped by a base as HCl salt. Subsequent electron delocalisation led to the formation of carbodiimide with p-toluenesulphonic acid being trapped as sulphonate salt. As suggested by the mechanism, the O-sulphonylisourea and the carbodiimide were in equilibrium. Thus in order to increase the yield of carbodiimide, it was necessary to prevent the backward reaction by efficient trapping of acids as salt.

On the other hand, if the salt formation with a base was not complete, the free p-toluenesulphonic acid would react with the carbodiimide, generating p-toluenesulphonyl anhydride and urea[253] (**Scheme 9**). The resultant sulphonyl anhydride would have similar reactivity as the sulphonyl chloride, and it would dehydrate the urea into carbodiimide. Hence, the reaction could be reversible. The reversibility of the reaction was not surprising as there were reports on the use of sulphonyl anhydride to dehydrate urea into carbodiimide[254], as well as the reaction of carbodiimide with sulphonic acid to give sulphonyl anhydride and urea[255].

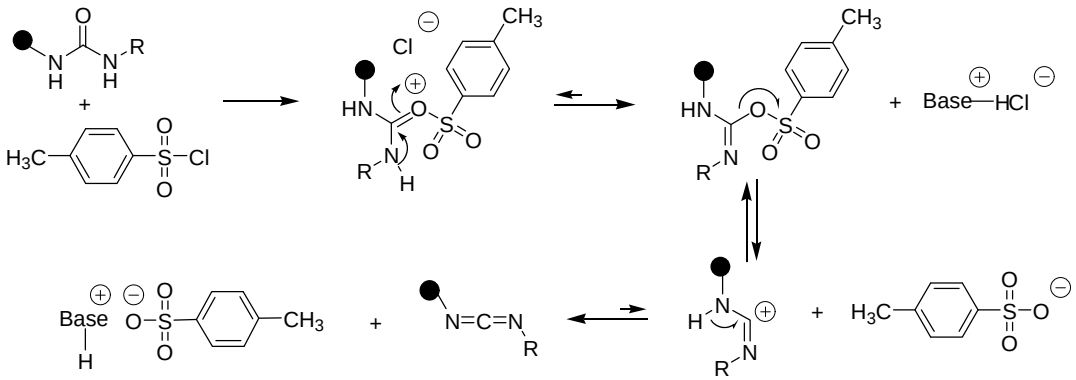

Scheme 8. Proposed mechanism of dehydration of urea by p-toluenesulphonyl chloride.

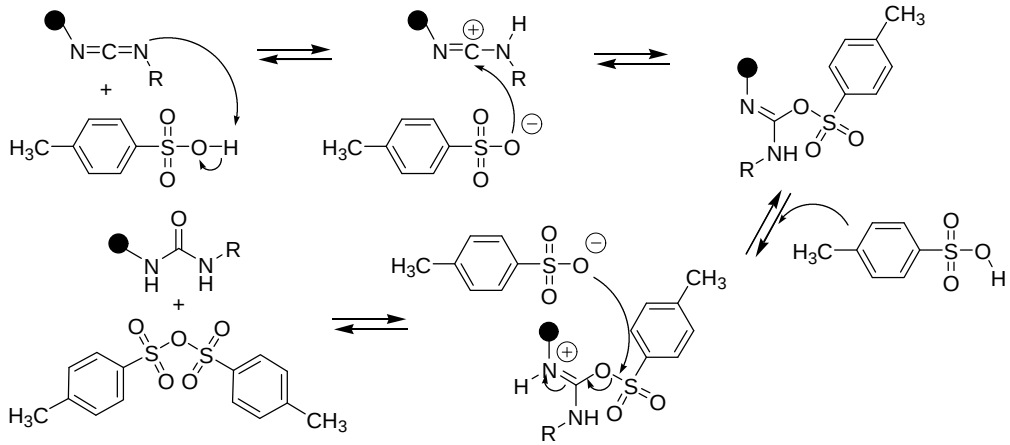

Scheme 9. Proposed mechanism of reaction between sulphonic acid with carbodiimide, resulting in urea formation together with sulphonyl anhydride.

Comparing the two mechanisms (**Scheme 8** and **Scheme 9**), the dehydration by TosylCl is likely to be non-reversible due to the weak basicity of Cl^-. However, this was not the case for the dehydration by Tosyl anhydride, which was reversible. Besides that, the two mechanisms shared a common intermediate, O-(p-toluenesulphonyl)-N-alkyl-N'-(RinkResin)-isourea, which highlighted the similarity between the two reactions. As a result, with the availability of sulphonic acid as a result of inefficient salt formation, a vicious cycle could be established. The urea was continuously dehydrated and regenerated through the common intermediate O-sulphonylisourea. Thus, the reaction could not proceed to completion and it was essential to remove the sulphonic acid. It was believed that the incomplete reaction in

the preceding studies was due to the inefficient salt formation of sulphonic acid with a base.

Following the above reviews, optimisation was performed in the direction of increasing the amount of base, as well as increasing equivalency of TosylCl. Since pyridine had been used as solvent for dehydration using TosylCl in solution phase reaction, TEA/pyridine (1:3) was used as the solvent instead of the reported TEA/dichloromethane (1:3) with the rationale that large excessive base would trap the sulphonic acid formed[256]. Through the study, the optimal condition identified was to react the resin-bound urea with 5 equivalents of TosylCl in triethylamine/pyridine (1:3) at ice-bath for 30 minutes followed by 4 hours of reflux. As expected, the percent of conversion of urea into carbodiimide was higher than the previous experiments. However, it was observed that an additional IR band was observed at 2200 cm^{-1}, which was the same band that appeared in the preliminary study using Ph_3PBr_2. This band occurred quite readily, even after only 30 minutes reaction at ice-bath temperature.

It appeared that the TEA/pyridine system was not the optimal base for urea dehydration due to side reactions. Hence, phase transfer catalyst (PTC) was employed as an alternative[257]. The use of PTC was theoretically an ideal approach, as the PTC would trap the sulphonic acid formed, and the partitioning of the sulphonate salt between different phases would minimise the availability of the sulphonic acid in the organic phase. Thus the backward reaction was prevented.

Triethylbenzylammonium chloride (TEBA-Cl) was used as the PTC, with the dehydration reaction occurred in the organic phase while the sulphonic acid partitioned into the complementary phase[257]. Two different systems, the 20 % NaOH solution and the sodium bicarbonate (Na_2CO_3) solid, were used as the complementing phase, and 5 equivalents of TEBA-Cl was applied[257]. However, the yield of carbodiimide as shown

by DRIFT was low when performing the dehydration in DCM/NaOH system at ice-bath temperature. By subjecting the reaction to reflux temperature for 24 hours, the yield of carbodiimide was still low. The use of Na_2CO_3 solid as the second phase gave higher yield as compared to the 20 % NaOH solution. Nevertheless, the yield of carbodiimide using PTC was lower than that of the TEA/pyridine system. As a result, the investigation using PTC was discontinued, and the focus of optimisation was reverted back to previously developed TEA/pyridine system.

In order to force the equilibrium forward to give carbodiimide, it was decided to increase the amount of TosylCl. To the on-bead urea, 10 equivalents of TosylCl in TEA/pyridine/DCM (2:1:1) were added and reacted at 64 °C for two hours. The yield of carbodiimide was satisfactory. However, the formation of an IR band at 2200 cm^{-1} still persisted. In a study using 9 equivalents of TosylCl in pyridine, a large IR band at 2249 cm^{-1}IR was observed, with minimal formation of carbodiimide at 2120 cm^{-1}.

A nitrile group could be responsible for IR band ($\nu_{C\equiv N}$) at 2200 cm^{-1}. The structure of the nitrile group was not elucidated, but a few possibilities were deduced theoretically (**Scheme 10**). The formation of nitrile could possibly arise from both urea and carbodiimide as suggested by literature reports[258,259,260].

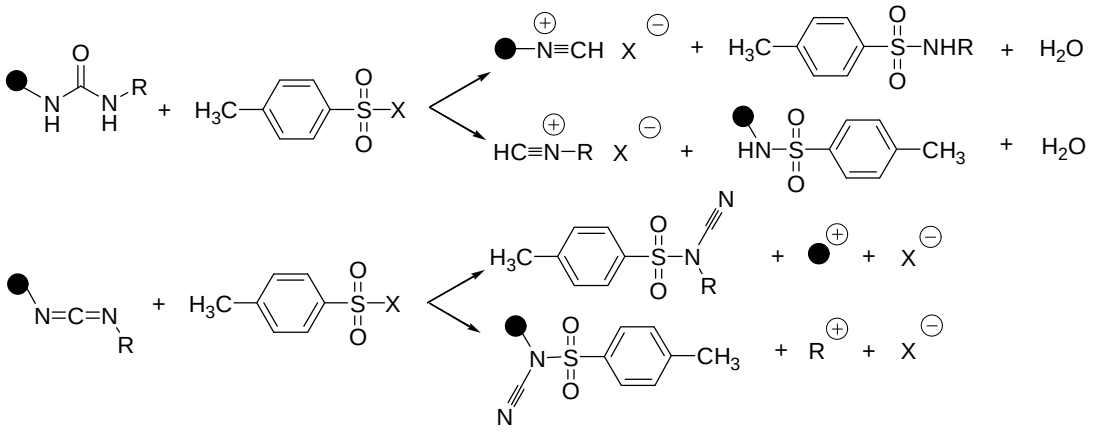

Scheme 10. The proposed formation of nitrile functional group which may be derived from either urea or carbodiimide. (X = Cl-, CH_3PhSO_3-)

As shown in the scheme, only half of the nitrile group was formed on the resin, while the other half was found in the solvent. Thus theoretically resin-bound nitrile, resin-bound sulphonyl and functionless resin should be observed under IR. However, the IR region for the sulphonyl function was indistinguishable from the background signals of the resin, while the functionless resin was not identifiable, thus only the nitrile band was observed. On the other hand, the use of LCMS was unable to elucidate the exact identity of the compounds.

Nevertheless, it was known from observations that the rate and yield of nitrile formation was enhanced under several conditions, such as high reaction temperature, long reaction duration and the presence of pyridine. The use of TEA without the use of pyridine resulted in low carbodiimide yield, and the reaction was stagnant after a few hours of reflux, after which, with longer duration of reflux, there is a decrease in peak area (absorbance mode) for $\nu_{C=N}$ (2120 – 30 cm^{-1}) accompanied by the appearance and increasing peak area (absorbance mode) for $\nu_{C\equiv N}$ (2200 cm^{-1}). On the other hand, the use of TEA with pyridine (acting as solvent and base) improved carbodiimide formation, but this also resulted in formation of nitrile. Interestingly the formation of nitrile seemed to be associated with the presence of pyridine. With pyridine, the nitrile bond (C≡N) was observed even only after 30 minutes of reaction in the ice-bath. As reaction progressed at 100 °C, more nitrile was formed with the consumption of carbodiimide, as evident from changes in the peak area of IR bands. Furthermore, with pyridine as the sole base, the yield of carbodiimide was extremely low, while the yield of nitrile group was high. This suggested the critical role of pyridine in producing the nitrile group. Hence the amount of pyridine was to be controlled carefully, and the role of pyridine was re-examined, and it was found that pyridine, which was initially believed to act as a base, could have actually behaved as catalyst[261]. TosylCl was

activated by pyridine to give a reddish colour complex, which was observed in the reaction. As a result, pyridine should be used as a catalyst in minimal amount, while the role of removing the sulphonic acid through salt formation should be performed by TEA.

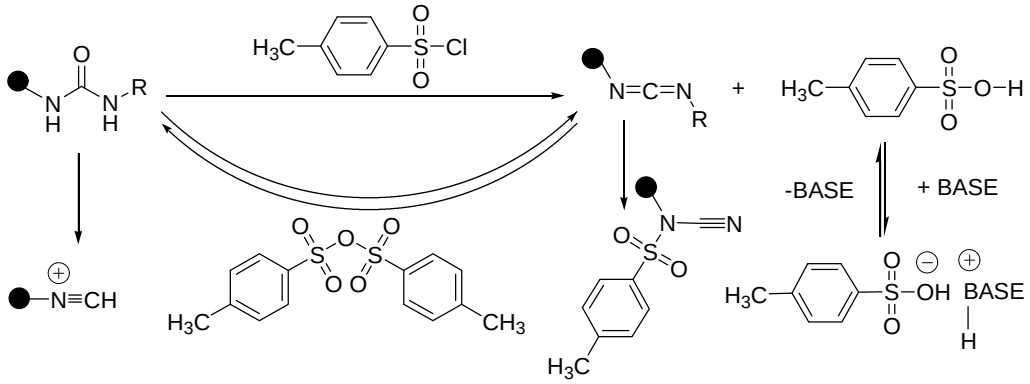

Scheme 11. A proposed scheme depicted the concurrent reactions in the process of urea dehydration.

Combining the three mechanisms of reaction, an overall picture of the reactions involved in the dehydration of urea using TosylCl could be mapped (**Scheme 11**). Several reactions were occurring concurrently. The urea was dehydrated by TosylCl to give carbodiimide, and this was followed by the equilibrium between urea and carbodiimide (though sulphonyl anhydride and sulphonic acid interconversion), and finally nitrile groups were formed, possibly from both urea and carbodiimide. This scheme could be used to explain the yield (around 70%) reported with solution phase synthesis, which was believed to be due to the urea-carbodiimide equilibrium and the degradation process.

As suggested by the **Scheme 11**, in order to increase the yield of carbodiimide, it was necessary to increase the amount of TosylCl and to remove the sulphonic acid formed. The removal of sulphonic acid could be achieved by salt formation, as well as physical removal of the salt from the reaction system. As for minimising the side

reaction, it was achievable through using milder reaction conditions, such as lower reaction temperature, shorter reaction duration and lower amount of catalytic pyridine.

The physical removal of sulphonate from the reaction system was achieved through washing cycles. It was observed that the reaction became stagnant after a period of reflux, and large amount of insoluble sulphonate salt appeared during the reaction. Hence, by splitting the reaction into several cycles with the use of fresh reagents mixture, the reaction system was supplied with fresh TosylCl for urea dehydration, while the sulphonates were physically removed. Therefore, the regeneration of urea as a result of carbodiimide-sulphonic acid reaction was minimised.

As a result, several approaches for optimising the dehydration of urea were attempted, which included the use of catalytic amount of pyridine and low reaction temperature, as well as performing the reaction in several cycles with the addition of fresh reagents. The optimisation study showed much improvement when these approaches were taken. The catalytic pyridine was used in one to one ratio to TosylCl. The reaction was monitored in blocks of 15-minute, and it was found that the reaction proceeded rapidly and significant dehydration was achieved in a short reaction time. Yellowish sulphonate crystals were formed within short period of time, and the dehydrated resin was found to be reddish orange in colour. Using on-bead N-(n-propyl)-N'-resin-urea as a model, the optimal dehydration condition was to react the resin-bound urea with a mixture of 0.5M TosylCl and 0.5M pyridine in TEA/DCM (1:1), with pyridine as catalyst and TEA as base. The reaction was carried out at room temperature with fresh addition of reagents in three intervals of 15/15/30 minutes. It was found that the yield of carbodiimide was maximised with minimal formation of nitrile.

However, this optimal condition had to be adjusted according to the bound urea because it was found that the rate of reaction was different with different N^2-alkyl substituents on the urea. Generally, a urea with a linear N^2-alkyl group would react faster than a urea with a N^2-benzyl or N^2-cyclohexyl group, probably due to the steric impediment of the N^2-alkyl group against the incoming TosylCl. Thus a different set of reaction duration was developed using the same reagent mixture for the dehydration of urea with hindered N-alkyl moiety. The optimised condition was to carry out the reaction at room temperature in three intervals of 30/30/60 minutes, with fresh addition of reagents at each interval.

Optimising Post-Cleavage Workup

Following the optimisation of carbodiimide formation, the conditions for all six steps of SPOS reaction were developed. However, the final yield obtained was low, which was a result of unoptimised post-cleavage workup. The direct evaporation of the cleavage solution using rotary evaporator was ineffective. After evaporating the solution at 40 °C, a yellowish thick liquid with strong acidic odour was obtained, and this suggested that the acid removal by evaporation was ineffective and the yellow liquid obtained was a concentrated TFA solution with dissolved guanidine. By rotary evaporating at higher temperature (50 – 60 °C) in order to get rid of the TFA, black residue was obtained, most probably as a result of acidic decomposition of the guanidines. Hence, it was necessary to remove the TFA completely, and it was also important to avoid the formation of concentrated TFA solution in the process of TFA removal.

Hence, liquid-liquid extraction between solution containing the cleaved product and NaOH solution was performed. Interestingly, guanidine was detected in both the aqueous phase and the organic phase as shown by LCMS. This resulted in a lower

guanidine yield as the guanidine in the aqueous layer could not be effectively recovered. In addition, the TFA salt might be soluble to some extent in the organic phase, thus multiple back extractions were required to remove the TFA salt, and this further lowered the final yield. Besides that, sodium hydroxide might decompose the guanidines[262]. Thus liquid-liquid extraction using NaOH solution was not advisable.

In order to overcome the above problems, several modifications were performed to the purification process. Water was added to the solution containing the cleaved product. Since the boiling point of TFA (75 °C) is lower than water, water remained as the last solvent to be evaporated off, and thus preventing the formation of concentrate TFA solution. Furthermore, the low water-solubility of the free base form of N^1,N^2-dialkylguanidine resulted in saturated solution and subsequently the appearance of brownish immiscible droplets in the aqueous concentrate. This served as a visual cue to stop the evaporation. Subsequently, DCM was added to the emulsion and extraction was performed twice using water. Both aqueous and organic extracts were analysed using LCMS. The aqueous layer was devoid of guanidine while the organic layer contained the guanidine. Furthermore, being more hydrophilic than the corresponding guanidine, the urea, if present, was partially removed by the aqueous phase. After drying with anhydrous sodium sulphate, the decanted DCM solution was rotary dried, and a thick yellowish liquid was obtained as the final product.

Optimised Condition for Synthesising N^1-Monoalkyl-N^2-(mono/di)alkylguanidines

After the optimisation studies, an optimised condition was obtained and illustrated in the following scheme (**Scheme 12**).

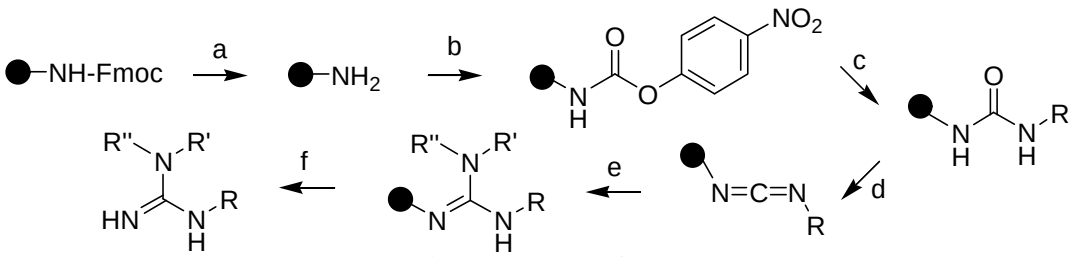

Scheme 12. Optimised SPOS of N^1-monoalkyl-N^2-(mono/di)alkylguanidine.
a. 20%v/v Piperidine/DMF, 30 minutes at room temperature
b. 0.5 M p-Nitrophenyl chloroformate and 0.5 M DIEA in THF/DCM (1:1), 30 minutes at room temperature
c. 0.5 M RNH_2 and 0.5 M TEA in DMF, 30 minutes at room temperature
d. 0.5 M p-Toluenesulfonyl Chloride and 0.5 M pyridine in TEA/DCM (1:1), three intervals: 15/15/30 minutes for unbranched alkyl chain, and 30/30/60 minutes for hindered alkyl chain at room temperature
e. 0.5 M, R'(R'')NH in THF/DCM (1:1), 24 hours at 50 °C
f. TFA/MeOH/DCM (5:1:94), two intervals of 15 minutes at room temperature

The optimised reaction for synthesising carbodiimide from urea would be a useful reaction with general applicability, not limited to the synthesis of guanidine. Carbodiimide is a versatile group that acts as a precursor for synthesising a variety of functional groups such as guanidines, ketenes, isourea, amide and anhydride[255]. With respect to the synthesis of N^1,N^2-dialkylguanidines, this optimised SPOS scheme had several advantages over the other published methods. The SPOS scheme allowed the use of structurally diverse and readily available alkylamines, which constitute the N^1-alkyl and N^2-alkyl substituents of the guanidine, as building blocks. The reaction was performed under rather mild conditions without the use of highly reactive or harmful reagents. The whole experiment could be completed within two working days. Furthermore, the cost of the experiment was kept minimal since the reagents were readily available commercially at low cost. However, due to the intrinsic nature of the reaction, the synthetic route was only suitable for the synthesis of N^1-monoalkyl-N^2-(mono/di)alkylguanidine, but not N^1-dialkyl-N^2-dialkylguanidine. Nevertheless, in terms of inhibiting NOS, this was not a concern as N^1-dialkyl-N^2-dialkylguanidine is unlikely to bind to the active site of NOS due to steric hindrance.

The optimisation of SPOS was quoted as the most time-consuming process in SPOS research[263]. From this study, it was shown that simple transfer of solution phase synthesis into solid phase synthesis using the same conditions was not feasible. The use of suitable analytical tool was critical for the optimisation study. Besides that, a good understanding of the mechanisms of reaction was important for optimising the reaction.

Chapter 7 Solid Phase Organic Synthesis of N^1,N^2-dialkylguanidines. Part III.

In the preceding chapters, the SPOS of N^1,N^2-alkylguanidines was designed and developed with reference to literature reports. With proper understanding of the mechanisms of the reaction, the dehydration of urea into carbodiimide was optimised. The optimised condition identified was to be put to practicality use by synthesising a series of N^1-(mono)alkyl-N^2-(mono/di)alkylguanidines.

Synthesis of N^1-Monoalkyl-N^2-(mono/di)alkylguanidines

Using the optimised conditions, six N^1-monoalkyl-N^2-(mono/di)alkylguanidines with representative N-alkyl groups were synthesised. The alkyl substituents were selected with the aims of evaluating the efficiency of using alkylamines as building blocks, as well as establishing the SAR of N^1,N^2-dialkylguanidines (**Table 3**). The $\%yield_{crude}$ reported was the yield of guanidine obtained after the post-cleavage liquid-liquid extraction. The purity was determined using LCMS. The $\%yield_{adj}$ (%yield adjusted to purity) was 3-75%. The varying

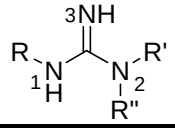

	R (N^1)	R' (N^2)	R'' (N^2)	$\%yield_{crude}$	% Purity	$\%yield_{adj}$
X	N^1-Propyl	N^2-Benzyl	H	46	83	38
XI	N^1-Propyl	N^2-Diphenylmethyl	H	38	52	20
XII	N^1-Propyl	N^2-(2,4-diCl-)Benzyl	H	128	59	75
XIII	N^1-Propyl	N^2-C_5H_{10}-N^2		17	30	5
XIV	N^1-Benzyl	N^2, N^2-Diethyl		32	11	3
XV	N^1-Cyclohexyl	N^2-C_5H_{10}- N^2		26	45	12

Table 3. The yield, purity and %yield (adjusted to purity) ($\%yield_{adj}$) of the N^1-(mono)alkyl-N^2-(mono/di)alkylguanidines.

%yield$_{adj}$ was rather unexpected. For all compounds, DRIFT study showed that carbodiimide $\nu_{C=N}$ band was present after the dehydration. Regardless of the N-alkyl substituents, the ratios of the peak area of carbodiimide $\nu_{C=N}$ peak to the peak area of reference peak were comparable. Thus this suggested that the synthesis of carbodiimide was successful and unlikely to result in the observed varying %yield$_{adj}$.

Compounds **X** – **XIII**, in which the N^2-substituent was varied while the N^1-substituent remained the same, were synthesised from the same carbodiimide intermediate. However, moderate %yield$_{adj}$ were obtained by reacting primary alkylamines with the carbodiimide (compounds **X** – **XII**) regardless of the bulkiness of the primary alkylamine. On the other hand, lower %yield$_{adj}$ was achieved when secondary alkylamine was used (compound **XIII**). This suggested that the efficiency of secondary alkylamine to react with carbodiimide was less than that of primary alkylamine. The inefficient addition of the secondary alkylamine to carbodiimide also observed for compounds **XIV** – **XV**, which were produced in low %yield$_{adj}$ regardless of the size of N^1-alkyl group on the carbodiimide. Hence the low %yield$_{adj}$ was probably attributed to the steric hindrance on access of the bulky secondary alkylamine to the carbodiimide. The carbodiimide was located close to the polymeric matrix as it was connected to the polystyrene matrix *via* a Rink linker, which was rather short and bulky. As a result, the conformational flexibility of the carbodiimide was restricted and the accessibility of carbodiimide to the bulky secondary alkylamine was limited.

While the lower %yield$_{adj}$ of N^2-disubstituted guanidines (**XIII** – **XV**) as compared to N^2-monosubstituted guanidines (**X** – **XII**) suggested that the varying %yield$_{adj}$ might be due to incomplete guanidine formation from carbodiimide, an alternative inference was that the incomplete cleavage of carbodiimide from the resins

was a contributing factor to the low %yield$_{adj}$. Due to the bulkiness of the N^1-(mono)alkyl-N^2-(di)alkylguanidine, which was located near to the resin matrix, the accessibility of the TFA to the Rink linker was restricted, and resulted in inefficient cleavage.

Generally, the reactions produced guanidines in moderate to low yield$_{adj}$. The yield$_{adj}$ of the reaction was dependent on the bulkiness of the N^2-alkyl moiety. However, in view of the involvement of 6-step reactions in the synthesis, the yield$_{adj}$ was acceptable. Nevertheless, the optimised condition for SPOS synthesis of carbodiimide from urea served as a good synthetic route with general applicability in synthesising carbodiimide, which is a general precursor to a variety of compounds[255].

Biological Evaluation of N^1-Monoalkyl-N^2-(mono/di)alkylguanidines

The six compounds were evaluated by the L-[^{3}H]citrulline assay using the three NOS isoforms. The concentration of guanidines prepared was adjusted for the purity of the sample. Initial screening was performed at 125 μM. Since the purities of some of the samples were moderate to low, it was decided that only compounds showing at least 50 % inhibition at 125 μM as compared to the predetermined 10% inhibition (**Chapter 13**) was to be further evaluated for the corresponding IC_{50} value (**Table 4**). The process of reaction optimisation for this SPOS reaction scheme was tedious and time-consuming. As a result, by the time this library of compounds were synthesised, significant biological data was already obtained for the other concurrent series of compounds, the N^1-alkyl-N^2-nitroguanidines (**Chapters 11**, **12**). Hence, the present data could be discussed and compared to the data obtained from the other concurrent studies.

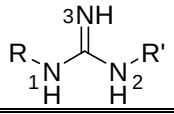

	nNOS		iNOS		eNOS	
	%Inh	IC_{50} ± SEM	%Inh	IC_{50} ± SEM	%Inh	IC_{50} ± SEM
X	< 50		< 50		< 50	
XI	73.8	54.6 ± 2.2	< 50		< 50	
XII	< 50		< 50		< 50	
XIII	< 50		< 50		< 50	
XIV	59.6	83.3 ± 3.6	< 50		< 50	
XV	< 50		< 50		< 50	

Table 4. % Inhibition at 125 μM and the corresponding IC_{50} (μM) values for compounds showing more than 50 % inhibition at 125 μM.

The most active compound was compound **XI**, N^1-(n-propyl)-N^2-(diphenyl)methylguanidine, and it was shown to be nNOS selective. Similarly, the compounds **XIV**, N^1-benzyl-N^2,N^2-diethylguanidine, showed inhibitory activity against nNOS while inactive against both iNOS and eNOS, suggestive of nNOS selective inhibition. The improved binding and nNOS selectivity of the compound **XI** was believed to be attributed to the N^1-(diphenyl)methyl substituent. This highlighted the binding enhancement though N-(diphenyl)methyl substituent, as well the larger active site cavity of nNOS than those of iNOS and eNOS. Similar information was obtained from the concurrent series of N^1-alkyl-N^2-nitroguanidines (**Chapters 11**, **12**), and this suggested that the N^2-nitro and N^2-propyl substituents did not differ much in their role in contributing to the affinity and selectivity of the N^1,N^2-(disubstituted)guanidines. On the other hand, comparing compound **XIV** with N-benzyl substituted compound **X**, it was found that the N^2,N^2-diethyl substituent could

result in enhanced binding to the nNOS, as well as improved selective nNOS inhibition. According to the understanding of X-ray crystallography of NOS (**Chapter 1**), it was probable that the N^2,N^2-diethyl substituent was directed towards the haem iron and formed hydrophobic contact with the small hydrophobic cavity above the haem. The cavity was shown to be larger in nNOS than in iNOS and eNOS, thus possibly explaining the selective inhibition observed.

The interpretation of biological results obtained was complicated by the low purity of the SPOS products. Nevertheless, the biological results for this series of compounds was comparable to the results obtained from the concurrent nitroguanidine series (**Chapter 11**, **12**), suggesting that similar SAR and molecular probing information could be obtained from the other concurrent studies. As a result, it was decided not to pursue further in this series of compounds.

Chapter 8 N^1-Alkyl-N^2-nitroguanidines. Part I.

Along with the optimisation of the SPOS of N^1,N^2-dialkylguanidines, a concurrent study on the NOS inhibitory activity of N^1-alkyl-N^2-nitroguanidines was initiated. The study on N^1-alkyl-N^2-nitroguanidine was initiated with reference to the prototypical NOS inhibitor L-NA. The Fe_{haem}-interacting N^{ω}-nitro group was not oxidised by NOS[36], and hence, nitroguanidino compounds were potential NOS inhibitors.

The aim of the study was to understand the SAR of N^1-alkyl-N^2-nitroguanidines as nNOS selective inhibitors, and to evaluate the role of hydrophobic interaction in RegG. For the series of N^1-alkyl-N^2-nitroguanidines, the N-substituents were limited to alkyl group, and the incorporation of additional functional groups was avoided in order to minimise confounding factors for the results interpretation.

Synthesis of N^1-Alkyl-N^2-nitroguanidines

As compared to N^1,N^2-dialkylguanidines, the synthesis of the N^1-alkyl-N^2-nitroguanidines was rather easy as the N^2-subsituent was nitrated, and only the N^1-alkyl group was varied for chemical diversity. The N^1-alkyl-N^2-nitroguanidines can be synthesised by several approaches[264]. Nitration of N^1-alkylguanidines by nitric acid produces N^1-alkyl-N^2-nitroguanidines[264]. However, the nitration reaction is not specific to guanidine. An alternative synthetic approach is a modified Rathke synthesis, which involves the substitution of alkylamines on nitroguanylating agents, such as N-nitroguanidine or S-methyl-N-nitroisothiourea (SMNNITU)[198,264]. For the substitution on N-nitroguanidine, the reaction is likely to be complicated by side reaction (dinitrogen oxide being produced), and it is not suitable for the synthesis involving higher secondary amines. Hence, the latter nitroguanylating agent, SMNNITU, was selected for this study.

The N^1-alkyl-N^2-nitroguanidine was synthesized through nucleophilic substitution of alkylamine on SMNNITU, which was in turn synthesized from the nitration of SMITUSO4 (**Scheme 13**)[198]. A series of structurally different N-alkyl subsitituents was selected for the synthesis, and these included primary alkyl (unbranched and branched chains), secondary alkyl, and benzyl groups. The chain length of the alkyl groups was kept short so that the alkyl chains would not interact with other sides beyond the RegG.

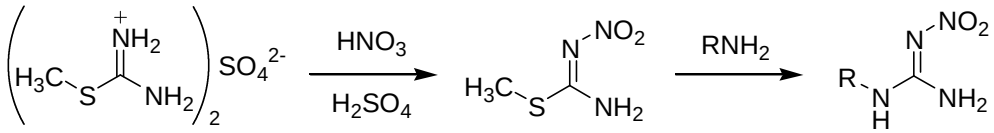

Scheme 13. Synthesis of N^1-alkyl-N^2-nitroguanidine.

The synthesis of SMNNITU was conducted at ice-bath temperature. The SMITUSO4 was added slowly into the nitrating mixture, consisting of fuming nitric acid and concentrated sulphuric acid, which produced the nitrating agent, nitronium ion (NO_2^+)[265]. The product was obtained as a precipitate by pouring the reaction mixture into crushed ice.

As compared to SMITUSO4, the SMNNITU is less basic due to the electron withdrawing effect of the nitro group. The presence of the nitro group results in a more electrophilic ureido carbon, hence SMNNITU reacts readily with a nucleophile (such as alkylamine). As compared to the reaction between SMITUSO4 and alkylamine (**Chapter 7**), the reaction between SMNNITU and alkylamine demanded both reagents to be in their free base form, as the alkylamine HCl salt was found to be unable to react with SMNNITU.

The yield of SMNNITU was reported as 90%[198]. However, in current study, lower yield of 40-60% was consistently obtained after the crude product was

recrystallised twice from aqueous ethanol. The difference in yield might be due to differences in experimental settings such as reaction temperature and duration, as well as recrystallisation process. It was found that with forced cyrstallisation at low temperature (to increase the yield) resulted a mixture of (mainly) needle-shape crystals and (a little of) cube-shape crystals, with the former shape was reported as the appearance of SMNNITU. Thus, the recrystallisation was performed at room temperature in order to have pure crystals (at the expense of lower yield).

The reaction between SMNNITU and alkylamines progressed well. All the alkylamines reacted smoothly with SMNNITU at reflux temperature with ethanol as solvent. It was found that the reaction could also progress under solventless condition (without the use of solvent as reaction medium) at room temperature, with the exception of secondary alkylamines which required mild heating under solventless condition. In order to ensure good yield and the completion of the reaction, the reflux approach was preferred to the solventless approach. It was noted that dicyclohexylamine, a bulky secondary alkylamines, was unable to react with SMNNITU despite long hours of reflux.

The reaction was monitored using TLC. Interestingly, the methylthiol produced in the reaction was a good indicator of the progress of the reaction. Cessation of the methylthiol production indicated the completion of the reaction. The crude yield of the reaction was generally in the range of 30-70%, depending on the solubility of the nitroguanidines in the reaction solvent (ethanol). The compounds were recrystallised from aqueous ethanol. The pure crystals were subsequently characterised and subjected to L-citrulline assay.

Biological Evaluation of N^1-Alkyl-N^2-nitroguanidines

The compounds were tested against nNOS, iNOS and eNOS using L-citrulline assay (**Table 5**). As shown in the table, the NOS inhibitory activities were demonstrated by two groups of nitroguanidines, the N^1-alkyl(unbranched)-N^2-nitroguanidines (**XVII**, **XVIII**) and N^1-benzyl-N^2-nitroguanidines (**XXIII** – **XXV**). On the other hand, the nitroguanidines with N^1-alkyl(branched) (**XIX**, **XX**) and N^1,N^1-dialkyl substituents (**XXI**, **XXII**) lacked NOS inhibitory activity. In terms of isoform selective inhibition, the series of compounds showed a general trend toward constitutive NOS inhibition over iNOS.

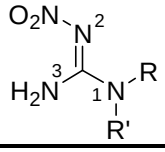

			nNOS		iNOS		eNOS	
	R	R’	%Inh	$IC_{50} \pm SEM$	%Inh	$IC_{50} \pm SEM$	%Inh	$IC_{50} \pm SEM$
XVI	H	H	23	377.4 ± 55.7	<10		20	367.1 ± 15.7
XVII	Methyl	H	32	285.0 ± 12.6	<10		34	265.6 ± 21.1
XVIII	Propyl	H	50	139.8 ± 35.3	<10		34	226.0 ± 27.6
XIX	Isobutyl	H	<10		<10		<10	
XX	Cyclohexyl	H	<10		<10		<10	
XXI	Methyl	Methyl	<10		<10		<10	
XXII	Ethyl	Ethyl	<10		<10		<10	
XXIII	Benzyl	H	34	192.6 ± 16.8	<10		23	383.8 ± 113.4
XXIV	*p*-Chlorobenzyl	H	26	343.2 ± 37.5	<10		<10	
XXV	*m*-Chlorobenzyl	H	101	60.6 ± 11.1	22	311.5 ± 24.1	38	231.9 ± 29.7

Table 5. Screening (%Inhibition at 125 μM) and IC_{50} values (μM) of preliminary library of N^1-alkyl-N^2-nitroguanidines.

With reference to the crystal structure of NOS bound with L-NA, it was assumed that this series of compounds would bind to the NOS with their N^2-nitro group facing the Fe_{haem}, while the N^1-alkyl substituents would be orientated towards the access channel. The unsubstituted N^3H_2 would likely be hydrogen bonded to both the carboxylic residue of Glu and the backbone amide carbonyl of Trp in the distal GBS.

With the above assumption on binding orientation of nitroguanidines, the results suggested that the RegG was rather hydrophobic but was sterically limited. The inactivity of N^1,N^1-dialkyl-N^2-nitroguanidines (**XXI** – **XXII**) could be attributed to either the inability for N^1H to form hydrogen bonding to carboxylic residue of Glu, or the steric collision between the N^1-substituents with the protein structure. On the other hand, the inactivity of N^1-alkyl(branched)-N^2-nitroguanidine (**XIX** – **XX**) suggested that branching was not tolerated at the NOS active site. However, this observation was in contradiction to the activity exhibited by N^1-benzyl-N^2-nitroguanidines, which was also sterically bulky. This difference in activity could be attributed to the electronic properties of the N^1-substituents. The benzyl group was electron rich and was able to participate in π-π stacking interaction. As a result, the π-π stacking interaction would probably represent an important interaction, on top of the hydrophobic interaction, in RegG. The π-π stacking interaction may also be responsible for the slight selective inhibition towards nNOS over iNOS and possible eNOS.

An alternative orientation of binding, in which the N^1-alkyl was orientated towards the Fe_{haem}, should also be considered. EPITU and L-NPA are known to inhibit NOS in this binding orientation[175,176]. The hydrophobic cavity above the haem can accommodate simple alkyl groups (such as ethyl and propyl). Re-examining the

results using this perspective led to a different interpretation of results. Consistent with the literature reports, the current series of compounds suggested that the hydrophobic cavity above the haem was rather small. Both N^1-methyl and N^1-propyl substituents could bind to the hydrophobic cavity above the haem, thus inhibiting NOS. However, the inactivity of N^1-alkyl-N^2-nitroguanidines with larger substituents (**XIX** – **XXII**) could be attributed to the inability of the bulky N^1-substituents to bind to the hydrophobic cavity above the haem. Besides that, the results also suggested that the sizes of this haem hydrophobic cavity were similar in both nNOS and eNOS while the haem hydrophobic cavity in iNOS was smaller, as the N^1-alkyl(unbranched)-N^2-nitroguanidines (**XVII** – **XVIII**) showed similar activity towards nNOS and eNOS, and were inactive against iNOS. On the other hand, with this alternative binding orientation, the N^2-nitro group would be orientated towards the access channel, thus suggesting that hydrophobic yet electron-rich moieties could be tolerated at the RegG. Nevertheless, this alternative binding orientation was not applicable in the N^1-benzyl-N^2-nitroguanidines, as the hydrophobic cavity above the haem was too small for the N^2-benzyl moiety.

However, the alternative binding orientation was to be evaluated with caution. With reference to the activities of compound **XIV** and L-AMMA, which suggest that the dialkyl group could be accommodated in the hydrophobic cavity above the haem, it was quite surprising to find the compounds **XXI** and **XXII** being inactive. As a result, it was believed that the contribution of the alternative binding orientation was minimal. On the other hand, the different activity profiles of compounds **XVI** – **XVIII** and compounds **XXIII** – **XXV** suggested that the alternative binding orientation plays a greater role in the binding of N^1-alkyl-N^2-nitroguanidines with

small N^1-alkyl groups, while it is unlikely for the the N^1-benzyl-N^2-nitroguanidines to bind in the latter binding orientation.

Generally, it was believed that the preferred binding orientation of N^1-alkyl-N^2-nitroguanidine was to position the N-nitro group facing the Fe_{haem}, while the alternative binding orientation, though cannot be totally ignored, could play a minor role for the binding of compound. Comparing the two binding orientations, the binding orientation with Fe_{haem}-facing N-nitro group showed greater applicability than the alternative orientation as more structural variation could be performed. Furthermore, the objective to probe for hydrophobic interaction in the RegG could only be achieved with the N^1-alkyl groups facing the access channel. As a result, short alkyl N^1-substituents, which were likely to bind in alternative binding orientation (and thus unsuitable for molecular probing study on RegG), were not suitable to be used for further studies. On the other hand, the improved inhibitory activity and nNOS selectivity were demonstrated by the N^1-benzyl-N^2-nitroguanidines. Hence, the RegG was likely to be hydrophobic in nature, and it could accommodate large and electron rich group. Besides that, with π-π interaction in the RegG was likely to be responsible for slight selectivity towards nNOS. As a result, the N^1-benzyl-N^2-nitroguanidines were identified as leads for further evaluation.

Chapter 9 N^1-Alkyl-N^2-nitroguanidines. Part II.

From the study on N^1-alkyl-N^2-nitroguanidines, the N^1-benzyl-N^2-nitroguanidines were identified as lead for further investigation as these compounds showed relatively good potency and selectivity for nNOS inhibition. As a result, a series of N^1-benzyl-N^2-nitroguanidines were synthesised and evaluated for the selective nNOS inhibition. In order to elucidate SAR information of N^1-benzyl-N^2-nitroguanidines and to gain insights into the RegG, structural modifications were introduced to the N^1-benzyl moiety. On the other hand, the N^2-nitro was left unmodified due to its importance for interacting with GBS.

Synthesis of N^1-Benzyl-N^2-nitroguanidines

In order to obtain the SAR of inhibitors interacting with the RegG, it was important to have structurally diverse N^1-benzyl group, which could be derived from benzylamine. Molecular diversity in terms of hydrophobic, electrostatic and steric properties of the benzyl group was introduced as substitutions on phenyl ring and methyl (α-carbon) group. The Craig's plot[266] was used as a reference to ensure that the ring substituents were diverse electrostatically and hydrophobically. With ring substitution, the hydrophobicity of the ring, and thus the participation of the ring in hydrophobic interaction with RegG, was modified. Besides that, the electronic property of the ring, thus the aromaticity of the ring and the involvement of π-π interaction with the RegG, was varied. On top of that, the possible involvement of electrostatic interaction in the RegG could also be evaluated. On the other hand, substitution on the methyl (α-carbon) group was a suitable approach for evaluating the contribution of steric and conformational factors on the binding of N^1-benzyl-N^2-nitroguanidine to the active site. The main impact of having α-carbon substitution

was the conformational restriction on the molecule. With various substituents introduced, the size and flexibility of the benzyl group were modified.

According to computational calculation using SYBYL6.6, the molecular properties of the reagents, benzylamines, were evaluated. The ClogP (partition coefficient) of the benzylamines selected for the synthesis ranged from –0.74 to 2.92, while the dipole moment ranged from 1.85 to 5.69 (debye) and the CMR (molar refractivity) ranged from 3.53 to 6.03. As for the computed surface area, volume, HOMO and LUMO of the benzylamine were calculated to be 139.83 – 210.07 ($Å^2$), 118.77 – 197.55 ($Å^3$), -8.06 – -9.98 (eV), and -1.26 – 0.58 (eV), respectively. Hence, a diverse selection of benzylamine was used in the synthesis, thus enabling a meaningful SAR and molecular probing studies.

The reactions of SMNNITU with primary amines were clean and generally completed within 12 hours of reflux. Upon cooling, the N^1-(substituted)benzyl-N^2-nitroguanidines precipitated out from the reaction solution, and the crude products were further recrystallised from aqueous ethanol. The identity and purity of the compounds were established prior to subjecting the compounds for L-[^{3}H]-citrulline assays.

Biological Evaluation of N^1-Benzyl-N^2-nitroguanidines

The compounds were screened at 125 μM using the L-citrulline assay against three NOS isoforms (**Table 6**). The IC_{50} values were determined for compounds showing more than 10% inhibition at 125 μM. Interestingly, the N^1-(substituted)benzyl-N^2-nitroguanidines demonstrated a tendency towards nNOS selective inhibition. At 125 μM, 18 out of the 22 compounds exhibited more than 10% inhibition against nNOS. One the other hand, only 4 of the compounds showed more than 10% inhibition at 125 μM against iNOS, while 10 of the compounds

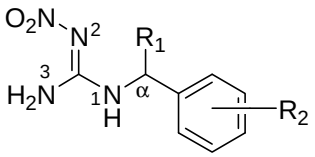

	Substitution		nNOS		iNOS		eNOS	
	R_1	R_2	%Inh	$IC_{50} \pm SEM$	%Inh	$IC_{50} \pm SEM$	%Inh	$IC_{50} \pm SEM$
XXIII	H	H	34	192.6 ± 16.8	<10		23	383.8 ± 113.4
XXIV	H	*p*-Cl	26	343.2 ± 37.5	<10		<10	
XXVI	H	*p*-F	43	229.4 ± 20.8	<10		<10	
XXVII	H	*p*-CH_3	<10		<10		14	959.2 ± 233.8
XXVIII	H	*p*-CF_3	13	634.7 ± 46.7	<10		<10	
XXIX	H	*p*-OCH_3	18	632.6 ± 6.5	<10		<10	
XXX	H	*p*-NO_2	33	269.2 ± 70.3	<10		26	269.7 ± 46.9
XXXI	H	*p*-NH_2	44	287.3 ± 59.4	<10		12	989.6 ± 219.9
XXXII	H	*p*-SO_2NH_2	36	323.0 ± 57.6	<10		16	431.8 ± 89.8
XXXIII	H	*p*-$C(CH_3)_3$	<10		<10		<10	
XXV	H	*m*-Cl	65	60.6 ± 11.1	22	311.5 ± 24.1	37	231.9 ± 29.7
XXXIV	H	*m*-CH_3	47	114.2 ± 34.7	<10		29	367.8 ± 75.4
XXXV	H	*m*-CF_3	48	131.2 ± 20.8	<10		11	771.5 ± 161.5
XXXVI	H	*m*-NO_2	86	39.5 ± 8.7	13	732.1 ± 60.2	34	250.5 ± 14.4
XXXVII	H	*m*-OCH_2O-*p*	21	502.4 ± 39.9	<10		<10	
XXXVIII	H	*o,p*-diCl	86	52.1 ± 9.7	13	909.4 ± 106.9	55	96.4 ± 13.2
XXXIX	H	*m,p*-diCl	35	215.7 ± 19.8	25	468.4 ± 207.7	<10	
XXXX	*S*-*a*-CH_3	H	<10		<10		<10	
XXXXI	*R*-*a*-CH_3	H	<10		<10		<10	
XXXXII	*a*-phenyl	H	71	58.0 ± 5.0	<10		<10	
XXXXIII	*a*-CH_2CH_2-*o*		51	122.7 ± 11.4	<10		<10	
XXXXIV	*a*-$CH_2CH_2CH_2$-*o*		24	384.6 ± 51.0	<10		<10	

Table 6. Screening (%Inhibition at 125 μM) and IC_{50} values (μM) of N^1-(substituted)benzyl-N^2-nitroguanidines.

demonstrated more than 10% inhibition at 125 μM against eNOS. Closer examination showed that the IC_{50} values were relatively higher against iNOS and eNOS, while moderate IC_{50} values were demonstrated against the nNOS.

With the unsubstituted N^1-benzyl-N^2-nitroguanidine (**XXIII**) as a reference, the N^1-(*para*-substituted)benzyl-N^2-nitroguanidines (**XXIV** – **XXXIII**) were generally found to result in lower binding affinities towards nNOS. Regardless of the nature of the *para* substituents, the $IC_{50(nNOS)}$ values were higher than **XXIII**, and the similar trends of decreased inhibition were also observed against eNOS and possibly iNOS. This suggested that the steric factor, rather than hydrophobic or the π-π stacking interactions, was the main reason for the decrease in inhibitory activities. The RegG facing the *para*-substituent was seemed to be restricted in size, and compound **XXXIII** was found to be inactive as a result of bulky *t*-butyl substituent. Hence, the data suggested that *para*-substituents were to be avoided. Of less significance, the *para*-substituents might be directed towards a site capable of hydrogen bonding or electrostatic interactions, as shown by a smaller degree of reduction in binding affinity for compounds with *para*-substituents capable of hydrogen bonding or electrostatic interaction (**XXIV** – **XXVI**, **XXX** – **XXXII**), as compared to those with hydrophobic non-hydrogen bonding *para*-substituents (**XXVII** – **XXIX**). With reference to the selectivity among NOS isoforms, the selectivity profile of N^1-(*para*-substituted)benzyl-N^2-nitroguanidine was similar to that of unsubstituted **XXIII** with no enhancement of isoform selectivity. As a result, the RegG facing the *para*-substituent was restricted in size and conserved among the isoforms.

A totally different picture was observed for N^1-*meta*-substituted-N^2-nitroguanidines (**XXV** – **XXXVI**), which showed improved binding affinities

towards all the three NOS isoforms as compared to unsubstituted **XXIII**. The data suggested that hydrophobic interaction predominates at RegG facing the *meta*-substituents, and hydrogen bonding or electrostatic interaction also played a role in the binding of the inhibitors. Notably the compound **XXXVI** demonstrated mid-micromolar $IC_{50(nNOS)}$ value. As compared to compound **XXIII**, the enhanced nNOS inhibition of compound **XXXVI** was complemented by improved inhibition against iNOS and eNOS, but the degree of improvement in eNOS inhibition was less than nNOS, while some of the *meta* substituents (**XXVII**, **XXV**) resulted in better iNOS inhibition. The data suggested that the RegG facing the *meta*-substituents would likely be hydrophobic in nature. However, this *meta*-substituent interacting area in RegG was more or less conserved among the isoforms, as demonstrated by little enhancement in isoform selectivity with *meta*-substituents. However, the hydrogen-bonding or electrostatic interaction seemed to be playing a greater role in nNOS, as demonstrated by the enhanced nNOS inhibition by compound **XXXVI** over both iNOS and eNOS inhibition.

As for N^1-(disubstituted)benzyl-N^2-nitroguanidines (**XXXVII** – **XXX**), the overall effects were cumulative of the effects of the individual substituent. The presence of *para*-substituent lowered the inhibitory activity while the *meta*-substituent enhance the inhibition. Thus, the resultant inhibitory activity was intermediate, as shown by compound **XXXIX** as compared to compounds **XXIV** and **XXV**. Surprisingly, the compound **XXXVIII** showed good inhibitory activity against nNOS and eNOS, and weak inhibition against iNOS. This suggested the role of *ortho*-substituent in enhancing the inhibitory activity. However, the *ortho*-substitution was not designed into the experiment because the *ortho*-substituent were positioned near to the GBS and thus provided little potential for enhancing isoform selectivity. The

design rationale was supported by compound **XXXVIII**, which showed negligible selectivity towards nNOS over eNOS, and the overall selectivity profile was similar to that of unsubstituted compound **XXIII**.

As discussed above, substitutions on the phenyl ring provided little enhancement in isoform selectivity profile, despite improvement in binding affinity was demonstrated by *meta*-substituents. This suggested that the RegG environment around the phenyl group was rather conserved in terms of steric, electronic and hydrophobic properties, which was fairly consistent with the X-ray crystallography data. On the other hand, promising isoform selective inhibition was observed with substitution on the α-methyl group (**XXXX** – **XXXXIV**), which argue against the active site conservation displayed in X-ray crystallography.

In order to evaluate the importance of stereo-orientation of the phenyl ring for binding to the RegG, enantiomeric N^1-(α-methyl)benzyl-N^2-nitroguanidines (**XXXX** and **XXXXI**) were studied. However, both S- and R-enantiomers were shown to be inactive. This indicated that methyl substitution on the α-carbon resulted in unfavourable orientation of the phenyl ring for proper interaction with the active site as compared to compound **XXIII**. However, with conformational restriction and molecular size increment through ethyl and propyl group bridging the α-carbon and the *ortho*-carbon of the phenyl ring (**XXXXIII** and **XXXXIV**), nNOS selective inhibition was demonstrated. The phenyl ring of compound **XXXXIII** was suitably orientated for interaction with the active site as compared to compound **XXXXIV**, as shown by the lower $IC_{50(nNOS)}$ value of compound **XXXXIII**. Interestingly, both compounds **XXXXIII** and **XXXXIV** were active against nNOS but not iNOS or eNOS. Since the surface topology of RegG interacting with the phenyl ring was conserved among the three NOS isoform, the absence of inhibition for iNOS and

eNOS by compounds **XXXXIII** and **XXXXIV** was probably a consequence of steric effect of the ethyl and propyl bridges rather than electronics or hydrophobic effects. The nNOS seemed to be able to accommodate these bulky structures.

Interestingly, mid-micromolar $IC_{50(nNOS)}$ value was demonstrated by N^1-(*a*-phenyl)benzyl-N^2-nitroguanidine (**XXXXII**). The presence of *a*-phenyl substituent resulted in proper orientation of the phenyl ring for active site interaction, and it was likely that the both phenyl rings were able to participate in hydrophobic and/or π-π stacking interaction with the RegG. More importantly, nNOS selective inhibition was demonstrated by **XXXXII**, which was inactive against both iNOS and eNOS. Once again, the data suggested that the active site of nNOS was more spacious and accommodative than that of iNOS and eNOS. This suggested either a more spacious nNOS active site, or the RegG of nNOS was more readily to undergo conformational changes upon induced fit of compounds.

As a result, a size-exclusion mechanism around RegG was suggested for achieving nNOS selective inhibition. For the future design of nNOS selective inhibitor, bulky and hydrophobic group (and preferentially aromatic in nature) whould be introduced as RegG-interacting group in order to exploit the size-exclusion mechanism. Re-examining the reported NOS inhibitors (**Chapter 2**), it was found that the size-exclusion mechanism was not exploited for achieving nNOS selective inhibition. None of the reported NOS inhibitors possesses an appropriately sized RegG-interacting bulky group at such a close distance to GBS as compound **XXXXII**. The only likely example of utilising the size-exclusion mechanism was demonstrated by 6-(4-(substituted)phenyl)-2-aminopyridines[174], assuming that the 2-aminopyridine was the group interacting with the GBS. With bulky 6-substituents, selective nNOS

inhibition was achieved. Hence, the size-exclusion mechanism was a potentially useful factor for achieving nNOS selective inhibition.

The size exclusion mechanism was likely to be a result of conformationally flexibility of RegG in nNOS. As shown by the data, the RegG was found to be hydrophobic. Since hydrophobic interaction is weak and nonspecific, the RegG could undergo conformational change induced by the binding of the nitroguanidine with bulky and aromatic N^1-benzyl group. Hence, although the size difference in the active site was not apparently observed in X-ray crystallography of NOS, induced-fit of bulky RegG-interacting group to nNOS selectively was likely to occur, as demonstrated by the current study.

Generally, the IC_{50} values of this series of compounds were in the micromolar range. As compared to the submicromolar IC_{50} values of L-NA, it was not surprising to observe the relatively weak binding affinity for the current series of N^1-benzyl-N^2-nitroguanidines, which were lack of NBS-interacting group and CBS-interacting group. Nevertheless, the mid-micromolar $IC_{50(nNOS)}$ value displayed by compound **XXXXII** was rather impressive, thus suggesting the significant contribution of the hydrophobic and π-π stacking interactions towards the binding of the compounds. Of more significance was the size-exclusion mechanism that contributed to the nNOS selective binding of compound **XXXXII**. The N^1-(α-phenyl)benzyl-N^2-nitroguanidine (**XXXXII**) was identified as the lead compound with selective nNOS inhibition with a $IC_{50(nNOS)}$ of 58.0 μM. Further in vivo study were to be conducted using **XXXXII** to determine its potential clinical application.

Chapter 10 Further Investigations Using Guanidino-containing Compounds

As shown in the preceding discussions, hydrophobic interaction in the RegG contributed to the binding of the inhibitor to the active site of NOS. However, it was of interest to evaluate whether ionic interaction, in addition to the hydrophobic interaction, would enhance the binding to the RegG. In this section of the study, the potential of guanidino containing heterocycles to inhibit NOS is also assessed.

The 2-(2-nitroguanidino)alkanoic acid (NGAA) has an carboxylic acid group attached at α-position to the nitroguanidino group, thus NGAA is useful for evaluating the involvement of anionic interacting site in RegG. On the other hand, the 1-alkyl-4-nitroimino-1,3,5-triazinane (TZN) is a saturated triazinane, in which a nitroguanidino moiety incorporated as part of the heterocycle. Since a tertiary nitrogen, which becomes cationic at physiological pH, is located at the a-position to the nitroguanidino moiety, the TZN serves as a useful probe for evaluating the involvement of cationic interacting site in the RegG. The 6-anilino-4-amino-1,2-dihydro-2,2-dimethyl-1,3,5-triazine (TZA), in which a guanidino group constitutes a part of a conjugated system, is charged under physiological pH. Thus it serves as an alternative strategy to probe the RegG for possibility of cationic interaction. Different from the compounds discussed in the preceding chapters, both TZN and TZA represented the attempts to evaluate the use of heterocyclic compounds as NOS inhibitors.

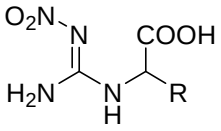

NGAA

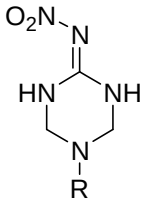

TZN

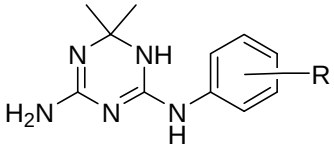

TZA

Synthesis and Biological Evaluation of 2-(2-Nitroguanidino)alkanoic acids (NGAA)

The 2-(2-nitroguanidino)alkanoic acids (NGAA) was synthesised by reacting *a*-amino acids with SMNNITU (**Scheme 14**). It was of interest to evaluate the influence of adjacent carboxylic acid group on the progress of the reaction, as well as the inhibitory activity on NOS. Racemic *dl-a*-amino acids with hydrophobic side chains, instead of side chains containing other functional groups, were used for the synthesis. Three α-amino acids selected (Gly, Val and Phe) varied in terms of hydrophobicity and the bulkiness of the side chains.

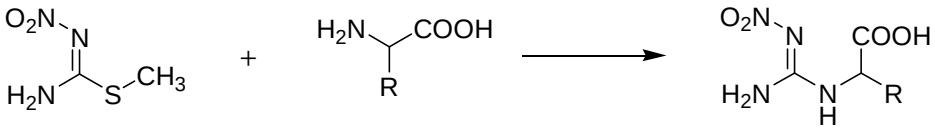

Scheme 14. Synthesis of NGAA.

The reaction between α-amino acids and SMNNITU in aqueous ethanol did not proceed well. Furthermore, the amino acids were weakly soluble in the aqueous ethanol, thus prevented the reaction from taking place. In order for the amino function to react with SMNNITU, it should exist in unprotonated form to act as a nucleophile. As a result, with the addition of a base to the reaction medium, the amino function was unprotontated. The use of the base also improved the dissolution of the α-amino acids in the reaction medium.

Attempts to use triethylamine as a base was unsuccessful. On the other hand, the use of sodium hydroxide was undesirable because NaOH solution is known to decompose nitroguanidine group. Hence, sodium carbonate was chosen as the base. Although Na_2CO_3 was reported to be less destructive to the nitroguanidino group[267], precaution was taken to minimise the base-induced decomposition of nitroguanidino

group through reducing the duration of heating. One equivalent of 1M Na_2CO_3 was added to the α-amino acid, and the reaction mixture was brought to reflux for 15 minutes. Subsequently, SMNNITU was added to the boiling reaction mixture. After the complete dissolution of SMNNITU, the reaction mixture was left to cool to room temperature with continuous stirring for 24 hours.

Following that, the strongly acidic Dowex-H^+ resins were added to the reaction mixture until the pH of the solution reached pH4 (using pH paper). Under this acidic condition, α-carboxylic acid was protonated while the unreacted α-amino group, together with other basic side products, would be charged and thus adsorbed onto the Dowex-H^+ resins. The filtrate containing NGAA was collected and rotary evaporated to dryness. Using this method, three compounds (**Table 7**) were successfully synthesised in moderate yield with good purity.

The use of solid phase extraction (SPE) as a purification step simplified the post-reaction workup. SPE represented one of the applications of solid phase organic chemistry, and the ability to separate impurities from solution through simple filtration was very helpful in accelerating the synthetic process[205]. Prior to the use of SPE, the reaction mixture was acidified with 2M HCl to either pH 2 (using pH paper). Subsequently, the solution was rotary evaporated, but the presence of HCl would decompose the nitroguanidino group upon heating. Liquid-liquid extraction was not suitable due to the limited solubility of NGAA in organic solvents. Thus the use of SPE largely simplified the purification step with the Dowex-H^+ acting as an acidifying agent as well as electronic trap for unwanted cationic species.

As shown in the table (**Table 7**), none of the NGAA showed more than 10% inhibition on three isoforms of NOS. Despite having close resemblance to compound **XVII** (N^1-methyl-N^2-nitroguanidine), compound **XXXXV** was found to be inactive,

indicating the incompatibility of the carboxylic function with RegG. With longer alkyl chain as in compound **XXXXVI**, no increase in inhibitory activity was observed. The introduction of a phenyl ring, which was capable of hydrophobic and π-π stacking interactions with the active site, did not improve the binding of compound **XXXXVII**. These data suggested that the absence of anionic binding site in the RegG.

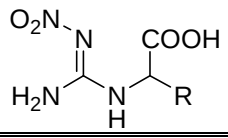

		% Inh		
	R	nNOS	iNOS	eNOS
XXXXV	H	< 10	< 10	< 10
XXXXVI	$CH_2CH(CH_3)_2$	< 10	< 10	< 10
XXXXVII	CH_2Ph	< 10	< 10	< 10

Table 7. %Inhibition at 125 μM for NGAA.

There was a possibility that the steric hindrance at α-carbon could result in inactive NGAA. However, the activities demonstrated by compounds **XXXXII** – **XXXXIV** argued against this possibility. Furthermore, given that phenyl ring of the compound **XXXXVI** was separated from the nitroguanidino group by an ethyl group (and thus possessed greater conformational flexibility), the lack of inhibitory activity was unlikely to be related to the improper orientation of the phenyl ring. Thus, electronic incompatibility instead of steric hindrance was likely to be the major cause of the absence of NOS inhibition by NGAA.

Synthesis and Biological Evaluation of 1-Alkyl-4-nitroimino-1,3,5-triazinanes (TZN)

For 1-alkyl-4-nitroimino-1,3,5-triazinane (TZN), the nitroguanidino moiety was incorporated as part of the parent 1,3,5-triazinane ring. The TZN represented one of the few heterocyclic compounds that could be derived from nitroguanidines, which was rarely used as starting material for the synthesis of heterocycles despite having several functional anchors for reaction, due to the low basicity and low nucleophilicity of nitroguanidines. The nitro group in the nitroguanidino fragment of the TZN lowered the basicity of the guanidino moeity, and only the ring nitrogen (N^1) was protonated under physiological pH. Due to the saturated ring system without electron conjugation in TZN, the positive charge on the protonated ring nitrogen (N^1) was localised. Hence, TZN is useful for evaluating the tolerance of the RegG to cations.

The TZN was a relatively less studied compound with limited literature reports available. There was no report on the biological activity of TZN. However, with suitable N-substituents, as in the 1-(3-furanyl)alkyl-2-nitroimino-3-alkyl-5-alkyl-1,3,5-triazinanes, pesticidal effects were reported[268]. On the other hand, in chemical synthesis, the TZN is treated as a protecting group for the nitroguanidino moiety. Upon transforming nitroguanidine into TZN, alkylation can be carried out on the guanidino nitrogens. Subsequently, acid-induced ring cleavage produces alkylnitroguanidine[269].

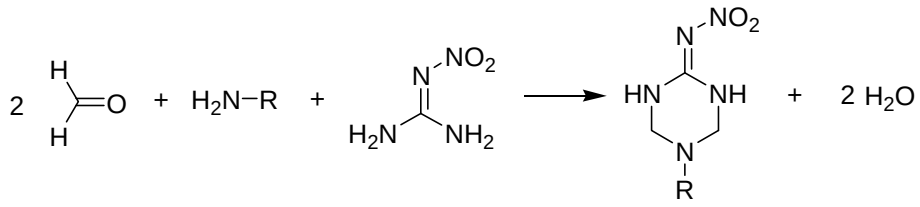

Scheme 15. Synthesis of TZN.

The TZN was synthesised by reacting 2 equivalents of formaldehyde and 1 equivalent of alkylamine with 1 equivalent of nitroguanidine, which was synthesised from SMNNITU (**Scheme 15**). The reaction progressed smoothly using 37% aqueous formaldehyde, with ethanol as solvent and the reaction was carried out at 50 °C for 5 hours[269]. As the reaction progressed, precipitation of the product occurred. The crude product was subsequently recrystallised from aqueous ethanol. Replacing the 37% aqueous formaldehyde by solid paraldehyde resulted in slow reaction rate and low yield. The use of higher temperature was undesirable. The mechanism of the reaction was unclear. However, it was believed to involve the formation of alkylimine and alkyliminium intermediates.

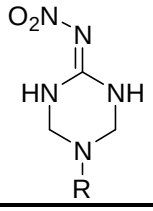

		% Inh		
	R	nNOS	iNOS	eNOS
XXXXVII	CH_3	< 10	< 10	< 10
XXXXIX	C_3H_7	< 10	< 10	< 10
L	$CH_2CH(CH_3)_2$	< 10	< 10	< 10
LI	Cyclohexyl	< 10	< 10	< 10
LII	Benzyl	< 10	< 10	< 10
LIII	2-Phenylethyl	< 10	< 10	< 10

Table 8. %Inhibition at 125 μM for TZN.

As demonstrated in the table (**Table 8**), none of the TZN showed more than 10% inhibition at 125 μM, regardless of the N^1-alkyl groups. This could be

interpreted that cationic interacting site was not present in RegG, and that a cation was not tolerated in this region. However, this inference should be accepted with caution, as the binding conformation of TZN was likely to be different from that of N^1-alkyl-N^2-nitroguanidine. Assuming that the nitroguanidino moiety of TZN would bind to the active site in a similar fashion as L-NA, steric hindrance could arise from N^3/N^5, which supposedly occupied the distal GBS. Furthermore, the N^1-alkyl group could be orientated to a different direction, as compared to the alkyl backbone of L-NA, which would probably result in additional steric hindrance. The lack of inhibitory activites with short N^1-alkyl chain or flexible N^1-(2-phenyl)ethyl chain suggested, to some extent, that TZN was incompatible with active site. As a result, the inactivity of TZN observed was probably due to the incompatibility of the cation at the active site as well as steric hindrance due to the cyclic structure and the N^1-alkyl group.

Synthesis and Biological Evaluation of 6-Anilino-4-amino-1,2-dihydro-2,2-dimethyl-1,3,5-triazine (TZA)

The 6-anilino-4-amino-1,2-dihydro-2,2-dimethyl-1,3,5-triazine (TZA) was first reported in the 1950s[270-274]. There were relatively few reports on biological effects of TZA, one of which was herbicidal activity[275]. For the TZA, a guanidino moiety is incorporated as part of the heterocyclic dihydrotriazine ring. Structurally, the TZA is an interesting molecule as there is an extended conjugated biguanide system spanned across the molecule. Comparing TZA to TZN, despite a lack of nitro group on the guanidino fragment, the TZA is more structurally related to the N^1-benzyl-N^2-nitroguanidinine series than the TZN in terms of the orientation of the phenyl ring with respect to the guanidino fragment. Furthermore, assuming that 4-amino group was bound to the distal GBS and the N^3 was located in the proximal

GBS facing the Fe_{haem}, the 2,2-dimethyl would be able to fit into the hydrophobic cavity above the haem, and the phenyl ring would be positioned into the RegG facing the substrate access channel. Hence, theoretically the TZA should be able to bind well to the active site and it is of interest to determine the potential of this guanidino containing heterocycle as NOS inhibitor. In addition, the TZA, being protonated at physiological pH, is an alternative probe in place of TZN for evaluating the presence of anionic interaction in the RegG.

The TZA was synthesized through Dimroth rearrangement of 1-(substituted)phenyl-4,6-diamino-1,2-dihydro-2,2-dimethyl-1,3,5-triazine (TZP), which was in turn synthesized through from cyanoguanidine, aniline and acetone (**Scheme 16**). The one-pot synthesis of TZP was a simple and clean reaction[273]. The subsequent rearrangement of TZP into TZA could be carried out under various conditions[271]. The reported reaction condition[273] (sodium hydroxide was added dropwise until pH11) resulted in incomplete reaction, which was attributed to incomplete conversion of TZP·HCl salt into free base form. Hence, in order to improve the rearrangement, it was necessary to ensure that all the TZP·HCl salt had been converted into the free base (from which Dimroth rearrangement could occur), with an excess of the base/alkali available as catalysts.

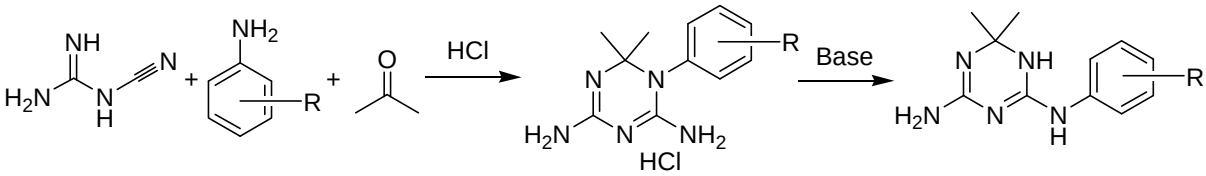

Scheme 16. Synthesis of TZA.

In order to determine the optimal base/alkali, the following bases were used for rearrangement: 10M NaOH, saturated Na_2CO_3, ethanolamine, TEA and piperidine. Using compound **LVI** (**Table 9**) as the model, the rearrangement from 1-

(4-chloro)phenyl-4,6-diamino-1,2-dihydro-2,2-dimethyl-1,3,5-triazine was completed in 15 minutes when either NaOH or Na_2CO_3 was used as base catalyst. On the other hand, the rearrangement took more than one hour to complete when organic bases were used. The crude yields were higher for inorganic bases (>80%) while the organic bases resulted in lower yields (82% for ethanolamine, 64% for piperidine and 22% for TEA). The variation in reaction duration and yield may be due to the differences in molecular size and the nucleophilicity of the nucleophiles. Furthermore, judging on the melting points and general appearance of the crude products, the catalysis by 10M NaOH yielded products of highest purity. Thus, the optimised condition was identified as the dropwise addition of 10M NaOH into a solution of TZPχHCl in 50% aqueous methanol, until pH 14 (by pH paper) was reached. The reaction mixture was then refluxed and the progress of the reaction was monitored by UV spectrophotometry.

A mechanism of rearrangement of TZP into TZA was proposed in 1954[273]. However, the proposal was found to be inconsistent with the generally accepted mechanism of Dimroth rearrangement[276] and failed to explain the occurrence of rearrangement under neutral condition. As a result, a new mechanism of rearrangement of TZP to TZA (**Scheme 17**), which was consistent with the generally accepted Dimroth rearrangement mechanism[276], was proposed.

The electron delocalised from the 6-amino ($N_\alpha H_2$) moiety led to the formation of an imine. The strong π-electrons localisation in the doubly bonded nitrogen atom resulted in an imbalance of electronic distribution over the N_1-C_2 bond, and led to the fissure of the N_1-C_2 bond, with the addition of nucleophiles such as hydroxide ions, ethanol or even water molecule. Following that, the N_α would be incorporated into

the dihydrotriazine ring system upon ring closure, where the N_1-C_2 bond was reestablished *via* nucleophilic attack of the imine nitrogen.

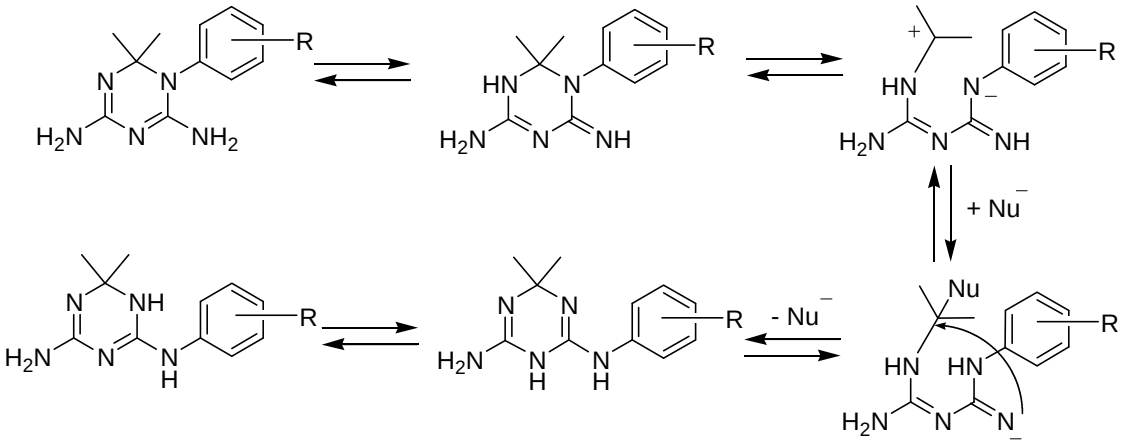

Scheme 17. Mechanism of Dimroth rearrangement of TZP into TZA under the presence of nucleophiles, such as hydroxide ions.

Reported reactions and observations in the literatures could be adequately explained by this new proposal for the mechanism of Dimroth rearrangement. First, the intermediate was predicted to be an arylbiguanide[273], the UV spectrum of which was similar to that of TZA and TZP, thus no abrupt change in UV spectra was to be expected during the course of the rearrangement. This was indeed shown to be the case as predicted. Secondly, this proposed mechanism explained the occurrence of Dimroth rearrangement under neutral condition, using water molecules as nucleophiles. Thirdly, the absence of Dimroth rearrangement under acidic condition could also be satisfactorily explained by this mechanism as the lack of free lone pair of electron for initialising the rearrangement process. In addition, the Dimroth rearrangement under molten state could be accounted by the proposed mechanism as having an imine moiety itself acting as a nucleophile, which catalysed the ring opening of another molecule in the intermediate state.

Thermodynamically, the Dimroth rearrangement is driven by both enthalpy and entropy of the reaction[276]. Most of the rearranged products were achieved at a

lower energy level as compared to the pre-rearrangement reactants. Both computer modelling and X-ray crystallography[277] studies showed that much steric strain was observed in TZP. The 1-phenyl ring was roughly perpendicular to the π-conjugation in dihydrotriazine ring, resulting in ineffective π electron conjugation between the two rings. Furthermore, the rotation of the 1-phenyl ring was highly restricted, resulting in atropisomerism of TZP. However, upon Dimroth rearrangement to TZA, the steric strain was relieved, and contributed to a decrease in enthalpy. On the other hand, higher rotational freedom of 6-phenyl ring and improved overall π-electron delocalisation resulted in an increase in entropy. Thus, TZA was thermodynamically preferred to TZP.

From the proposed mechanism of Dimroth rearrangement, it was expected that an electron-donating substituent on the aryl ring would partly restore the charge imbalances over the N_1-C_2 bond and thus reduce the rate of Dimroth rearrangement, and *vice versa* for electron-withdrawing substituent. In fact, a slow rate of rearrangement was observed in 4-amino-1,2-dihydro-2,2-dimethyl-6-(3,4-dimethyl)anilino-1,3,5-triazine (r9008).

As shown in **Scheme 17**, the rearrangement reaction is expected to be reversible. However, in this study, the Dimroth rearrangement of TZP into TZA was virtually irreversible. This was because the 6-amino group of TZP was unsubstituted, and so the resulted TZA was favoured sterically. However, for N^1,N^6-disubstituted TZP, Dimroth rearrangement was reported to be reversible. A study on two-component condensation [r9008] between N^1-(4-chloro)phenyl-N^2-methylbiguanide and acetone showed that the reaction produced solely 4-amino-1-(4-chloro)phenyl-6-(N-methyl)amino-1,2-dihydro-2,2-dimethyl-1,3,5-triazine under acid-catalysis, and solely 4-amino-6-(4-chloro)anilino-1-methyl-1,2-dihydro-2,2-dimethyl-1,3,5-triazine

under base-catalysis. However, when either of the two compounds was placed in the alkali aqueous solution, Dimroth rearrangement occurred and resulted in a mixture of two components, with a ratio of 1 part of the former to 3-4 parts of the latter. This was consistent with the general observation about Dimroth rearrangement [r9013], in which the nitrogen with bulkier and/or more electron-withdrawing substituent would prefer to be exocyclic.

With the optimised Dimroth rearrangement condition and an understanding of the mechanism of reaction, a series of TZA was synthesised and evaluated using L-citrulline assay (**Table 9**).

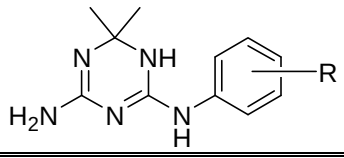

		% Inh		
	R	nNOS	iNOS	eNOS
LIV	H	< 10	< 10	< 10
LV	3-Cl	< 10	< 10	< 10
LVI	4-Cl	< 10	< 10	< 10
LVII	3-Br	< 10	< 10	< 10
LVIII	4-Br	< 10	< 10	< 10
LIX	3-CH_3	< 10	< 10	< 10
LX	4-CH_3	< 10	< 10	< 10
LXI	3-OCH_3	< 10	< 10	< 10
LXII	4-OCH_3	< 10	< 10	< 10
LXIII	3-NO_2	< 10	< 10	< 10

Table 9. %Inhibition at 125 μM for TZA.

As shown in the above table, all the compounds showed less than 10% inhibition at 125 μM. This suggested that the low affinity of TZA to the active site of NOS was probably due to the incompatibility of the positively charged dihydrotriazine ring system with the RegG. Hence, together with TZN, it was suggested that the cationic interaction was less likely to play a role in inhibitor binding to the RegG.

All the three series of compounds (NGAA, TZN and TZA) were found to be inactive against NOS. The lack of inhibitory activity was likely to be attributed to the intolerance of charged species in the RegG, although the role of steric hindrance could not be ruled out for heterocyclic series. It was shown that in the RegG, the involvement of both cationic and anionic interactions (at a close distance to GBS) was negligible. As a result, the future design of NOS inhibitors should refrain from having a charged group as the RegG-interacting group, which would reduce the binding affinity of the compounds.

Chapter 11 *In Vivo* Evaluation

From the preceding series of guanidino compounds studied, N^1-(*a*-phenyl)benzyl-N^2-nitroguanidine (**XXXXII**) was identified as the lead compound with moderate potency and good nNOS selectivity. Hence, compound **XXXXII** was subjected to further biological evaluation using *in vivo* neuroprotection model. The chemical-induced convulsion model, pentylenetetrazole test (PTZ test), was used[278]. If neuroprotection effect was present, the mice would suffer less or delayed brain damage, and thus was able to survive for a longer duration. The PTZ test was done in complementary with the rotarod test for detecting the manifestation of neuromotor side effects such as muscle incoordinations and imbalances[278].

The nNOS-derived NO has been speculated to participate in the epileptic episodes. However, the role of NO in epilepsy is found to be controversial. Various reports suggested that NO is anti-convulsive[279,280]. However, pro-convulsive effect of NO has also been documented[281]. The inconclusive literature data was attributed to the variations in convulsive models, the doses of seizure-inflicting agent, and the types of NOS inhibitors[282]. However, in this study, it was suggested (as discussed below) that the NO does not play primary convulsant/anticonvulsant role, but is involved in the destructive processes following the initiation of convulsion.

Most of the *in vivo* effect of nNOS inhibition is determined using 7-nitroindazole (7-NI). Although 7-NI is claimed to be nNOS selective *in vivo*, it is known to be non-selective *in vitro*, with equipotency in inhibiting nNOS (IC_{50} 0.7 μM), eNOS (IC_{50} 0.78 μM) and iNOS (IC_{50} 5.8 μM)[283]. The validity of *in vivo* selectivity of 7-NI had been debated, and the reason for the observed *in vivo* selectivity is still unknown. As a result, despite being widely used as a selective *in*

vivo inhibitor of nNOS in recent years, the results are to be accepted with caution[284,285].

Biological (*in vivo*) Evaluation using PTZ and Rotarod Tests

In the PTZ-induced convulsion model, a high dose of PTZ (120 mg/kg) was employed for inducing both clonic and tonic convulsion[278]. The negative control using DMSO provided no neuroprotection against PTZ induced convulsion and this was taken as the reference for comparison (**Table 10**). On the other end, the positive control of 2 mg/kg DZP provided full protection against PTZ induced convulsion with none of the mice developed into jumping and the subsequent convulsive stages. However, a 10-fold decrease in DZP dose (0.2 mg/kg) was shown to delay but not prevent the occurrence of convulsive events and the neuronal damages. For the 100 mg/kg **XXXXII** and 100 mg/kg 7-NI, complete protection from PTZ-induced convulsion was not achievable, but delays in the occurrence of convulsive events were observed.

Initial statistical analysis using 1-way ANOVA with Bartlett's test for equal variance showed that the variances of each group were statistically significant. As a result, non-parametric 1-way ANOVA, the Kruskal-Wallis test, was used to evaluate the data, and Dunn's multiple comparison test was carried out for inter-group comparison (**Table 11**). Since none of the 2 mg/kg DZP treated mice showed any response, the data from this positive control mice was not used for comparison.

As for the rotarod test, the negative control DMSO, 0.2 mg/kg DZP and 100 mg/kg **XXXXII** were found to be devoid of motor incoordination (**Table 12**). As expected, the 2 mg/kg DZP resulted in sedation in the mice with short rotarod staying duration. As for the 100 mg/kg 7-NI, the treated mice were found to exhibit serious motor incoordination (catalepsy), showing short rotarod staying duration.

	Latency (seconds) (Cut-off time: 1800 seconds)		
	Jumping	Full Extension	Death
	Mean ± SEM	Mean ± SEM	Mean ± SEM
DMSO (-ve ctrl)	102 ± 7	265 ± 30	301 ± 32
DZP 0.2 mg/kg	206 ± 22	977 ± 56	1117 ± 146
XXXXII 100 mg/kg	188 ± 22	446 ± 52	1407 ± 198
7-NI 100 mg/kg	234 ± 31	845 ± 155	1684 ± 74
DZP 2 mg/kg (+ve ctrl)	1800 ± 0	1800 ± 0	1800 ± 0

Table 10. Latencies (seconds) to various convulsive responses for different treatment groups (n=6).

	Jumping	Hind limb extension	Death
Kruskal-Wallis test			
P value	P < 0.01	P < 0.001	P < 0.001
Dunn's Test	P value	P value	P value
DMSO vs DZP_0.2	P < 0.05	P < 0.01	P > 0.05
DMSO vs **XXXXII**	P > 0.05	P > 0.05	P < 0.05
DMSO vs 7-NI	P < 0.01	P < 0.01	P < 0.001
DZP_0.2 vs **XXXXII**	P > 0.05	P > 0.05	P > 0.05
DZP_0.2 vs 7-NI	P > 0.05	P > 0.05	P > 0.05
XXXXII vs 7-NI	P > 0.05	P > 0.05	P > 0.05

Table 11. Kruskal-Wallis test with Dunn’t test for various convulsive responses.

	Staying duration (seconds)
	Mean ± SEM
DMSO (-ve ctrl)	300 ± 0
Z2 (DZP 0.2 mg/kg)	300 ± 0
XXXXII 100 mg/kg	300 ± 0
7-NI 100 mg/kg	43 ± 18
DZP 2 mg/kg (+ve ctrl)	48 ± 17

Table 12. Rotarod test for different treatment groups (n=6).

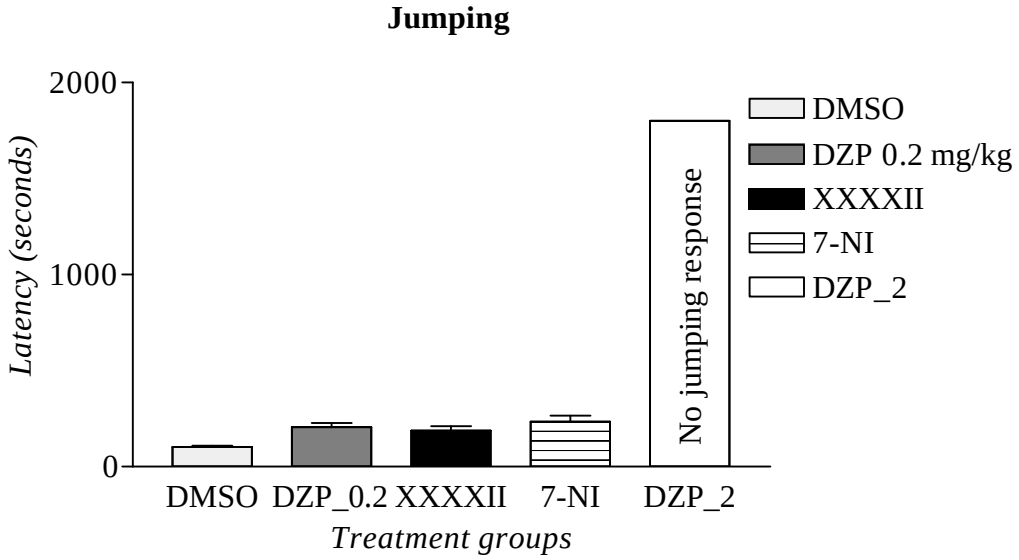

Figure 8. Latency to jumping response for different treatment groups.

With respect to jumping response (**Figure 8**), all of the test compounds showed a delay in jumping, with the exception of 100 mg/kg **XXXXII**. On the other hand, Dunn's test revealed that there was no statistical significance observed among the delay in response caused by 100 mg/kg **XXXXII**, 100 mg/kg 7-NI and 0.2 mg/kg DZP, although numerically the 7-NI showed longest delay among the three compounds (probably due to 7-NI induced catalepsy). The ultimate manifestation of jumping response for 7-NI treated mice suggested that the pathways for catalepsy

induced by 7-NI was either different from or overcome by the pathways for jumping response induced by PTZ.

After the jumping response, the mice were found to be jerking and immobilised, and finally manifested hind limb extension. In high dose PTZ-induced convulsion model, the hind limb extension is a response that indicates tonic stage of convulsion. Similar to the jumping response, both 0.2 mg/kg DZP and 100 mg/kg 7-NI, but not 100 mg/kg **XXXXII**, produced longer latencies to hind limb extension as compared to DMSO (**Figure 9**). However, among the three test compounds, there was no statistical significant difference when compared in pairs using Dunn's test. Nevertheless, it was found that numerically, the mice treated with nNOS inhibitors manifested hind limb extension earlier than the low dose 0.2 mg/kg DZP. Furthermore, as compared to mice treated with 0.2 mg/kg DZP and 100 mg/kg 7-NI, the mice treated with 100 mg/kg **XXXXII** progressed into the hind limb extension in a relatively short duration after the jumping response.

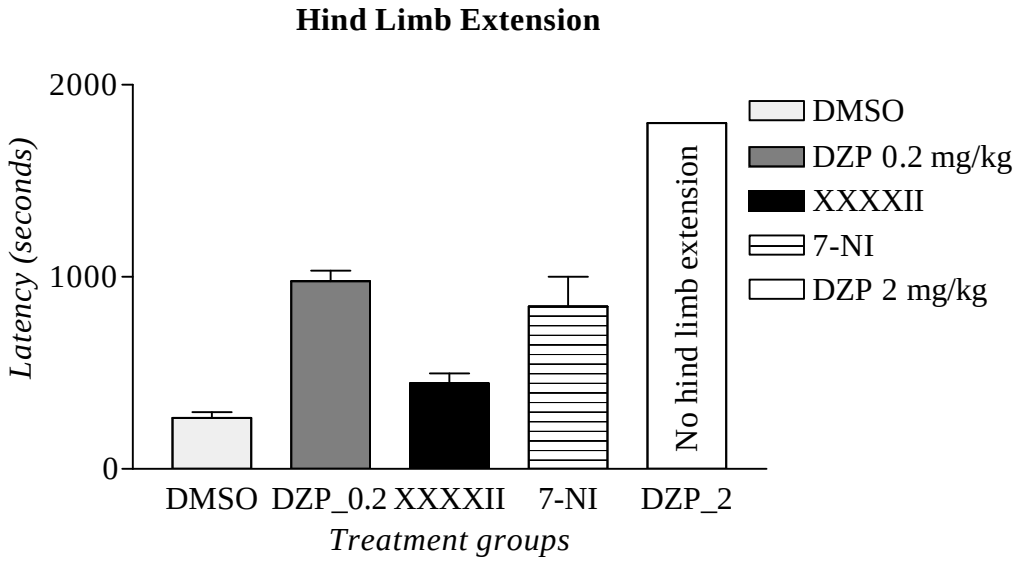

Figure 9. Latency to hind limb extension for different treatment groups.

Due to ethical consideration, observation was carried out in 1800 seconds. Within the 1800 seconds of observation, all the 2 mg/kg DZP treated mice were alive

as expected (**Figure 10**). As for the three test compounds, not only the latencies to death were prolonged, some of the mice were also protected from death. One, two and four out of the six mice were alive after being treated with 0.2 mg/kg DZP, 100 mg/kg **XXXXII** and 100 mg/kg 7-NI respectively. However, all the living mice (except positive control mice) were suffering with extended convulsion during the observation period.

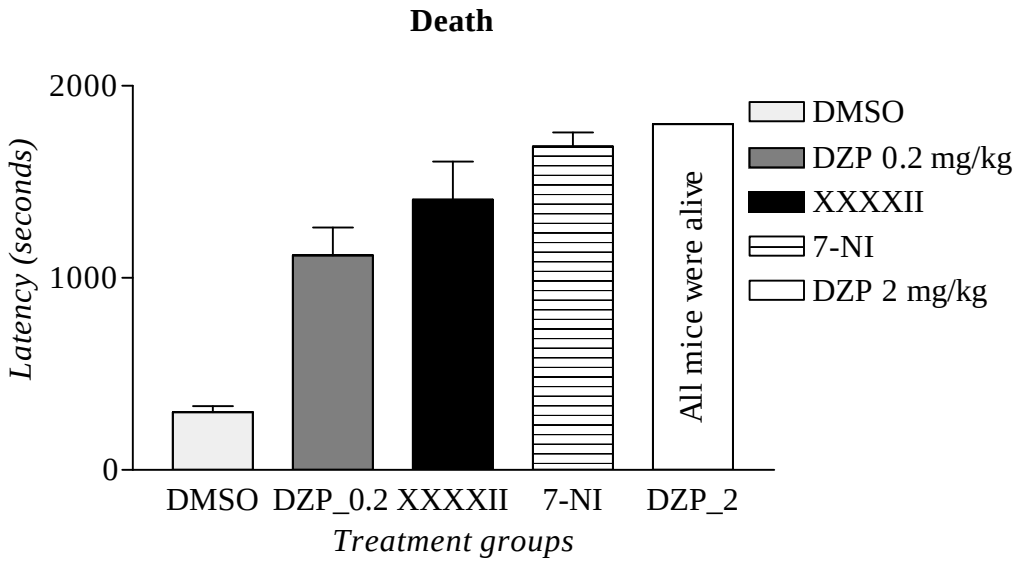

Figure 10. Latency to death for different treatment groups.

For the 0.2 mg/kg DZP treated mice, the mice usually died immediately after hind limp extension. However, for the mice treated with100 mg/kg 7-NI and 100 mg/kg **XXXXII**, it was found that after the first episode of hind limp extension, the mice would proceed into convulsive stage with continuous kicking motion, and some of the 100 mg/kg 7-NI mice might experience various episode of hind limb extension; and some of the mice even recovered from the hind limb extension and relapsed into the jerking and jumping stage for a brief period of time.

With the alive mice death latency taken as 1800 seconds, statistical analyses were performed and the comparison among the three compounds revealed that the nNOS inhibitors, 100 mg/kg **XXXXII** and 100 mg/kg 7-NI, were comparable to each

other and were superior to 0.02 mg/kg DZP. An interesting result was that 0.2 mg/kg DZP was shown to be statistically insignificant as compared to DMSO by Dunn's Test. This might be due to the underlying principle of Dunn's Test that compares the ranking instead of numerically value of the data.

As suggested by the data presented above, it was shown that the nNOS inhibitors were lack of anti-convulsive activity. On the other hand, the nNOS inhibitors were also devoid of pro-convulsive activity. The result was rather different from the heavily debated argument regarding the role of nNOS-derived NO as either anti-convulsant or pro-convulsant[279-282]. Nevertheless, in this study, an analysis of the response profiles of the mice suggested the role of nNOS inhibitor as a neurological protector against neurodegenerative pathways.

The negative control, DMSO-treated mice, progressed rapidly from jumping response, through hind limb extension, into death. On the other extreme, the mice treated with 2 mg/kg DZP (positive control) were completely protected from the manifestation of convulsive responses. This highlighted the efficiency of DZP to act as anticonvulsant, which serves to prevent the excitation of neurons and the initiation of convulsion. The use of DZP at lower dose (0.2 mg/kg) gives a insight to the response profile of DZP. The 0.2 mg/kg DZP treated mice were found to stay in the transitional phase between jumping response and hind limb extension for an extended period, and the mice died shortly after the hind limb extension (**Figure 11**), a response profile which was different from that of the mice treated with nNOS inhibitors. This suggested that DZP was useful in preventing the initialisation of convulsion (thus the slow manifestation of hind limb extension), but it did not offer neuroprotection after the start of the convulsion (rapid progress to death after hind limb extension).

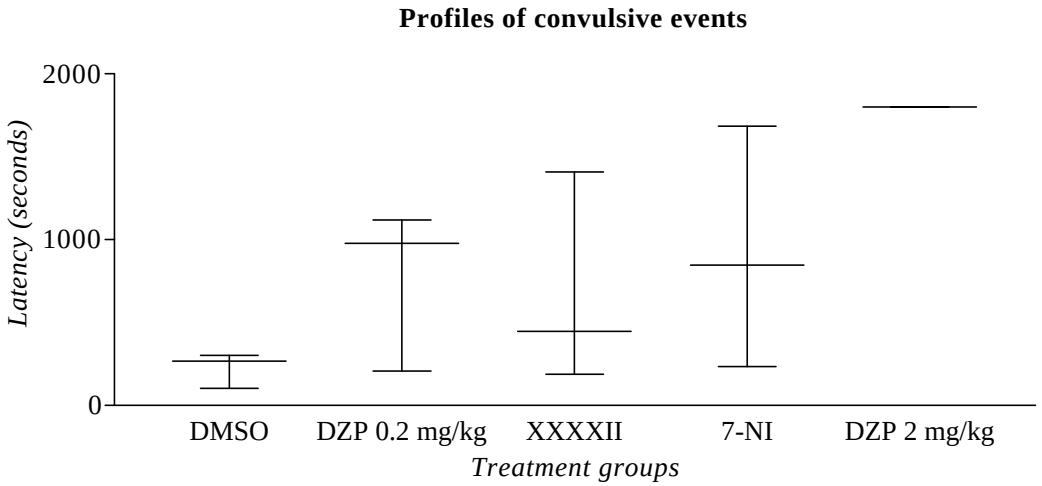

Figure 11. Profiles of convulsive events for different treatment groups.

DZP acts on benzodiazepine receptor that allosterically modulate $GABA_A$ receptor, which in turn activates the Cl^- ion channel[186]. As a result, DZP is able to increase influx of Cl^- ions and subsequently prevent the polarisation of the membranes. In other word, the initiation of convulsion is inhibited. It is known that the convulsion process will lead to a series of downstream pathways that might lead to cellular damages and ultimately the demise of the neurons. Hence, after convulsion was initialised, the DZP offered no protection against the resulting neuronal damages. As a result, DZP is not a neuroprotector in the sense that it does not prevent the cellular damaging responses after the initiation of an insulting event.

A different response profile was observed for the mice treated with nNOS inhibitors, thus suggesting that nNOS inhibitors behaving dissimilarly as the DZP. The mice developed rather rapidly into the hind limb extension, which was indicative of the inability of the nNOS inhibitor to prevent the initiation of convulsion. Since PTZ-induced convulsion was postulated to arise from disruption of GABA-ergic neurons[286], inactivity of nNOS inhibitors implied a limited, if any, contribution of nNOS in PTZ-induced convulsion. Hence, nNOS inhibitor is not considered an anti-convulsant. Nevertheless, it was found that the mice were able to survive for a longer

duration after the hind limb extension, a response profile which was different from that of mice treated with 0.2 mg/kg DZP. This suggested that the nNOS inhibitors offered protection against the neuro-damaging downstream events following the initial insult. Hence, the nNOS was shown to provide neuroprotection against the neurodegenerative pathways.

A comparison of the two nNOS inhibitors used in this study showed that 7-NI was more effective than compound **XXXXII** at the same dose of 100 mg/kg. At 100 mg/kg, the compound **XXXXII** only provided moderate neuroprotection as compared to 7-NI. This was as expected from a comparison of *in vitro* IC_{50} values. The compound **XXXXII** ($IC_{50(nNOS)}$ 58 μM) was 80 times less active than 7-NI ($IC_{50(nNOS)}$ 0.7 μM).

The use of high dose of 7-NI was to evaluate the effect of full nNOS inhibition. The dose of 100 mg/kg was higher than commonly applied 7-NI dose, but the 7-NI was still unable to prevent the initiation of convulsion. This suggested that the nNOS-derived NO was a determining factor for the initiation of convulsion. It was reasonable to assume that 100 mg/kg 7-NI resulted in full inhibition of the nNOS, thus the nNOS was only partially inhibited by compound **XXXXII** at a dose of 100 mg/kg. At this partial inhibitory dose, compound **XXXXII** was able to offer secondary protection against convulsive damages, and at the same time devoid of neuromotor side effects as shown by rotarod test. It was known that nNOS-derived NO played important physiological functions. Although the importance of nNOS inhibition in cases of overproduction of nNOS-derived NO was recognised, there had been concerns on the suitable degree of nNOS inhibition to be achieved in order to provide therapeutic effects, which was devoid of disruption of normal physiological functioning of nNOS[58]. A complete full inhibition of nNOS was undesirable, as

suggested by catalepsy associated with 7-NI in rotarod test. On the other hand, a partial nNOS inhibition by compound **XXXXII** was shown to offer neuronal protection with minimal side effects.

The *in vivo* biological study using compound **XXXXII** demonstrated the *in vitro* activity of the compound was translatable to *in vivo* activity. Even though compound **XXXXII** provided moderate neuroprotection, it was yet to be considered an ideal nNOS selective inhibitor because the dose used in the study was rather high. Nevertheless, the results obtained in this study held promise in using **XXXXII** as a leading template for the further search of nNOS selective inhibitor.

Chapter 12 Conclusion

The nNOS is an important biological target with potential clinical significance. Hyperactive nNOS has been implicated in various neurodegenerative conditions. There were various attempts to search for NOS inhibitors, and inhibitors with good potencies had been reported. However, relatively few inhibitors were found to be nNOS selective.

For inhibitors with guanidino mimicking groups that bind to GBS, good binding affinity is attained with the presence of groups that interact with NBS and/or CBS. In addition, the groups that bind to GBS, SacBS, and (to some extend) CBS are the selectivity-contributing groups. As suggested by X-ray crystallography, the active sites of the three NOS isoforms were highly conserved and rigid, and hence the search for selective inhibitors seemed futile. However, the presence of isoform selective inhibitors argued against the pessimistic views, and recent X-ray crystallographic reports refuted the general perception of rigid active site[176]. Differential induced-binding of inhibitors to the active site could be accounting for the selectivity of reported inhibitors.

The RegG is strategically located immediately adjacent to GBS, and thus it is inevitable for an inhibitor to interact with RegG. However, the RegG is a less studied and under-utilised binding site, and the group binding to RegG is generally considered as a passive element instead of active contributor towards binding affinity and selectivity of an inhibitor. Limited data has suggested that hydrophobic interactions are involved in RegG[102], and hydrophobic interactions have been suggested to be the major driving force for induced-fitting of inhibitors to the active site[108]. Thus, it was hypothesised that by exploiting the RegG, selective nNOS inhibition and improved

nNOS binding affinity can be achieved through differently substituted guanidino compounds, thus may give rise to useful therapeutic value.

Six series of compounds, with guanidino group as the GBS- interacting group and a range of hydrophobic, cationic and anionic groups as the RegG-interacting groups, were synthesised and evaluated as NOS inhibitors, as well as molecular probes of the RegG. From a synthetic point of view, the optimisation of the syntheses of N^1,N^2-dialkylguanidines, NGAA and TZA were challenging. The optimisation of SPOS of N^1,N^2-dialkylguanidines demanded a good understanding of the mechanism of reactions. The solid-phase extraction was applied to the synthesis of NGAA, which required careful control of reaction pH and temperature, while the synthesis of TZA demanded the selection of optimal base and reaction pH. Nevertheless, although the optimisation studies were tedious and time-consuming, the learning process was enjoyable and enriching.

It was known that N^1,N^2,N^3-(trisubstituted)guanidines could not bind to the GBS[106], thus only N^1-(monosubstituted)guanidines and N^1,N^2-(disubstituted)guanidines were evaluated. With additional N^2-substitutent, the N^1,N^2-(disubstituted)guanidines were more potent than N^1-(monosubstituted)guanidines and exhibited a tendency towards selective inhibition, but there was a size limitation on the N^2-susbtituent. Both N^2-nitro and N^2-propyl were found to show similar potency and selectivity profiles.

With charged (both anionic and cationic) N-substituents, the compounds were inactive as NOS inhibitors. As for the hydrophobic N-substituents, the N-benzyl groups were shown to be better than N-alkyl groups in terms of both potency and selectivity. For certain N^1-(ring-substituted)benzyl-N^2-nitroguanidines, especially the electron-rich *meta*-substituted compounds, marked improvement in binding potency

was observed. Nevertheless, despite showing some tendency of nNOS inhibition, the compounds demonstrated no improvement in nNOS selectivity regardless of the nature of the ring substituents. On the other hand, a completely different selectivity profile was observed with N^1-(*a*-substituted)benzyl groups. With bulky and hydrophobic α-substituents, nNOS selective inhibition was demonstrated. The compound **XXXXII**, N^1-(diphenyl)methyl-N^2-nitroguanidine, was found to be nNOS selective with mid-micromolar IC_{50} value (58.0±5 μM).

The results suggested that the RegG was hydrophobic in nature, and it was intolerant of charged species. Besides that, π-π stacking interaction could also be involved in the binding of inhibitor to RegG. Consistent with the X-ray crystallographic studies, the surface topology of the RegG seemed to be highly conserved when the RegG-interacting group was not steric challenging. With bulky, hydrophobic and aromatic RegG-interacting group, the RegG of nNOS could undergo induced-conformational change to accommodate the compound. However, the induced-conformational change was not observed in iNOS and eNOS.

Induced fitting of a ligand to the active site is frequently encountered[107]. Being a non-specific and weak binding force, groups involved in hydrophobic interactions could easily undergo conformational with minimal energetic penalty. In the literatures, hydrophobic interactions were overwhelmingly implicated in cases of induced-fit[107]. Many of the cases of induced-fit could not be predicted by conventional medicinal chemistry approach, which tended to focus on stronger interactions (such as ionic and hydrogen bonding interactions)[107]. In the case of NOS, differential induced fitting of nNOS (but not iNOS and eNOS) active site to the inhibitor was likely to be the reason for selective nNOS inhibition, and this led to a proposal of a size-exclusion mechanism for achieving nNOS selective binding. The

different capacities of the active sites to undergo induced-conformational changes were likely due to the differences in protein residues found in the protein core[176].

The lead compound **XXXXII** was subjected to further *in vivo* testing, and it was found that the *in vitro* activity was translatable into *in vivo* activity. The compound **XXXXII** showed moderate neuroprotection with minimal neuromotor side effects. The results tended to suggest that full nNOS inhibition was undesirable, while a partial nNOS inhibition was preferred. The nNOS inhibitor was found to be neither a proconvulsant nor an anticonvulsant, but instead offered protection against the convulsive neurological damages.

With the information obtained in the current study, several further studies could be identified. Since compound **XXXXII** was shown to be nNOS selective and well tolerated in *in vivo* model, it could be used as a template for future inhibitors, in which the bulky hydrophobic RegG-interacting group is to be retained in order to exploit the size-exclusion mechanism for achieving nNOS selective inhibition. Additional groups interacting with NBS, CBS and/or SacBS can be introduced in order to enhance the potency of compound **XXXXII**. Besides that, in order to understand the structural basis for the size-exclusion mechanism, X-ray crystallography of nNOS, iNOS and eNOS bound with compound **XXXXII** shall be performed. Further SAR study can also be performed with the aim to evaluate the optimal orientation of the phenyl ring for achieving π-π stacking interaction. Since neurodegeneration is usually a multifaceted and long-term disease, nNOS inhibitors obtained shall also be tested using additional *in vivo* neurodegenerative models.

Finally, the hypothesis of the study was proven true; that guanidino compounds such as N^1-substituted-N^2-nitroguanidines showed reasonably good binding to nNOS and that they exhibited good isoform selectivity. The RegGs of the

three NOS isoforms were found to show different capacities to undergo induced-conformational changes, thus enabling a size exclusion mechanism for achieving nNOS selective inhibition.

Materials and Methods

Material and Analysis. All the solvents and reagents used in the synthesis were purchased from Sigma, Aldrich, Fluka, Merck and Tokyo Kasei. The Rink Resin was obtained from Advanced ChemTech. All the solvents and reagents were obtained commercially and used without purification. Melting points (mp) were determined in °C using Gallenkamp melting point apparatus, and were recorded without correction. UV spectra were obtained using Shimadzu UV-160A spectrophotometer and λ_{max} were reported in nm. IR spectra were obtained using Jasco FT/IR-430 spectrometer and representative peaks were reported as cm^{-1}. TLC was carried out using silica gel coated aluminium plates with fluorescent indicator, and was visualized with UV light of wavelength 254nm, as well as iodine vapour chamber. LCMS was performed in a Finnagan LCMS system. LCMS analysis of SPOS products was performed on Eclipse XDB-C8 (4.6 mm x 15 cm) column using the following gradient elution system: 0 min (50% A, 50% B), 0.1 min (50% A, 50% B), 4.1 min (5% A, 95% B), 6.0 min (5% A, 95% B), 10.0 min (50% A, 50% B), 11.0 min (50% A, 50% B), 14.5 min (100% A), 24.5 min (100% A), 28.0 min (50% A, 50% B), 40.0 min (50% A, 50% B), where mobile phase A is 0.01%v/v TFA/methanol and mobile phase B is 0.01%v/v TFA/H_2O. ^1H and ^{13}C NMR spectra were recorded by Bruker-Spectrospin 300 Ultrashield spectrometer and the chemical shifts (δ) were reported in parts per million (ppm) relative to internal standard TMS: s = singlet, d = doublet, dd = double doublet, t = triplet, m = multiplet. Deuterium oxide (D_2O) exchange ^1H NMR was also performed. The MS spectra were obtained on a Finnagan LCQ Ion Trap MS Mass Spectrometer under electron-spay ionization (ESI) (50% aqueous methanol as solvent) or atmospheric pressure chemical ionization (APCI) (acetone as solvent) mode, and the m/z ratios (and relative intensity) of $[M+1]^+$ or $[M-NO_2]^+$ were

reported. Elemental analyses were performed using a Perkin Elmer Elemental Analyzer 2400 CHN and a Perkin Elmer Series II CHNS Analyzer 2400 (by Elemental Analysis Laboratory, National University of Singapore).

Synthesis of N^1-monoalkylguanidines (I – IX). S-Methylisothiourea sulphate (0.01 mol) was added to a conical flask containing 50% methanol/water solution of alkylamine (0.01 mol) and the reaction mixture was refluxed for 24 hours. The cooled solution was then put into refrigerator at 4 °C. If no precipitation occurred, the solution was rotary evaporated to dryness.

N^1-(1-Propyl)guanidine sulphate (I). White crystals (yield 81%), recrystallised from water: mp 243 – 6 °C; λ_{max} (MeOH) 202.2 nm; IR (KBr disc) 3343, 3138, 1661, 1118, 620 cm^{-1}; ^1H NMR (D_2O): δ 3.19 (t, 2H, CH), 1.63 (m, 2H, CH), 0.98 (t, 3H, CH) ppm; ^{13}C NMR (D_2O): δ 157.50, 43.53, 22.03, 10.95 ppm; MS (ESI) (50% MeOH) $[M+1]^+$ m/z 102.1 (100%).

N^1-(2-Methylpropyl)guanidine sulphate (II). Pale white crystals (yield 84%), recrystallised from water: mp 202 – 5 °C; λ_{max} (MeOH) 204.4 nm; IR (KBr disc) 3340, 3169, 1661, 1117, 620 cm^{-1}; ^1H NMR (D_2O): δ 3.00 (d, 2H, CH), 1.87 (m, 1H, CH), 0.94 (d, 6H, CH) ppm; ^{13}C NMR (D_2O): δ 159.13, 50.70, 29.77, 21.27 ppm; MS (ESI) (50% MeOH) $[M+1]^+$ m/z 116.1 (100%).

2-Piperidinylamidine sulphate (III). White crystals (yield 51%), recrystallised from water: mp 288 – 92 °C (ref.[287] 284 – 287 °C (decomposed)); λ_{max} (MeOH) 204.4 nm; IR (KBr disc) 3354, 3188, 2942, 2858, 1631, 1115, 619 cm^{-1}; ^1H NMR (D_2O): δ 3.32 (t, 4H, CH), 1.54 (t, 6H, CH) ppm; ^{13}C NMR (D_2O): δ 157.60, 48.71, 26.71, 25.10 ppm; MS (ESI) (50% MeOH) $[M+1]^+$ m/z 128.2 (100%).

N^1-(Phenylmethyl)guanidine sulphate (IV). White crystals (yield 86%), recrystallised from aqueous propanol and aqueous ethanol: mp 205 – 7 °C (ref.[288] 204

°C); λ_{max} (MeOH) 207.8 nm; IR (KBr disc) 3451, 3315, 3151, 1663, 1455, 1112, 618, 457 cm^{-1}; ^{1}H NMR (DMSO-d_6): δ 8.98 (s, NH), 7.81 (s, NH), 7.27 (m-overlap, 5H, Ar-H), 3.35 (s, 2H, CH) ppm; ^{13}C NMR (DMSO-d_6): δ 156.98, 137.12, 128.44, 127.37, 127.11, 43.80 ppm; MS (ESI) (50% MeOH) $[M+1]^+$ m/z 150.0 (100%).

N^1-((*p*-Chloro)phenylmethyl)guanidine sulphate (V). White crystals (yield 98%), recrystallised from aqueous propanol and aqueous ethanol: mp 222 – 5 °C (ref.[289] 220 – 222 °C); λ_{max} (MeOH) 203.4, 220.2 nm; IR (KBr disc) 3330, 3134, 1662, 1636, 1490, 1112, 807, 619, 541 cm^{-1}; ^{1}H NMR (DMSO-d_6): δ 9.04 (s, NH), 7.81 (s, NH), 7.31 (m, 4H, Ar-H), 4.25 (s, 2H, CH) ppm; ^{13}C NMR (D_2O): δ 157.09, 136.84, 131.60, 128.83, 128.13, 42.75 ppm; MS (ESI) (50% MeOH) $[M+1]^+$ m/z 184.1 (100%), 186.1.

N^1-((*p*-Methyl)phenylmethyl)guanidine sulphate (VI). White crystals (yield 56%), recrystallised from aqueous propanol and aqueous ethanol: mp 209 – 12 °C; λ_{max} (MeOH) 212.0 nm; IR (KBr disc) 3477, 3339, 3161, 1664, 1115, 809, 619 cm^{-1}; ^{1}H NMR (DMSO-d_6): δ 8.93 (s, NH), 7.79 (s, NH), 7.18 (dd, 2H, Ar-H, J = 7.9 Hz), 7.09 (dd, 2H, Ar-H, J = 8.3 Hz), 4.19 (s, 2H, CH), 2.25 (s, 3H, CH) ppm; ^{13}C NMR (DMSO-d_6): δ 157.05, 136.00, 134.76, 128.75, 127.02, 43.22, 20.58 ppm; MS (ESI) (50% MeOH) $[M+1]^+$ m/z 163.7 (100%).

N^1-((*p*-Nitro)phenylmethyl)guanidine sulphate (VII). Golden yellow crystals (yield 63%), recrystallised from aqueous propanol and aqueous ethanol: mp 238 – 9 °C (decomposed); λ_{max} (MeOH) 204.2, 265.8 nm; IR (KBr disc) 3464, 3335, 3169, 3093, 1694, 1627, 1515, 1345, 1107, 1059, 732, 619, 468 cm^{-1}; ^{1}H NMR (DMSO-d_6): δ 9.19 (s, NH), 7.87 (s, NH), 8.08 (dd, 2H, Ar-H, J = 9.0 Hz), 7.52 (dd, 2H, Ar-H, J = 8.6 hz), 4.41 (s, 2H, CH) ppm; ^{13}C NMR (DMSO-d_6): δ 157.23, 146.40, 145.82,

127.90, 123.22, 42.92, 22.82 ppm; MS (ESI) (50% MeOH) $[M+1]^+$ m/z 194.6 (100%).

N^1-((*p*-Amino)phenylmethyl)guanidine sulphate (VIII). Yellow crystals (yield 26%), recrystallised from aqueous propanol and aqueous ethanol: mp 216 – 8 °C; λ_{max} (MeOH) 205.0, 242.2 nm; IR (KBr disc) 3464, 3365, 3151, 1636, 1115, 1048, 824, 620 cm^{-1}; ^1H NMR (DMSO-d_6): δ 8.58 (s, NH), 7.71 (s, NH), 6.97 (dd, 2H, Ar-H, J = 8.3 Hz), 6.52 (dd, 2H, Ar-H, J = 8.3 hz), 4.99 (s, 2H, NH), 4.05 (s, 2H, CH) ppm; ^{13}C NMR (DMSO-d_6): δ 156.83, 147.71, 128.15, 124.39, 113.66, 43.45 ppm; MS (ESI) (50% MeOH) $[M+1]^+$ m/z 164.3 (100%).

N^1-((*m,p*-Dichloro)phenylmethyl)guanidine sulphate (IX). White crystals (yield 55%), recrystallised from aqueous propanol and aqueous ethanol: mp 236 – 7 °C; UV λ_{max} (MeOH) 206.0 nm; IR (KBr disc) 3475, 3326, 3093, 1685.96, 1626, 1468, 1402, 1051, 971, 761, 615, 590, 431 cm^{-1}; ^1H NMR (DMSO-d_6): δ 9.14 (s, NH), 7.83 (s, NH), 7.50 (m-overlay, 2H, Ar-H), 7.28 (d, H, Ar-H, J = 8.7 Hz), 4.27 (s, 2H, CH) ppm; ^{13}C NMR (DMSO-d_6): δ 157.09, 139.04, 130.81, 130.34, 129.60, 129.02, 127.23, 42.33 ppm; MS (ESI) (50% MeOH) $[M+1]^+$ m/z 217.5 (100%), 219.5.

Synthesis of N^1,N^2-dialkylguanidine (X – XV). 0.5g of Rink resin (1.05 mmol/g) was soaked in DCM for at least 6 hours, and subsequently washed with DCM (5ml) and DMF (2 x 5ml). The Rink resin was deprotected by reacting with 20%v/v piperidine/DMF for 30 minutes at room temperature, followed by two washing cycles of DMF (5ml) and THF/DCM (1:1) (5ml). Subsequently, the resin was reacted with a reaction mixture of 0.5 M p-nitrophenyl chloroformate and 0.5 M DIEA in THF/DCM (1:1) at room temperature for 30 minutes, and followed by two washing cycles of THF/DCM (1:1) (5ml) and DMF (5ml). After that, the resin was reacted with a reaction mixture of 0.5 M alkylamine and 0.5 M TEA in DMF at room temperature

for 30 minutes, and followed by two washing cycle of DMF (5ml) and THF/DCM (1:1) (5ml). Subsequently, three cycles of reaction mixture of 0.5 M TosylCl and 0.5 M pyridine in TEA/DCM (1:1) was added at room temperature to the resin. The reaction interval for each cycle was 15/15/30 minutes for unbranched alkyl chain and 30/30/60 minutes for hindered alkyl chain, with three washing cycles of DMF (5ml) and THF/DCM (1:1) (5ml) after each reaction. Following that, the resin was reacted with 0.5 M alkylamine in THF/DCM (1:1) at 50 °C for 24 hours, and this was followed by two washing cycles of THF/DCM (1:1) (5ml) and DMF (5ml). Subsequently, the resin was washed with a series of solvents in sequence: THF/DCM (1:1) (2 x 5ml), DMF (2 x 5ml), acetone (2 x 5ml), water (5ml), acetone (2 x 5ml), DMF (2 x 5ml), THF/DCM (1:1) (2 x 5ml), DCM (2 x 5ml). After that, the product was cleaved from the resin using TFA/MeOH/DCM (5:1:94). The cleavage reaction was performed as two reaction cycles at room temperature for 15 minutes. The cleaved resin was washed with DCM (2 x 5ml) and water (5ml). The combined filtrate was concentrated using vacuum evaporator until saturation and DCM (5ml) was added to the concentrate. This was followed by a liquid-liquid extraction (2x) of the concentrate using water. The organic phase was subsequently evaporated to dryness.

N^1-Benzyl-N^2-propylguanidine (X). Yellow liquid (yield 46 %, purity (LCMS) 83.1 %): ^{1}H NMR (DMSO-d_6) δ 7.37 (m, 5H, Ar-H) 4.41 (d, 2H, CH) 3.11 (q, 2H, CH) 1.50 (m, 2H, CH) 0.86 (t, 3H, CH) ppm; MS (ESI) (50% MeOH) $[M+1]^+$ m/z 191.5 (100%).

N^1-Diphenylmethyl-N^2-propylguanidine (XI). Yellow liquid (yield 38 %, purity (LCMS) 51.5 %): ^{1}H NMR (DMSO-d_6) δ 7.61-7.24 (m, 10H, Ar-H) (an CH is

overlapped with water peak), 2.91 (t, 2H, CH), 1.47 (m, 2H, CH), 0.84 (m, 3H, CH) ppm; MS (ESI) (50% MeOH) $[M+1]^+$ m/z 267.3 (100%).

N^1-(2,4-Dichlorobenzyl)-N^2-propylguanidine (XII). Yellow liquid (yield 128 %, purity (LCMS) 58.6 %): ^{1}H NMR (DMSO-d_6) δ 7.69 (d, 1H, Ar-H, J = 2.3Hz), 7.49 (d, 1H, Ar-H, J = 1.9Hz), 7.35 (s, 1H, Ar-H), 4.45-4.43 (d, 2H, CH_2), 3.10 (m, 2H, CH_2), 1.51 (m, 2H, CH), 0.85 (m, 3H, CH) ppm; MS (ESI) (50% MeOH) $[M+1]^+$ m/z 260.6 (100%).

2-(N-Piperidinyl)-1-propylamidine (XIII). Yellow liquid (yield 17 %, purity (LCMS) 29.5 %: ^{1}H NMR (DMSO-d_6) δ 3.37 (m, 4H, CH), 3.13 (q, 2H, CH), 1.54 (m, 8H, CH), 0.85 (m, 3H, CH) ppm; MS (ESI) (50% MeOH) $[M+1]^+$ m/z 170.2 (100%).

N^1-Benzyl-N^2,N^2-diethylguanidine (XIV). Yellow liquid (yield 32 %, purity (LCMS) 11.0 %): ^{1}H NMR (DMSO-d_6) δ 7.35 (m, 5H, Ar-H), 4.47 (d, 2H, CH), 3.39 (m, 4H, CH), 1.09 (m, 6H, CH) ppm; MS (ESI) (50% MeOH) $[M+1]^+$ m/z 206.2 (5%).

1-Cyclohexyl-2-(N-piperidinyl)amidine (XV). Yellow liquid (yield 26 %, purity (LCMS) 45.3 %): ^{1}H NMR (DMSO-d_6) δ 3.35 (s, 4H, CH), 1.75 (m, 4H, CH), 1.60-1.51 (s, 6H, CH), 1.26 (s, 4H, CH), 1.10 (m, 2H, CH) ppm; MS (ESI) (50% MeOH) $[M+1]^+$ m/z 209.4 (100%).

Synthesis of S-methyl-N-nitroisothiourea (SMNNITU). S-methylisothiourea sulphate (20 g) was added slowly over 5 minutes to a mixture of fuming nitric acid (20 ml) and concentrated sulphuric acid (60 ml) in an ice-bath. After continuous stirring for another 15 minutes, the reaction mixture was poured slowly into a beaker of ice (850 g). The white precipitate formed was collected by vacuum filtration after the ice had melted. Two recrystallisations from aqueous ethanol afforded clear, white

needle crystals (50 – 60 % yield): mp 161 – 163 °C (ref.[198] 163 – 164 °C); λ_{max} (MeOH) 279.8 nm; IR (KBr disc) 3377, 3279, 3112, 1627, 1457, 1250, 1122, 978, 732, 581 cm^{-1}; ^{1}H NMR (DMSO-d_6) δ 9.13 (b, 2H, NH), 2.41 (s, 3H, CH) ppm; MS (ESI) (50% MeOH) $[M+1]^+$ m/z 136.1 (100%).

Synthesis of N^1-alkyl-N^2-nitroguanidine (XVI – XXXXIV). To a solution of alkylamine (0.01 mole) in ethanol (15ml), S-methyl-N-nitroisothiourea (0.01 mole) was added and the reaction mixture was stirred and refluxed for 12 hours. If hydrochloride salt of alkylamine was used, then the free base form was obtained with by neutralization with triethylamine (0.02 mole) prior to the addition of S-methyl-N-nitroisothiourea. For ammonia and alkylamines with boiling point lower than aqueous ethanol, two equivalents of amines was used for each equivalent of SMNNITU, and the reation was conducted at room temperature with continuous stirring. The product precipitated occurred during the reaction or upon cooling, and was collected by vacuum filtration. Recrystallizations from aqueous ethanol afforded purified compounds for characterizations.

N^1-Nitroguanidine (XVI). White needle crystals (yield 59.6%), recrystallised from aqueous ethanol: mp 240 – 242 °C (decomposed) (ref.[290] 246 – 247 °C); λ_{max} (MeOH) 221.6nm, 264.8 nm; IR (KBr disc) 3454, 3398, 3342, 3199, 1667, 1635, 1526, 1406, 1280, 1150, 1040, 781, 562 cm^{-1}; ^{1}H NMR (DMSO-d^6) δ 7.50 (b, 5H, NH) ppm; ^{13}C NMR (DMSO-d^6) δ 161.54 ppm.

N^1-Methyl-N^2-nitroguanidine (XVII). White powders (yield 18.86%), recrystallised from aqueous ethanol: mp 161.1 – 161.9 °C (ref.[291] 159 – 161 °C); λ_{max} (MeOH) 270.2 nm; IR (KBr disc) 3409, 3319, 3243, 3119, 1647, 1603, 1407, 1286, 1139, 1071, 782, 591 cm^{-1}; ^{1}H NMR (DMSO-d^6) δ 8.55 (s, 1H, NH), 7.82 (s, 2H, NH), 2.76 (s, 3H, CH) ppm; MS (ACPI) (50% MeOH) $[M-NO_2+2]^+$ m/z 74.0 (100%).

N^1-Propyl-N^2-nitroguanidine (XVIII). White crystals (yield 11%), recrystallised from aqueous ethanol: mp 97.9 – 98.7 °C (ref.[292] 98 – 98.5 °C); λ_{max} (MeOH) 270.2 nm; IR (KBr disc) 3386, 3308, 3158, 2965, 1652, 1597, 1558, 1425, 1319, 1092, 762, 577 cm^{-1}; ^1H NMR (DMSO-d^6) δ 8.54 (s, 1H, NH), 7.91 (s, 2H, NH), 3.11 (q, 2H, CH) 1.50 (q, 2H, CH), 0.87 (t, 3H, CH) ppm; MS (ACPI) (50% MeOH) $[M\text{-}NO_2+2]^+$ m/z 102.0 (100%).

N^1-Isobutyl-N^2-nitroguanidine (XIX). White flakes (yield 7.51%), recrystallised from aqueous ethanol: mp 121.0 – 121.7 °C (ref.[291] 120 – 121 °C); λ_{max} (MeOH) 270.0nm; IR (KBr disc) 3375, 3322, 3175, 2959, 1652, 1601, 1553, 1422, 1323, 1105, 759, 605, 558 cm^{-1}; ^1H NMR (DMSO-d^6) δ 8.58 (s, 1H, NH), 7.89 (s, 1H, NH), 6.96 (s, 1H, NH), 2.96 (s, 2H, CH), 1.78 (s, 2H, CH) 0.88 (d, 6H, CH) ppm; MS (ACPI) (50% MeOH) $[M\text{-}NO_2+2]^+$ m/z 116.1 (100%).

N^1-Cyclohexyl-N^2-nitroguanidine (XX). White powders (yield 59.46%), recrystallised from aqueous ethanol: mp 198.2 – 199.7 °C (ref.[198] 197 – 198 °C); λ_{max} (MeOH) 270.4nm; IR (KBr disc) 3419, 3308, 3160, 2929, 2851, 1636, 1520, 1436, 1385, 1260, 1140, 724, 576 cm^{-1}; ^1H NMR (DMSO-d^6) δ 8.39 (s, 1H, NH), 8.03 (s, 1H, NH), 1.50 (m, 11H, CH) ppm; MS (ACPI) (50% MeOH) $[M\text{-}NO_2+2]^+$ m/z 142.1 (100%).

N^1,N^1-Dimethyl-N^2-nitroguanidine (XXI). White crystals (yield 55.30%), recrystallised from aqueous ethanol: mp 196.9 – 199.2 °C (ref.[291] 193.5 – 195 °C); λ_{max} (MeOH) 270.8nm; IR (KBr disc) 3398, 3266, 2936, 1611, 1589, 1492, 1355, 1298, 782, 559 cm^{-1}; ^1H NMR (DMSO-d^6) δ 8.29 (s, 2H, NH), 2.97 (s, 6H, CH) ppm; MS (ACPI) (50% MeOH) $[M\text{-}NO_2+2]^+$ m/z 89.0 (100%).

N^1,N^1-Diethyl-N^2-nitroguanidine (XXII). White crystals (yield 6.25%), recrystallised from aqueous ethanol: mp 93.7 – 95.1 °C; λ_{max} (MeOH) 280.0nm; IR

(KBr disc) 3378, 3260, 2978, 1611, 1582, 1483, 1385, 1268, 1198, 1081, 778, 605 cm^{-1}; ^1H NMR (DMSO-d^6) δ 8.33 (s, 2H, NH), 1.09 (s, 10H, CH) ppm; MS (ACPI) (50% MeOH) $[M\text{-}NO_2+2]^+$ m/z 116.1 (100%).

N^1-Benzyl-N^2-nitroguanidine (XXIII). White flaky crystals, recrystallised from aqueous ethanol (yield 75 %): mp 181 – 183 °C (ref.[293] 179 – 180.5 °C); λ_{max} (MeOH) 270.8 nm; IR (KBr disc) 3378, 3177, 1654, 1596, 1307 740, 707 cm^{-1}. ^1H NMR (DMSO-d_6) δ 8.89 (b, 1H, NH), 7.99 (b, 2H, NH), 7.33 (m, 5H, Ar-H), 4.42 (s, 2H, CH) ppm; MS (APCI) (acetone) $[M\text{-}NO_2]^+$ m/z 148.1 (100%).

N^1-(*p*-Chloro)benzyl-N^2-nitroguanidine (XXIV). White crystal, recrystallised from aqueous ethanol (yield 38 %): mp 197 – 199 °C (ref.[293] 195 – 197 °C); λ_{max} 269.8 (MeOH) nm; IR (KBr disc) 3371, 3177, 1645, 1589, 1301, 818 cm^{-1}. ^1H NMR (DMSO-d_6) δ 8.95 (b, 1H, NH), 8.01 (b, 2H, NH), 7.43 (dd, 2H, Ar-H, J = 8.3 Hz), 7.32 (dd, 2H, Ar-H, J = 8.7 Hz), 4.40 (d, 2H, CH) ppm; MS (APCI) (acetone) $[M\text{-}NO_2]^+$ m/z 182.1 (100%), 184.0.

N^1-(*m*-Chloro)benzyl-N^2-nitroguanidine (XXV). White powders, recrystallised from aqueous ethanol (yield 25 %): mp 169 – 170 °C (ref.[293] 166 – 167 °C); λ_{max} (MeOH) 270.2 nm; IR (KBr disc) 3376, 3161, 1652, 1595, 1309, 783, 726 cm^{-1}. ^1H NMR (DMSO-d_6) δ 8.97 (b, 1H, NH), 8.05 (b, 2H, NH), 7.35 (m, 4H, Ar-H), 4.43 (d, 2H, CH) ppm; MS (APCI) (acetone) $[M\text{-}NO_2]^+$ m/z 182.1 (100%), 184.1.

N^1-(*p*-Fluoro)benzyl-N^2-nitroguanidine (XXVI). White flaky crystals, recrystallised from aqueous ethanol (yield 69 %): mp 205 – 206 °C (ref.[293] 205 – 206 °C); λ_{max} (MeOH) 270.0 nm; IR (KBr disc) 3382, 3178, 1652, 1592, 1307, 832 cm^{-1}. ^1H NMR (DMSO-d_6) δ 8.96 (b, 1H, NH), 8.01 (b, 2H, NH), 7.28 (m, 4H, Ar-H), 4.40 (d, 2H, CH) ppm; MS (APCI) (acetone) $[M\text{-}NO_2]^+$ m/z 166.1 (100%).

N^1-(*p*-Methyl)benzyl-N^2-nitroguanidine (XXVII). White crystals, recrystallised from aqueous ethanol (yield 54 %): mp 186 – 187 °C (ref.[293] 181 – 183 °C); λ_{max} (MeOH) 270.6 nm; IR (KBr disc) 3380, 3162, 1650, 1593, 1306, 805 cm^{-1}. ^1H NMR (DMSO-d_6) δ 8.97 (b, 1H, NH), 7.96 (b, 2H, NH), 7.18 (m, 4H, Ar-H), 4.36 (s, 2H, CH), 2.90 (s, 3H, CH) ppm; MS (APCI) (acetone) $[M\text{-}NO_2]^+$ m/z 162.1 (100%); Anal. ($C_9H_{12}N_4O_2$) C, H, N: calcd, 40.17, 3.79, 29.28; found, 40.19, 3.80, 29.17.

N^1-(*p*-Trifluoromethyl)benzyl-N^2-nitroguanidine (XXVIII). White needlelike crystals, recrystallised from aqueous ethanol (yield 61 %): mp 156 – 158.5 °C; λ_{max} (MeOH) 268.0 nm; IR (KBr disc) 3385, 3180, 1653, 1596, 1330, 832 cm^{-1}. ^1H NMR (DMSO-d_6) δ 9.05 (b, 1H, NH), 8.05 (b, 2H, NH), 7.74 (dd, 2H, Ar-H, J = 8.3 Hz), 7.51 (dd, 2H, Ar-H, J = 8.2 Hz), 4.51 (d, 2H, CH) ppm; MS (APCI) (acetone) $[M\text{-}NO_2]^+$ m/z 216.1 (100%); Anal. ($C_9F_3H_9N_4O_2$) C, H, N: calcd, 41.23, 3.46, 21.37; found, 41.24, 3.39, 21.43.

N^1-(*p*-Methoxy)benzyl-N^2-nitroguanidine (XXIX). White crystals, recrystallised from aqueous ethanol (yield 68 %): mp 191 – 192 °C (ref.[293] 191.5 – 192.5 °C); λ_{max} (MeOH) 271.4 nm; IR (KBr disc) 3374, 3185, 1653, 1595, 1302, 1238, 1096, 820 cm^{-1}. ^1H NMR (DMSO-d_6) δ 8.94 (b, 1H, NH), 7.94 (b, 2H, NH), 7.25 (dd, 2H, Ar-H, J = 8.7 Hz), 6.92 (dd, 2H, Ar-H, J = 8.7 Hz), 4.33 (s, 2H, CH), 3.74 (s, 3H, CH_3) ppm; MS (APCI) (acetone) $[M\text{-}NO_2]^+$ m/z 178.1 (100%).

N^1-(*p*-Nitro)benzyl-N^2-nitroguanidine (XXX). White needlelike crystals, recrystallised from aqueous ethanol (yield 75 %): mp 178 – 179 °C; λ_{max} (MeOH) 271.8 nm; IR (KBr disc) 3405, 3235, 1652, 1609, 1340, 844 cm^{-1}. ^1H NMR (DMSO-d_6) δ 9.06 (b, 1H, NH), 8.91 (b, 2H, NH), 8.24 (dd, 2H, Ar-H, J = 9.0 Hz), 7.56 (dd, 2H, Ar-H, J = 9.1 Hz), 4.57 (d, 2H, CH) ppm; MS (APCI) (acetone) $[M\text{-}NO_2]^+$ m/z

193.1 (100%); Anal. ($C_8H_9N_5O_4$) C, H, N: calcd, 40.17, 3.79, 29.28; found, 40.19, 3.80, 29.17.

N^1-(*p*-Amino)benzyl-N^2-nitroguanidine (XXXI). Pale yellowish golden flaky crystals, recrystallised from aqueous ethanol (yield 63 %): mp 205 – 208 °C; λ_{max} (MeOH) 269.8 nm; IR (KBr disc) 3373, 3089, 1644, 1607, 1352, 1280, 832, cm^{-1}. ^1H NMR (DMSO-d_6) δ 8.86 (b, 1H, NH), 7.88 (b, 2H, NH), 6.69 5 (dd, 2H, Ar-H, J = 8.3 Hz), 6.55 (dd, 2H, Ar-H, J = 8.3 Hz), 5.04 (s, 2H, Ar-NH), 4.20 (s, 2H, CH) ppm; MS (APCI) (acetone) $[M\text{-}NO_2]^+$ m/z 163.1 (100%); Anal. ($C_8H_{11}N_5O_2$) C, H, N: calcd, 45.93, 5.30, 33.48; found, 45.93, 5.28, 32.99.

N^1-(*p*-Aminosulphonyl)benzyl-N^2-nitroguanidine (XXXII). White powders, recrystallised from aqueous ethanol (yield 59 %): mp 198 – 200 °C; λ_{max} (MeOH) 270.8 nm; IR (KBr disc) 3400, 3181, 1644, 1588, 1167, 1322, 811 cm^{-1}. ^1H NMR (DMSO-d_6) δ 9.03 (b, 1H, NH), 8.05 (b, 2H, NH), 7.82 (m, 2H, Ar-H), 7.47 (m, 2H, Ar-H), 7.34 (m, 2H, SO_2NH_2), 4.51 (s, 2H, CH) ppm; MS (APCI) (acetone) $[M\text{-}NO_2]^+$ m/z 227.2 (100%); Anal. ($C_8H_{11}N_5O_4S_1$): C, H, N, S: calcd, 35.16, 4.06, 25.63, 11.73; found, 35.38, 4.51, 25.23, 12.12.

N^1-(*p*-t-Butyl)benzyl-N^2-nitroguanidine (XXXIII). White powdery crystals, recrystallised from aqueous ethanol (yield 39 %): mp 170 – 172 °C; λ_{max} (MeOH) 270.2 nm; IR (KBr disc) 3388, 3208, 2950, 1661, 1599, 1311, 821 cm^{-1}. ^1H NMR (DMSO-d_6) δ 8.96 (b, 1H, NH), 7.94 (b, 2H, NH), 7.38 (dd, 2H, Ar-H, J = 8.3 Hz), 7.23 (dd, 2H, Ar-H, J = 8.3 Hz), 4.36 (s, 2H, CH), 1.27 (s, 9H, CH) ppm; MS (APCI) (acetone) $[M\text{-}NO_2]^+$ m/z 204.2 (100%); Anal. ($C_{12}H_{18}N_4O_2$): C, H, N: calcd, 57.58, 7.25, 22.38; found, 57.61, 7.32, 21.85.

N^1-(*m*-Methyl)benzyl-N^2-nitroguanidine (XXXIV). White crystals, recrystallised from aqueous ethanol (yield 48 %): mp 152 – 154 °C (ref.[293] 151 – 153 °C); λ_{max}

(MeOH) 270.0 nm; IR (KBr disc) 3396, 3160, 1650, 1595, 1303, 751, 702 cm^{-1}. ^1H NMR (DMSO-d_6) δ 8.96 (b, 1H, NH), 7.98 (b, 2H, NH), 7.18 (m, 4H, Ar-H), 4.38 (d, 2H, CH), 2.30 (s, 3H, CH) ppm; MS (APCI) (acetone) $[M\text{-}NO_2]^+$ m/z 162.1 (100%).

N^1-(*m*-Trifluoromethyl)benzyl-N^2-nitroguanidine (XXXV). White crystals, recrystallised from aqueous ethanol (yield 27 %): mp 164 – 165 °C (ref.[293] 164 – 165 °C); λ_{max} (MeOH) 270.4 nm; IR (KBr disc) 3489, 3157, 1651, 1618, 1329, 778, 705 cm^{-1}. ^1H NMR (DMSO-d_6) δ 9.00 (b, 1H, NH), 8.08 (b, 2H, NH), 7.66 (m, 4H, Ar-H), 4.51 (s, 2H, CH) ppm; MS (APCI) (acetone) $[M\text{-}NO_2]^+$ m/z 216.1 (100%).

N^1-(*m*-Nitro)benzyl-N^2-nitroguanidine (XXXVI). Milky white powders, recrystallised from aqueous ethanol (yield 62 %): mp 202 – 203 °C; λ_{max} (MeOH) 268.8 nm; IR (KBr disc) 3379, 3151, 1645, 1596, 1346, 769, 732 cm^{-1}. ^1H NMR (DMSO-d_6) δ 9.10 (b, 1H, NH), 8.16 (b, 2H, NH), 8.17 (t, 2H, Ar-H, J = 8.3 Hz), 7.78 (d, 1H, Ar-H, J = 7.5 Hz), 7.68 (t, 1H, Ar-H, J = 7.9 Hz), 4.55 (d, 2H, CH) ppm; MS (APCI) (acetone) $[M\text{-}NO_2]^+$ m/z 193.1 (100%); Anal. ($C_8H_9N_5O_4$): C, H, N: calcd, 40.17, 3.79, 29.28; found, 40.22, 3.84, 28.84.

N^1-Piperonyl-N^2-nitroguanidine (XXXVII). Milky white flaky crystals, recrystallised from aqueous ethanol (yield 78 %): mp 209 – 210 °C (ref.[293] 207.5 – 209 °C); λ_{max} (MeOH) 273.0 nm; IR (KBr disc) 3369, 3158, 1651, 1598, 1308, 1259, 1094, 813, 770, 704 cm^{-1}. ^1H NMR (DMSO-d_6) δ δ 8.90 (b, 1H, NH), 7.94 (b, 2H, NH), 6.89 (t, 1H, Ar-H, J= 4.5 Hz J = 3.4 Hz), 6.88 (s, 1H, Ar-H), 6.81 (d, 1H, Ar-H, J = 8.3 Hz), 5.99 (s, 2H, CH), 4.31– 4.29 (d, 2H, CH) ppm; MS (APCI) (acetone) $[M\text{-}NO_2]^+$ m/z 192.1 (100%).

N^1-(*o,p*-Dichloro)benzyl-N^2-nitroguanidine (XXXVIII). White powdery crystals, recrystallised from aqueous ethanol (yield 59 %): mp 205.5 – 207.5 °C (ref.[293] 200 – 202 °C); λ_{max} (MeOH) 269.4 nm; IR (KBr disc) 3379, 3176, 1652, 1600, 1306, 822,

694 cm^{-1}. ^1H NMR (DMSO-d_6) δ 8.88 (b, 1H, NH), 8.10 (b, 2H, NH), 7.64– 7.64 (d, 1H, Ar-H, J = 1.9 Hz), 7.47 (dd, 1H, Ar-H, J = 8.3 Hz), 7.34 (dd, 1H, Ar-H, J = 8.3 Hz), 4.46 (s, 2H, CH) ppm; MS (APCI) (acetone) $[M+1]^+$ m/z 216.2 (100%), 218.1, 220.1; Anal. ($C_8Cl_2H_8N_4O_2$): C, H, N: calcd, 36.52, 3.07, 21.30; found, 36.57, 3.05, 21.26.

N^1-(*m,p*-Dichloro)benzyl-N^2-nitroguanidine (XXXIX). White powdery crystals, recrystallised from aqueous ethanol (yield 41 %): mp 209 – 211 °C (ref.[293] 208 – 210 °C); λ_{max} (MeOH) 269.6 nm; IR (KBr disc) 3372, 3161, 1652, 1594, 1308, 824, 784, 737 cm^{-1}. ^1H NMR (DMSO-d_6) δ 8.96 (b, 1H, NH), 8.05 (b, 2H, NH), 7.63 (dd, 1H, Ar-H, J = 8.3 Hz), 7.57 (d, 1H, Ar-H, J = 1.9 Hz), 7.30 (dd, 1H, Ar-H, J = 8.3 Hz), 4.41 (d, 2H, CH) ppm; MS (APCI) (acetone) $[M-NO_2]^+$ m/z 216.1 (100%), 218.1, 220.0.

S-(-)-N^1-(α-Methyl)benzyl-N^2-nitroguanidine (XXXX). White flaky powders, recrystallised from aqueous ethanol (yield 37 %): mp 123 – 125 °C (ref.[293] 126 – 127 °C); λ_{max} (MeOH) 271.2 nm; IR (KBr disc) 3397, 3210, 1659, 1590, 1456, 1411, 1364, 1300, 754, 698 cm^{-1}. ^1H NMR (DMSO-d_6) δ 8.76 (b, 1H, NH), 7.92 (b, 2H, NH), 7.37 (m, 4H, Ar-H), 7.28 (m, 1H, Ar-H), 4.89 (m, 1H, CH), 1.43– 1.41 (d, 3H, CH) ppm; MS (APCI) (acetone) $[M-NO_2]^+$ m/z 162.1 (100%); Anal. ($C_9H_{12}N_4O_2$): C, H, N: calcd, 51.92, 5.81, 26.91; found, 52.13, 5.48, 26.68.

R-(+)-N^1-(α-Methyl)benzyl-N^2-nitroguanidine (XXXXI). White crystals, recrystallised from aqueous ethanol (yield 7 %): mp 124.5 – 126 °C (ref.[293] 126 – 127 °C); λ_{max} (MeOH) 271.0 nm; IR (KBr disc) 3400, 3208, 1658, 1590, 1456, 1410, 1364, 1298, 753, 698 cm^{-1}. ^1H NMR (DMSO-d_6) δ 8.73 (b, 1H, NH), 7.94 (b, 2H, NH), 7.36 (m, 4H, Ar-H), 7.29 (m, 1H, Ar-H), 4.89 (m, 1H, CH), 1.42 (d, 3H, CH)

ppm; MS (APCI) (acetone) $[M+1]^+$ m/z 162.1 (100%); Anal. ($C_9H_{12}N_4O_2$): C, H, N: calcd, 51.92, 5.81, 26.91; found, 51.96, 5.83, 26.90.

N^1-(α-Phenyl)benzyl-N^2-nitroguanidine (XXXXII). White powders, recrystallised from aqueous ethanol (yield 34 %): mp 231 – 232 °C (ref.[293] 236 – 237 °C); λ_{max} (MeOH) 272.8 nm; IR (KBr disc) 3429, 3321, 3249, 1634, 1586, 1453, 1387, 1257, 746, 717 cm^{-1}. ^1H NMR (DMSO-d_6) δ 9.23 (b, 1H, NH), 7.87 (b, 2H, NH), 7.32 (m, 10H, Ar-H), 6.09 (d, 1H, CH) ppm; MS (APCI) (acetone) $[M-NO_2]^+$ m/z 224.3 (100%); Anal. ($C_{14}H_{14}N_4O_2$): C, H, N: calcd, 62.21, 5.22, 20.73; found, 62.49, 5.27, 20.35.

N^1-(1-Indanyl)-N^2-nitroguanidine (XXXXIII). White powders, recrystallised from aqueous ethanol (yield 24 %): mp 156 – 158 °C; λ_{max} (MeOH) 271.8 nm; IR (KBr disc) 3379, 3184, 1646, 1584, 1422, 1348, 1309, 750, 700 cm^{-1}. ^1H NMR (DMSO-d_6) δ 8.12 (b, 3H, NH), 7.25 (m, 4H, Ar-H), 5.23 (m, 1H, CH), 3.96 (m, 1H, CH), 2.80 (m, 1H, CH), 2.50 (m, 1H, CH), 1.86 (s, 1H, CH) ppm; MS (APCI) (acetone) $[M-NO_2]^+$ m/z 174.1 (100%); Anal. ($C_{10}H_{12}N_4O_2$): C, H, N: calcd, 54.53, 5.49, 25.53; found, 54.49, 5.36, 25.42.

N^1-(1,2,3,4-Tetrahydro-1-napthyl)-N^2-nitroguanidine (XXXXIV). White powders, recrystallised from aqueous ethanol (yield 26 %): mp 175.5 – 177 °C; λ_{max} (MeOH) 272.2 nm; IR (KBr disc) 3392, 3168, 2930, 1645, 1590, 1420, 1366, 1301, 786, 717 cm^{-1}. ^1H NMR (DMSO-d_6) δ 8.06 (b, 3H, NH), 7.20 (m, 3H, Ar-H), 7.14 (m, 1H, Ar-H), 4.91 (s, 1H, CH), 2.74 (m, 2H, CH), 1.95 (s, 1H, CH), 1.78 (m, 3H, CH) ppm; MS (APCI) (acetone) $[M-NO_2]^+$ m/z 188.1 (100%); Anal. ($C_{11}H_{14}N_4O_2$): C, H, N: calcd, 56.40, 6.02, 23.91; found, 56.46, 5.93, 24.03.

Synthesis of 1-alkyl-4-nitroimino-1,3,5-triazinane (NGAA) (XXXXV – XXXXVII). To 0.01 moles of *dl*-α-amino acid, 10ml of 1M sodium carbonate was

added and the reaction mixture was heated to boil. Subsequently 0.01 moles of S-methyl-N-nitroisothiourea was added to the boiling mixture. When the S-methyl-N-nitroisothiourea was fully dissolved, the reaction mixture was left to cool to room temperature with continuous stirring for 24 hours.

2-(2-nitroguanidino)-ethanoic acid (XXXXV). Whitish orange powders (yield 78%), recyrstallised from aqueous ethanol: mp 176.2 °C (decomposed) (ref.[294] 179 °C (decomposed)); λ_{max} (MeOH) 270.2 nm; IR (KBr disc) 3379, 3291, 3202, 1704, 1666, 1621, 1537, 1463, 1317, 1133, 929, 784,730, 531 cm^{-1}; ^{1}H NMR (DMSO-d^{6}) δ 8.89 (s, 1H, NH), 8.00 (s, 1H, NH), 7.12 (s, 1H, NH), 2.52 (s, 2H, CH), 1.06 (s, 1H, COOH) ppm; MS (ESI) (50% MeOH) $[M+1]^{+}$ m/z 161.6 (100%).

2-(2-nitroguanidino)-4-methyl-pentanoic acid (XXXXVI). Orange powders (yield 17%), recyrstallised from aqueous ethanol: mp 143.6 – 144.6 °C; λ_{max} (MeOH) 270.6 nm; IR (KBr disc) 3412, 3298, 3244, 3170, 2959, 1752, 1719, 1641, 1526, 1454, 1398, 1258, 1176, 785, 742, 581 cm^{-1}; ^{1}H NMR (DMSO-d^{6}) δ 7.99 (m, 3H, NH) 4.26 (s, 1H, CH) 1.63 (s, 2H, CH) 0.90 (s, 6H, CH) ppm; MS (ESI) (50% MeOH) $[M+1]^{+}$ m/z 218.7 (100%).

2-(2-nitroguanidino)-3-phenyl-propanoic acid (XXXXVII). Orange crystals (yield 65%), recyrstallised from aqueous ethanol: mp 113.4 – 116.7 °C; λ_{max} (MeOH) 270.4nm; IR (KBr disc) 3545, 3421, 3331, 1705, 1628, 1581, 1524, 1438, 1394, 1272, 1185, 1121, 875, 814, 784, 702, 615 cm^{-1}; ^{1}H NMR (DMSO-d^{6}) δ 8.84 (s, 1H, NH), 7.97 (s, 2H, NH), 7.28 (m, 5H, Ar-H), 4.53 (s, 1H, CH), 3.08 (d, 2H, CH) ppm; MS (ESI) (50% MeOH) $[M+1]^{+}$ m/z 253.0 (100%).

Synthesis of 1-alkyl-4-nitroimino-1,3,5-triazinane (TZN) (XXXXVIII – LIII). To 0.0025 moles of nitroguanidine, 10 ml of 50% aqueous ethanol was added, followed by 0.0025 moles of alkylamine and 0.005 moles of formaldehyde (37% aqueous

solution). The reaction mixture was heated to 50 °C for 5 hours. The product was precipitated after being cooled to room temperature or 0 °C, and was collected by vacuum filtration. The product from recrystallized from aqueous ethanol.

1-Methyl-4-nitroimino-1,3,5-triazinane (XXXXVIII). White crystals (yield 51 %), recrystallized from aqueous ethanol: mp 206.1 – 208.5 °C; λ_{max} (MeOH) 270.8 nm; IR (KBr disc) 3344, 3211, 3131, 1615, 1449, 1389, 1320, 1108, 784, 714 cm^{-1}; ^{1}H NMR (DMSO-d^{6}) δ 8.71 (s, 2H, NH) 4.18 (s, 4H, CH) 2.41 (s, 3H, CH) ppm; MS (ESI) (50% MeOH acidified) $[M]^{+}$ m/z 159.0 (100%).

1-Propyl-4-nitroimino-1,3,5-triazinane (XXXXIX). White flakes (yield 71 %), recrystallized from aqueous ethanol: mp 186.0 – 187.5 °C; λ_{max} (MeOH) 271.0 nm; IR (KBr disc) 3342, 3207, 3129, 1616, 1454, 1385, 1321, 1107, 784, 715 cm^{-1}; ^{1}H NMR (DMSO-d^{6}) δ 8.68 (s, 2H, NH) 4.24 (s, 4H, CH), 2.53 (t, 2H, CH), 1.47 (m, 2H, CH), 0.88 (t, 3H, CH) ppm; MS (ESI) (50% MeOH acidified) $[M]^{+}$ m/z 187.1 (100%).

1-(2-Methyl)propyl-4-nitroimino-1,3,5-triazinane (L). White flakes (yield 64 %), recrystallized from aqueous ethanol: mp 183.1 – 184.9 °C; λ_{max} (MeOH) 270.8 nm; IR (KBr disc) 3335, 3212, 3133, 1613, 1459, 1388, 1318, 1105, 784, 713 cm^{-1}; ^{1}H NMR (DMSO-d^{6}) δ 8.69 (s, 2H, NH) 4.22 (s, 4H, CH), 2.35 (d, 2H, CH), 1.74 (m, 1H, CH), 0.89 (m, 6H, CH) ppm; MS (ESI) (50% MeOH acidified) $[M]^{+}$ m/z 200.9 (100%).

1-Cyclohexyl-4-nitroimino-1,3,5-triazinane (LI). White crystals (yield 76 %), recrystallized from aqueous ethanol: mp 180.2 – 182.0 °C; λ_{max} (MeOH) 271.6 nm; IR (KBr disc) 3346, 3208, 3124, 2926, 1607, 1475, 1383, 1298, 1108, 784, 719 cm^{-1}; ^{1}H NMR (DMSO-d^{6}) δ 8.64 (s, 2H, NH), 4.34 (s, 4H, CH_2), 1.88 (d, 2H, CH), 1.73

(d, 2H, CH), 1.56 (m, 1H, CH), 1.19 (m, 6H, CH) ppm; MS (ESI) (50% MeOH acidified) $[M]^+$ m/z 226.7 (100%).

1-Benzyl-4-nitroimino-1,3,5-triazinane (LII). White crystals (yield 85 %), recrystallized from aqueous ethanol: mp 215.0 – 217.2 °C (ref.[295] 217 – 218°C); λ_{max} (MeOH) 271.6 nm; IR (KBr disc) 3358, 3191, 3122, 1595, 1482, 1389, 1310, 1109, 998, 777, 742, 715, 699 cm^{-1}; ^1H NMR (DMSO-d^6) δ 8.77 (s, 2H, NH), 7.34 (m, 5H, Ar-H), 4.24 (s, 4H, CH), 3.79 (s, 2H, CH) ppm; MS (ESI) (50% MeOH acidified) $[M]^+$ m/z 234.5 (100%).

1-(2-Phenyl)ethyl-4-nitroimino-1,3,5-triazinane (LIII). White needle (yield 90 %), recrystallized from aqueous ethanol: mp 196.0 – 197.5 °C; λ_{max} (MeOH) 271.2 nm; IR (KBr disc) 3346, 3120, 3114, 1603, 1468, 1398, 1371, 1314, 1106, 782, 751, 741, 697 cm^{-1}; ^1H NMR (DMSO-d^6) δ 8.72 (s, 2H, NH), 7.20 (m, 5H, Ar-H), 4.29 (s, 4H, CH), 2.81 (m, 4H, CH) ppm; MS (ESI) (50% MeOH acidified) $[M]^+$ m/z 248.4 (100%).

Synthesis of 1-(substituted)phenyl-2,4-diamino-1,2-dihydro-2,2-dimethyl-1,3,5-triazine HCl (TZP^{x}HCl). In the synthesis of **TZP**, a mixture of substituted anilines (0.02 mole), cyanoguanidine (1.86g, 0.022 mole), acetone (30ml) and concentrated hydrochloric acid (1.7ml, 0.02 mole) was refluxed for 2 hours to 30 hours depending on the type of aniline used. The progress of the reaction was monitored by TLC and biguanide-test The reaction was stopped if the substituted anilines were consumed completely (by TLC), or when no further consumption of the anilines by 30th hour of reaction (by TLC), or when the biguanide-tests gave positive results on two successive hours. Precipitation occurred when the reaction solution was cooled down to room temperature. The reaction mixture was then vacuum filtered. The product obtained was recrystallised from ethanol-water mixture. Without further

characterisations, except melting point determination and UV absorption spectra determination, **TZP**·HCl was used for Dimroth rearrangement.

Synthesis of 6-(substituted)anilino-4,6-diamino-1.2-dihydro-2,2-dimethyl-1,3,5-triazine (LIV – LXIII). 1g of **TZP**·HCl was dissolved in 20ml of 50% methanol in water. Usually complete dissolution occurred or else, heat was applied to encourage dissolution. After complete dissolution, a base, such as 10M NaOH, was added dropwise until no further change in pH (i.e. pH14 for NaOH, by using pH paper) or maximum precipitation of free base **TZP** occurred. The reflux was started, and the progress of the rearrangement was monitored by UV spectrophotometry spectrum scanning (from 200nm to 400nm). The reaction was stopped when there was no further shift in the λ_{max} value on two consecutive measurements (usually at first one hour as suggested by literature, as well as the first one and a half hour). The reaction solution was then kept in a freezer for at least 24 hours for crystallisation. If a sticky mass was produced instead of crystals, the reaction solution was kept in the refrigerator for a longer period until the mass became non-sticky. This was then harvested, by suction filtration, as crystals or powder. Recrystallisations were carried out using mixtures of methanol and water.

4-Amino-6-anilino-1.2-dihydro-2,2-dimethyl-1,3,5-triazine (LIV). White crystals (yield 85 %), recrystallised from aqueous methanol: mp 187 – 188 °C (ref.[273] 187 – 189 °C); λ_{max} (MeOH) 250.6 nm; IR (KBr disc) 3422, 3373, 3075, 2976, 1668, 1618, 1575, 1543, 1479, 1395 cm^{-1}; ^{1}H NMR (DMSO-d_6) δ 7.68 (d, 2H, Ar-H, J = 7.9 Hz), 7.11 (t, 2H, Ar-H, J = 7.9 Hz), 6.74 (t, 1H, Ar-H, J = 7.9 Hz), 1.27 (s, 6H, CH) ppm; MS (ESI) (50% MeOH) $[M+1]^+$ m/z 218.2 (100%).

4-Amino-6-(3-chloro)anilino-1.2-dihydro-2,2-dimethyl-1,3,5-triazine (LV). White powder (yield 46%), recrystallised from aqueous methanol: mp 142 – 146 °C; λ_{max}

(MeOH) 261.2nm; IR (KBr disc) 3396, 2970, 1666, 1574, 1478, 1409, 1355 cm^{-1}; ^1H NMR (DMSO-d_6) δ 7.83 (s, 1H, Ar-H), 7.50 (d, 1H, Ar-H, J = 8.3 Hz), 7.21 (t, 1H, Ar-H, J = 8.3 Hz), 6.91 (d, 1H, Ar-H, J = 7.9 Hz,), 1.32 (s, 6H, CH) ppm; MS (ESI) (50% MeOH) $[M+1]^+$ m/z 252.3 (100%).

4-Amino-6-(4-chloro)anilino-1.2-dihydro-2,2-dimethyl-1,3,5-triazine (LVI). Yellowish white crystals (yield 98%), recrystallised from aqueous methanol: mp 131 – 134° C (ref.[273] 135 – 137 °C); λ_{max} (MeOH) 263.4nm; IR (KBr disc) 3422, 3375, 3075, 2977, 1669, 1618, 1576, 1543, 1480, 1395 cm^{-1}; ^1H NMR (DMSO-d_6) δ 7.75 (d, 2H, Ar-H, J = 9.1 Hz), 7.12 (d, 2H, Ar-H, J = 9.1 Hz), 1.24 (s, 6H, CH) ppm; MS (ESI) (50% MeOH) $[M+1]^+$ m/z 252.3 (100%).

4-Amino-6-(3-bromo)anilino-1.2-dihydro-2,2-dimethyl-1,3,5-triazine (LVII). White crystals (yield 86%), recrystallised from aqueous methanol: mp 162 – 165 °C; λ_{max} (MeOH) 260.8nm; IR (KBr disc) 2966, 2835, 1671, 1580, 1488, 1413, 1356 cm^{-1}; ^1H NMR (DMSO-d_6) δ 8.05 (s, 1H, Ar-H), 7.62 (d, 1H, Ar-H, J = 8.3 Hz), 7.06 (t, 1H, Ar-H, J = 8.3 Hz), 6.90 (d, 1H, Ar-H), 1.26 (s, 6H, CH) ppm; MS (ESI) (50% MeOH) $[M+1]^+$ m/z 296.3 (100%).

4-Amino-6-(4-bromo)anilino-1.2-dihydro-2,2-dimethyl-1,3,5-triazine (LVIII). White crystals (yield 95%), recrystallised from aqueous methanol: mp 141 – 145 °C; λ_{max} (MeOH) 265.2nm; IR (KBr disc) 3422, 3370, 3059, 2976, 1670, 1618, 1573, 1543, 1478, 1392 cm^{-1}; ^1H NMR (DMSO-d_6) δ 7.69 (d, 2H, Ar-H, J = 9.0 Hz), 7.24 (d, 2H, Ar-H, J = 9.0 Hz), 1.24 (s, 6H, CH) ppm; MS (ESI) (50% MeOH) $[M+1]^+$ m/z 296.3 (100%).

4-Amino-1.2-dihydro-2,2-dimethyl-6-(3-methyl)anilino-1,3,5-triazine (LIX). White crystals (yield 47%), recrystallised from aqueous methanol: mp 171 – 175 °C; λ_{max} (MeOH) 258.8nm; IR (KBr disc) 2979, 1673, 1581, 1488, 1408, 1356 cm^{-1}; ^1H

NMR (DMSO-d_6) δ 7.60 (d, 1H, Ar-H, J = 7.9 Hz), 7.40 (s, 1H, Ar-H), 6.99 (t, 1H, Ar-H, J = 7.9 Hz), 6.57 (d, 1H, Ar-H, J = 7.9 Hz), 2.20 (s, 3H, CH), 1.25 (s, 6H, CH) ppm; MS (ESI) (50% MeOH) $[M+1]^+$ m/z 232.2 (100%).

4-Amino-1.2-dihydro-2,2-dimethyl-6-(4-methyl)anilino-1,3,5-triazine (LX). White powder (yield 94%), recrystallised from aqueous methanol: mp 155 – 157 °C; λ_{max} (MeOH) 258.0nm; IR (KBr disc) 3445, 2977, 1654, 1578, 1514, 1401, 1358 cm^{-1}; ^{1}H NMR (DMSO-d_6) δ 7.58 (d, 2H, Ar-H, J = 7.9 Hz), 6.91 (d, 2H, Ar-H, J = 7.9 Hz), 2.18 (s, 3H, CH), 1.23 (s, 6H, CH) ppm; MS (ESI) (50% MeOH) $[M+1]^+$ m/z 232.2 (100%).

4-Amino-1.2-dihydro-2,2-dimethyl-6-(3-methoxy)anilino-1,3,5-triazine (LXI). White powder (yield 75%), recrystallised from aqueous methanol: mp 156 – 161 °C; λ_{max} (MeOH) 262.2nm; IR (KBr disc) 3490, 3384, 2970, 1671, 1574, 1475, 1410, 1356 cm^{-1}; ^{1}H NMR (DMSO-d_6) δ 7.58 (s, 1H, Ar-H), 7.12-7.14 (d, 1H, Ar-H), 7.00 (m, 1H, Ar-H), 6.33 (d, 1H, Ar-H, J = 6.8 Hz), 3.67 (s, 3H, CH), 1.25 (s, 6H, CH) ppm; MS (ESI) (50% MeOH) $[M+1]^+$ m/z 248.2 (100%).

4-Amino-1.2-dihydro-2,2-dimethyl-6-(4-methoxy)anilino-1,3,5-triazine (LXII). White powder (yield 34%), recrystallised aqueous methanol: mp 190 – 193 °C; λ_{max} (MeOH) 255.6nm; IR (KBr disc) 2980, 2833, 1512, 1489, 1407, 1356 cm^{-1}; ^{1}H NMR (DMSO-d_6) δ 7.57 (d, 2H, Ar-H, J = 9.0 Hz), 6.74 (d, 2H, Ar-H, J = 9.0 Hz), 3.67 (s, 3H, CH), 1.26(s, 6H, CH) ppm; MS (ESI) (50% MeOH) $[M+1]^+$ m/z 248.2 (100%).

4-Amino-1.2-dihydro-2,2-dimethyl-6-(3-nitro)anilino-1,3,5-triazine (LXIII). Bright yellow crystals (yield 98%), recrystallised from aqueous methanol: mp 214 – 216 °C; λ_{max} (MeOH) 260.4nm; IR (KBr disc) 3479, 3441, 3380, 3347, 2964, 1651, 1521, 1397, 1347 cm^{-1}; ^{1}H NMR (DMSO-d_6) δ 8.82 (d, 1H, Ar-H), 7.97 (s, 1H, Ar-H,

J = 8.3 Hz), 7.56 (d, 1H, Ar-H, J = 7.5 Hz), 7.37 (t, 1H, Ar-H, J = 7.9 Hz), 1.28 (s, 6H, CH) ppm; MS (ESI) (50% MeOH) $[M+1]^+$ m/z 256.8 (100%).

L-Citrulline Assay (*in vitro*).

A variety of *in vitro* assays are available for characterisation NOS activity, mainly by detecting the NO (or products of NO-related reactions), or the L-citrulline[296-298]. However, the radiolabelled L-citrulline assay has become the standard assay for determining the activity of NOS because of its high sensitivity, low false positive and simple assay procedures[296,297]. As a radiolabelled assay, the technique is very sensitive with limit of detection in the picomole range. Besides that, the assay is likely to be specific to NOS pathway as the direct consumption of L-Arg in eukaryotic cells is unprecedented. Furthermore, the ease of separating L-Cit from L-Arg enables hundreds of samples to be tested in a relatively short time.

The principal of L-citrulline assay is based on the difference in pK_a of guanidine (pK_a 13.6) and urea (pK_a 0.1). Upon oxidation of L-Arg, L-Cit is produced in stoichiometric ratio of 1:1 to NO. With basic guanidino side chain, the L-Arg is positively charged at neutral pH, while the L-Cit with an ureido side chain has zero net charge. Thus, when the reaction mixture containing both L-Arg and L-Cit is passed through a column containing anionic Dowex resin (kept at pH <8), the L-Arg is retained on the resin but the L-Cit is eluted out. Subsequently, the amount of L-Cit eluted, which reflects the NO produced, is quantified by scintillation counting.

In the early phase of the current research, the L-Citrulline assay was performed using crude NOS extracted from rat cerebellum. Majority of the NOS activity could be attributed to nNOS, but a minor fraction of eNOS also contributed to the NOS activity. Besides that, crude tissues were also known to have intact urea

cycle, which consumes urea, as well as both arginine succinate synthase and arginosuccinase, which recycle L-Cit into L-Arg, are known to be present in crude neurons[297]. As a result, it was decided to replace the crude nNOS extract with commercially available NOSs. The nNOS (rat recombinant), iNOS (murine macrophage) and eNOS (bovine recombinant) were obtained from Cayman Chemical Company (USA).

The protocol used in the study was developed with reference to the Current Protocols in Pharmacology[299]. The incubation period was optimised to produce a linear time-activity relationship, thus ensuring the consistency and extrapolatibility of the data. The incubations of nNOS and eNOS were carried out at 37 °C, with the incubation periods of 10 and 20 minutes for nNOS and eNOS respectively. As for the iNOS, it was found that the activity of the enzyme at 37 °C deteriorated within a short period, which is too brief for proper execution of assay. Hence, the iNOS was incubated at a lower temperature (30 °C) for 15 minutes, after which the bath temperature was raised to 37 °C for another 15 minutes of incubation.

The [^{3}H]L-Citrulline assays. All the chemicals were obtained from Sigma. The L-[2,3,4,5-^{3}H]-Arginine HCl and scintillation cocktail was obtained from Amersham. The enzymes were obtained from Cayman Chemicals Company. The incubation mixture containing 125 µl drug solution, 10 µl of deionized water, 20 µl of reaction buffer (350 mM HEPES pH 7.4, 10 mM EDTA, 12.5 mM $CaCl_2$, 0.15 µCi [^{3}H]-L-arginine) and 45 µl of enzyme mixture (enzyme aliquot, 5 µl 20 mM NADPH, 5 µl 40 mM DTT, 5 µl 400 µg/ml CaM, 5 µl 360 µM BH4 and 25 µl 50mM HEPES pH7.4) was incubated at 37 °C. The reactions were initiated by the addition of the cold enzyme mixture and were terminated by 200 µl of the stopping buffer (160 mM HEPES pH5.5, 16 mM EDTA). Since the iNOS is Ca^{2+}-independent, the stopping

buffer with high concentration of L-Arg in place of Ca^{2+}-chelator was used instead (160 mM HEPES pH5.5, 80 mM L-Arginine). The reaction mixture was passed through the Dowex-Na^+ (pH < 8) column, followed by 500 µl of deionised water to rinse column. 5 ml of the scintillation cocktail was added to the eluent and radioactivity was measured in count per minute (cpm) using liquid scintillation counter (Beckman LS3801). Each set of assays was performed in triplicate. L-NA was used as positive controls. The compounds were screened at a concentration of 125 µM. Compounds, which showed at least 10% inhibition at 125 µM, were selected for further evaluation of IC_{50} values. The analysis of experimental raw data and statistical evaluation were performed using the software Prism 3.

	nNOS			iNOS			eNOS		
	%Inh	IC_{50}	± SEM	%Inh	IC_{50}	± SEM	%Inh	IC_{50}	± SEM
L-NA	100	0.083	± 0.0084	95	7.26	± 0.63	99	0.184	± 0.068

MES Test (*in vivo* neuroprotection)

The chemical-induced convulsion model, pentylenetetrazol-induced convulsions (PTZ test), was used to evaluate the neuroprotective potential of the compound. PTZ convulsion model is the one of the two standard convulsion model used for initial screening of anticonvulsants[300]. PTZ is a chemoconvulsant that reliably causes convulsion in mammals[286]. The mechanism of action of PTZ is not yet well understood, although PTZ was shown to be a $GABA_A$ receptor antagonist[286]. The impaired GABA-mediated inhibition results in increased excitability of the neurons, and thus convulsion. The amount of PTZ used can be tailored for inducing tonic-clonic convulsion at high doses and clonic convulsion at low doses[278].

Convulsion leads to neuronal damages. Neuronal excitation results in a series of downstream events, which produces neuronal necrosis and apoptosis, and finally the demise of the animal. As a result, if a compound could provide neuroprotection, the mice would suffer less or delayed brain damage, and thus survive for a longer duration.

The rotarod test[278] is commonly performed in conjunction to the PTZ test. In rotarod test, the animal is placed on a rod that rotates at an accelerating speed. If the animal is unable to stay on the rotating rod during a specified period, then it is likely that the animal is suffering neuromotor side effects, such as muscle incoordination and imbalance, of the compounds.

PTZ and rotarod tests. The experimental protocols were adapted from Current Protocols in Pharmacology[278], and the experiments were designed and performed in accordance to ethical and scientific requirements. All the chemicals were obtained from Sigma except the diazepam which was obtained from Merck. The experiments were performed using Swiss Albino mice (male, 20-25g). The mice were kept 6-8 in a cage at room temperature with 12/12 hours of day/night lighting cycle, and were provided with free access to food and water. All the drugs were dissolved in DMSO and given intraperitoneally (*i.p.*) with injection volume of 5 ml/kg. The test compounds were given at a dose of 100 mg/kg. The diazepam (DZP, Merck) was used as the positive control at a dose of 2 mg/kg, and the DMSO was used as the negative control. Due to ethical consideration, six mice (n=6) were used for each treatment group. The rotarod test was carried out on Rotarod machine (Accelerating rota-rod (Jones and Robers) for mice 7650, Ugo Basile, Italy) for 300 seconds, a period during which the speed of rotarod accelerated from 16 rpm to 32 rpm. The tests were carried out at 15^{th} minutes after the mice were injected with drugs. In PTZ

test, the pentetrazole (PTZ, Sigma) was given at a dose of 120 mg/kg subcutaneously (*s.c.*) using saline as vehicle. At 30th minute after a mouse was treated with drug, PTZ was injected and the mouse was observed in isolated cage for a period of 30 minutes. Latencies to each stage of convulsive events (jumping, full hind-limps extension and death) were recorded. The mice were sacrificed after 30 minutes of observation. The data was analysed with Prism 3 and reported as mean (± standard error of mean). Kruskal-Wallis test (non-parametric one-way ANOVA) with Dunn's multiple comparison test were performed using Prism 3.

Bibliography

1. **The Nobel Prize in physiology or medicine 1998** http://www.nobel.se/medicine/laureates/1998/presentation-speech.html The Nobel Foundation. Accessed on 23rd July 2004.
2. **About Viagra**. http://www.viagra.com/consumer/aboutViagra/index.asp Pfizer Incorporation. Accessed on 23rd July 2004.
3. **The molecule of the year**. Koshland D E Jr. Science (1992), 258(5090), 1861.
4. **Section 10 Table 10-1**. Lange's Handbook of Chemistry. Dean, John A. McGraw-Hill. New York. (1985), 10-6.
5. **Influence of pH and ionic strength upon solubility of nitric oxide in aqueous solution.** Armor, John N. Journal of Chemical and Engineering Data (1974), 19(1), 82-4.
6. **Oxygen exchange between nitric oxide and water.** Bonner, Francis T. Inorganic Chemistry (1970), 9(1), 190-3.
7. **Signal transduction mechanisms involving nitric oxide.** Ignarro, Louis J. Biochemical Pharmacology (1991), 41(4), 485-90.
8. **Biochemistry of nitric oxide and its redox-activated forms.** Stamler, Jonathan S.; Singel, David J.; Loscalzo, Joseph. Science (1992), 258(5090), 1898-902.
9. **Direct and indirect effects of nitric oxide in chemical reactions relevant to biology.** Wink, David A.; Grisham, Matthew B.; Mitchell, James B.; Ford, Peter C. Methods in Enzymology (1996), 268(Nitric Oxide, Part A), 12-31.
10. **Reactions of the bioregulatory agent nitric oxide in oxygenated aqueous media: Determination of the kinetics for oxidation and nitrosation by intermediates generated in the nitric oxide/oxygen reaction.** Wink, David A.; Darbyshire, John F.; Nims, Raymond W.; Saavedra, Joseph E.; Ford, Peter C. Chemical Research in Toxicology (1993), 6(1), 23-7.
11. **Autoxidation kinetics of aqueous nitric oxide**. Ford, Peter C; Wink, David A; Stanbury, David M FEBS letters (1993), 326(1-3), 1-3.

12. **Photochemistry of nitric oxide adducts of water-soluble iron(III) porphyrin and ferrihemoproteins studied by nanosecond laser photolysis.** Hoshino, Mikio; Ozawa, Koji; Seki, Hiroshi; Ford, Peter C. Journal of the American Chemical Society (1993), 115(21), 9568-75.

13. **Guanylate cyclase activation by nitroprusside and nitrosoguanidine is related to formation of S-nitrosothiol intermediates.** Ignarro, Louis J.; Barry, Barbara K.; Gruetter, Darlene Y.; Edwards, James C.; Ohlstein, Eliot H.; Gruetter, Carl A.; Baricos, William H. Biochemical and Biophysical Research Communications (1980), 94(1), 93-100.

14. **Inhibition of cytochromes P450 by nitric oxide and a nitric oxide-releasing agent.** Wink, David A.; Osawa, Yoichi; Darbyshire, John F.; Jones, Collins R.; Eshenaur, Steven C.; Nims, Raymond W. Archives of Biochemistry and Biophysics (1993), 300(1), 115-23.

15. **Oxidation of nitrogen oxides by bound dioxygen in hemoproteins.** Doyle, Michael P.; Hoekstra, James W. Journal of Inorganic Biochemistry (1981), 14(4), 351-8.

16. **Nitric oxide as an antioxidant.** Kanner, Joseph; Harel, Stela; Granit, Rina. Archives of Biochemistry and Biophysics (1991), 289(1), 130-6.

17. **Critical review of rate constants for reactions of hydrated electrons, hydrogen atoms and hydroxyl radicals ($^{\cdot}OH/^{\cdot}O^{-}$) in aqueous solution.** Buxton, George V.; Greenstock, Clive L.; Helman, W. Philip; Ross, Alberta B. Journal of Physical and Chemical Reference Data (1988), 17(2), 513-31.

18. **The reaction of nitric oxide with organic peroxyl radicals.** Padmaja, S.; Huie, R. E. Biochemical and Biophysical Research Communications (1993), 195(2), 539-44.

19. **Nitric oxide protects against cellular damage and cytotoxicity from reactive oxygen species.** Wink, David A.; Hanbauer, Ingeborg; Krishna, Murali C.; DeGraff, William; Gamson, Janet; Mitchell, James B. Proceedings of the National Academy of Sciences of the United States of America (1993), 90(21), 9813-17.

20. **Apparent hydroxyl radical production by peroxynitrite: implications for endothelial injury from nitric oxide and superoxide**. Beckman, Joseph S.; Beckman, Tanya W.; Chen, Jun; Marshall, Patricia A.; Freeman, Bruce A. Proceedings of the National Academy of Sciences of the United States of America (1990), 87(4), 1620-4.

21. **The chemistry of peroxonitrites.** Edwards, John O.; Plumb, Robert C. Progress in Inorganic Chemistry (1994), 41, 599-635.

22. **The chemistry of peroxynitrite: a product from the reaction of nitric oxide with superoxide.** Pryor, William A.; Squadrito, Giuseppe L. American Journal of Physiology (1995), 268(5, Pt. 1), L699-L722.

23. **Peroxynitrite oxidation of sulfhydryls. The cytotoxic potential of superoxide and nitric oxide.** Radi, Rafael; Beckman, Joseph S.; Bush, Kenneth M.; Freeman, Bruce A. Journal of Biological Chemistry (1991), 266(7), 4244-50.

24. **Peroxynitrite-mediated tyrosine nitration catalyzed by superoxide dismutase**. Ischiropoulos, Harry; Zhu, Ling; Chen, Jun; Tsai, Michael; Martin, James C.; Smith, Craig D.; Beckman, Joseph S. Archives of Biochemistry and Biophysics (1992), 298(2), 431-7.

25. **Nitric oxide reactions important to biological systems: a survey of some kinetics investigations.** Wink, David A.; Ford, Peter C. Methods (1995), 7(1), 14-20.

26. **Reaction kinetics for nitrosation of cysteine and glutathione in aerobic nitric oxide solutions at neutral pH. Insights into the fate and physiological effects of intermediates generated in the NO/O2 reaction.** Wink, David A.; Nims, Raymond W.; Darbyshire, John F.; Christodoulou, Danae; Hanbauer, Ingeborg; Cox, George W.; Laval, Francoise; Laval, Jacques; Cook, John A.; et al. Chemical Research in Toxicology (1994), 7(4), 519-25.

27. **Inhibition of tumor cell ribonucleotide reductase by macrophage-derived nitric oxide.** Kwon, Nyoun Soo; Stuehr, Dennis J.; Nathan, Carl F. Journal of Experimental Medicine (1991), 174(4), 761-7.

28. **Nitric oxide and nitric oxide-generating agents induce a reversible inactivation of protein kinase C activity and phorbol ester binding.** Gopalakrishna, Rayudu; Chen, Zhen Hai; Gundimeda, Usha. Journal of Biological Chemistry (1993), 268(36), 27180-5.

29. **Nitric oxide-induced S-nitrosylation of glyceraldehyde-3-phosphate dehydrogenase inhibits enzymic activity and increases endogenous ADP-ribosylation.** Molina y Vedia, Luis; McDonald, Brad; Reep, Bryan; Bruene, Bernhard; Di Silvio, Mauricio; Billiar, Timothy R.; Lapetina, Eduardo G. Journal of Biological Chemistry (1992), 267(35), 24929-32.

30. **Inhibition by nitric oxide of the repair protein, O6-methylguanine-DNA-methyltransferase.** Laval, Francoise; Wink, David A. Carcinogenesis (1994), 15(3), 443-7.

31. **The Fpg protein, a DNA repair enzyme, is inhibited by the biomediator nitric oxide in vitro and in vivo.** Wink, David A.; Laval, Jacques. Carcinogenesis (1994), 15(10), 2125-9.

32. **Metallothionein protects against the cytotoxic and DNA-damaging effects of nitric oxide.** Schwarz, Margaret A.; Lazo, John S.; Yalowich, Jack C.; Allen, William P.; Whitmore, Mark; Bergonia, Hector A.; Tzeng, Edith; Billiar, Timothy R.; Robbins, Paul D.; et al. Proceedings of the National Academy of Sciences of the United States of America (1995), 92(10), 4452-6.

33. **Nitric oxide, an endothelial cell relaxation factor, inhibits neutrophil superoxide anion production via a direct action on the NADPH oxidase.** Clancy, Robert M.; Leszczynska-Piziak, Joanna; Abramson, Steven B. Journal of Clinical Investigation (1992), 90(3), 1116-21.

34. **Effects of superoxide on nitric oxide-dependent N-nitrosation reactions.** Miles, Allen M.; Gibson, Michael F.; Kirshna, Murali; Cook, John C.; Pacelli, Robert; Wink, David; Grisham, Matthew B. Free Radical Research (1995), 23(4), 379-90.

35. **Diffusion of free nitric oxide.** Lancaster, Jack R., Jr.. Methods in Enzymology (1996), 268(Nitric Oxide, Part A), 31-50.

36. **Pharmacological modulation of nitric oxide synthesis by mechanism-based inactivators and related inhibitors.** Bryk, Ruslana; Wolff, Donald J. Pharmacology & Therapeutics (1999), 84(2), 157-78.

37. **Mammalian nitric oxide synthases.** Stuehr, Dennis J.; Griffith, Owen W. Advances in Enzymology and Related Areas of Molecular Biology (1992), 65, 287-346.

38. **Nitric oxide synthase structure and mechanism.** Marletta, Michael A. Journal of Biological Chemistry (1993), 268(17), 12231-4.

39. **Nitric oxide synthases: properties and catalytic mechanism.** Griffith, Owen W.; Stuehr, Dennis J. Annual Review of Physiology (1995), 57, 707-36.

40. **Heme coordination and structure of the catalytic site in nitric oxide synthase.** Wang, Jianling; Stuehr, Dennis J.; Ikeda-Saito, Masao; Rousseau, Denis L. Journal of Biological Chemistry (1993), 268(30), 22255-8.

41. **Tetrahydrobiopterin-deficient nitric oxide synthase has a modified heme environment and forms a cytochrome P 420 analog.** Wang, Jianling; Stuehr, Dennis J.; Rousseau, Denis L. Biochemistry (1995), 34(21), 7080-7.

42. **Structure-function aspects in the nitric oxide synthases**. Stuehr, Dennis J. Annual Review of Pharmacology and Toxicology (1997), 37, 339-59.

43. **Tetrahydrobiopterin, a cofactor for rat cerebellar nitric oxide synthase, does not function as a reactant in the oxygenation of arginine.** Giovanelli, John; Campos, Kenneth L.; Kaufman, Seymour. Proceedings of the National Academy of Sciences of the United States of America (1991), 88(16), 7091-5.

44. **Allosteric modulation of rat brain nitric oxide synthase by the pterin-site enzyme inhibitor 4-aminotetrahydrobiopterin.** Pfeiffer, Silvia; Gorren, Antonius C. F.; Pitters, Eva; Schmidt, Kurt; Werner, Ernst R.; Mayer, Bernd. Biochemical Journal (1997), 328(2), 349-52.

45. **The pteridine binding site of brain nitric oxide synthase. Tetrahydrobiopterin binding kinetics, specificity, and allosteric interaction with the substrate domain.** Klatt, Peter; Schmid, Martin; Leopold, Eva; Schmidt, Kurt; Werner, Ernst R.; Mayer, Bernd. Journal of Biological Chemistry (1994), 269(19), 13861-6.

46. **Nitric oxide synthases reveal a role for calmodulin in controlling electron transfer.** Abu-Soud, Husam M.; Stuehr, Dennis J. Proceedings of the National Academy of Sciences of the United States of America (1993), 90(22), 10769-72.

47. **The calmodulin-nitric oxide synthase interaction. Critical role of the calmodulin latch domain in enzyme activation.** Su, Zenghua; Blazing, Michael A.; Fan, Daju; George, Samuel E. Journal of Biological Chemistry (1995), 270(49), 29117-22.

48. **Calmodulin controls neuronal nitric-oxide synthase by a dual mechanism. Activation of intra- and interdomain electron transfer.** Abu-Soud, Husam M.; Yoho, Laura L.; Stuehr, Dennis J. Journal of Biological Chemistry (1994), 269(51), 32047-50.

49. **Heme iron reduction and catalysis by a nitric oxide synthase heterodimer containing one reductase and two oxygenase domains.** Siddhanta, Uma; Wu, Chaoqun; Abu-Soud, Husam M.; Zhang, Jingli; Ghosh, Dipak K.; Stuehr, Dennis J. Journal of Biological Chemistry (1996), 271(13), 7309-12.

50. **Domain swapping in inducible nitric-oxide synthase. Electron transfer occurs between flavin and heme groups located on adjacent subunits in the dimer.** Siddhanta, Uma; Presta, Anthony; Fan, Baochen; Wolan, Denis; Rousseau, Denis L.; Stuehr, Dennis J. Journal of Biological Chemistry (1998), 273(30), 18950-8.

51. **Complementation analysis of mutants of nitric oxide synthase reveals that the active site requires two hemes.** Xie, Qiao-wen; Leung, Mary; Fuortes, Michele; Sassa, Shigeru; Nathan, Carl. Proceedings of the National Academy of Sciences of the United States of America (1996), 93(10), 4891-6.

52. **Characterization of heme-deficient neuronal nitric-oxide synthase reveals a role for heme in subunit dimerization and binding of the amino acid substrate and**

tetrahydrobiopterin. Klatt, Peter; Pfeiffer, Silvia; List, Barbara M.; Lehner, Dieter; Glatter, Otto; Baechinger, Hans Peter; Werner, Ernst R.; Schmidt, Kurt; Mayer, Bernd. Journal of Biological Chemistry (1996), 271(13), 7336-42.

53. **Nw-Hydroxy-L-arginine is an intermediate in the biosynthesis of nitric oxide from L-arginine.** Stuehr, Dennis J.; Kwon, Nyoun Soo; Nathan, Carl F.; Griffith, Owen W.; Feldman, Paul L.; Wiseman, Jeffrey. Journal of Biological Chemistry (1991), 266(10), 6259-63.

54. **Analysis of neuronal NO synthase under single-turnover conditions: Conversion of Nw-hydroxyarginine to nitric oxide and citrulline.** Abu-Soud, Husam M.; Presta, Anthony; Mayer, Bernd; Stuehr, Dennis J. Biochemistry (1997), 36(36), 10811-6.

55. **On the mechanism of the nitric oxide synthase-catalyzed conversion of Nw-hydroxyl-L-arginine to citrulline and nitric oxide.** Korth, Hans Gert; Sustmann, Reiner; Thater, Claudia; Butler, Anthony R.; Ingold, Keith U. Journal of Biological Chemistry (1994), 269(27), 17776-9.

56. **Nitric oxide in excitable tissues: physiological roles and disease.** Christopherson, Karen S.; Bredt, David S. Journal of Clinical Investigation (1997), 100(10), 2424-9.

57. **Acylation targets endothelial nitric oxide-synthase to plasmalemmal caveolae.** Shaul, Philip W.; Smart, Eric J.; Robinson, Lisa J.; German, Zohre; Yuhanna, Ivan S.; Ying, Yunshu; Anderson, Richard G. W.; Michel, Thomas. Journal of Biological Chemistry (1996), 271(11), 6518-22.

58. **Blocking NO synthesis: how, where and why?** Vallance, Patrick; Leiper, James. Nature Reviews Drug Discovery (2002), 1(12), 939-50.

59. **Nitric oxide: A physiologic messenger molecular.** Bredt, David S.; Snyder, Solomon H. Annual Review of Biochemistry (1994), 63, 175-95.

60. **Nitric oxide synthases: structure, function and inhibition.** Alderton, Wendy K.; Cooper, Chris E.; Knowles, Richard G. Biochemical Journal (2001), 357(3), 593-615.

61. **Nitric oxide synthases: roles, tolls, and controls.** Nathan, Carl; Xie, Qiao-Wen. Cell (1994), 78(6), 915-8.

62. **Nitric oxide and macrophage function.** MacMicking, John; Xie, Qiaowen; Nathan, Carl. Annual Review of Immunology (1997), 15, 323-50.

63. **Constitutive expression of inducible nitric oxide synthase in the mouse ileal mucosa.** Hoffman, Rosemary A.; Zhang, Guisheng; Nuessler, Natascha C.; Gleixner, Susan L.; Ford, Henri R.; Simmons, Richard L.; Watkins, Simon C. American Journal of Physiology (1997), 272(2, Pt. 1), G383-92.

64. **Induction of calcium-dependent nitric oxide synthases by sex hormones.** Weiner, Carl P.; Lizasoain, Ignacio; Baylis, Sally A.; Knowles, Richard G.; Charles, Ian G.; Moncada, Salvador. Proceedings of the National Academy of Sciences of the United States of America (1994), 91(11), 5212-16.

65. **Nitric oxide synthases.** Knowles, R. G. Biochemical Society Transactions (1996), 24(3), 875-8.

66. **An autoinhibitory control element defines calcium-regulated isoforms of nitric oxide synthase.** Salerno, John C.; Harris, Dawn E.; Irizarry, Kris; Patel, Binesh; Morales, Arturo J.; Smith, Susan M. E.; Martasek, Pavel; Roman, Linda J.; Masters, Bettie Sue S.; Jones, Caroline L.; Weissman, Ben A.; Lane, Paul; Liu, Qing; Gross, Steven S. Journal of Biological Chemistry (1997), 272(47), 29769-77.

67. **Cloned and expressed macrophage nitric oxide synthase contrasts with the brain enzyme.** Lowenstein, Charles J.; Glatt, Charles S.; Bredt, David S.; Snyder, Solomon H. Proceedings of the National Academy of Sciences of the United States of America (1992), 89(15), 6711-5.

68. **PIN: an associated protein inhibitor of neuronal nitric oxide synthase.** Jaffrey, Samie R.; Snyder, Solomon H. Science (1996), 274(5288), 774-7.

69. **Activation of nitric oxide synthase in endothelial cells by Akt-dependent phosphorylation.** Dimmeler, Stefanie; Fleming, Ingrid; Fissithaler, Beate; Hermann, Corinna; Busse, Rudi; Zeiher, Andreas M. Nature (1999), 399(6736), 601-5.

70. **Direct interaction of endothelial nitric-oxide synthase and caveolin-1 inhibits synthase activity.** Ju, Hong; Zou, Rong; Venema, Virginia J.; Venema, Richard C. Journal of Biological Chemistry (1997), 272(30), 18522-5.

71. **Nitrergic transmission: nitric oxide as a mediator of non-adrenergic, non-cholinergic neuro-effector transmission.** Rand, M. J. Clinical and Experimental Pharmacology and Physiology (1992), 19(3), 147-69.

72. **Neural roles for heme oxygenase: contrasts to nitric oxide synthase.** Baranano, David E.; Snyder, Solomon H. Proceedings of the National Academy of Sciences of the United States of America (2001), 98(20), 10996-11002.

73. **Deletion of exon 6 of the neuronal nitric oxide synthase gene in mice results in hypogonadism and infertility.** Gyurko, Robert; Leupen, Sarah; Huang, Paul L. Endocrinology (2002), 143(7), 2767-74.

74. **Nitric oxide in skeletal muscle.** Kobzik, Lester; Reid, Michael B.; Bredt, David S.; Stamler, Jonathan S. Nature (1994), 372(6506), 546-8.

75. **Nitric oxide synthase complexed with dystrophin and absent from skeletal muscle sarcolemma in Duchenne muscular dystrophy.** Brenman, Jay E.; Chao, Daniel S.; Xia, Houhui; Aldape, Ken; Bredt, David S. Cell (1995), 82(5), 743-52.

76. **Renal NO production and the development of hypertension.** Persson, A. E. G.; Gutierrez, A.; Pittner, J.; Ring, A.; Ollerstam, A.; Brown, R.; Liu, R.; Thorup, C. Acta Physiologica Scandinavica (2000), 168(1), 169-74.

77. **Nitric oxide regulates the heart by spatial confinement of nitric oxide synthase isoforms.** Barouch, Uli A.; Harrison, Robert W.; Skaf, Michel W.; Rosas, Gisele O.; Cappola, Thomas P.; Kobeissi, Zoulficar A.; Hobal, Ion A.; Lemmon, Christopher A.; Burnett, Arthur L.; O'Rourke, Brian; Rodriguez, E. Rene; Huang, Paul L.; Lima, Joao A. C.; Berkowitz, Dan E.; Hare, Joshua M. Nature (2002), 416(6878), 337-40.

78. **Contribution of nitric oxide synthases 1, 2, and 3 to airway hyperresponsiveness and inflammation in a murine model of asthma**. De Sanctis, George T.; MacLean, James A.; Hamada, Kaoru; Mehta, Sanjay; Scott, Jeremy A.; Jiao, Aiping; Yandava,

Chandri N.; Kobzik, Lester; Wolyniec, Walter W.; Fabian, Attila J.; Venugopal, Changaram S.; Grasemann, Hartmut; Huang, Paul L.; Drazen, Jeffrey M. Journal of Experimental Medicine (1999), 189(10), 1621-30.

79. **Nitric oxide: a cytotoxic activated macrophage effector molecule.** Hibbs, John B., Jr.; Taintor, Read R.; Vavrin, Zdenek; Rachlin, Elliot M. Biochemical and Biophysical Research Communications (1988), 157(1), 87-94.

80. **Nitric oxide and the immune response.** Bogdan, Christian. Nature Immunology (2001), 2(10), 907-916.

81. **Effects of nitric oxide on the induction and differentiation of Th1 cells.** Niedbala, Wanda; Wei, Xiao-Qing; Piedrafita, David; Xu, Damo; Liew, Foo Yew. European Journal of Immunology (1999), 29(8), 2498-2505.

82. **Requirement of the inducible nitric oxide synthase pathway for IL-1-induced osteoclastic bone resorption.** van't Hof, R. J.; Armour, K. J.; Smith, L. M.; Armour, K. E.; Wei, X. Q.; Liew, F. Y.; Ralston, S. H. Proceedings of the National Academy of Sciences of the United States of America (2000), 97(14), 7993-8.

83. **Critical role for nitric oxide signaling in cardiac and neuronal ischemic preconditioning and tolerance.** Nandagopal, Krishnadas; Dawson, Ted M.; Dawson, Valina L. Journal of Pharmacology and Experimental Therapeutics (2001), 297(2), 474-8.

84. **Inducible nitric oxide synthase (iNOS) activity promotes ischemic skin flap survival.** Kane, Anthony J.; Barker, Jane E.; Mitchell, Geraldine M.; Theile, David R. B.; Romero, Rosalind; Messina, Aurora; Wagh, Milind; Fraulin, Frankie O. G.; Morrison, Wayne A.; Stewart, Alastair G. Journal of Pharmacology (2001), 132(8), 1631-8.

85. **Hypertension in mice lacking the gene for endothelial nitric oxide synthase.** Huang, Paul L.; Huang, Zhihong; Mashimo, Hiroshi; Bloch, Kenneth D.; Moskowitz, Michael A.; Bevan, John A.; Fishman, Mark C. Nature (1995), 377(6546), 239-2.

86. **Endothelial nitric oxide synthase and LTP**. Wilson, Rachel I.; Yanovsky, Jevgenij; Godecke, Axel; Stevens, David R.; Schrader, Jurgen; Haas, Helmut L. Nature (1997), 386(6623), 338.

87. **Cytokine-induced venodilatation in humans in vivo: eNOS masquerading as iNOS.** Bhagat, Kiran; Hingorani, Aroon D.; Palacios, Miriam; Charles, Ian G.; Vallance, Patrick. Cardiovascular Research (1999), 41(3), 754-64.

88. **Nitric oxide and septic shock.** Ruetten, Hartmut; Thiemermann, Christoph. Nitric Oxide (2000), 747-57.

89. **Nitric oxide in asthma. Pathogenic, therapeutic, or diagnostic?** Sanders, Scherer P. American Journal of Respiratory Cell and Molecular Biology (1999), 21(2), 147-9.

90. **The role of nitric oxide in nociception**. Luo, Z. David; Cizkova, Dasa. Current Review of Pain (2000), 4(6), 459-66.

91. **Gene expression profiling of mouse bladder inflammatory responses to LPS, substance P, and antigen-stimulation.** Saban, Marcia R.; Nguyen, Ngoc-Bich; Hammond, Timothy G.; Saban, Ricardo. American Journal of Pathology (2002), 160(6), 2095-110.

92. **Effects of cerebral ischemia in mice deficient in neuronal nitric oxide synthase.** Huang, Zhihong; Huang, Paul L.; Panahian, Nariman; Dalkara, Turgay; Fishman, Mark C.; Moskowitz, Michael A. Science (1994), 265(5180), 1883-5.

93. **Biosynthesis and action of nitric oxide in mammalian cells.** Mayer, Bernd; Hemmens, Benjamin. Trends in Biochemical Sciences (1997), 22(12), 477-81.

94. **Nitric oxide mediates glutamate neurotoxicity in primary cortical cultures.** Dawson, Valina L.; Dawson, Ted M.; London, Edythe D.; Bredt, David S.; Snyder, Solomon H. Proceedings of the National Academy of Sciences of the United States of America (1991), 88(14), 6368-71.

95. **Nitric oxide in the central nervous system.** Paakkari, Ilari; Lindsberg, Perttu. Annals of Medicine (Helsinki) (1995), 27(3), 369-77.

96. **Manganese superoxide dismutase protects nNOS neurons from NMDA and nitric oxide-mediated neurotoxicity.** Gonzalez-Zulueta, Mirella; Ensz, Lisa M.; Mukhina, Galina; Lebovitz, Russell M.; Zwacka, Ralf M.; Engelhardt, John F.; Oberley, Larry W.; Dawson, Valina L.; Dawson, Ted M. Journal of Neuroscience (1998), 18(6), 2040-55.

97. **Mechanisms of nitric oxide-mediated neurotoxicity in primary brain cultures.** Dawson, Valina L.; Dawson, Ted M.; Bartley, Duane A.; Uhl, George R.; Snyder, Solomon H. Journal of Neuroscience (1993), 13(6), 2651-61.

98. **Inducible nitric oxide synthase: a little bit of good in all of us**. Kubes, Paul. Gut (2000), 47(1), 6-9.

99. **The structure of nitric oxide synthase oxygenase domain and inhibitor complexes.** Crane, Brian R.; Arvai, Andrew S.; Gachhhui, Rtaan; Wu, Chaoqun; Ghosh, Dipak K.; Getzoff, Elizabeth D.; Steuhr, Dennis J.; Tainer, John A. Science (1997), 278(5337), 425-31.

100. **Structure of nitric oxide synthase oxygenase dimer with pterin and substrate.** Crane, Brian R.; Arvai, Andrew S.; Ghosh, Dipak K.; Wu, Chaoqun; Getzoff, Elizabeth D.; Stuehr, Dennis J.; Tainer, John A. Science (1998), 279(5359), 2121-6.

101. **Crystal structure of constitutive endothelial nitric oxide synthase: a paradigm for pterin function involving a novel metal center.** Raman, C. S.; Li, Huiying; Martasek, Pavel; Kral, Vladimir; Masters, Bettie Sue S.; Poulos, Thomas L. Cell (1998), 95(7), 939-50.

102. **Structural characterization of nitric oxide synthase isoforms reveals striking active-site conservation.** Fischmann, Thierry O.; Hruza, Alan; Niu, Xiao Da; Fossetta, James D.; Lunn, Charles A.; Dolphin, Edward; Prongay, Andrew J.; Reichert, Paul; Lundell, Daniel J.; Narula, Satwant K.; Weber, Patricia C. Nature Structural Biology (1999), 6(3), 233-42.

103. **Crystal structures of zinc-free and -bound heme domain of human inducible nitric-oxide synthase. Implications for dimer stability and comparison with**

endothelial nitric-oxide synthase. Li, Huiying; Raman, C. S.; Glaser, Charles B.; Blasko, Eric; Young, Tish A.; Parkinson, John F.; Whitlow, Marc; Poulos, Thomas L. Journal of Biological Chemistry (1999), 274(30), 21276-84.

104. **Mapping the active site polarity in structures of endothelial nitric oxide synthase heme domain complexed with isothioureas.** Li, Huiying.; Raman, C. S.; Martasek, Pavel; Kral, V.; Masters, Bettie Sue S.; Poulos, Thomas L. Journal of Inorganic Biochemistry (2000), 81(3), 133-9.
105. **The Novel Binding Mode of N-Alkyl-N'-hydroxyguanidine to Neuronal Nitric Oxide Synthase Provides Mechanistic Insights into NO Biosynthesis.** Li, Huiying; Shimizu, Hideaki; Flinspach, Mack; Jamal, Joumana; Yang, Weiping; Xian, Ming; Cai, Tingwei; Wen, Edward Zhong; Jia, Qiang; Wang, Peng George; Poulos, Thomas L. Biochemistry (2002), 41(47), 13868-75.
106. **L-Arginine binding to nitric-oxide synthase. The role of H-bonds to the nonreactive guanidinium nitrogens.** Babu, Boga Ramesh; Frey, Christopher; Griffith, Owen W. Journal of Biological Chemistry (1999), 274(36), 25218-26.
107. **Application and limitations of X-ray crystallographic data in structure-based ligand and drug design.** Davis, Andrew M.; Teague, Simon J.; Kleywegt, Gerard J. Angewandte Chemie, International Edition (2003), 42(24), 2718-36.
108. **Hydrogen bonding, hydrophobic interactions, and failure of the rigid receptor hypothesis.** Davis, Andrew M.; Teague, Simon J. Angewandte Chemie, International Edition (1999), 38(6), 736-49.
109. **Protein dynamics from NMR.** Ishima, Rieko; Torchia, Dennis A. Nature Structural Biology (2000), 7(9), 740-3.
110. **NO synthase isoenzymes have distinct substrate binding sites.** Fan, Baochen; Wang, Jianling; Stuehr, Dennis J.; Rousseau, Denis L. Biochemistry (1997), 36(42), 12660-5.

111. **Potent and Selective Inhibition of Neuronal Nitric Oxide Synthase by Nw-Propyl-L-arginine.** Zhang, Henry Q.; Fast, Walter; Marletta, Michael A.; Martasek, Pavel; Silverman, Richard B. Journal of Medicinal Chemistry (1997), 40(24), 3869-70.

112. **Active site topologies and cofactor-mediated conformational changes of nitric-oxide synthases.** Gerber, nancy Counts; Rodriguez-Crespo, Ignacio; Nishida, Clinton R.; Ortiz de Montellano, Paul R. Journal of Biological Chemistry (1997), 272(10), 6285-90.

113. **NO news is not necessary good.** Editorial. Nature Structural Biology (1999), 6(3), 201-2.

114. **Inhibitors of human nitric oxide synthase isoforms with the carbamidine moiety as a common structural element.** Moore, William M.; Webber, R. Keith; Fok, Kam F.; Jerome, Gina M.; Kornmeier, Christine M.; Tjoeng, Foe S.; Currie, Mark G. Bioorganic & Medicinal Chemistry (1996), 4(9), 1559-64.

115. **1H-Pyrazole-1-carboxamidines: new inhibitors of nitric oxide synthase.** Lee, Y.; Martasek, P.; Roman, L. J.; Silverman, R. B. Bioorganic & Medicinal Chemistry Letters (2000), 10(24), 2771-4.

116. **2-Iminopiperidine and other 2-iminoazaheterocycles as potent inhibitors of human nitric oxide synthase isoforms.** Moore, William M.; Webber, R. Keith; Fok, Kam F.; Jerome, Gina M.; Connor, Jane R.; Manning, Pamela T.; Wyatt, Pamela S.; Misko, Thomas P.; Tjoeng, Foe S.; Currie, Mark G. G. D. Journal of Medicinal Chemistry (1996), 39(3), 669-72.

117. **NG-methylarginine, an inhibitor of endothelium-derived nitric oxide synthesis, is a potent pressor agent in the guinea pig: does nitric oxide regulate blood pressure in vivo?** Aisaka, Kazuo; Gross, Steven S.; Griffith, Owen W.; Levi, Roberto. Biochemical and Biophysical Research Communications (1989), 160(2), 881-6.

118. **Endogenous dimethylarginine as an inhibitor of nitric oxide synthesis.** Vallance, Patrick; Leone, Anna; Calver, Alison; Collier, Joe; Moncada, Salvador. Journal of Cardiovascular Pharmacology (1992), 20(12), S60-2.

119. **Characterization of cell selectivity of two novel inhibitors of nitric oxide synthesis.** Lambert, Laurie E.; French, John F.; Whitten, Jeffrey P.; Baron, Bruce M.; McDonald, Ian A. European Journal of Pharmacology (1992), 216(1), 131-4.

120. **Synthesis of Ethylene-Bridged (Nd to Nw) Analogues of Arginine.** Lundquist, Joseph T.; Orwig, Kevin S.; Dix, Thomas A. Journal of Organic Chemistry (1999), 64(25), 9265-7.

121. **Asymmetric Synthesis of Conformationally Restricted L-Arginine Analogs as Active Site Probes of Nitric Oxide Synthase.** Atkinson, Robert N.; Moore, Lisa; Tobin, Joseph; King, S. Bruce. Journal of Organic Chemistry (1999), 64(10), 3467-75.

122. **N-Phenylamidines as Selective Inhibitors of Human Neuronal Nitric Oxide Synthase: Structure-Activity Studies and Demonstration of In Vivo Activity.** Collins, Jon L.; Shearer, Barry G.; Oplinger, Jeffrey A.; Lee, Shuliang; Garvey, Edward P.; Salter, Mark; Duffy, Claire; Burnette, Thimysta C.; Furfine, Eric S. Journal of Medicinal Chemistry (1998), 41(15), 2858-71.

123. **Conformationally-restricted arginine analogs as alternative substrates and inhibitors of nitric oxide synthases.** Lee, Younghee; Marletta, Michael A.; Martasek, Pavel; Roman, Linda J.; Masters, Bettie Sue Siler; Silverman, Richard B. Bioorganic & Medicinal Chemistry (1999), 7(6), 1097-104.

124. **Conformationally restricted arginine analogs as inhibitors of human nitric oxide synthase.** Shearer, Barry G.; Lee, Shuliang; Franzmann, Karl W.; White, Helen A.R.; Sanders, Daniella C. J.; Kiff, Rachel J.; Garvey, Edward P.; Furfine, Eric S. Bioorganic & Medicinal Chemistry Letters (1997), 7(13), 1763-1768.

125. **a-Guanidinoglutaric acid, an endogenous convulsant, as a novel nitric oxide synthase inhibitor.** Yokoi, Isao; Kabuto, Hideaki; Habu, Hitoshi; Mori, Akitane. Journal of Neurochemistry (1994), 63(4), 1565-7.

126. **Guanidine-substituted imidazoles as inhibitors of nitric oxide synthase.** Atkinson, Robert N.; King, S. Bruce. Bioorganic & Medicinal Chemistry Letters (1999), 9(20), 2953-8.

127. **L-NG-nitro arginine (L-NOARG), a novel, L-arginine-reversible inhibitor of endothelium-dependent vasodilatation in vitro.** Moore, P. K.; Al-Swayeh, O. A.; Chong, N. W. S.; Evans, R. A.; Gibson, A. British Journal of Pharmacology (1990), 99(2), 408-12.

128. **Inhibition of nitric oxide synthesis by NG-nitro-L-arginine methyl ester (L-NAME): requirement for bioactivation to the free acid, NG-nitro-L-arginine.** Pfeiffer, Silvia; Leopold, Eva; Schmidt, Kurt; Brunner, Friedrich; Mayer, Bernd. British Journal of Pharmacology (1996), 118(6), 1433-40.

129. **Selective Inhibition of Neuronal Nitric Oxide Synthase by Nw-Nitroarginine- and Phenylalanine-Containing Dipeptides and Dipeptide Esters.** Silverman, Richard B.; Huang, Hui; Marletta, Michael A.; Martasek, Pavel. Journal of Medicinal Chemistry (1997), 40(18), 2813-2817.

130. **Nw-Nitroarginine-Containing Dipeptide Amides. Potent and Highly Selective Inhibitors of Neuronal Nitric Oxide Synthase.** Huang, Hui; Martasek, Pavel; Roman, Linda J.; Masters, Bettie Sue Siler; Silverman, Richard B. Journal of Medicinal Chemistry (1999), 42(16), 3147-53.

131. **Reduced Amide Bond Peptidomimetics. (4S)-N-(4-Amino-5-[aminoalkyl]aminopentyl)-N'-nitroguanidines, Potent and Highly Selective Inhibitors of Neuronal Nitric Oxide Synthase.** Hah, Jung-Mi; Roman, Linda J.; Martasek, Pavel; Silverman, Richard B. Journal of Medicinal Chemistry (2001), 44(16), 2667-70.

132. **Synthesis and evaluation of peptidomimetics as selective inhibitors and active site probes of nitric oxide synthases.** Huang, Hui; Martasek, Pavel; Roman, Linda J.; Silverman, Richard B. Journal of Medicinal Chemistry (2000), 43(15), 2938-45.

133. **Aromatic Reduced Amide Bond Peptidomimetics as Selective Inhibitors of Neuronal Nitric Oxide Synthase.** Hah, Jung-Mi; Martasek, Pavel; Roman, Linda J.; Silverman, Richard B. Journal of Medicinal Chemistry (2003), 46(9), 1661-9.

134. **Dipeptides containing L-arginine analogs: new isozyme-selective inhibitors of nitric oxide synthase.** Kobayashi, Nobutaka; Higuchi, Tsunehiko; Urano, Yasuteru; Kikuchi, Kazuya; Hirobe, Masaaki; Nagano, Tetsuo. Biological & Pharmaceutical Bulletin (1999), 22(9), 936-40.

135. **Minimal amidine structure for inhibition of nitric oxide biosynthesis.** Billack, Blase; Heck, Diane E.; Porterfield, D. Marshall; Malchow, R. Paul; Smith, Peter J. S.; Gardner, Carol R.; Laskin, Debra L.; Laskin, Jeffery D. Biochemical Pharmacology (2001), 61(12), 1581-6.

136. **Substituted 2-Iminopiperidines as Inhibitors of Human Nitric Oxide Synthase Isoforms.** Webber, R. Keith; Metz, Suzanne; Moore, William M.; Connor, Jane R.; Currie, Mark G.; Fok, Kam F.; Hagen, Timothy J.; Hansen, Donald W., Jr.; Jerome, Gina M.; Manning, Pamela T.; Pitzele, Barnett S.; Toth, Mihaly V.; Trivedi, Mahima; Zupec, Mark E.; Tjoeng, F. Siong. Journal of Medicinal Chemistry (1998), 41(1), 96-101.

137. **2-Iminohomopiperidinium Salts as Selective Inhibitors of Inducible Nitric Oxide Synthase (iNOS).** Hansen, Donald W., Jr.; Peterson, Karen B.; Trivedi, Mahima; Webber, Ronald K.; Tjoeng, Foe S.; Moore, William M.; Jerome, Gina M.; Kornmeier, Christine M.; Manning, Pamela T.; Connor, Jane R.; Misko, Thomas P.; Currie, Mark G.; Pitzele, Barnett S. Journal of Medicinal Chemistry (1998), 41(9), 1361-6.

138. **2-Iminopyrrolidines as Potent and Selective Inhibitors of Human Inducible Nitric Oxide Synthase.** Hagen, Timothy J.; Bergmanis, Arija A.; Kramer, Steven W.; Fok, Kam F.; Schmelzer, Albert E.; Pitzele, Barnett S.; Swenton, Lydia; Jerome, Gina M.; Kornmeier, Christine M.; Moore, William M.; Branson, Linda F.; Connor, Jane R.; Manning, Pamela T.; Currie, Mark G.; Hallinan, E. Ann. Journal of Medicinal Chemistry (1998), 41(19), 3675-83.

139. **3-Hydroxy-4-methyl-5-pentyl-2-iminopyrrolidine: A potent and highly selective inducible nitric oxide synthase inhibitor.** Tsymbalov, Sofya; Hagen, Timothy J.; Moore, William M.; Jerome, Gina M.; Connor, Jane R.; Manning, Pamela T.; Pitzele, Barnett S.; Hallinan, E. Ann. Bioorganic & Medicinal Chemistry Letters (2002), 12(22), 3337-9.

140. **A Potent Inhibitor of Inducible Nitric Oxide Synthase, ONO-1714, a Cyclic Amidine Derivative.** Naka, Masao; Nanbu, Toshiyuki; Kobayashi, Kaoru; Kamanaka, Yoshihisa; Komeno, Masaharu; Yanase, Ryo; Fukutomi, Tatsushi; Fujimura, Shinsei; Seo, Han Geuk; Fujiwara, Noriko; Ohuchida, Shuichi; Suzuki, Keiichiro; Kondo, Kigen; Taniguchi, Naoyuki. Biochemical and Biophysical Research Communications (2000), 270(2), 663-7.

141. **Design and synthesis of orally bioavailable inhibitors of inducible nitric oxide synthase. Part 1: synthesis and biological evaluation of dihydropyridin-2-imines.** Kawanaka, Yasufumi; Kobayashi, Kaoru; Kusuda, Shinya; Tatsumi, Tadashi; Murota, Masanori; Nishiyama, Toshihiko; Hisaichi, Katsuya; Fujii, Atsuko; Hirai, Keisuke; Naka, Masao; Komeno, Masaharu; Nakai, Hisao; Toda, Masaaki. Bioorganic & Medicinal Chemistry Letters (2002), 12(17), 2291-4.

142. **Design and synthesis of orally bioavailable inhibitors of inducible nitric oxide synthase. Synthesis and biological evaluation of dihydropyridin-2(1H)-imines and 1,5,6,7-tetrahydro-2H-azepin-2-imines.** Kawanaka, Yasufumi; Kobayashi, Kaoru; Kusuda, Shinya; Tatsumi, Tadashi; Murota, Masayuki; Nishiyama, Toshihiko; Hisaichi, Katsuya; Fujii, Atsuko; Hirai, Keisuke; Nishizaki, Minoru; Naka, Masao; Komeno, Masaharu; Nakai, Hisao; Toda, Masaaki. Bioorganic & Medicinal Chemistry (2003), 11(5), 689-702.

143. **Design and Synthesis of Orally Bioavailable Inhibitors of Inducible Nitric Oxide Synthase. Identification of 2-Azabicyclo[4.1.0]heptan-3-imines.** Kawanaka, Yasufumi; Kobayashi, Kaoru; Kusuda, Shinya; Tatsumi, Tadashi; Murota, Masayuki; Nishiyama, Toshihiko; Hisaichi, Katsuya; Fujii, Atsuko; Hirai, Keisuke; Naka, Masao;

Komeno, Masaharu; Odagaki, Yshihiko; Nakai, Hisao; Toda, Masaaki. Bioorganic & Medicinal Chemistry (2003), 11(8), 1723-43.

144. **Synthesis and Biological Characterization of L-N6-(1-Iminoethyl)lysine 5-Tetrazole-amide, a Prodrug of a Selective iNOS Inhibitor.** Hallinan, E. Ann; Tsymbalov, Sofya; Dorn, Clifford R.; Pitzele, Barnett S.; Hansen, Donald W., Jr.; Moore, William M.; Jerome, Gina M.; Connor, Jane R.; Branson, Linda F.; Widomski, Deborah L.; Zhang, Yan; Currie, Mark G.; Manning, Pamela T. Journal of Medicinal Chemistry (2002), 45(8), 1686-9.

145. **N5-(1-Imino-3-butenyl)-L-ornithine. A neuronal isoform selective mechanism-based inactivator of nitric oxide synthase.** Babu, Boga Ramesh; Griffith, Owen W. Dep. Biochem., Medical College Wisconsin, Milwaukk, WI, USA. Journal of Biological Chemistry (1998), 273(15), 8882-9.

146. **Conformationally constrained NO synthase inhibitors: rigid analogs of L-N-iminoethylornithine.** Eustache, Jacques; Grob, Alfred; Lam, Charles; Sellier, Odile; Schulz, Gerhard. Bioorganic & Medicinal Chemistry Letters (1998), 8(21), 2961-6.

147. **Synthesis and evaluation of trans 3,4-cyclopropyl L-arginine analogues as isoform selective inhibitors of nitric oxide synthase.** Fishlock, Dan; Perdicakis, Basil; Montgomery, Heather J.; Guillemette, J. Guy; Jervis, Eric; Lajoie, Gilles A. Bioorganic & Medicinal Chemistry (2003), 11(6), 869-73.

148. **Inhibition of inducible nitric oxide synthase by acetamidine derivatives of hetero-substituted lysine and homolysine.** Young, Robert J.; Beams, Richard M.; Carter, Keith; Clark, Helen A. R.; Coe, Diane M.; Chambers, C. Lynn; Davies, P. Ifeyinwa; Dawson, John; Drysdale, Martin J.; Franzman, Karl W.; French, Colin; Hodgson, Simon T.; Hodson, Harold F.; Kleanthous, Savvas; Rider, Peter; Sanders, Daniela; Sawyer, David A.; Scott, Keith J.; Shearer, Barry G.; Stocker, Richard; Smith, Steven; Tackley, Miriam C.; Knowles, Richard G. Bioorganic & Medicinal Chemistry Letters (2000), 10(6), 597-600.

149. **Syntheses of new conformationally constrained S-[2-[(1-iminoethyl)amino]ethyl]homocysteine derivatives as potential nitric oxide synthase inhibitors.** Wang, Lijuan J.; Grapperhaus, Margaret L.; Pitzele, Barnett S.; Hagen, Timothy J.; Fok, Kam F.; Scholten, Jeffrey A.; Spangler, Dale P.; Toth, Mihaly V.; Jerome, Gina M.; Moore, William M.; Manning, Pamela T.; Sikorski, James A. Heteroatom Chemistry (2002), 13(1), 77-83.

150. **Structural requirements for human inducible nitric oxide synthase substrates and substrate analog inhibitors.** Grant, Stephan K.; Green, Barbara G.; Stiffey-Wilusz, Janet; Durette, Philippe L.; Shah, Shrenik K.; Kozarich, John W. Biochemistry (1998), 37(12), 4174-80.

151. **Acetamidine Lysine Derivative, N-(5(S)-amino-6,7-dihydroxyheptyl)ethanimidamide Dihydrochloride: A Highly Selective Inhibitor of Human Inducible Nitric Oxide Synthase.** Hallinan, E. Ann; Tsymbalov, Sofya; Finnegan, Patricia M.; Moore, William M.; Jerome, Gina M.; Currie, Mark G.; Pitzele, Barnett S. Journal of Medicinal Chemistry (1998), 41(6), 775-7.

152. **1400W is a slow, tight binding, and highly selective inhibitor of inducible nitric-oxide synthase in vitro and in vivo.** Garvey, Edward P.; Oplinger, Jeffrey A.; Furfine, Eric S.; Kiff, Rachel J.; Laszlo, Ferenc; Whittle, Brenden J. R.; Knowles, Richard G. Journal of Biological Chemistry (1997), 272(8), 4959-63.

153. **Discovery and development of neuronal nitric oxide synthase inhibitors.** Reif, D. W.; McCarthy, D. J.; Cregan, E.; Macdonald, J. E. Free Radical Biology & Medicine (2000), 28(10), 1470-7.

154. **Novel lipoic acid analogues that inhibit nitric oxide synthase.** Harnett, Jeremiah J.; Auguet, Michel; Viossat, Isabelle; Dolo, Christine; Bigg, Dennis; Chabrier, Pierre-E. Bioorganic & Medicinal Chemistry Letters (2002), 12(11), 1439-42.

155. **Time-dependence and preliminary SAR studies in inhibition of nitric oxide synthase isoforms by homologues of thiocitrulline.** Goodyer, Claire L. M.; Chinje,

Edwin C.; Jaffar, Mohammed; Stratford, Ian J.; Threadgill, Michael D. Bioorganic & Medicinal Chemistry Letters (2003), 13(21), 3679-80.

156. **L-Thiocitrulline. A stereospecific, heme-binding inhibitor of nitric-oxide synthases.** Frey, Christopher; Narayanan, Krishnaswamy; McMillan, Kirk; Spack, Larry; Gross, Steven S.; Masters, Bettie Sue; Griffith, Owen W. Journal of Biological Chemistry (1994), 269(42), 26083-9.

157. **Synthesis of N-benzyl- and N-phenyl-2-amino-4,5-dihydrothiazoles and thioureas and evaluation as modulators of the isoforms of nitric oxide synthase.** Goodyer, Claire L. M.; Chinje, Edwin C.; Jaffar, Mohammed; Stratford, Ian J.; Threadgill, Michael D. Bioorganic & Medicinal Chemistry (2003), 11(19), 4189-206.

158. **Preparation and evaluation of new L-canavanine derivatives as nitric oxide synthase inhibitors.** Li, Xiaofeng; Atkinson, Robert N.; King, S. Bruce. Tetrahedron (2001), 57(30), 6557-65.

159. **Isothioureas: potent inhibitors of nitric oxide synthases with variable isoform selectivity.** Southan, Garry J.; Szabo, Csaba; Thiemermann, Christoph. British Journal of Pharmacology (1995), 114(2), 510-16.

160. **Potent and selective inhibition of human nitric oxide synthases. Inhibition by non-amino acid isothioureas.** Garvey, Edward P.; Oplinger, Jeffery A.; Tanoury, Gerald J.; Sherman, Paula A.; Fowler, Marc; Marshall, Scott; Harmon, Marilyn F.; Paith, Jerilin; Furfine, Eric S. Journal of Biological Chemistry (1994), 269(43), 26669-76.

161. **Novel potent and selective inhibitors of inducible nitric oxide synthase.** Nakane, Masaki; Klinghofer, Vered; Kuk, Jane E.; Donnelly, Jennifer L.; Budzik, Gerald P.; Pollock, Jennifer S.; Basha, Fatima; Carter, George W. Molecular Pharmacology (1995), 47(4), 831-4.

162. **Substituted N-Phenylisothioureas: Potent Inhibitors of Human Nitric Oxide Synthase with Neuronal Isoform Selectivity.** Shearer, Barry G.; Lee, Shuliang; Oplinger, Jeffrey A.; Frick, Lloyd W.; Garvey, Edward P.; Furfine, Eric S. Journal of Medicinal Chemistry (1997), 40(12), 1901-5.

163. **Potent and selective inhibition of human nitric oxide synthases. Selective inhibition of neuronal nitric oxide synthase by S-methyl-L-thiocitrulline and S-ethyl-L-thiocitrulline.** Furfine, Eric S.; Harmon, Marilyn F.; Paith, Jerilin; Knowles, Richard G.; Salters, Mark; Kiff, Rachel J.; Duffy, Claire; Hazelwood, Robert; Oplinger, Jeffery; Garvey, Edward P. Journal of Biological Chemistry (1994), 269(43), 26677-83.

164. **Synthesis and Evaluation of New Sulfur-Containing L-Arginine-Derived Inhibitors of Nitric Oxide Synthase.** Ichimori, Kohji; Stuehr, Dennis J.; Atkinson, Robert N.; King, S. Bruce. Journal of Medicinal Chemistry (1999), 42(10), 1842-8.

165. **S-alkyl-L-thiocitrullines. Potent stereoselective inhibitors of nitric oxide synthase with strong pressor activity in vivo.** Narayanan, Krishnaswamy; Spack, Larry; McMillan, Kirk; Kilbourn, Robert G.; Hayward, Michael A.; Masters, Bettie Sue Siler; Griffith, Owen W. Journal of Biological Chemistry (1995), 270(19), 11103-10.

166. **Preparation and evaluation of new L-canavanine derivatives as nitric oxide synthase inhibitors.** Li, Xiaofeng; Atkinson, Robert N.; King, S. Bruce. Tetrahedron (2001), 57(30), 6557-65.

167. **Nitric oxide synthase inhibition by dimaprit and dimaprit analogues.** Paquay, Jos B. G.; 't Hoen, Peter A. Chr.; Voss, Hans-Peter; Bast, Aalt; Timmerman, Henk; Haenen, Guido R. M. M. British Journal of Pharmacology (1999), 127(2), 331-4.

168. **Selective inhibition of human inducible nitric oxide synthase by S-alkyl-L-isothiocitrulline-containing dipeptides.** Park, Jung-Min; Higuchi, Tsunehiko; Kikuchi, Kazuya; Urano, Yasuteru; Hori, Hiroyuki; Nishino, Takeshi; Aoki, Junken; Inoue, Keizo; Nagano, Tetsuo. British Journal of Pharmacology (2001), 132(8), 1876-82.

169. **Heterocyclic analogues of L-citrulline as inhibitors of the isoforms of nitric oxide synthase (NOS) and identification of Nd-(4,5-dihydrothiazol-2-yl)ornithine as a potent inhibitor.** Ulhaq, Saraj; Chinje, Edwin C.; Naylor, Matthew A.; Jaffar, Mohammed; Stratford, Ian J.; Threadgill, Michael D. Bioorganic & Medicinal Chemistry (1999), 7(9), 1787-96.

170. **Crystal Structure of Nitric Oxide Synthase Bound to Nitro Indazole Reveals a Novel Inactivation Mechanism.** Raman, C. S.; Li, Huiying; Martasek, Pavel; Southan, Garry; Masters, Bettie Sue S.; Poulos, Thomas L. Biochemistry (2001), 40(45), 13448-55.

171. **Conformational Changes in Nitric Oxide Synthases Induced by Chlorzoxazone and Nitroindazoles: Crystallographic and Computational Analyses of Inhibitor Potency.** Rosenfeld, Robin J.; Garcin, Elsa D.; Panda, Koustubh; Andersson, Gunilla; Aberg, Anders; Wallace, Alan V.; Morris, Garrett M.; Olson, Arthur J.; Stuehr, Dennis J.; Tainer, John A.; Getzoff, Elizabeth D. Biochemistry (2002), 41(47), 13915-25.

172. **Substituted 2-aminopyridines as inhibitors of nitric oxide synthases.** Hagmann, William K.; Caldwell, Charles G.; Chen, Ping; Durette, Philippe L.; Esser, Craig K.; Lanza, Thomas J.; Kopka, Ihor E.; Guthikonda, Ravi; Shah, Shrenik K.; MacCoss, Malcolm; Chabin, Renee M.; Fletcher, Daniel; Grant, Stephan K.; Green, Barbara G.; Humes, John L.; Kelly, Theresa M.; Luell, Sylvie; Meurer, Roger; Moore, Vernon; Pacholok, Stephen G.; Pavia, Tony; Williams, Hollis R.; Wong, Kenny K. Bioorganic & Medicinal Chemistry Letters (2000), 10(17), 1975-8.

173. **A new class of selective and potent inhibitors of neuronal nitric oxide synthase.** Lowe, John A., III; Qian, Weimin; Volkmann, Robert A.; Heck, Steven; Nowakowski, Jolanta; Nelson, Robert; Nolan, Charles; Liston, Dane; Ward, Karen; Zorn, Stevin; Johnson, Celeste; Vanase, Michelle; Faraci, W. Stephen; Verdries, Kimberly A.; Baxter, James; Doran, Shawn; Sanders, Martin; Ashton, Mike; Whittle, Peter; Stefaniak, Mark. Bioorganic & Medicinal Chemistry Letters (1999), 9(17), 2569-72.

174. **Structure-Activity Relationships of Potent, Selective Inhibitors of Neuronal Nitric Oxide Synthase Based on the 6-Phenyl-2-aminopyridine Structure.** Lowe, John A., III; Qian, Weimin; Drozda, Susan E.; Volkmann, Robert A.; Nason, Deane; Nelson, Robert B.; Nolan, Charles; Liston, Dane; Ward, Karen; Faraci, Steve; Verdries, Kim; Seymour, Pat; Majchrzak, Michael; Villalobos, Anabella; White, W. Frost. Journal of Medicinal Chemistry (2004), 47(6), 1575-86.

175. **Implications for isoform-selective inhibitor design derived from the binding mode of bulky isothioureas to the heme domain of endothelial nitric-oxide synthase.** Raman, C. S.; Li, Huiying; Martasek, Pavel; Babu, Boga Ramesh; Griffith, Owen W.; Masters, Bettie Sue S.; Poulos, Thomas L. Journal of Biological Chemistry (2001), 276(28), 26486-91.

176. **Structural Basis for the Specificity of the Nitric-oxide Synthase Inhibitors W1400 and Nw-Propyl-L-Arg for the Inducible and Neuronal Isoforms.** Fedorov, Roman; Hartmann, Elisabeth; Ghosh, Dipak K.; Schlichting, Ilme. Journal of Biological Chemistry (2003), 278(46), 45818-25.

177. **Crystallographic studies on endothelial nitric oxide synthase complexed with nitric oxide and mechanism-based inhibitors.** Li, Huiying; Raman, C. S.; Martasek, Pavel; Masters, Bettie Sue S.; Poulos, Thomas L. Biochemistry (2001), 40(18), 5399-406.

178. **Structural basis for dipeptide amide isoform-selective inhibition of neuronal nitric oxide synthase.** Flinspach, Mack L.; Li, Huiying; Jamal, Joumana; Yang, Weiping; Huang, Hui; Hah, Jung-Mi; Gomez-Vidal, Jose Antonio; Litzinger, Elizabeth A.; Silverman, Richard B.; Poulos, Thomas L. Nature Structural & Molecular Biology (2004), 11(1), 54-9.

179. **The nature of p-p interactions.** Hunter, Christopher A.; Sanders, Jeremy K. M. Journal of the American Chemical Society (1990), 112(14), 5525-34.

180. **Basic strengths of methylated guanidines.** Angyal, S. J.; Warburton, W. K. Journal of the Chemical Society, Abstracts (1951), 2492-4.

181. **An original traceless linker strategy for solid-phase synthesis of N,N',N''-substituted guanidines.** Gomez, Laurent; Gellibert, Francoise; Wagner, Alain; Mioskowski, Charles. Chemistry--A European Journal (2000), 6(21), 4016-20.

182. **A versatile synthesis of novel N,N,N''-trisubstituted guanidines.** Rasmussen, C. R.; Villani, F. J., Jr.; Reynolds, B. E.; Plampin, J. N.; Hood, A. R.; Hecker, Leonard R.; Nortey, S. O.; Hanslin, A.; Costanzo, Michael J.; et al. Synthesis (1988), (6), 460-6.

183. **Preface**. Mori, Akitane. Guanidines 2: further explorations of the biological and clinical significance of guanidino compounds. Mori, Akitane; Cohen, Burton D.; Koide, Hikaru. Plenum Press, New York (1989), vii-viii.

184. **Guanidines as Drugs**. Cohen, Burton D. Guanidines 2: further explorations of the biological and clinical significance of guanidino compounds. Mori, Akitane; Cohen, Burton D.; Koide, Hikaru. Plenum Press, New York (1989), 109-13.

185. **Nitric oxide synthase inhibitors: biology and chemistry.** Granik, V. G.; Grigor ev, N. B. Russian Chemical Bulletin (Translation of Izvestiya Akademii Nauk, Seriya Khimicheskaya) (2002), 51(11), 1973-95.

186. **Basic and clinical pharmacology.** Katzung, B.G. Appleton and Lange, US (1999).

187. **Functions containing an iminocarbonyl group and any elements other than a halogen or chalcogen.** Cliffe, I.A. Comprehensive organic functional group transformation. Katritzky, A. R.; Meth-Cohn; Rees, C.W. Pergamon (1995) 639-55.

188. **New Route to Guanidines from Bromoalkanes.** Vaidyanathan, Ganesan; Zalutsky, Michael R. Journal of Organic Chemistry (1997), 62(14), 4867-9.

189. **Synthesis and properties of phenyl substituted derivatives of 2-phenyl-1,1,3,3-tetramethylguanidine.** Pruszynski, Przemyslaw. Canadian Journal of Chemistry (1987), 65(3), 626-9.

190. **Guanidine compounds. II. Preparation of mono and N,N-dialkylguanidines.** Bannard, Robert A. B.; Casselman, Alfred A.; Cockburn, W. F.; Brown, G. M. Canadian Journal of Chemistry (1958), 36, 1541-9.

191. **Reactions of isocyanide dihalides and their derivatives.** Kuehle, Engelbert; Anders, Bertram; Klauke, Erich; Tarnow, Horst; Zumach, Gerhard. Angewandte Chemie, International Edition in English (1969), 8(1), 20-34.

192. **Carbodiimides. I. Conversion of isocyanates to carbodiimides with phospholine oxide catalyst.** Campbell, Tod W.; Monagle, John J.; Foldi, Veronika S. Journal of the American Chemical Society (1962), 84, 3673-7.

193. **Synthesis and properties of a series of sterically hindered guanidine bases.** Barton, Derek H. R.; Elliott, John D.; Gero, Stephan D. Journal of the Chemical Society, Perkin Transactions 1: Organic and Bio-Organic Chemistry (1972-1999) (1982), (9), 2085-90.

194. **Synthesis and antiviral properties of 1-adamantylguanidine. A modified method for preparing tert-alkylguanidines.** Geluk, H. W.; Schut, J.; Schlatmann, J. L. M. A. Journal of Medicinal Chemistry (1969), 12, 712-5.

195. **4-(4-Pyrimidinyl)pyridinium salts. Analogs of hypoglycemic 4-pyrazolylpyridinium salts.** Bauer, Victor J.; Dalalian, Harry P.; Safir, S. R. Journal of Medicinal Chemistry (1968), 11, 1263-4.

196. **A Versatile One-Pot Synthesis of 1,3-Substituted Guanidines from Carbamoyl Isothiocyanates.** Linton, Brian R.; Carr, Andrew J.; Orner, Brendan P.; Hamilton, Andrew D. Journal of Organic Chemistry (2000), 65(5), 1566-8.

197. **A convenient synthesis of guanidines from thioureas.** Maryanoff, Cynthia A.; Stanzione, Robin C.; Plampin, James N.; Mills, John E. Journal of Organic Chemistry (1986), 51(10), 1882-4.

198. **The preparation and reactions of 2-alkyl-1(or 3)-nitro-2-thiopseudourea. I. Reaction with amines.** Fishbein, Lawrence; Gallaghan, John A. Journal of the American Chemical Society (1954), 76, 1877-9.

199. **Solid phase peptide synthesis. I. The synthesis of a tetrapeptide.** Merrifield, Robert B. Journal of the American Chemical Society (1963), 85(14), 2149-54.

200. **The nobel prize in chemistry 1984**. http://www.nobel.se/chemistry/laureates/1984/ The Nobel Foundation. Accessed on 2nd August 2004.

201. **Glossary of terms used in combinatorial chemistry.** Maclean, D.; Baldwin, J. J.; Ivanov, V. T.; Kato, Y.; Shaw, A.; Schneider, P.; Gordon, E. M. Pure and Applied Chemistry (1999), 71(12), 2349-65.

202. **Solid phase synthesis.** Brown, Angus R.; Hermkens, Pedro H. H.; Ottenheijm, Harry C. J.; Rees, David C. Synlett (1998), (8), 817-827.

203. **Combinatorial chemistry libraries, analysis of**. Kibbey, Christopher E. Encyclopedia of Analytical Chemistry. Meyers, Robert A. John Wiley & Sons Ltd., UK (2000), 7100-43.

204. **Analytical methods in combinatorial chemistry**. Yan, Bing. Technomic Publiching Company, Inc. USA. (2000).

205. **Solid-supported combinatorial and parallel synthesis of small-molecular-weight compound libraries**. Obrecht, Daniel; Villalgordo, Jose, M. Elsevier Science Ltd. UK. (1998).

206. **Combinatorial Chemistry**. Terrett, Nicholas K. Oxford University Press, NY (1998).

207. **Linkers and Cleavage Strategies in Solid-Phase Organic Synthesis and Combinatorial Chemistry.** Guillier, Fabrice; Orain, David; Bradley, Mark. Chemical Reviews (2000), 100(6), 2091-157.

208. **Linkers for solid phase organic synthesis.** James, Ian W. Tetrahedron (1999), 55(16), 4855-946.

209. **Solid-phase synthesis of disubstituted guanidines.** Kearney, Patrick C.; Fernandez, Monica; Flygare, John A. Tetrahedron Letters (1998), 39(18), 2663-6.

210. **Novel linker for the solid-phase synthesis of guanidines.** Josey, John A.; Tarlton, Catherine A.; Payne, Courtney E. Tetrahedron Letters (1998), 39(33), 5899-902.

211. **Solid-phase synthesis of N-acyl-N'-carbamoylguanidines.** Lin, Peishan; Ganesan, A. Tetrahedron Letters (1998), 39(52), 9789-92.

212. **Solid-Phase Synthesis of N-Acyl-N'-Alkyl/Aryl Disubstituted Guanidines.** Ghosh, Ajit K.; Hol, Wim G. J.; Fan, Erkang. Journal of Organic Chemistry (2001), 66(6), 2161-4.

213. **Solid-phase synthesis of N,N'-substituted guanidines.** Dodd, Dharmpal S.; Wallace, Owen B. Tetrahedron Letters (1998), 39(32), 5701-4.

214. **A traceless linker approach to the solid phase synthesis of substituted guanidines utilizing a novel acyl isothiocyanate resin.** Wilson, Lawrence J.; Klopfenstein, Sean R.; Li, Min. Tetrahedron Letters (1999), 40(21), 3999-4002.

215. **A simple solid-phase synthesis of disubstituted guanidines using Rink amide resin as an amine component.** Li, Min; Wilson, Lawrence J.; Portlock, David E. Tetrahedron Letters (2001), 42(12), 2273-5.

216. **Solid phase synthesis of oligomeric guanidiniums.** Schneider, Stephen E.; Bishop, Patricia A.; Salazar, Mary Alice; Bishop, Owen A.; Anslyn, Eric V. Tetrahedron (1998), 54(50), 15063-86.

217. **Solid phase synthesis of guanidines.** Robinson, Shaughnessy; Roskamp, Eric J. Tetrahedron (1997), 53(19), 6697-705.

218. **Soluble polymer-supported synthesis of N,N-di(Boc)-protected guanidines.** Shey, Jing-Ying; Sun, Chung-Ming. Synlett (1998), (12), 1423-5.

219. **Solid phase synthesis of a diketopiperazine catalyst containing the unnatural amino acid (S)-norarginine.** Kowalski, Jennifer; Lipton, Mark A. Tetrahedron Letters (1996), 37(33), 5839-40.

220. **Solid-Phase Synthesis of Arginine-Containing Peptides by Guanidine Attachment to a Sulfonyl Linker.** Zhong, H. Marlon; Greco, Michael N.; Maryanoff, Bruce E. Journal of Organic Chemistry (1997), 62(26), 9326-30.

221. **The solid phase synthesis of a guanidinium based 'tweezer' receptor.** Bonnat, Murielle; Bradley, Mark; Kolburn, Jeremy D. Tetrahedron Letters (1996), 37(30), 5409-12.

222. **A Novel Solid-Phase Synthesis of Highly Diverse Guanidines: Reactions of Primary Amines Attached to the T2 Linker.** Dahmen, Stefan; Braese, Stefan. Organic Letters (2000), 2(23), 3563-5.

223. **Solid-phase synthesis of trisubstituted guanidines.** Drewry, David H.; Gerritz, Samuel W.; Linn, James A. Tetrahedron Letters (1997), 38(19), 3377-80.

224. **Solid-phase synthesis of 3,4-dihydroquinazoline.** Wang, Fengjlang; Hauske, James R. Tetrahedron Letters (1997), 38(50), 8651-4.

225. **Polynitrogen strong bases: 1 New syntheses of biguanides and their catalytic properties in transesterification reactions.** Gelbard, Georges; Vielfaure-Joly, Florence. Tetrahedron Letters (1998), 39(18), 2743-6.

226. **Solid-Phase Synthesis of Trisubsituted Guanidines.** Hopkins, Thutam P.; Dener, Jeffrey M.; Boldi, Armen M. Journal of Combinatorial Chemistry (2002), 4(2), 167-74.

227. **Solid-Phase Synthesis of Substituted Guanidines Using a Novel Acid Labile Linker.** Patek, Marcel; Smrcina, Martin; Nakanishi, Eiji; Izawa, Hiroyuki. Journal of Combinatorial Chemistry (2000), 2(4), 370-7.

228. **Solid-phase synthesis of N,N'-substituted acylguanidines.** Dodd, Dharmpal S.; Zhao, Yufen Tetrahedron Letters (2001), 42(7), 1259-62.

229. **Heterocumulenes. Imine, nitrones, and isocyanides**. Tennant, G. Comprehensive organic chemistry: the synthesis and reactions of organic compounds. Sir Barton, Derek; Ollis, W. David. Pergamon Press Oxford (1979), 513-27.

230. **Functions with at least one nitrogen and no chalcogens**. Muthyala, Ramaiah. Comprehensive organic functional group transformation. Katritzky, A. R.; Meth-Cohn; Rees, C.W. Pergamon (1995) 5.1062-85.

231. **Carbodiimide chemistry: recent advances**. Williams, Andrew; Ibrahim, Ibrahim T. Chemical Reviews (1981), 81, 589-636.

232. **A convenient method for the preparation of carbodiimides using 2-chloropyridinium salt.** Shibanuma, Tadao; Shiono, Manzo; Mukaiyama, Teruaki. Chemistry Letters (1977), (5), 575-6.

233. **Advances in the chemistry of carbodiimides.** Kurzer, Frederick; Douraghi-Zadeh, K. Chemical Reviews (1967), 67(2), 107-52.

234. **Synthesis of Isocyanates and Carbodiimides**. Ulrich, Henry; Sayigh, Adnan A. R. Angewandte Chemie, International Edition (1966), 5(8), 704.

235. **N,N'-Dicyclohexylcarbodiimide. Preparation from urea and cyclohexylamine.** Amiard, Gaston; Heymes, Rene. Bulletin de la Societe Chimique de France (1956), 1360-1.

236. **Acylcarbodiimides. V. Preparation of (N-alkylbenzimidoyl)- and (N-arylbenzimidoyl)carbodiimides; their rearrangement to aminoquinazolines and dihydro-1,3,5-triazines.** Goerdeler, Joachim; Eggers, Wolfgang. Chemische Berichte (1986), 119(12), 3737-48.

237. **Carbodiimides from isocyanates.** Neumann, Wolfram; Fischer, Peter. Angew. Chem. (1962), 74(21), 801-6.

238. **Synthetic reactions by complex catalysts. XVIII. Reaction of an azide with isocyanide using an iron carbonyl catalyst. New route to carbodiimide.** Saegusa, Takeo; Ito, Yoshihiko; Shimizu, Toyoji. Journal of Organic Chemistry (1970), 35(11), 3995-6.

239. **Synthetic reactions by complex catalysts. XXXVII. Novel and versatile method of carbodiimide synthesis oxidation of carbene palladium(II) complex with silver oxide.** Ito, Yoshihiko; Hirao, Toshikazu; Saegusa, Takeo. Journal of Organic Chemistry (1975), 40(20), 2981-2.

240. **A general method for the solid phase synthesis of ureas.** Hutchins, Steven M.; Chapman, Kevin T. Tetrahedron Letters (1994), 35(24), 4055-8.

241. **A strategy for urea linked diamine libraries.** Hutchins, Steven M.; Chapman, Kevin T. Tetrahedron Letters (1995), 36(15), 2583-6.

242. **Polymeric carbodiimide. I. Preparation**. Weinshenker, Ned M.; Shen, Chan M.; Wong, Jack Y. Organic Synthesis (1976), 56, 95-99.

243. **Advanced Chemtech Handbook of Combinatorial and Solid Phase Organic Chemistry**. Bennett, William D.; Christensen, James W.; Hamaker, Linda K.; Peterson, Mark L.; Phodes, Monte R.; Saneii, Hossain H. Advanced ChemTech Inc. US (1998).

244. **Nucleophile/base-labile protecting groups**. Protecting group chemistry Robertson,Jeremy. Oxford University Press, NY (2000), Unit3.4, 62-5.

245. **9-Fluorenylmethoxycarbonyl amino-protecting group.** Carpino, Louis A.; Han, Grace Y. Journal of Organic Chemistry (1972), 37(22), 3404-9.

246. **Peptide synthesis. Part 2. Procedures for solid-phase synthesis using Na-fluorenylmethoxycarbonyl amino acids on polyamide supports. Synthesis of substance P and of acyl carrier protein 65-74 decapeptide.** Atherton, Eric; Logan, Christopher J.; Sheppard, Robert C. Journal of the Chemical Society, Perkin Transactions 1: Organic and Bio-Organic Chemistry (1972-1999) (1981), (2), 538-46.

247. **Alkylation of Rink's amide linker on polystyrene resin: a reductive amination approach to modified amine-linkers for the solid phase synthesis of N-substituted amide derivatives.** Brown, Edward G.; Nuss, John M. Tetrahedron Letters (1997), 38(49), 8457-60.

248. **Convenient synthesis of water-soluble carbodiimides.** Sheehan, John C.; Cruickshank, Philip A.; Boshart, Gregory L. Journal of Organic Chemistry (1961), 26, 2525-8.

249. **Convenient and improved synthesis of unstable carbodiimides.** Palomo, Claudio; Mestres, Ramon. Synthesis (1981), (5), 373-4.

250. **Notiz uber eine neue Carbodiimid-Synthese.** Appel, Rolf; Kleinstuck, Roland; Ziehn, Klaus-Dieter. Chemische Berichte (1071), 104, 1335-6.

251. **Carbodiimides. Dehydration of ureas.** Stevens, Calvin L.; Singhal, Gopal H.; Ash, Arthur B. Journal of Organic Chemistry (1967), 32(9), 2895.

252. **A new reagent for dehydrating primary amides under mild conditions**. Stephens, C. R.; Bianco, E. J.; Pilgrim, F. J. Journal of The American Chemical Society (1955), 77, 1701-2703.

253. **Carbodiimides. II. The reaction of sulfonic acids with carbodiimides. A new method of preparation of sulfonic anhydrides.** Khorana, H. G. Canadian Journal of Chemistry (1953), 31 585-8.

254. **Carbodiimides. VIII. Observations on the reactions of carbodiimides with acids and some new applications in the synthesis of phosphoric acid esters**. Smith, Michael; Moffatt, J.G.; Khorana, H.G. Journal of The American Chemical Society (1958), 80, 6204-12.

255. **The chemistry of carbodiimides.** Khorana, H. G. Chemical Reviews (1953), 53, 145-66.

256. **1-Ethyl-3-(3-dimethylamino)propylcarbodiimide hydrochloride and metiodide**. Sheehan, John C.; Cruickshank, Philip A. Organic Syntheses (1968), 48, 83-86.

257. **Preparation of carbodiimide using phase-transfer catalysis**. Jazay, Zsuzsa M.; Petnehazy, Imre; Toke, Laszlo; Szajani, Bela. Synthesis (1987), 520-22.

258. **A Novel Preparation of Isonitriles.** Hertler, W.R.; Corey, E. J. Journal of The Chemical Society (1958), 23, 1221-2.

259. **Uber Carbodiimide, III. Die reaction von carbodiimiden mit saurehalogeniden**. Hartke, Klaus; Palou, Emilio. Chemische Berichte (1966), 99, 3155-62.

260. **Uber Carbodiimide, IV. Eliminierung von schwefelwasserstoff mit acylierten carbodiimiden**. Hartke, Klaus. Chemische Berichte (1966), 99, 3163-72.

261. **Pyridine and hydrogenated derivatives**. Pyridine and its derivatives. Part one. Newkome, George R. Interscience Publishers, NY (1960), 37-9.

262. **The alkaline hydrolysis of guanidine hydrochloride.** Eloranta, Jorma. Suomen Kemistilehti B (1961), 34B 107-10. (Chemical Abstract Number 56:35402).

263. **Key Factors in the translation of solution-phase chemistry to the solid phase**. Hermkens, Pedro H. H.; Hamersma, Hans; Man, Adrianus, P.A. de. Optimisation of solid-phase combinatorial synthesis. Yan, Bing.; Czarnik, Anthony W. Marcel Dekker Inc. NY (2002) 69-90.

264. **Nitroguanidines**. McKay, A. F. Chemical Reviews (1952), 301-46.

265. **Practical organic chemistry**. Mann, Frederick George; Saunders, Bernard Charles. Longman, London (1978), 155.

266. **Interdependence between physical parameters and selection of substituent groups for correlation studies**. Craig, Paul N. Journal of Medicinal Chemistry (1971), 14(8), 680-4.

267. **Nitroguanidine**. The Merck Index 11th edition. Budavari, Susan; O'Neil, Maryadele J.; Smith, Ann; Heckelmer, Patricia E. Merck and Co. Inc. US (1989), 1046.

268. **Preparation of 1-(tetrahydro-3-furanylmethyl)-2-(nitroimino)-1,3,5-triazine derivatives as insecticides and method for production thereof.** Odaka, Kenji; Kinoshita, Katsutoshi; Wakita, Takeo; Shiraishi, Shiro; Oonuma, Kazutomi. Jpn. Kokai Tokkyo Koho (1995), 13 pp. JP 07173157.

269. **A novel method for the preparation of N,N'-disubstituted N''-nitroguanidines, including a practical synthesis of the neonicotinoid insecticide clothianidin.** Maienfisch, Peter; Huerlimann, Hanspeter; Haettenschwiler, Joerg. Tetrahedron Letters (2000), 41(37), 7187-91.

270. **A metabolite of paludrine with high antimalarial activity.** Carrington, H. C.; Crowther, A. F.; Davey, D. G.; Levi, A. A.; Rose, F. L. Nature (1951), 168, 1080.

271. **Synthetic antimalarials. XLIX. The structure and synthesis of the dihydrotriazine metabolite of Proguanil.** Carrington, H. C.; Crowther, A. F.; Stacey, G. J. Journal of the Chemical Society, Abstracts (1954), 1017-31.

272. **A series of new, biologically significant dihydrotriazines.** Modest, Edward J.; Foley, Geo. E.; Pechet, Maurice M.; Farber, Sidney. Journal of the American Chemical Society (1952), 74, 855-6.

273. **Chemical and biological studies of 1,2-dihydro-s-triazines. II. Three-component synthesis.** Modest, Edward J. Journal of Organic Chemistry (1956), 21, 1-13.

274. **Chemical and biological studies of 1,2-dihydro-s-triazines. III. Two-component synthesis.** Modest, Edward J. Journal of Organic Chemistry (1956), 21, 14-20.

275. **1,2-Dihydro-s-triazines.** Newman, Howard; Moon, Edward L.; English, Jackson P. U.S. (1966), 2 pp. US 3287366.

276. **Amidine rearrangements (the Dimroth rearrangements).** Brown, Desmond J. Mechanisms of Molecular Migrations (1968), 1, 209-45.

277. **The crystal structure of the hydrochloride and hydrobromide of the dihydrotriazine metabolite of proguanil.** Bailey, M. Acta Cryst. (1954), 7, 366-9.

278. **Models of epilepsy: Electroshock and chemical Induced convulsions in the mouse**. Giardina, William J. Current Protocols in Pharmacology. Enna, S. J.; Williams, Michael. John Wiley and Sons. NY. Unit 5.22.

279. **Study on the influence of potent inhibitors of neuronal nitric oxide synthase on the antinociceptive and anticonvulsant activity of benzodiazepines in mice.** Fidecka, Sylwia. Polish Journal of Pharmacology (2003), 55(2), 193-201.

280. **Abnormal Expression of Neuronal Nitric Oxide Synthase Triggers Limbic Seizures and Hippocampal Damage in Rat.** Bagetta, Giacinto; Paoletti, Anna Maria; Leta, Aida; Del Duca, Claudio; Nistico, Robert; Rotiroti, D.; Tiziana Corasaniti, M. Biochemical and Biophysical Research Communications (2002), 291(2), 255-60.

281. **Further studies on anti- and proconvulsant effects of inhibitors of nitric oxide synthase in rodents**. Alexander, Corrinne B.; Ellmore, Timothy M.; Kokate, Tushar G.; Kirkby, R. Duncan. European Journal of Pharmacology (1998), 344, 15-25.

282. **Anticonvulsant and proconvulsant roles of nitric oxide in experimental epilepsy models**. Del-Bel E. A.; Oliveira, P. R.; Oliveira, J. A. C.; Mishra, P. K.; Jobe, P. C.; Garcia-Cairasco, N. Brazilian Journal of Medical and Biological Research (1997), 30, 971-9.

283. **7-Nitro indazole derivatives are potent inhibitors of brain, endothelium and inducible isoforms of nitric oxide synthase.** Bland-Ward, Philip A.; Moore, Philip K. Life Sciences (1995), 57(11), PL131-PL135.

284. **On the selectivity of 7-nitroindazole as an inhibitor of neuronal nitric oxide synthase. Comments.** Reiner, Anton; Zagvazdin, Yuri. Trends in Pharmacological Sciences (1998), 19(9), 348-50.

285. **On the selectivity of 7-nitroindazole as an inhibitor of neuronal nitric oxide synthase. Reply to comments.** Handy, Rachel L. C.; Moore, Philip K. Trends in Pharmacological Sciences (1998), 19(9), 350.

286. **Experimental models of status epilepticus**. Treiman, David M.; Heinemann, Uwe. Epilepsy: A Domprehensive Texbook. Engel, Jerome Jr.; Pedley, Timothy A. Lippincott-Raven Publishers US (1997), 443-55.

287. **Guanidine compounds. II. Preparation of mono and N,N-dialkylguanidines.** Bannard, R. A. B.; Casselman, A. A.; Cockburn, W. F.; Brown, G. M. Canadian Journal of Chemistry (1958), 36, 1541-9.

288. **Determination of the ionization constants of guanidine and some of its alkylated derivatives.** Davis, Tenny L.; Elderfield, Robert C. Journal of the American Chemical Society (1932), 54 1499-503.

289. **Sympathetic nervous system blocking agents. Derivatives of guanidine and related compounds.** Short, James H.; Biermacher, Ursula; Dunnigan, Daniel A.; Leth, Thomas D. Journal of Medicinal Chemistry (1963), 6, 275-83.

290. **Physical properties of certain nitro compounds.** Devergnes, Louis. Revue de Chimie Industrielle et le Moniteur Scientifique de Quesneville Reunis (Paris) (1929), 38, 265-6.

291. **1-Substituted-3-nitroguanidines.** McKay, Arthur F. US 2559085 (1951).

292. **Preparation of alkyl-, alkenyl- and alkynylnitroguanidines as cytokinin plant growth regulants.** Lutz, Albert W.; Rodaway, Shirley J. US 4677226 (1987).

293. **Substituted Nitro- and Cyanoguanidines and Their Use in Increasing Crop Yields**. Spelt, L. M.; Walworth, B. L.; Pavlista, A. D. *Ger. Offen.* **1984**, 25pp. DE 3345281.

294. **Conversion of the amino group of amino acids into the nitroguanidino group**. Heyboer, N.; Visser, G. Heymens; Kerling, K. E. T. Recueil des Travaux Chimiques des Pays-Bas (1962), 81, 69-72.

295. **Chlorine-assisted nitrolysis of cyclic tertiary amines**. Cliff, Matthew D. Heterocycles (1998) 48(4), 657-69.

296. **Purification, Assay and Properties of Mammalian Nitric Oxide Synthases**. Stuehr, Dennis J.; Griffith, Owen W. in Methods in Nitric Oxide Research. Edited by Feelisch, Martin; Stamler, Jonathan S. John Wiley & Sons Ltd. UK (1996), 177-86.

297. **The Citrulline Assay**. Bredt, D. S; Schmidt, H.H.H.W. in Methods in Nitric Oxide Research. Edited by Feelisch, Martin; Stamler, Jonathan S. John Wiley & Sons Ltd. UK (1996), 249-58.

298. **Measurement of NO-related Activities – Which Assay for Which Purpose?** Feelisch, M; Stamler, J.S. in Methods in Nitric Oxide Research. Edited by Feelisch, Martin; Stamler, Jonathan S. John Wiley & Sons Ltd. UK (1996), 177-86.

299. **Nitric Oxide Assays**. Zhang, Jie. Current Protocols in Pharmacology. Enna, S. J.; Williams, Michael. John Wiley and Sons. NY. Unit 2.4.

300. **The NIH Anticonvulsant Drug Development (ADD) Program: preclinical anticonvulsant screening project**. Stables, James P.; Kupferberg, Harvey J. http://www.ninds.nih.gov/about_ninds/clusters/addadd_review.pdf National Institute of Neuroloigal Disorders and Stroke, National Institutes of Health. Accessed 23rd July 2004.